2021-07-21

Investigating the role of RACK-1 in the C. elegans germ line

Vanden Broek, Kara Dawn

UNIVERSITY OF CALGARY

Investigating the role of RACK-1 in the *C. elegans* germ line

by

Kara Dawn Vanden Broek

A THESIS

SUBMITTED TO THE FACULTY OF GRADUATE STUDIES

IN PARTIAL FULFILMENT OF THE REQUIREMENTS FOR THE

DEGREE OF DOCTOR OF PHILOSOPHY

GRADUATE PROGRAM IN BIOLOGICAL SCIENCES

CALGARY, ALBERTA

JULY, 2021

Abstract:

Stem cells are central to the development of multi-cellular organisms, including *C. elegans* and humans. Key to their function is their ability to differentiate into more specialized cells or proliferate to maintain their population for future use. Germline stem cells (GSCs) are a class of stem cells that are crucial for an organism's reproductive success. GSCs proliferate to maintain the stem cell pool (self-renew) and differentiate to produce gametes (sperm/oocytes). A balance between proliferation and differentiation is necessary for proper germline function and the production of offspring throughout an organism's life. This thesis uses the *C. elegans* hermaphrodite germline as an *in vivo* model to investigate the molecular mechanisms that regulate the proliferation/differentiation balance.

In this thesis I have characterized RACK-1 as a modulator of the stem cell proliferation/differentiation balance. I found that RACK-1 is required for the proper activity of the conserved STAR family, RNA-binding protein, GLD-1/Quaking. GLD-1 is expressed throughout the cytoplasm in wildtype germlines, whereas in the absence of *rack-1,* GLD-1 levels are reduced, and GLD-1 becomes mislocalized to perinuclear aggregates (germ granules). This leads to a decrease, but not a complete loss, of GLD-1 activity. Specifically, a loss of *rack-1* in combination with a loss of GLD-2 pathway function results in an over-proliferation phenotype. This phenocopies a partial reduction of *gld-1* (*gld-1(het)*), but not a complete loss of *gld-1*, in the same genetic background. Additionally, loss of *rack-1* rescues the proliferation defects in an *fbf-1(0) fbf-2(0)* mutant background similar to a reduction of *gld-1* (*gld-1(het)*). Loss of *rack-1* enhances the defective

progression through meiosis phenotype associated with reduced GLD-1 activity. This data supports the model that *rack-1* functions to modulate GLD-1 activity through controlling GLD-1's subcellular localization and levels, thereby maintaining the proper proliferation/differentiation balance. This thesis reveals a novel mechanism that fine-tunes the activity of a key meiotic protein, GLD-1, to provide an additional layer of regulation in the proliferation/differentiation balance in the *C. elegans* germline.

Preface

This thesis is original, unpublished, independent work by the author Kara Dawn Vanden Broek.

Acknowledgments

I am incredibly grateful to all the people who have supported me and kept me laughing throughout my PhD journey. A huge thank you to my supervisor Dr. Dave Hansen. I have a ton of appreciation and admiration for him as a scientist and supervisor, and even more for him as a person. His support, knowledge, and humour have made my PhD experience exceptionally better. I feel very fortunate to have had him as my supervisor.

I owe a lot of my knowledge and success to previous lab members specifically Dr. Xin Wang, Dr. Prat Gupta, Dr. Ryan Smit and Dr. Brett Lancaster who trained me on all things related to science, *C. elegans* and grad school. I owe an even bigger thank you to Dr. Ramya Singh and Dr. Chris Wang for sharing their knowledge and passion of science with me. Picking worms beside them are some of my fondest PhD memories. I would also like to thank the current lab members that got me to the end of my degree: Dr. Xue "Cheryl" Han, the lab mom, for her compassion and troubleshooting assistance that kept me sane; Dan Zhang, the little egg, for all the scientific and life chats that influenced a lot of my decisions; Lauren McMillan; the little potato, for always keeping me laughing and ensuring me that "it's fine, it's fine, everything's fine" even when it wasn't; Sadaf Sangari, the sweet one, for her kindness and positive attitude that brightened even the toughest of lab days.

I would like to thank Dr. John Cobb, and my committee members Dr. Peng Huang and Dr. Marcus Samuel, for their input and support throughout my degree. I would also

like to thank my exam committee members, Dr. Ekaterina Voronina and Dr. Savraj Grewal, for their input on my research and discussion during my exam.

I owe the Worm group both past and present a huge thanks for sharing their science and ideas with me. They made Monday morning meetings enjoyable, especially Dr. Jim McGhee, Dr. Paul Mains, Dr. Maja Tarailo-Graovac, Tammy Lu, Amanda Stuart, Dr. Francesca Hargreaves, and Dr. Xiao Li.

I have many friends who listened to me ramble on about my research throughout my degree, so thank you for helping me celebrate my successes and supporting me through the lows. I really am incredibly lucky to have such an amazing support system. I owe a special thank you to Erika Reinarz, Nina Pattar, Julie Fisher and last, but not least, my book club ladies: Yesha Manani, Isabella Skuplik, Lindsay Phillips, Danielle Blackwell, Jasper Greysson-Wong, Tika Kocha, Amanda Stuart, Francesca Hargreaves; my life is much brighter and better with you all in it, thank you for being the very best of friends.

I am most grateful to my parents, Robyn and Frank, for their love and support. I would not have made it through any of my endeavours without them, and simply cannot thank them enough. They are the best support system, cheerleaders, and role models I could ever ask for. I am so lucky they are my parents and I really owe them the world.

List of abbreviations

Abbreviation	Definition
ASC	Adult stem cell
Cas9	CRISPR associated protein 9
CGC	*Caenorhabditis* genetics center
CRISPR	Clustered regularly interspaced short palindromic repeats
CSL	CBF1 /Su(H)/LAG-1
DAPI	4', 6- diamidino-2-phenylindole dihydrochloride
ddH_2O	Double distilled H_2O
dsDNA	Double stranded DNA
DSL	Delta/Serrate/LAG -2
DTC	Distal tip cell
ECL	Enhanced chemical luminescence
EMS	Ethyl-methane-sulphonate
ERK	Extracellular signal-regulated kinases
gf	Gain-of-function
GFP	Green fluorescent protein
Glp	Germline proliferation abnormal
GSC	Germline stem cell
IP	Immunoprecipitation
KH	K Homology
L3	Larval 3

L4	Larval 4
lf	Loss-of-function
LNR	LIN-12/Notch Repeats
MAPK	Mitogen-activated protein kinases
miRISC	microRNA-induced silencing complex
miRNA	microRNA
Mog	Masculinization of the germline
MS	Mass spectrometry
MSP	Major sperm protein
NBRP	National BioResource Project
NGM	Nematode growth media
NICD	Notch intracellular domain
PBS	phosphate buffered saline
PBT	Phosphate buffer saline with tween-20
PCR	Polymerase chain reaction
PGC	Primordial germ cell
Pro	Proximal proliferation tumour
PUF	Pumilio and FBF family
PZ	Proximal zone
RFP	Red fluorescent protein
RNAi	RNA interference

RNP	Ribonucleoprotein
SBP	Streptavidin binding peptide
SCF	SKR-2 CUL-1 PROM-1
SDS-PAGE	Sodium dodecyl sulfate- polyacrylamide gel electrophoresis
SIMR	siRNA-defective and mortal germline
siRNA	small interfering
TBS	Tris Buffer Saline
TBST	Tris Buffer Saline with Tween-20
ts	Temperature Sensitive
TZ	Transition Zone
WLB	Worm Lysis Buffer

List of gene names

Gene	Expanded name
alg-1/2	Argonaute (plant)-like gene
apx-1	Anterior Pharynx in excess
asc1	Absence of growth Suppressor of Cyp1
car-1	Cytokinesis, apoptosis, RNA-associated
cdk1	Cyclin-dependent Kinase 1
ced-1	Cell death abnormality
cep-1	*C. elegans* p-53-like protein
csr-1	Chromosome-segregation and RNAi deficient
cul-1	Culllin-1
cye-1	Cyclin E
dcr-1	Dicer related
deps-1	Defective P granules and sterile
dlc-1	Dynein light chain
ego-1	Enhancer of *glp-1*
fbf-1/-2	*fem-3* mRNA binding factor
gld-1/-2/-3	Defective in germ line development
glh-1/-4	Germ line helicase
glp-1	Germ line proliferation abnormal
him-3	High incidence of males
ife-1	Initiation factor 4E family

kin-10	Protein kinase
lag-1	*lin-12* and *glp-1* phenotype
lin-12	Abnormal cell lineage
lst-1	Lateral signaling target
mex-3	Muscle excess
mpk-1	Map kinase
mrg-1	Mortality factor-related gene
nos-1/-2/-3	Nanos related
pgl-1/-3	P granule abnormality
prg-1	Piwi related gene
prom-1	Progression of meiosis
prp-17	Yeast PRP (splicing factor) related
puf-5/-3/-11	Pumilio/FBF domain-containing
rack-1	Receptor of activated C kinase
rec-8	Recombination abnormal
rfp-1	Ring finger protein
simr-1	siRNA-defective and mortal germline
skr-1	Skp1 related (ubiquitin ligase complex component)
spn-4	Spindle orientation defective
sygl-1	Synthetic germline proliferation defective
teg-1/-4	Tumorous enhancer of *glp-1(gf)*

tra-2	Transformer: XX animals transformed into males
unc-115	Uncoordinated

Units of measurements

Units	Definition
°C	Degrees Celsius
%	Percentage
au	Arbitrary units
bp	Base pairs
g	Grams
gcd	Germ cell diameters
kDa	KiloDalton
M	Molar
mg	milligrams
mL	millilitres
mM	millimolar
ms	milliseconds
ng	nanogram
nmol	nanomole
pmol	picomole
μg	Microgram
μm	micrometer
μM	micromolar
S	Svedberg units
xg	Unit of relative centrifugal force (RCF)

Table of Contents

List of Figures

List of Tables

Chapter 1: Introduction

1.1 Stem cells

Stem cells are unspecified cells that possess the ability to self-renew through mitotic cellular divisions (proliferation) or to develop into more specialized mature cell types (differentiation) (Reviewed in: (Zakrzewski et al., 2019)). The existence of stem cells was first established in 1963 by Ernest Armstrong McCulloh and James Edgar Till (Becker et al., 1963; McCulloch & Till, 1960). Their experiment, transplanting bone marrow derived cells into irradiated mice, led to the realization that these cells had the ability to both self-renew and to mature into more specialized cells (Becker et al., 1963; McCulloch & Till, 1960). Mouse embryonic stem cells (ESCs) were later isolated and grown *in vitro* in 1981 by Sir Martin John Evans and Matthew Kaufman, followed by human ESCs in 1988 by James Alexander Thomson (Evans & Kaufman, 1981; Thomson et al., 1998).

The ability of stem cells to self-renew allows for a pool of stem cells to be maintained throughout development and the life of the organism. The ability of stem cells to develop, or differentiate, into other more specialized cell types allows for the development of the multiple different cell types needed for the formation of a complete organism (Zakrzewski et al., 2019). Additionally stem cell differentiation allows for tissue repair and maintenance throughout an organism's life (Zakrzewski et al., 2019). Proper development of all multi-cellular organisms, including *C. elegans* and humans, requires both stem cell proliferation and differentiation; therefore, a precise balance between proliferation and differentiation is required, such that an organism can maintain the stem cell pool for future use, while also allowing for tissue formation and repair to occur (Zakrzewski et al., 2019).

Pluripotent embryonic stem cells (ESC) are required for early development of an organism, as ESCs give rise to all cell types found within the organism (Zakrzewski et al., 2019). Adult stem cells (ASCs) have a reduced differentiation capacity and are only able to give rise to a limited subset, or specific type of cell, referred to as multi- or unipotent (Zakrzewski et al., 2019). ASCs are required for tissue homeostasis throughout an organism's life. Germline stem cells (GSCs) are a specific subset of ASCs. GSC research using model organisms, such as *C. elegans* and *Drosophila,* has provided valuable information on how stem cell proliferation and differentiation is regulated *in vivo* (Spradling et al., 2011).

1.2 Germline stem cells

Germline Stem Cells (GSCs) are responsible for the reproductive success, or fitness (ability to produce offspring), of an organism (Spradling et al., 2011). Organisms require a fine-tuned balance between GSC proliferation (self-renewal) and differentiation (production of gametes (sperm and/or oocyte)), throughout their life for them to successfully reproduce. Excessive GSC differentiation leads to depletion of the stem cell pool, which removes the organism's ability to further produce gametes (Spradling et al., 2011). Conversely, excessive GSC proliferation leads to tumour formation, which results in a decrease in the production of gametes and reduced ability for the production offspring; therefore, disruption in this balance, in either direction, has serious implications for an organism's fitness (Spradling et al., 2011).

GSCs arise from a subset of cells, primordial germ cells (PGCs), which are specified to give rise to the germline during embryonic development. PGCs were proposed to be

specified by the inheritance of ‘germ plasm’ (Parker et al., 1893; Weismann, 1892). Continued research identified a component of germ plasm, later referred to as germ granules, which are maternally supplied proteins and RNAs that form distinct granules in many organisms, including *Drosophila,* zebrafish, *Xenopus*, mice and *C. elegans* (Clark & Eddy, 1975; Ikenishi et al., 1996; Knaut et al., 2000; Mahowald, 1968; Spiegelman & Bennett, 1973; Strome & Wood, 1982). Germ granules contain components that are conserved across many species including RNA regulatory proteins, and components of small RNA pathways, suggesting a role in RNA metabolism and gene expression (Reviewed in (Voronina et al., 2011). Research on *C. elegans* germ granules supports the model that they are involved in RNA metabolism, required for animal fertility, and has uncovered their involvement in epigenetic inheritance (Section 1.81) (Sundby et al., 2021).

Stem cells are housed in a specific micro-environment known as the niche (Schofield, 1978). Schofield first proposed the idea of the ‘niche’ in 1978 by suggesting that stem cells retain their “stemness” through localization to a specific physical environment. The niche has since been identified for germline stem cell pools in various model organisms including *C. elegans, Drosophila and* mice (Brinster, 2002; Kiger et al., 2001; Kimble & White, 1981; Meng et al., 2000; Tulina & Matunis, 2001; Xie & Spradling, 2000; Yomogida et al., 2003). GSCs residing in the niche undergo mitotic divisions. These division can produce two identical daughter cells that both remain in the niche, and therefore remain GSCs, or can produce two non-identical daughter cells, one that remains in the niche (GSC) and one that exits the niche and can begin to differentiate. The niche provides

signals that maintain the stem cell fate/identity of GSCs; however, only a defined number of cells can be maintained by the niche (Reviewed in: (Morrison & Spradling, 2008). GSC proliferation and GSC exit from the niche establishes a balance between proliferation and differentiation that is required for proper germline function throughout an organism's life. Although the presence and function of the niche is conserved between organisms, the specific cells and signaling pathways differ.

GSC fate in *Drosophila* ovaries and testis is maintained through BMP signaling. The niche cells express BMP ligands, *dpp* and *gbb,* which trigger the BMP signaling cascade within in the GSC, resulting in the repression of *bam*, a differentiation promoting gene (Kawase et al., 2004; Song et al., 2004). In the ovaries the GSCs are surrounded by the cap and escort cells, which function as the niche (Kirilly & Xie, 2007; Lin, 2002; Xie & Spradling, 2000). In the *Drosophila* testis the somatic cyst and hub cells function as the niche (Kawase et al., 2004; Tran et al., 2000; Tulina & Matunis, 2001; Wieschaus & Szabad, 1979; Xie & Spradling, 2000). Direct contact between the niche and GSCs are required to maintain GSC fate (Hardy et al., 1979; Jan et al., 1999; Kawase et al., 2004; Tran et al., 2000; Xie & Spradling, 2000; Yamashita et al., 2003). As GSCs proliferate, one daughter cell loses contact with the niche and begins to differentiate (Wieschaus & Szabad, 1979; Xie & Spradling, 2000). The ovarian niche maintains only 2-3 GSCs, whereas in the testis, the niche maintains a population of ~7-10 GSCs (Kawase et al., 2004; Tran et al., 2000; Tulina & Matunis, 2001; Wieschaus & Szabad, 1979; Xie & Spradling, 2000). In the mammalian testis, Sertoli cells function as the niche. These cells express GDNF (glial derived neurotrophic factor), a TGFβ family member, which is

required to maintain the proliferative fate of a single GSC (spermatogonial stem cell) by activating a number of downstream pathways, including Src signaling and Ras/ERK1/2 signaling (Braydich-Stolle et al., 2007; He et al., 2008; Hofmann et al., 2005; Kubota et al., 2004; Meng et al., 2000; Yomogida et al., 2003).

The mechanisms controlling the *C. elegans* GSC population are the focus of this thesis and will be described in detail in the following sections.

1.3 *C. elegans*

C. elegans are small, transparent, free-living nematodes, with a relatively short reproductive cycle (~3 days), and exist in two sexes, male (XO) and a self-fertilizing hermaphrodite (XX) (Porta-de-la-Riva et al., 2012). The research presented in this thesis focuses on the hermaphrodite germline. In the hermaphrodite, embryogenesis begins *in utero* upon fertilization of mature oocytes. At the gastrula stage (embryo made up of pluripotent cells) the embryos are laid and the rest of embryogenesis occurs *ex utero* (Corsi et al., 2015). The end of embryogenesis is marked by hatching that gives rise to the first of the four larval stages, L1 (Corsi et al., 2015). The larval stages L1, L2, L3, and L4, are separated from each other by molting (replacement of a new protective cuticle). At one day post L4, the worm is considered an adult and the life cycle can continue by self-fertilization in a hermaphrodite or through mating with a male (Corsi et al., 2015).

1.3.1 *C. elegans* germline development

The germline arises from two primordial germ cells (PGCs), Z2 and Z3, which are quiescent during embryonic development until the first larval stage (L1) when they begin to proliferate upon access to nutrients (Hirsh et al., 1976; Kimble & Hirsh, 1979). The

somatic gonad arises from the Z1 and Z4 cells, descendants of the MS lineage (Kimble & Hirsh, 1979). The PGCs and somatic gonad precursors proliferate throughout the first three larval stages giving rise to a pool of stem cells and the somatic gonad primordium (Hirsh et al., 1976; Kimble & Hirsh, 1979). The distal tip cell (DTC) is an important somatic cell that is required for proper migration of the developing gonad (Kimble & Hirsh, 1979). During the L3 stage, the most proximal cells enter meiosis, which is referred to as 'initial meiosis' (Austin & Kimble, 1987; Kimble & White, 1981). In the hermaphrodite germline the first cells to undergo meiosis differentiate as sperm with primary spermatocytes becoming visible during the mid-L4 stage, and all sperm (~150/gonad arm) being produced by the L4 molt (Hirsh et al., 1976; Kimble & White, 1981). The switch from spermatogenesis to oogenesis occurs after the L4 molt with oocyte production continuing throughout the organism's adult life (Hirsh et al., 1976). The oocytes mature in a distal-proximal fashion, with the most mature oocytes being located most proximally next to the spermathecae resulting in fertilized embryos being housed in the uterus, next to the vulva to be laid (Hirsh et al., 1976).

1.3.2 Anatomy of the gonad

The DTC caps the distal end of the u-shaped gonad arm, where it functions as the proliferative niche needed to maintain the mitotic GSC population (Kimble & White, 1981). This most distal zone of the germline, where the stem cell pool is housed, is referred to as the proliferative zone (PZ). As the cells proliferate, they move proximally, away from the DTC/niche and begin to enter meiosis (differentiation) (Austin & Kimble, 1987; Kimble & White, 1981). This region is defined by distinct crescent shaped nuclear morphology that marks the exit from the mitotic cell cycle and transition into early meiotic pachytene

stages (lepotene/zygotene) (MacQueen & Villeneuve, 2001). This region is referred to as the transition zone (TZ). In the meiotic region located proximally to the TZ, cells progress through pachytene until the bend in the gonad arm (loop region) where they are either removed by apoptosis or progress through diplotene and arrest in diakinesis of meiosis, forming mature oocytes at the most proximal end.

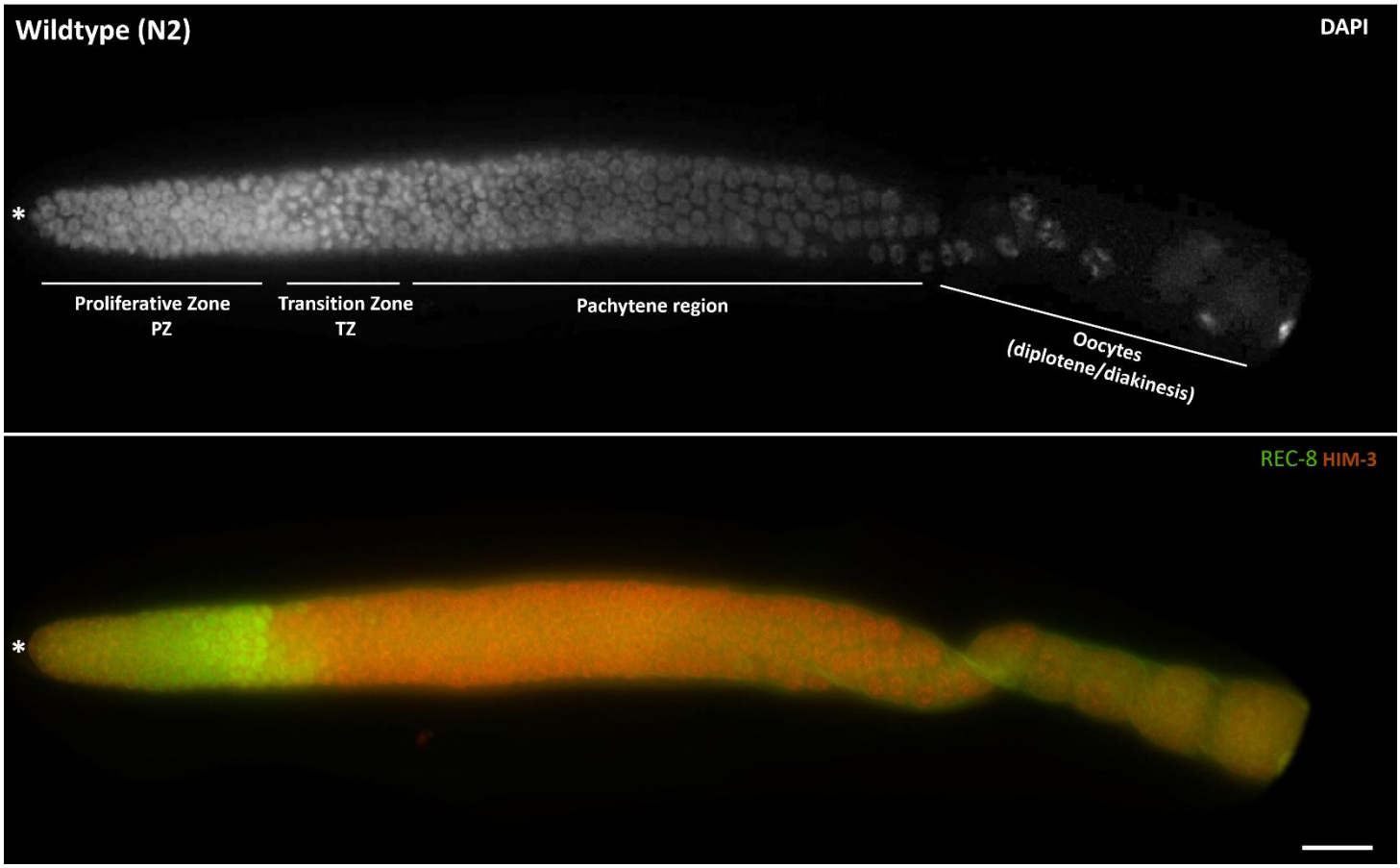

Figure 1.1 - Dissected adult hermaphrodite gonad. Representative image of a young adult wildtype (N2) gonad. Animals were raised at 20 °C and dissected one day past the L4 stage, fixed, and stained with DAPI to visualize nuclear morphology, α-REC-8 antibodies to mark proliferative cells (mitotic), and α-HIM-3 antibodies to mark differentiating cells (meiotic). The distal end, which is capped by the somatic distal tip cell (DTC) is marked with an *. The DTC supplies the proliferative niche to maintain a pool of mitotic GSCs in the proliferative zone (PZ). As the cells proliferate, they exit the niche, and begin the transition into meiosis. This region is referred to as the transition zone (TZ) and is marked by crescent-shaped nuclei. The cells continue through meiotic pachytene

until the loop region where they progress into diplotene/diakinesis forming mature oocytes.

1.4 The DTC and GLP-1/Notch signaling

The DTC, which caps the distal end of the gonad arm, creates a proliferative niche that functions to maintain a population of mitotic stem cells within the proliferative zone. This somatic cell extends processes ("DTC plexus") that allows the DTC to maintain contact with germ cells up to 20 cell diameters away (Byrd et al., 2014; Crittenden et al., 2006; Hall et al., 1999). The niche is estimated to maintain approximately 60-80 GSCs and 130-160 mitotically cycling cells, with the remaining germ cells in the PZ being mostly in meiotic S phase (Crittenden et al., 2006; Fox et al., 2011; Fox & Schedl, 2015; Maciejowski et al., 2006). These populations make up the pool of germ cells found within the PZ (~230 cells) (Crittenden et al., 2006; Fox et al., 2011; Fox & Schedl, 2015; Maciejowski et al., 2006). As the cells move out of the proliferative niche, they lose the proliferative signal and begin to differentiate. Cells that exit the niche in S or G2 phase will complete the mitotic cell cycle before progressing through to meiotic S-phase in the daughter cells (Fox et al., 2011). The more proximal end of the proliferative zone therefore contains a mix of mitotic and meiotic cells (Crittenden et al., 1994; Fox et al., 2011; Hansen, Hubbard, et al., 2004). Laser ablation of the DTC and DTC repositioning experiments demonstrated that the DTC functions as the niche and is needed for the PGCs and GSCs to remain proliferative (Kimble & White, 1981). In the absence of the DTC, the GSCs prematurely enter meiosis resulting in a Glp (germline proliferation abnormal) phenotype (four to eight mature sperm produced) (Figure 1.2) (Austin &

Kimble, 1987; Kimble & White, 1981). These results demonstrated that the DTC functions as the niche and is required to maintain the GSC pool.

1.4.1 GLP-1/Notch signaling

The DTC expresses LAG-2 and APX-1, DSL (Delta/Serrate/LAG -2) family ligands, on its cell surface, which interact with the GLP-1/Notch receptor present on the GSCs (Crittenden et al., 1994; Fitzgerald & Greenwald, 1995; Nadarajan et al., 2009). Loss of *glp-1,* which encodes a Notch family transmembrane receptor, within the GSCs resulted in Glp germlines, phenocopying the loss of the DTC (Austin & Kimble, 1987; Kimble & White, 1981; Lambie et al., 1991). Conversely, in *glp-1* gain-of-function mutants GSCs fail to enter meiosis and instead GSC over-proliferation occurs resulting in a germline tumour (Figure 1.2) (Berry et al., 1997; Pepper et al., 2003). Taken together this data suggested that GLP-1/Notch signaling is the main regulator of GSC proliferation/differentiation.

Interaction between APX-1/LAG-2 and GLP-1/Notch is predicted to result in three proteolytic cleavage events in the GLP-1/Notch receptor that result in the release of the of the Notch intracellular domain (NICD) (Reviewed (Hubbard & Schedl, 2019)). NICD has only recently been visualized within the GSCs and their nuclei within the proliferative zone of *C. elegans* (Gutnik et al., 2018; Sorensen et al., 2020). NICD translocates into the nucleus where it functions as a transcriptional activation complex alongside LAG-1 CSL family member (CBF1 /Su(H)/LAG-1), and LAG-3/SEL-8 (Christensen et al., 1996; Doyle et al., 2000; Lambie et al., 1991; Petcherski & Kimble, 2000).

1.4.2 Direct GLP-1/Notch targets - LST-1 and SYGL-1

The GLP-1/Notch/LAG-1/LAG-3/SEL-8 complex functions as a translational activator. Analysis of putative GLP-1/Notch targets identified two redundant genes, *lst-1* and *sygl-1,* which when simultaneously knocked out phenocopy a loss of GLP-1/Notch signaling (Glp phenotype) (Figure 1.2) (Kershner et al., 2014). Interestingly, both *lst-1* and *sygl-1* do not contain any conserved protein domain sequences and do not appear to be conserved in other species (Kershner et al., 2014). SYGL-1 is expressed within the proliferative zone up to 11-13 germ cell diameters (gcd) from the DTC (Kocsisova et al., 2019; Shin et al., 2017). LST-1 expression is more restricted being expressed only up to 5 gcd from the DTC (Kocsisova et al., 2019; Shin et al., 2017). Loss of *lst-1* alone slightly reduces the stem cell pool, whereas loss of *sygl-1* reduces the PZ by about half (Brenner & Schedl, 2016; Kershner et al., 2014; Shin et al., 2017). Increased *sygl-1* expression corresponds with an increase in the proliferative zone size, with ubiquitous expression of *lst-1* and *sygl-1* resulting in germline tumours (Figure 1.2) (Shin et al., 2017). Analysis of various downstream GLP-1/Notch signaling targets determined that most require the activity of *lst-1* and *sygl-1,* rather than GLP-1/Notch transcriptional activation (Chen et al., 2020; Shin et al., 2017). It is thought that *lst-1* and *sygl-1* are the only direct targets of GLP-1/Notch that function to promote GSC proliferation (Chen et al., 2020; Shin et al., 2017). The identification of these two targets has provided researchers with a direct readout of GLP-1/Notch activity, which has been useful in characterizing various proliferation/differentiation mutants (Chen et al., 2020; Kocsisova et al., 2019; Shin et al., 2017).

1.4.3 The PUF hub

Four PUF (Pumilio and FBF family) RNA binding proteins, *fbf-1, fbf-2, puf-3* and *puf-11* work as a hub ('PUF hub') to promote GSC proliferation (Crittenden et al., 2002; Haupt et al., 2020). Loss of these four PUF proteins phenocopies the Glp phenotype of *glp-1/*Notch or *lst-1 sygl-1* null mutants (Haupt et al., 2020).

fbf-1 and *fbf-2* were the first two PUF hub genes identified (Crittenden et al., 2002; Zhang et al., 1997). *fbf-1* and *fbf-2* are thought to promote mitosis through repressing the expression of genes required for meiosis (Crittenden et al., 2002; Lamont et al., 2004; Zhang et al., 1997). They were found to play a role in regulating GSC proliferation, downstream of GLP-1/Notch, as loss of both *fbf-1* and *fbf-2* resulted in Glp germlines; however, unlike *glp-1* null mutants [or *lst-1(0) sygl-1(0)*], the GSCs in these mutants proliferate until the L4 stage and then prematurely enter meiosis resulting in a germline filled with ~400 sperm, instead of only four to eight sperm as in *glp-1* or *lst-1 sygl-1* null germlines (Figure 1.2) (Crittenden et al., 2002). FBF-1 and FBF-2 share the majority of their target mRNAs, possess 89% identity and were originally thought to be largely redundant for their role in GSC proliferation, being collectively referred to as FBF (Crittenden et al., 2002; Kershner & Kimble, 2010; Zhang et al., 1997); however, independent roles for *fbf-1* and *fbf-2* within the germline have been uncovered (Lamont et al., 2004; Voronina et al., 2012; Wang et al., 2020).

FBF-1 is expressed within the proliferative zone of the adult germline and functions to repress its targets through poly-A deadenylation with the CCR-4-NOT deadenylase complex leading to target degradation (Crittenden et al., 2002; Lamont et al., 2004;

Voronina et al., 2012; Wang et al., 2020). FBF-1 is required to prevent meiotic entry with loss of *fbf-1* resulting in a decrease in the PZ size (Lamont et al., 2004; Wang et al., 2020). FBF-2 expression is low in the first few cell rows of the PZ but increases and is detectable throughout the PZ (Lamont et al., 2004; Voronina et al., 2012). FBF-2 represses target genes in a deadenylation-independent manner, through the formation of ribonucleoprotein (RNP) complexes with its target mRNAs (Wang et al., 2020). FBF-2 functions to promote cell division, with loss of *fbf-2* resulting in an increase in the proliferative zone size (Lamont et al., 2004; Wang et al., 2020). These separate functions are regulated by divergent sequences within these genes (Wang et al., 2020) .

Analysis of other *C. elegans* PUF family proteins led to the identification of *puf-3* and *puf-11* playing a role in GSC proliferation (Haupt et al., 2020). Alone *puf-3* and *puf-11* have no effect on GSC proliferation (Haupt et al., 2020); however, loss of either *puf-3* or *puf-11* in combination with *fbf-1(0) fbf-2(0)* resulted in a decrease in GSC proliferation as determined by a reduction in the number of sperm produced per germline (Haupt et al., 2020). A loss of both *puf-3* and *puf-11*, in combination with *fbf-1(0)* and *fbf-2(0)*, resulted in a Glp phenotype resembling that of *glp-1* null mutants (Figure 1.2) (Haupt et al., 2020). PUF-3 and PUF-11 are expressed within the PZ, consistent with their role in regulating GSCs (Haupt et al., 2020).

Interestingly, all components of the PUF hub have been found to interact with LST-1 and all but PUF-11 appear to interact with SYGL-1 (Haupt et al., 2019; Qiu et al., 2019; Shin et al., 2017). Mutations of FBF binding sites in *lst-1* disrupted its ability to promote

GSC proliferation (Haupt et al., 2019; Qiu et al., 2019). The working model is that interactions between PUF hub components and LST-1 and SYGL-1 are required for proper target repression and ultimately GSC proliferation (Haupt et al., 2020; Shin et al., 2017).

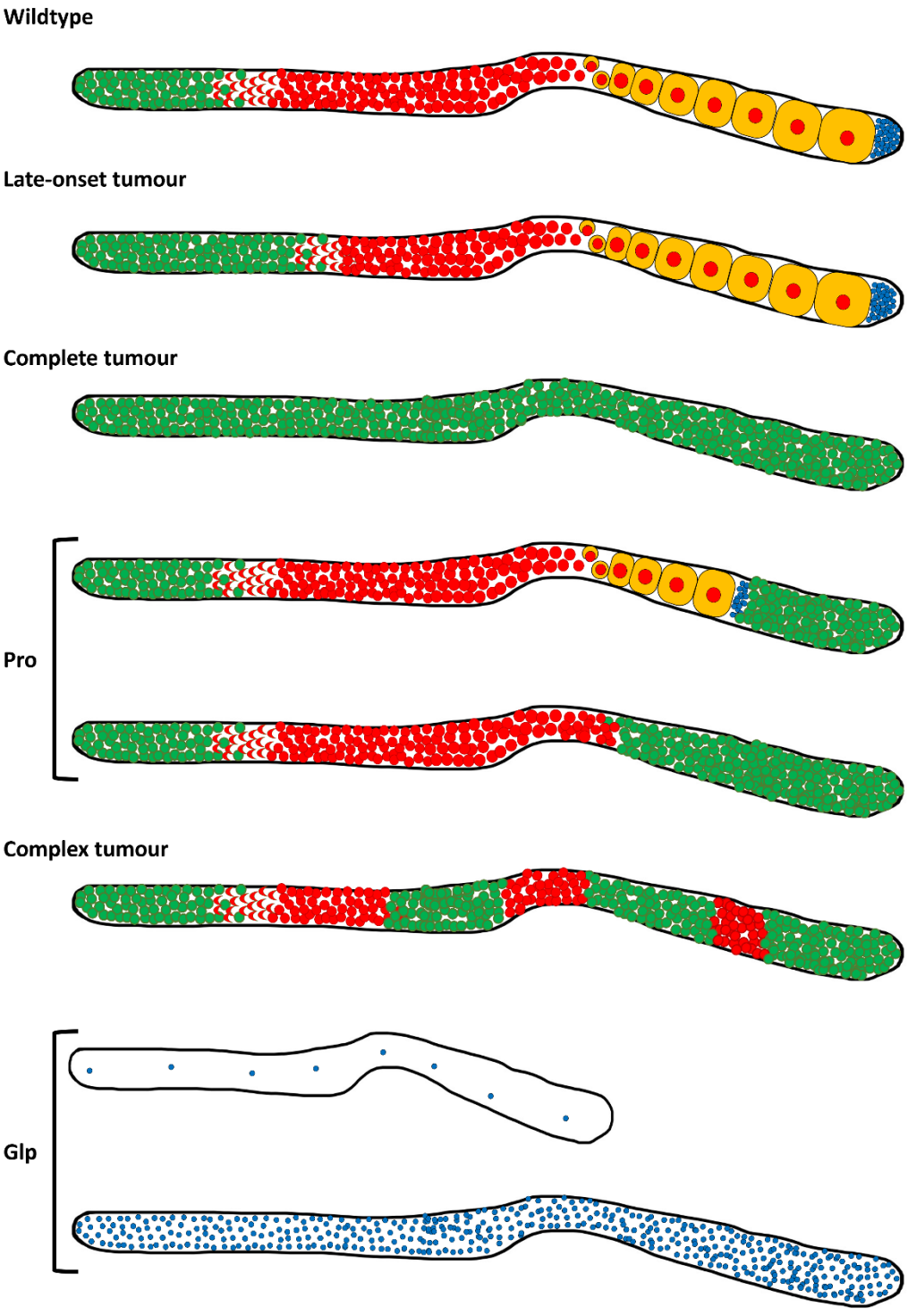
Wildtype
Late-onset tumour
Complete tumour
Pro
Complex tumour
Glp

Figure 1.2 – Germline phenotypes associated with defects in the proliferation/differentiation balance in the adult germline. Cartoon representations of germline phenotypes associated with changes in the proliferation/differentiation balance. The distal end is on the left-hand side. Green cells represent mitotic cells, red cells represent meiotic cells, blue cells represent mature sperm, and yellow represents developing oocytes. Wildtype germlines have a proper balance between proliferation and differentiation resulting in maintenance of the stem cell pool (green) and production of gametes (sperm and oocytes (blue and yellow)). Disruptions to the balance between proliferation and differentiation results in a variety of germline phenotypes. Increased proliferation, as seen in *glp-1(ar202gf)* mutants at the permissive temperature, results in a late-onset tumour detectable by the increased stem cell pool (green). If the balance is completely disrupted such that only proliferation can occur a complete tumour is formed, as seen in *glp-1(ar202gf)* mutants at the restrictive temperature. Proximal tumours (Pro) have a pool of ectopic proliferating cells present at the proximal end of the germline. Pro germlines may have visible gametes (as seen in *glp-1(oz264gf)* or *glp-1(ar202gf)* at the restrictive temperature (top germline), or they may lack gametes as seen in *gld-1(q485)* (bottom germline). A complex tumour has patches of meiotic and mitotic cells throughout the germline. These tumours may have proliferating cells (Pro) or meiotic cells at the proximal end of the germline. Defective proliferation results in a Glp (abnormal germline proliferation) phenotype. Glp germlines have only meiotic cells (mature sperm) present within the germline. The top germline represents a Glp phenotype associated with

complete loss of GSC proliferation (*glp-1* null mutants, *lst-1(0) sygl-1(0),* loss of PUF hub), and the bottom represents Glp phenotype associated with *fbf-1(0) fbf-2(0)* mutants.

1.5 Meiotic entry pathways

Active GLP-1/Notch signaling promotes proliferation through regulating the expression of *lst-1* and *sygl-1* (Figure 1.3). These genes function alongside of the PUF hub to inhibit meiosis, through repressing the expression of meiosis promoting factors, allowing proliferation to occur (Haupt et al., 2020; Shin et al., 2017). Three redundant pathways that are required for the entry into meiosis – the GLD-1 pathway, the GLD-2 pathway, and the SCF^{PROM-1} mediated protein degradation pathway (Figure 1.3) (Reviewed in (Hubbard & Schedl, 2019)). Loss of one these pathways has no effect on meiotic entry; however, loss of two of these pathways disrupts GSC entry into meiosis, with few meiotic cells detectable within the germline (Eckmann et al., 2004; Hansen, Hubbard, et al., 2004; Kadyk & Kimble, 1998; Mohammad et al., 2018). Additional unidentified factors are required to promote entry into meiosis as meiotic cells are detected in germlines mutant for all three pathways (GLD-1, GLD2, and SCF^{PROM-1}) (Figure 1.3) (Mohammad et al., 2018).

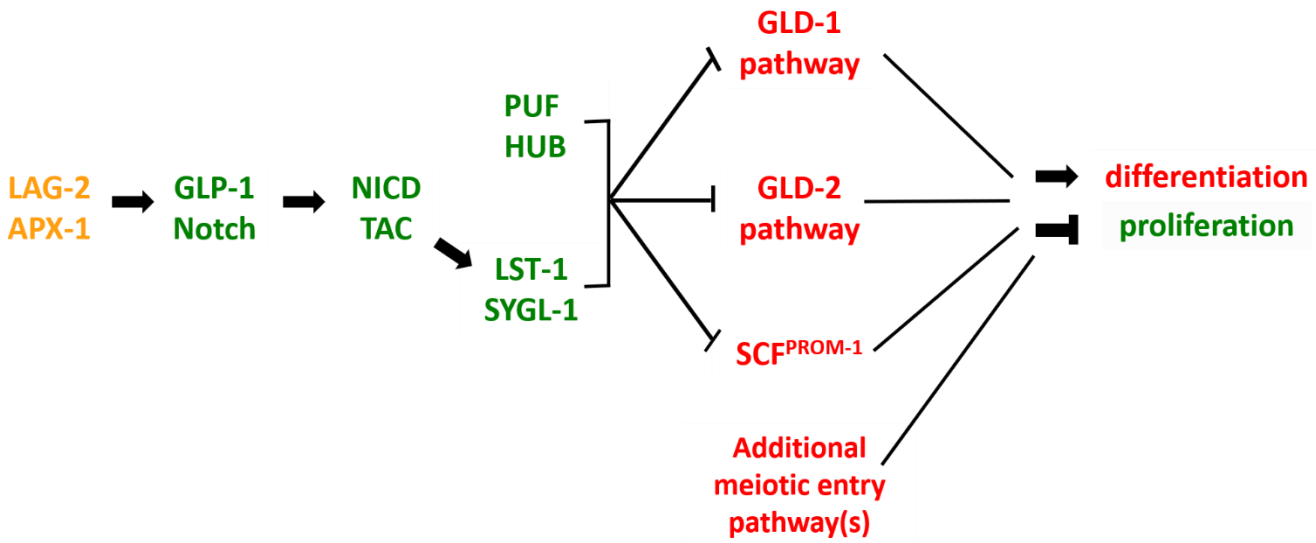

Figure 1.3 - The genetic pathway regulating the balance between GSC proliferation and differentiation in the germline of *C. elegans.* The DSL ligands, LAG2 and APX-1, are expressed on the surface of the DTC where they interact with the GLP-1/Notch receptor present on GSC cell surfaces. This interaction results in proteolytic cleavage of the receptor and release of GLP-1/Notch intracellular domain (NICD). NICD translocates to the nuclease forming a transcriptional activation complex, activating the expression of LST-1 and SYGL-1. These two proteins interact with components of the PUF HUB (*fbf-1, fbf-2, puf-3, puf-11)* and inhibit meiosis through repressing the downstream meiotic entry pathways, GLD-1 (*gld-1, nos-3),* GLD-2 (*gld-2, gld-3)*, SCF^{PROM-1} (*skr-2, cul-1, prom-1*). Proliferation promoting proteins are labeled in green, meiosis promoting proteins are in red, and DTC expressed components are yellow. Adapted from (Hubbard & Schedl, 2019).

1.5.1 GLD-1 pathway

The identification of multiple mutant alleles displaying germline defects in hermaphrodites led to the discovery and identification of *gld-1* (Francis et al., 1995). GLD-1 is a member of the KH/Star domain family, with homologs How in *Drosophila* and mammalian QUAKING and SAM68 (Ebersole et al., 1996; Jan et al., 1999; Jones et al., 1996; Jones & Schedl, 1995; Lock et al., 1996). The identification of over 30 mutant alleles with varying defects in germline development (loss-of-function/separation-of-function alleles) allowed for the characterization of GLD-1's functions within the germline (Francis et al., 1995; Jones et al., 1996).

GLD-1 functions redundantly with components of the other meiotic promoting pathways (GLD-2 and SCF^{PROM-1}) to promote GSC entry into meiosis (Eckmann et al., 2004; Hansen, Hubbard, et al., 2004; Kadyk & Kimble, 1998; Mohammad et al., 2018). GLD-1 is also required for the progression through meiosis, as complete loss of *gld-1* results in germ cells failing to progress through meiotic pachytene and re-entering the mitotic cell cycle (de-differentiation) (Figure 1.2) (Francis et al., 1995). Additionally, a subset of *gld-1* mutant alleles display late meiotic pachytene arrest, rather than mitotic re-entry (Francis et al., 1995; Schumacher et al., 2001). This arrested pachytene phenotype uncovered a role for *gld-1* in regulating germline apoptosis, which occurs during oogenesis at the late pachytene stage (Schumacher et al., 2001). Interestingly, the progression through meiosis defect is restricted to germ cells undergoing oogenesis (Francis et al., 1995). Additionally, a subset of *gld-1* mutant alleles result in the formation of defective oocytes (Francis et al., 1995); therefore, *gld-1* is required during various

stages of oocyte development. *gld-1* is also involved in promoting the specification of the male germline fate, with *gld-1(0)* hermaphrodites having no masculinized germ cells (lacking sperm) (Francis et al., 1995). GLD-1 is not required for meiotic progression, or spermatogenesis, in male germlines (Francis et al., 1995).

GLD-1 is thought to control these processes through its activity as a translational repressor (Jan et al., 1999; Jungkamp et al., 2011; Lee & Schedl, 2004; Marin & Evans, 2003; Merritt et al., 2008; Mootz et al., 2004; Schumacher et al., 2005) **.** Many *gld-1* mRNA targets have been identified, including genes involved in sex determination (*tra-2*), apoptosis (*cep-1, lin-45*), meiotic progression (*cye-1, lin-45)*, oocyte development (*puf-5, spn-4*) and the meiotic entry decision (*glp-1, mex-3)* (Ariz et al., 2009; Biedermann et al., 2009; Ellenbecker et al., 2019; Lee & Schedl, 2004; Lublin & Evans, 2007; Marin & Evans, 2003; Merritt et al., 2008; Mootz et al., 2004; Schumacher et al., 2005). Interestingly, GLD-1 has been found to be required for stabilization/protection of a subset of its target mRNAs, in addition to its role in translational repression (Biedermann et al., 2009; Lee & Schedl, 2004; Scheckel et al., 2012). How exactly GLD-1 functions to either repress its target genes, or stabilize its targets, remains unclear but may be mediated through interactions with other proteins and/or complexes (Ellenbecker et al., 2019; Lee & Schedl, 2010; Scheckel et al., 2012; Wang et al., 2016; Zhang et al., 1997)

GLD-1's expression pattern is consistent with it being required for meiotic entry and progression. GLD-1 is expressed at low levels in the distal most end of the germline (Brenner & Schedl, 2016; Hansen, Wilson-Berry, et al., 2004; Jones et al., 1996). Prior to

GSC entry into meiosis GLD-1 levels increase and remain high through the meiotic pachytene phase of the germline until the loop region (developing oocytes) where GLD-1 expression is lost (Brenner & Schedl, 2016; Hansen, Wilson-Berry, et al., 2004; Jones et al., 1996). GLD-1 is mainly expressed within the cytoplasm of meiotic germ cells; however, a portion of GLD-1 is enriched in RNP germ granules (P granules) in the germline and embryo (Ellenbecker et al., 2019; Jones et al., 1996). Repression of GLD-1 in the distal end of the germline is thought to be regulated by FBF-1, LST-1 and SYGL-1, as loss of these genes results in elevated GLD -1 levels in the distal end of the germline (Brenner & Schedl, 2016; Crittenden et al., 2002; Shin et al., 2017).

nos-3, one of three *C. elegans* Nanos homologs, is another core component of the GLD-1 pathway (Hansen, Wilson-Berry, et al., 2004; Kraemer et al., 1999). NOS-3 is expressed throughout the germline in the cytoplasm of all germ cells except sperm (Kraemer et al., 1999). *nos-3* was first identified for its role in the sex determination pathway where it mediates the switch from spermatogenesis to oogenesis in hermaphrodite germlines (Kraemer et al., 1999). *nos-3* was subsequently identified to play a role in the GLD-1 pathway, as mutations in *nos-3,* in combination with GLD-2 or SCF^{PROM-1} components, results in germline over-proliferation (Hansen, Wilson-Berry, et al., 2004; Mohammad et al., 2018). *nos-3* is thought to promote meiotic entry, in part, through regulating the accumulation of GLD-1, redundantly with GLD-2, in opposition of FBF-1's translational repression (Brenner & Schedl, 2016; Hansen, Wilson-Berry, et al., 2004); however, no other targets regulating meiotic entry have been identified.

1.5.2 GLD-2 pathway

GLD-2 is a catalytic subunit of a cytoplasmic poly(A) polymerase that promotes the accumulation of target mRNAs through stabilization upon the addition of a poly(A) tail (Kim et al., 2010; Nousch et al., 2017; Suh et al., 2006; Wang et al., 2002). GLD-2 is expressed throughout the cytoplasm of germ cells with higher levels in the meiotic pachytene region and developed oocytes (Wang et al., 2002). *gld-2* was initially identified for its role in promoting meiotic progression in both male and hermaphrodite germlines; a loss of *gld-2* results in cells arresting in an abnormal pachytene state and gametogenesis failing to occur (Kadyk & Kimble, 1998). Additionally, *gld-2* functions redundantly with the GLD-1 and SCF^{PROM-1} pathways to promote entry into meiosis (Eckmann et al., 2004; Hansen, Hubbard, et al., 2004; Kadyk & Kimble, 1998; Mohammad et al., 2018). GLD-2 promotes meiotic entry, in part, through regulating GLD-1 expression redundantly with *nos-3* (Brenner & Schedl, 2016; Hansen, Wilson-Berry, et al., 2004; Nousch et al., 2017; Suh et al., 2006; Wang et al., 2002). Additional GLD-2 targets that promote entry into meiosis have not yet been identified.

GLD-2 lacks an RNA-binding domain and requires interaction with other proteins for complete poly(A) polymerase activity (Wang et al., 2002). Two RNA-binding proteins, GLD-3 and RNP-8, have been identified that bind to, and stimulate, GLD-2's poly(A) activity (Eckmann et al., 2002; Kim et al., 2009, 2010; Suh et al., 2006; Wang et al., 2002). The working model is that the RNA-binding component provides target specificity allowing GLD-2 poly(A) polymerase to regulate a diverse range of targets (Kim et al., 2009, 2010). The identification of RNP-8 as an additional GLD-2 interacting protein provides insight

into the differences in synthetic mutant phenotypes observed between *gld-2* and *gld-3* null mutants and other GLP-1/Notch components (Eckmann et al., 2004; Macdonald et al., 2008; Mohammad et al., 2018).

As mentioned above, GLD-3, a member of the Bicaudal-C RNA binding protein family, complexes with GLD-2 to form a functional poly(A) polymerase (Eckmann et al., 2002; Kim et al., 2009, 2010; Suh et al., 2006; Wang et al., 2002). GLD-3 is expressed throughout the germline in the cytoplasm of germ cells with a portion of GLD-3 localizing to P granules (Eckmann et al., 2002). GLD-3 expression is low in the distal end of the germline and the meiotic pachytene region; however, GLD-3 levels increase in the transition zone and are most abundant in developing oocytes (Eckmann et al., 2002). GLD-3's expression is, in part, regulated by *fbf-1* and/or *fbf-2* as GLD-3 levels increase throughout the germline in *fbf-1 fbf-2* mutant germlines (Eckmann et al., 2004). GLD-3 functions to promote spermatogenesis in male and hermaphrodite germlines (Eckmann et al., 2002). Loss of *gld-3* in hermaphrodite germlines results in abnormal or stacked oocytes and sterility due to defective spermatogenesis (Eckmann et al., 2002).

1.5.3 SCF^{PROM-1} mediated protein degradation pathway

The SCF^{PROM-1} E3 ubiquitin-ligase complex is made up of SKR-2, CUL-1 and PROM-1 (Fox et al., 2011; Mohammad et al., 2018). E3 ligases, such as SCF^{PROM-1}, function to provide target specificity within the ubiquitin mediated protein degradation pathway (Crews, 2003; Komander, 2009; Pickart, 2001). The SCF^{PROM-1} complex was found to promote meiotic entry through mediating the degradation of mitotic cell cycle proteins including *cye-1,* a known GLD-1 target, as well as positively regulating

homologous chromosome pairing (Biedermann et al., 2009; Fox et al., 2011; Jantsch et al., 2007; Mohammad et al., 2018; Nayak et al., 2002). Loss of SCF^{PROM-1} alone does not disrupt entry into meiosis; however, SCF^{PROM-1} functions redundantly with GLD-1 and GLD-2 pathways to promote meiotic entry (Mohammad et al., 2018). Loss of all three meiotic entry pathways (*gld-2(0) gld-1(0); prom-1(0)*) resulted in a significant reduction in the number of meiotic cells throughout the germline; however, low levels of meiotic entry was still detected in these mutants (Mohammad et al., 2018). This data highlights that additional unidentified regulators exist that function redundantly to promote entry into meiosis.

1.5.4 Additional factors/pathways regulating GSC proliferation/differentiation

The pathways described above are the core regulators of stem cell fate within the *C. elegans* germline; however, additional factors/pathways that function to modulate the proliferation/differentiation balance within the germline have been identified (Hubbard & Schedl, 2019). Partial reduction of the proteasome in sensitized backgrounds results in over-proliferation of GSCs, suggesting proteins necessary for proliferation are selectively degraded in order for meiotic entry to occur (Macdonald et al., 2008). In addition to SCF^{PROM-1}, other E3 ligases have been shown to be required to promote meiosis (Gupta et al., 2015). Loss of five E3 ligases/SRSs, specifically *rfp-1*, resulted in GSC over-proliferation (Gupta et al., 2015). Further analysis of RFP-1 identified a downstream proliferation promoting protein, MRG-1 (Gupta et al., 2015). Other proliferation promoting proteins, or mitotic cell cycle regulators, are likely targeted by other E3 ligases functioning

to redundantly control GSC entry into meiosis alongside of the core meiotic entry pathways.

In addition to the post-translational modulators, various genes within the pre-mRNA splicing pathway have been identified of modulators of GSC proliferation/differentiation balance (Belfiore et al., 2004; Kerins et al., 2010; Mantina et al., 2009; Wang et al., 2012; Tsukamoto et al., 2020). Loss of various splicing factors, including *prp-17*, *teg-4,* and *teg-1* result in GSC over-proliferation in sensitized genetic backgrounds (Belfiore et al., 2004; Kerins et al., 2010; Mantina et al., 2009; Wang et al., 2012; Tsukamoto et al., 2020). Further genetic analyses determined that these factors are required to promote entry into meiosis.

Sensitized backgrounds were required to identify the role of these modulators, with loss of the modulator alone having little to no impact on the proliferation/differentiation balance. This highlights that multiple mechanisms function redundantly to fine-tune the proliferation/differentiation balance alongside of the genetic core pathways.

1.6 RNP germ granules

Ribonucleoprotein (RNP) granules, such as stress granules, processing bodies (P body) and germ granules, are non-membrane bound organelles found in almost all animals (Reviewed by: (Marnik & Updike, 2019; Schisa, 2012; Voronina et al., 2011)). These organelles are thought to form due to RNA-RNA, and RNA-protein interactions, with many RNP proteins containing intrinsically disorder regions (Reviewed by (Marnik & Updike, 2019; Schisa, 2012; Tauber et al., 2020; Voronina et al., 2011)).

Germ granules, a type of RNP granule, have been identified in *Drosophila, Xenopus,* zebrafish, mice and *C. elegans* (Reviewed by: (Marnik & Updike, 2019; Schisa, 2012; Voronina et al., 2011)). Germ granules are thought to play a role in germ cell differentiation, germ cell fate specification, mRNA metabolism (posttranscriptional and translational regulation) and contribute to the function of small RNA pathways (Reviewed by:(Lev & Rechavi, 2020; Marnik & Updike, 2019; Schisa, 2012; Sundby et al., 2021; Voronina et al., 2011)).

1.6.1 *C. elegans* germline specific RNP granules

Germ granules in *C. elegans* were first characterized by Strome and Woods in 1982. Germ granules are present within the one-cell zygote and segregate to the P cell lineage, and subsequent primordial germ cells Z2 and Z3, during embryogenesis (Strome & Wood, 1982). These germ granules are referred to as P granules due to their localization to the P cell lineage (Strome & Wood, 1982). P granules are present within all germ cells of the adult gonad except sperm (Strome & Wood, 1982). P granules localize to the nuclear periphery until oocyte development where, similar to embryonic cells, the P granules disperse throughout the cytoplasm (Strome & Wood, 1982).

Maternal mRNAs necessary for embryonic germ cell specification and/development are passed down to offspring by accumulating in P granules of the developing oocyte (Lee et al., 2020; Seydoux & Fire, 1994). Additionally, a number of proteins localize to P granules in the embryo and adult germline, most of which possess RNA binding domains and/or function in RNA metabolism (Sundby et al., 2021; Updike & Strome, 2010). Among these are proteins involved in the proliferation/differentiation

balance including GLD-1, GLD-2, GLD-3, and FBF-2 (Eckmann et al., 2002; Ellenbecker et al., 2019; Jones et al., 1996; Voronina et al., 2012; Wang et al., 2002). DEPS-1, GLH-1, PGL-1, and IFE-1 have been shown to be necessary for P granule formation, P granule function and recruitment of downstream P granule proteins (Amiri et al., 2001; Kawasaki et al., 1998; Spike et al., 2008). Loss of P granule associated genes, such as the four listed above, results in temperature sensitive sterility (Amiri et al., 2001; Kawasaki et al., 1998; Spike et al., 2008). This highlights the role P granules play in germ line development, as a complete loss of P granules results in sterility due to delayed oogenesis. Moreover, P granules play a role in regulating gene expression, as loss of P granules results in germ cells losing their identity and expressing somatic markers (Updike et al., 2014). Various components of small RNA pathways, such as CSR-1, WAGO-1, PRG-1(PIWI), and EGO-1 have been found to localize to P granules in the adult germline (Batista et al., 2008; Claycomb et al., 2009; Gu et al., 2009).

Three other classes of germ granules have recently been identified; Mutator foci, Z granules and SIMR, which are all localized adjacent to P granules (Ishidate et al., 2018; Manage et al., 2020; Phillips et al., 2012; Wan et al., 2018). Mutator foci are independent granules that form in close contact to P granules. Mutator foci are required for siRNA amplification and contain *mutator* proteins, as well as the RNA dependent polymerase RRF-1 (Phillips et al., 2012). Loss of Mutator foci components results in a decrease in small RNAS (22G siRNAs) (Phillips et al., 2012). Z granules, containing WAGO-4 and ZNFX-1, are thought to promote the production of 22G siRNAs in order to maintain transgenerational piRNA-induced silent epigenetic states (Ishidate et al., 2018; Wan et

al., 2018). Loss of Z granule components results in a loss of inherited gene silencing in offspring (Ishidate et al., 2018; Wan et al., 2018). SIMR (siRNA-defective and mortal germline) granules contain the Tudor domain protein SIMR-1, which is thought to function to promote siRNA production by the *mutator* complex (Manage et al., 2020). Interestingly, P granules, Mutator Foci, and Z granules are found assembled in 'PZM tri-condensates assemblages' with Z granules functioning as a bridge between P granules and Mutator foci (Wan et al., 2018). This PZM aggregate is thought to regulate and localize the function of small RNA pathways allowing for nascent transcripts to be licensed via the CSR-1/EGO-1 pathway, or repressed by the PRG-1/WAGO pathway (Sundby et al., 2021). Taken together, this highlights the role for these granules in regulating gene expression, epigenetic inheritance, and fertility (Sundby et al., 2021).

1.7 The miRISC pathway

The microRNA Induced Silencing Complex (miRISC) is an RNP complex that functions to post-transcriptionally suppress target gene expression. In *C. elegans* miRISC silencing in the soma, but not the germline, involves mRNA destabilization (Dallaire et al., 2018). miRNAs, a class of noncoding-RNAs, provide sequence specificity to the miRISC allowing for targeted repression. There are two classes of miRNAS identified in *C. elegans;* in one class miRNAs regulate a single target, while in the other class multiple miRNAs act redundantly with others to regulate multiple targets (Ambros & Ruvkun, 2018). miRNA silencing requires proper transcription, processing, and loading of miRNAs onto the miRISC to regulate mRNA translation. In *C. elegans* pre-miRNA is processed into a mature miRNA by DCR-1 and then bound by an Argonaute protein (mainly ALG-

1/-2), which facilitates the recruitment of additional factors forming a complete miRISC (Ambros & Ruvkun, 2018). A number of additional proteins have been identified to interact with the miRISC, including GLD-1, VIG-1, GLH-1, CGH-1, CAR-1, KIN-10 and RACK-1 (Akay et al., 2013; Alessi et al., 2015; Dallaire et al., 2018; Jannot et al., 2011; Zhang et al., 2007). Several of these miRISC interacting proteins localize to P granules (GLH-1, CGH-1, CAR-1) (Dallaire et al., 2018). Moreover, mRNAs targeted by miRISC are found to accumulate near P granules (Dallaire et al., 2018). The localization of miRISC factors to P granules, and the localization of target mRNAs near P granules, suggests that P granules may be involved in miRNA mediated gene silencing (Dallaire et al., 2018).

Disruptions to miRISC, through loss of *alg-1/-2* or select miRNAs, in the DTC results in a decrease in the stem cell pool (PZ size), reduced number of oocytes and a reduction in brood size (Irfan et al., 2012). This data highlights a role for miRISC in regulating *C. elegans* germ cell development, although non-autonomously. miRNAs have been identified to be germline enriched, specifically the *mir-35-41* family, suggesting miRNA regulation may occur within germ cells themselves (Bezler et al., 2019; McEwen et al., 2016; Minogue et al., 2018). Similar to *alg-1/-2* mutants, loss of the *mir-35-41* family results in a decrease in the stem cell pool (PZ size) (Liu et al., 2011). Moreover, the *mir-35-41* family was found to regulate pachytene progression and oogenesis within the germline through regulating germ cell apoptosis (Doll et al., 2019; Minogue et al., 2018; Tran et al., 2019). The *mir-44* family has been shown to promote spermatogenesis, as a loss of *mir-44 or mir-45* results in a decrease in the production of sperm (Maniates et al., 2021). The continued identification and investigation into germline enriched miRNAs may

uncover additional regulatory mechanisms governing germline development, including GSC proliferation.

1.8 Receptor of Activated C Kinase RACK-1

Receptor of Activated C Kinase, RACK1, was first isolated and cloned from a rat brain cDNA library and identified for to its ability to bind activated Protein Kinase C (PKCβII) (Guillemot et al., 1989; Ron et al., 1994, 1995; Ron & Mochly-Rosen, 1995; Stebbins & Mochly-Rosen, 2001). RACK1 is highly conserved between eukaryotic species including humans (RACK1), yeast (Asc1 – 52%), *Drosophila melanogaster* (RACK1 – 76%), *Arabidopsis thaliana* (RACK1 – 66%), and *C. elegans* (RACK-1 – 80%) (Jannot et al., 2011; Ullah et al., 2008). RACK1, and its orthologs, are WD (tryptophan aspartic acid) repeat containing proteins. Structural analysis uncovered that RACK1 orthologs in human and yeast form a seven β-propellor blade structure that is relatively conserved between species (Guillemot et al., 1989; Ron et al., 1994, 1995; Ron & Mochly-Rosen, 1995; Stebbins & Mochly-Rosen, 2001). These blades arrange around a hollow core, resembling a propellor (Figure 1.4) (Guillemot et al., 1989; Ron et al., 1994, 1995; Ron & Mochly-Rosen, 1995; Stebbins & Mochly-Rosen, 2001). This propellor structure, which is characteristic of WD family proteins, enables interaction with a number of partners simultaneously, as interactions can occur on all 'blades' and surfaces of the protein (Stirnimann et al., 2010); therefore, WD family proteins are thought to function as scaffold proteins facilitating various protein-protein interactions.

In agreement with a role as scaffold protein, mammalian RACK1 can interact with various protein domains including C2, SH2, and plextrin homology (PH), allowing for

interactions with over 100 proteins (Reviewed in (Adams et al., 2011; Gandin et al., 2013)); therefore, RACK1 plays a role in many cellular processes including ribosome assembly/protein translation (Reviewed in (Adams et al., 2011; Gandin et al., 2013)) , cell cycle regulation (Mamidipudi et al., 2007; McLeod et al., 2000; Núñez et al., 2010), and the miRNA pathway (Brosnan et al., 2021; Jannot et al., 2011; Otsuka et al., 2011; Speth et al., 2013).

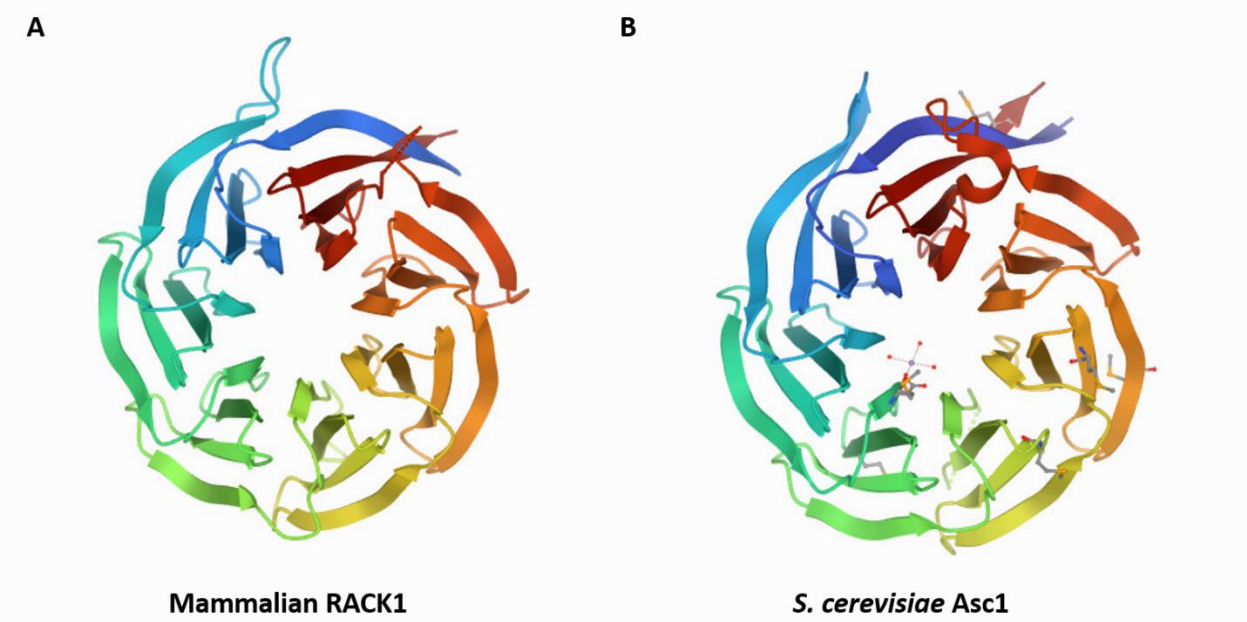

Figure 1.4 – Crystal structures of RACK-1/Asc1. Cartoon representations of the seven β-propellor blade structures of (A) mammalian (human) RACK1 and (B) *Saccharomyces cerevisiae* Asc1/RACK1. The individual blades are depicted in different colours surrounding the hollow core. Mammalian RACK1 resolution 2.45 Å. *S. cerevisiae* resolution is 2.13 Å. Images from RCSB PDB (rcsb.org) of (A) PDB ID 4AOW (Ruiz Carrillo et al., 2012) (B) PDB ID 3FRX (Coyle et al., 2009).

1.8.1 RACK1's role in ribosome assembly and protein translation

RACK1's interaction with PKCβII was determined to regulate PKCβII's localization and activity through stabilizing PKCβII in its active confirmation, in mammalian cell lines (Chinese Hamster Ovary cells, neonatal rat cardiac myocytes and NG108-15 mouse neuroblastoma X rat glioma hybrid cells) (Ron et al., 1994, 1999; Stebbins & Mochly-Rosen, 2001). RACK1 interacts with PKCβII's C2 domain and is required to 'shuttle' active PKCβII to various sub-cellular locations, facilitating PKCβII substrate interactions (Ron et al., 1995, 1999; Stebbins & Mochly-Rosen, 2001).

In human cell lines, RACK1 is required for ribosomal assembly through bridging PKCβII substrate interactions (Ceci et al., 2003; Dobrikov et al., 2018). RACK1 is a conserved component of the eukaryotic ribosome and predicted to function through recruiting PKCβII and other proteins (Reviewed in: (Adams et al., 2011). Eukaryotic ribosomal assembly requires recruitment of the 40S ribosomal subunit to mRNA (Reviewed by: (Jackson et al., 2010). eIF4G initiation factor functions to recruit other initiation factors, including eIF3, which is bound to the 40S ribosomal subunit (43S pre-initiation complex) (Dobrikov et al., 2018; Villa et al., 2013). RACK1 is required for PKCβII phosphorylation of both eIF4G1 and eIF3a, which is required for eIF4G1 and eIF3a interaction, and 40S ribosomal assembly on mRNA in human cell lines (Dobrikov et al., 2018; Villa et al., 2013). Additionally, the RACK1 PKCβII interaction in human cell lines facilitates the phosphorylation of another initiation factor, eIF6 (Ceci et al., 2003). eIF6 binds to the 60S ribosomal subunit and prevents 80S formation (Ceci et al., 2003).

Phosphorylation of eIF6 by PKCβII causes eIF6 release from the 60S subunit allowing for the formation of the 80S ribosomal subunit (Ceci et al., 2003). In yeast, Asc1/RACK1 has been shown to be required to promote, and inhibit translation (Thompson et al., 2016). Similar to RACK1, an interaction between Asc1 and eIF4G was proposed to be required for proper ribosome assembly and translation (Thompson et al., 2016). Conversely, another study on Asc1-ribosome interaction revealed that Asc1/RACK1 depleted yeast strains were found to have increased translational activity**;** however, no mechanism was proposed (Gerbasi et al., 2004). Overall, RACK1's association with the ribosome, and RACK1's recruitment of additional factors such as PKCβII, are required for proper ribosome assembly and function (Ceci et al., 2003; Dobrikov et al., 2018).

1.8.2 RACK1's role in the miRNA pathway

As discussed above, the miRNA pathway functions to suppress mRNA translation, which can be coupled to transcript decay or transcript stabilization (Brosnan et al., 2021; Dallaire et al., 2018). A role for RACK1 in the miRISC pathway has been identified in humans, *Arabidopsis,* and *C. elegans* (Brosnan et al., 2021; Jannot et al., 2011; Otsuka et al., 2011; Speth et al., 2013); however, RACK1 appears to function in different steps in the miRISC pathway between the three species (Speth & Laubinger, 2014). In *Arabidopsis,* loss of *rack1* results in a decrease in a subset of pre-miRNAs (early miRNA biogenesis), leading to a decrease in miRNA levels and an overall decrease in miRNA-mediate gene expression (higher translation) (Speth et al., 2013). Loss of mammalian RACK1 also results in a decrease in a subset of miRNA-mediated gene expression (Jannot et al., 2011; Otsuka et al., 2011); however, RACK1 is required for recruitment of

mature miRNAs to the miRISC, which may be mediated by its interaction with KSRP, a protein involved in the maturation of miRNAs (Otsuka et al., 2011; Trabucchi et al., 2009). In *C. elegans* RACK-1 is required to recruit miRISC to active ribosomes, facilitating miRISC-mRNA interactions (Jannot et al., 2011).

The differences in function in the same pathway between the three organisms is thought to be due to differences in RACK-1 protein interactions (Reviewed in: (Speth & Laubinger, 2014). In agreement with this, RACK1 interacts with ALG-2 in mammalian cells, and ALG-1/AGO1 in *Arapidopsis* and *C. elegans* (Jannot et al., 2011; Otsuka et al., 2011; Speth et al., 2013). The interaction between ALG-2 and RACK1 appears to be conserved in *Drosophila* (Kuhn et al., 2017). Overall, these results demonstrate RACK1's role in regulating gene expression via the miRISC pathway. Additionally, it demonstrates how RACK-1 may function to repress gene expression through mediating miRISC-ribosome interactions (Gerbasi et al., 2004; Jannot et al., 2011).

1.8.3 RACK-1's roll in regulating the cell cycle

Analysis of RACK1 in mammalian cell lines has demonstrated that it may be involved in regulating the cell cycle at various checkpoints (Chang et al., 2002; Chang et al., 1998; Mamidipudi et al., 2007; Mamidipudi et al., 2004). RACK-1 interacts with a number of enzymatic proteins, including protein tyrosine kinases (Gandin et al., 2013). These interactions either promote a protein's function, as is the case for PKCβII, or inhibit their function, as is the case for the protein tyrosine kinase Src (B Y Chang et al., 1998; Betty Y Chang et al., 2002; Ron et al., 1995, 1999; Stebbins & Mochly-Rosen, 2001). RACK1 binds and inhibits the activity of Src in mammalian cell lines (Chang et al., 2002;

Chang et al., 1998). The inhibition of Src activity results in a loss of the downstream phosphorylation cascade required for proper expression of cell cycle regulators, including cyclin D1 and Myc (Chang et al., 2002; Chang et al., 1998; Mamidipudi et al., 2007; Mamidipudi et al., 2004). Overexpression of RACK-1 inhibits Src activity, resulting in delayed G1/S progression (Chang et al., 2002; Chang et al., 1998; Mamidipudi et al., 2007; Mamidipudi et al., 2004). Conversely, loss of RACK1 expression accelerated G1/S transition, similar to what is seen with Src overexpression (Chang et al., 2002; Chang et al., 1998; Mamidipudi et al., 2007; Mamidipudi et al., 2004). This data demonstrates that RACK1 functions as a negative regulator of G1/S progression by controlling the activity of Src. The RACK1-Src interaction is regulated by Src phosphorylation of RACK1, thereby facilitating RACK1's binding to Src (Chang et al., 2002). This provides a mechanism to maintain an appropriate level of Src repression for proper cell cycle progression.

RACK-1 overexpression in mammalian cell lines also resulted in delayed exit from mitosis (G2/M progression) (Mamidipudi et al., 2007). This cell cycle delay depends on RACK1's interaction and inhibition of Src activity. Src is required to inactivate downstream cell cycle regulators including cyclin B/CDK1 complex and Sam68 (Mamidipudi et al., 2007). Inactivation of both are required for exit from mitosis (Mamidipudi et al., 2007). RACK1's regulation of G2/M progression is conserved in fission yeast; however, Cpc2/RACK1 had no effect on the G1/S progression (Núñez et al., 2010). Loss of Cpc2/RACK1 results in a delay at the G2/M transition (Núñez et al., 2010). This delay appears to be dependent on Cpc2/RACK1's ribosome association and regulation of the protein levels of the mitotic inhibitory kinase Wee1 (Núñez et al., 2010).

Interestingly, Cpc2/RACK1 also plays a role in regulating the mitotic to meiotic transition in *S. pombe*. Loss of Cpc2/RACK-1 results in a G2/M delay, similar to an activation of the meiotic inhibitory kinase Ran1 (Iino & Yamamoto, 1985; McLeod et al., 2000; McLeod & Beach, 1988). Inactivation of Ran1, via protein-protein interactions, facilitates the entry into meiosis (Iino & Yamamoto, 1985; McLeod & Beach, 1988). Interestingly, Cpc2/RACK1 is not required for proper Ran1 levels, or activity as in the previous examples, but instead is required for proper Ran1 localization (McLeod et al., 2000). This suggests that Cpc2/RACK1 may be required to mediate Ran1 protein-protein interactions that inhibit its activity thereby promoting entry into meiosis.

These examples highlight that although RACK1 is highly conserved between species, as well as its function within pathways, how it exerts its influence varies widely based on its interaction with a diverse array of proteins.

1.9 RACK-1 in *C. elegans*

As previously mentioned, RACK1 is highly conserved (80% identity) between humans and *C. elegans* (Jannot et al., 2011). Similar to yeast, *rack-1 C. elegans* mutants are viable but relatively unhealthy and slow growing (Demarco & Lundquist, 2010; Gerbasi et al., 2004; Núñez et al., 2010); whereas *rack1* mutants result in lethality in mice (at gastrulation) and *Drosophila* (in early larval stages) (Kadrmas et al., 2007; Volta et al., 2013). Loss of *rack-1* in *C. elegans,* through RNA interference (knockdown) or mutant alleles, results in a decrease in the number of progeny produced (brood size - 60% and 92% respectively) (Ai et al., 2009; Demarco & Lundquist, 2010). Investigation into this phenotype uncovered a conserved role of *rack-1* in embryonic development, as loss of

rack-1 resulted in embryonic lethality in *C. elegans*, with 51% of embryos displaying cytokinesis defects (Ai et al., 2009). *rack-1* controls embryonic development, in part, through regulating the localization of RAB-11 recycling endosomes, which are required to mediate cytokinesis (Ai et al., 2009; Giansanti et al., 2007). Skop *et al.,* also identified defects in the germline membrane when *rack-1* is knocked down, suggesting *rack-1* may play a role in germline development, as well as embryogenesis. Additionally, the embryos produced by *rack-1* depleted hermaphrodites were abnormally shaped and smaller in size (Ai et al., 2009). This small embryo phenotype was also observed upon loss of *RACK1* in *Drosophila* (Kadrmas et al., 2007).

rack-1 is also required for proper neuronal axon pathfinding, acting cell-autonomously in the UNC-115/abLIM pathway to regulate axon outgrowth (Demarco & Lundquist, 2010). How exactly *rack-1* regulates axon pathfinding remains unclear; however, *rack-1* could be required for proper localization of UNC-115, or be required to maintain UNC-115 in an active state, similar to PKCβIII, as an interaction between RACK-1 and UNC-115 was identified (Demarco & Lundquist, 2010). RACK-1 expression within the DTC is also required for proper DTC migration during development, with 32% of animals displaying DTC migration defects; however, no possible interacting proteins were identified to explain how RACK-1 regulates this process (Demarco & Lundquist, 2010). RACK-1 is also involved in the miRNA pathway in *C. elegans* (as discussed in Section 1.10.1) (Jannot et al., 2011).

In *C. elegans* RACK-1 appears to be required in various tissues and pathways in order for proper development to occur, which is consistent with RACK-1's expression. Using extrachromosomal transgenes expressing labeled RACK-1, Demarco *et al.,* determined that RACK-1 was expressed in the majority of cells in the hermaphrodite including neurons, DTC, and gut cells, but germline expression was not addressed (Demarco & Lundquist, 2010). RACK-1 was detected primarily in the cytoplasm with little to no expression within the nucleus (Demarco & Lundquist, 2010); however, RACK-1 has been detected in nuclear fractions from *C. elegans* extracts (Chu et al., 2014). Additionally, RACK-1 was detected in small puncta throughout the cytoplasm, and at the centrosomes and kinetochores of the developing embryo (Ai et al., 2009).

The defects in embryo size and development, combined with disorganization of the germline membrane, suggests that *rack-1* may play a role within the germline of *C. elegans* (Ai et al., 2009). In support of this, loss of *rack-1* in the germline resulted in GSC over-proliferation in a sensitized background (Wang, 2013). This data demonstrates a requirement for *rack-1* in the proliferation/differentiation balance of GSCs in *C. elegans.*

1.10 Thesis goal and outline

The goal of my thesis is to characterize the role of *rack-1* in regulating the proliferation/differentiation balance. As RACK-1 is a scaffold protein, I hypothesize that RACK-1 is required to regulate the localization and/or activity of key proteins within the GLP-1/Notch signaling pathway or the downstream meiotic entry pathways. Genetic analysis was performed with components of the GLP-1/Notch signaling pathway and meiotic entry pathways to determine if *rack-1* function is required within these pathways

to regulate the proliferation/differentiation balance (Chapter 3). RACK-1's expression within the germline was investigated using CRISPR generated tagged alleles (Chapter 4). RACK-1 was then identified as a regulator of GLD-1 levels, and sub-cellular localization within the germline (Chapter 5). Finally, RACK-1's regulation of GLD-1 (localization and levels) was determined to be required for proper GLD-1 function within the germline (Chapter 6).

Chapter 2: Materials and Methods

2.1 Strain maintenance

Animals were maintained at 20 °C as per standard methods unless otherwise noted (Brenner, 1974). Briefly, animals were maintained on Nematode Growth Media (NGM) plates with *E. coli* OP50 bacterial lawns (Brenner, 1974). Strains were maintained by expanding one L4 (larval stage 4) hermaphrodite to a fresh plate every ~ five days. For experimental purposes worms were grown at 15 °C and 25 °C. For a list of all strains and genotype descriptions can be found in Appendix F.

2.2 Bleaching to synchronize

Plates close to clearing (many worms with little to no bacterial lawn remaining) were cut into small pieces (~0.7 cm^2) using a sterilized spatula and placed on new plates ('chunked' - one plate to ~ eight plates) in order to generate a large quantity of gravid adults and embryos. After two to three days of growing, the gravid adults and embryos were washed off the plates using double distilled H_2O (ddH_2O) and transferred into a 15 mL falcon tube using a Pasteur pipette. The worms were pelleted by centrifugation for one minute at maximum speed (~1625 xg, setting 7, IEC centrifuge). The supernatant was removed by aspiration. Five mL of freshly prepared bleach solution (0.2 g NaOH, 2.5 mL 5% Sodium hypochlorite, 7.5 mL ddH_2O) was added to the worm pellet and vortexed vigorously for five minutes. The released eggs were pelleted by centrifugation for one minute at maximum speed (~1625 xg) and the bleach solution was removed by aspiration. Sterile phosphate buffered saline (PBS) was used to wash the pellet and remove any remaining bleach solution. Five mL of PBS was added, centrifuged for one minute at maximum speed (~1625 xg) and the supernatant removed by aspiration. This was

repeated three times. The pellet was then transferred (poured) to a 50 mL falcon tube after resuspending in ten mL sterile PBS. To allow for aeration, the cap was not sealed completely and instead was left slightly ajar and tapped down. The 50 mL tube was placed on an orbital shaker at 20 °C for one to two nights. Due to the absence of nutrients, the collected embryos hatch and arrest at the L1 stage. Following the overnight arrest, the worms were transferred (poured) into a 15 mL falcon tube and centrifuged for one minute at medium speed (~600 xg, setting 4-5, IEC centrifuge). The supernatant was removed by aspiration and the pellet was washed two times by adding five mL sterile PBS and centrifuged for one minute at medium speed (~600 xg) and the supernatant removed by aspiration. The pellet was then resuspended by gentle mixing with a sterile Pasteur pipette. The synchronized worms were then dropped onto fresh NGM OP50 plates using a sterile Pasteur pipette. The worms were then put at the appropriate temperature required for experimentation. For majority of the experiments the synchronized worms were placed at 20 °C for two days until they reached the L4 stage. For all experiments, animals carrying *rack-1(tm2262)* or *rack-1(ok3676)* were left for three nights to reach the L4 stage.

2.3 Whole worm lysis

In order to access the DNA from worms for genotyping through PCR amplification, the worm, and its cells, need to be lysed. To do this, single or multiple worms of interest were placed into a PCR tube containing five μL of worm lysis buffer (WLB – 50 mM KCl, 10 mM Tris-HCl pH 8.2, 25mM MgCl2, 0.45 % NP-40, 0.45 % Tween-20, 0.01 % gelatin and 100 μg/mL Proteinase K). The tubes were sealed with lids, and quickly dipped in

liquid Nitrogen for freeze cracking. The PCR tubes are then placed in a thermocycler and incubated for 60 minutes at 60 °C followed by 95 °C for ten minutes. The released DNA can then be used for PCR amplification or stored at -80 °C for future use.

2.4 PCR amplification

To perform PCR amplification, 2.5 μL or 5 μL of worm lysis was mixed with 1x PCR reaction buffer to a volume of 25 μL. 1x PCR reaction buffer contains 2.5 μL 10x PCR buffer (100 mM Tris-HCL pH 8.3, 500 mM KCl), 1 μL 50 mM $MgCl_2$, 0.5 μL 10mM dNTPs, 1 μL forward primer (10 pmol/μL), 1 μL reverse primer (10 pmol/μL), 0.5 μL 1x Taq Polymerase (homemade) and 16.5 μL ddH_2O). The PCR amplification program consisted of 35x cycles (94 °C 5 mins, [denature - 94 °C 30 sec, anneal – 50-57 °C 30 sec, elongation – 72 °C 30 sec- 1 min 45 sec] 35 times, 72 °C 7 mins, 21 °C hold].

Following PCR, 6 μL of 5X Loading dye (0.4 % Bromophenol Blue, 0.4 % Xylene Cyanol, 50 % glycercol in ddH_2O) was added to each tube, unless the sample was to be sent for sequencing (see below). 12.5 μL of the mixture was then loaded onto a 1-2 % agarose gel made in 0.5 X TBE (45 mM Tris-borate, 1 mM EDTA) and electrophoresed at 120 V until proper separation was achieved.

For all primers and sequences used in this thesis refer to Appendix E.

2.5 Sequencing preparation

If the amplified sample was prepared for genotyping by sequencing, only five μL of the PCR amplified reaction was used for PCR verification. To do this five μL was added to ten μL of ddH_2O and five μL of 5x Loading Dye. This mixture was loaded onto a 1 - 2%

agarose gel and electrophoresed at 120 V until proper separation was achieved. This gel analysis was performed to verify that the correct sequence was amplified, with no background bands present. The remaining PCR reaction was subject to PCR clean up with the Promega Wizard SV Gel and PCR Clean-up System (A9282), following the manufactures protocol. The only deviation from protocol was during the final elution, where 25 μL nuclease-free water (Thermofisher Scientific, Catalog #AM9939) was used instead of the supplied elution buffer. ~100 ng of purified PCR product was mixed with one μL of primer (10 pmol/μL) in nuclease-free water up to 20 μL total volume to prepare final sequencing mixture to be sent to the University of Calgary Core DNA services for sequencing analysis.

2.6 Brood size assay

To analyze the number of embryos laid and progeny produced per worm of a specific genotype a brood size assay was performed. L4 hermaphrodites were placed on individual plates and allowed to lay eggs for 24 hours. After 24 hours the worm was picked onto a new plate. This process was repeated until no embryos were produced (~six days). On the same day the parental worm was transferred of the plate, the embryos on that plate were counted. The embryos were allowed to hatch and develop for two to three nights at which point the number of hatched worms on each plate were counted. For each individual worm, the number of embryos produced, and number of hatched worms produced was summed. These values were then averaged for all worms of a specific genotype (n > ten), and the standard deviation determine. The percent embryonic viable

was determined by dividing the average number of hatched worms by the average number of embryos produced.

2.7 Gonad dissection

For analysis of germline protein expression and/or germline phenotypes, one day past L4 (adult) animals were used. ~150 animals were picked per genotype at the L4 stage onto a fresh NGM OP50 plate and left to grow overnight at the respective temperature (15 – 20 °C). The following day the worms were transferred from the plate into a clean microcentrifuge tube (rinsed with PBS plus 0.1% Tween-20 (PBT)) using ddh_2O (2 x 750 μL washes) and a Pasteur pipette. The worms were pelleted by centrifugation at 1,000 g and the supernatant removed by aspiration. The pellet was rinsed one to three times with ddH_2O (one mL) to remove any bacteria. The worms were then transferred to clean watch glass (cleaned with compressed air to remove any fibers and rinsed with PBT) using 1.5 mL ddH_2O. To paralyze the worms, five μL of 100 mM Levamisole was added to the watch glass. The worms were then dissected but cutting the head away from the rest of the body of the worm using two ten mL syringes with 10 $^{5/8}$G needles. Once all of the worms were dissected as much PBS as possible was carefully removed using a Pasteur pipette ensuring no dissected animals or extruded gonad arms were removed. Gonad arms were immediately fixed with 600 μL of 3 % paramformaldehyde/0.1 M K_2HPO_4 in ddH_2O for seven minutes. At the six-minute time point, the dissected worms were transferred, using a Pasteur pipette, into a small glass culture tube cleaned with compressed air (6 x 60 mM Kimax-51). The dissected worms were spun down at ~600 xg (setting 4-5, IEC centrifuge), the supernatant was aspirated

off. The pellet was washed three times with 500 μL of PBT, spinning down at (~600 xg) and removing the supernatant in between.

If primary and secondary antibodies were used for subsequent analysis, 500 μL of ice-cold methanol (stored at -20 °C) was added following the three PBT washes. The tubes were covered with parafilm and stored at -20 °C until subsequent processing. After at least one night incubation, the dissected worms are washed three times with 500 μL of PBT.

2.8 Detection of endogenously expressed fluorescent proteins and immunostaining

If endogenously expressed proteins (such as GFP or RFP) were to be detected, the above protocol was followed but after following the three PBT washes, 500 μL of 0.5 % Triton in PBS was added to the tubes and incubated for ten minutes. Following the incubation, the tubes were centrifuged at ~600 xg (setting 4-5) for one minute and the supernatant removed by aspiration. The worms were then washed three times with 500 μL of PBT. All analyses using strains with endogenously expressed fluorescent proteins still required detection of other proteins using antibodies; therefore, the remaining immunostaining steps are the same as in the follow section.

2.9 Immunostaining

Following the final PBT washes from the protocols above, the dissected animals were then blocked using ~100 μL of 3 % Goat Serum in PBS for one hour and 30 minutes at room temperature. The tubes were centrifuged at ~600 xg (setting 4-5) for one minute and the blocking solution removed by aspiration. A minimum of 50 μL of primary antibody

diluted in 3% goat serum was added to each tube. The tubes were covered with parafilm and incubated overnight at 4 °C. For information on primary antibodies used in this thesis refer to Table 2.1. The following day, the tubes were centrifuged at ~600 xg (setting 4-5) for one minute and the antibody solution was removed by aspiration. The dissected worms were then washed three times with 500 μL of PBT with a five-minute wait between each wash. The tubes were centrifuged at ~600 xg (setting 4-5) for one minute, and supernatant removed by aspiration in between the washes. The secondary antibody diluted in 3% goat serum was then added to each tube, the tubes were incubated in the dark at room temperature for one hour 30 minutes. For information on secondary antibodies used in this thesis refer to Table 2.2. Following secondary incubation, the dissected worms were washed three times with 500 μL with five-minute incubations in between, the same as described above. During incubation steps the tubes were kept in the dark. The dissected worms were then washed once with PBS and incubated for five minutes with 500 μL of DAPI (1 mg/mL - 4', 6- diamidino-2-phenylindole dihydrochloride) diluted 1:1000 in PBS. The DAPI solution was removed by aspiration following a one minute spin at ~600 xg (setting 4-5). The stained gonads were either mounted immediately for imaging, or topped with 500 μL of PBS, covered with parafilm and foil, and stored at 4 °C for up to five days.

For imaging, the majority of the liquid was removed from the tubes and the dissected gonads were transferred onto a slide containing a 1% agarose pads using a Pasteur pipette. Excess liquid was removed using a Kimwipe. Additionally, extruded

gonad arms and the remaining worm carcasses were spread out on the agarose pad using a torn edge of a Kimwipe prior to covering with a coverslip. Images were acquired using a Zeiss Axioimager Z1 microscope with AxioVision software.

Table 2.1 – Primary antibodies used for immunostaining

Antibody	Source	Catalog #	Species	Dilution
REC-8	Loidl lab		Rat	1:200
HIM-3	Zetka lab		Rabbit	1:750
RACK-1	Santa Cruz	SC-17754	Mouse	1:500
FLAG M2	Sigma	F1804	Mouse	1:1000
V5	Invitrogen	R960-25	Mouse	1:1000
GLD-1	Schedl lab		Rabbit	1:100
c-MYC	DSHB	9E10[a]	Mouse	50 μL/tube
MSP[b]	DSHB	4A5	Mouse	50 μL/tube

[a] 9E 10 was deposited to the DSHB by Bishop, J.M. (DSHB Hybridoma Product 9E 10).
[b] 4A5 was deposited to the DSHB by Greenstein, D. (DSHB Hybridoma Product 4A5).

Table 2.2 – **Secondary antibodies used for immunostaining**

Antibody	Source	Catalog #	Species	Dilution
Alexa488	Invitrogen	A21208	Rat	1:200
Alexa 488	Invitrogen	A21202	Mouse	1:400
Alexa488	Invitrogen	R37118	Rabbit	1:400
Alexa594	Invitrogen	A21207	Rabbit	1:500

2.10 Staining protocol for intensity measurement comparisons

For experiments when the intensity measurements of a protein of interest (SYGL-1::3XFLAG or GLD-1) was compared between two different genetic backgrounds the immunostaining protocol differs from above after the blocking step. One genotype was incubated with a primary antibody solution (typically α-REC-8) in 3% goat serum overnight while the other genotype remained in only 3% goat serum, in order to differentiate between the two genotypes as they will be on the same slide. The following day, the tube containing the antibody solution was spun down at ~600 xg (setting 4-5) for one minute and the antibody solution was removed by aspiration. The dissected worms were then washed four to five times with 500 μL of PBT with a five-minute wait between each wash. The tube was centrifuged at ~600 xg (setting 4-5) for one minute, and the supernatant removed by aspiration between the washes. The tube containing only goat serum was centrifuged at ~600 xg (setting 4-5) for one minute, and the supernatant was removed by aspiration. The primary antibody incubated genotype was transferred to the tube with the other genotype using 500 μL of PBT and a Pasteur pipette. The combined worms were pelleted using a one-minute spin at ~600 xg (setting 4-5). The second primary antibody raised against the protein whose expression was to be compared (α-GLD-1 or α-FLAG) diluted in 3 % goat serum was added to the tube. The tube was covered with parafilm and left overnight at 4 °C. The remaining steps of the protocol were the same as described above.

Since both genotypes were mounted on the same slide, the intensity measurements for the protein of interest can be more accurately compared. Three

individual gonads from each genotype were first measured. The shortest exposure time that was automatically determined by the software was recorded (meaning the highest measured intensity) and was manually further reduced by at least 100 ms in order to ensure that there was no overexposure; that exposure time was used to image all remaining germlines on the slide. Images were acquired using a Zeiss Axioimager Z1 microscope with AxioVision software.

2.11 Image analysis for intensity measurements

In order to determine intensity measurements, images were analyzed using FIJI (Schindelin et al., 2012). The segmented line tool was used to manually draw a line along the area of interest (from the distal tip to loop, for example). The 'line width' was set to 25 pixels and spline-fit was selected in FIJI. Plot profile was used to determine the pixel intensity data across the length of the line. The value at each distance was the average of all values obtained across the 25 pixel width. The plot prolife and distance for each gonad analyzed was saved in an excel file. For each genotype, the plot profiles of all measured gonads were averaged, and the standard deviation determined. The average plot profiles were utilized to graph and compare the expression profile between genotypes. The plot profiles for each genotype ends at the same intensity measurement. This was thought of as the baseline or background value for the proximal end of the germline. The area under the curve for each genotype was calculated using excel. The percent reduction was obtained by dividing the area for the genotype of interest by the control genotypes area and subtracting that value from 100.

The image analysis for SYGL-1::3XFLAG expression was conducted by Dr. Ryan Smit. The analysis was similar to what is described above; however, the manual line was drawn from the distal tip to beyond the end of detectable SYGL-1 expression. This allowed for background staining inside the germline to be determined. For control animals the average background staining was ~1709 arbitrary units vs 1773 arbitrary units in *rack-1(tm2262)* germlines, demonstrating that the background was comparable between genotypes. Each individual germline was then corrected based on its internal background measured (the last value obtained from the plot profile). These corrected values were averaged for each genotype and the standard deviation obtained. The average plot profiles were utilized to graph and compare the expression prolife between genotypes. As the area of interest was primarily the proliferative zone, the distance obtained from the plot profile was corrected to germ cell diameters by dividing the distance in μm by 4.5 μm/gcd, a previously determined conversion factor based on the average germ cell size (Lee et al., 2016). Additionally, the SYGL-1 expression extent was determined by counting the distance in germ cell diameters from the distal tip to the end of SYGL-1 expression, as described below. The values obtained were very similar; N2 converted distance = 13.3 gcd vs counted = 13 gcd; rack-1 converted = 10.5 gcd vs counted = 11 gcd. This demonstrates that the conversion factor 4.5 μm/gcd can accurately be used.

2.12 Analyzing the size of the proliferative zone

FIJI was used to determine the extent of REC-8 (proliferative marker) expression as measured in germ cell diameters. Images were opened in FIJI using the hyperstack option so it was easy to switch between channels. The segmented line tool was used to

draw a line starting at the distal most end of the germline until the end of REC-8 expression. Once the channel was switched to DAPI the line was then saved onto the image using the draw tool (CTRL D). The nuclei were counted along the edge of the germline on both sides and averaged to obtain the extent of REC-8 positive cells per germline. The multipoint tool was used to mark off each counted nuclei. Once all germlines had been counted the averages and standard deviation for each genotype was calculated.

To count the total number of cells within the proliferative zone, Z-stack images were obtained of the distal end of each germline. FIJI was used for image analysis using the cell counter window. A different cell counter colour was used every three stacks to ensure that new nuclei were counted until all the stacks had been analyzed. After all germlines were counted the average and standard deviation was determined for each genotype.

2.13 Whole mount DAPI

Some germline phenotypes were able to be identified by whole mount DAPI staining, specifically looking for Glp germlines, as the missing germline cells are quite obvious while looking through the animal body. For these experiments, ~150 animals were picked per genotype at the L4 stage onto a fresh NGM OP50 plates and left to grow overnight at the respective temperature (15 – 25 °C). The following day the worms were transferred from the plate into a clean microcentrifuge tube using ddH_2O (2 x 750 μL washes) and a Pasteur pipette. The worms were pelleted by centrifugation at 1,000 xg for one minute and the supernatant removed by aspiration. One mL PBS containing 2.5

μL levamisole was added to the tube and left for five – seven minutes. The worms were pelleted by centrifugation at 1,000 xg for one minute and the supernatant removed by aspiration. The worms were transferred into a small glass culture tube cleaned with compressed air (6 x 60 mM Kimax-51) using 600 μL PBS and a Pasteur pipette. The tubes were centrifuged at 600 xg (setting 4-5) for one minute, and supernatant removed by aspiration. 600 μL of cold methanol (stored at -20 °C) was added to the tube. The tube was covered with parafilm and stored at – 20 °C overnight. The following day the tubes were centrifuged at 600 xg (setting 4-5) for one minute, and the methanol removed by aspiration. The tubes were washed two – three times with 500 μL PBT (spinning at 600 xg (setting 4-5) in between washes). 500 μL of DAPI diluted in PBS (1:1000) was added to the tube and incubated for five minutes. The DAPI solution was removed by aspiration following a one-minute spin at ~600 xg (setting 4-5). The worms were either mounted immediately for imaging, or topped with 500 μL of PBS, covered with parafilm and foil, and stored at 4 °C for up to five days.

2.14 Western Blot analysis and intensity measurements

For western blot analysis, 100 L4 or one day past L4 worms were used. For one day past L4 stage, 100 L4s were picked on to a fresh NGM OP50 plate and left to grow overnight at 20 °C. If using L4 animals, 100 L4 animals were picked to a new NGM OP50 plate and washed off the same day. The worms were washed off the plate and transferred to a clean microcentrifuge tube using ddH_2O (2 x 750 μL washes) and a Pasteur pipette. The worms were pelleted by centrifugation at 1,000 xg and the supernatant removed by

aspiration. The worms were washed three to four times with PBS (one mL) with five-minute waits in between washes. The worms were centrifuged at 1,000 xg for one minute and the supernatant was removed by aspiration. Once all the bacteria was washed out (supernatant clear), the volume in the tube was reduced to approximately 20 μL volume. Five μL of 5X sample buffer (250 mM Tris-HCl, pH 6.8, 10 % SDS, 20 % glycerol, 0.05 % bromophenol blue, 5% 2-mercaptoethanol) and stored at -80 °C for future use or ran on an SDS-PAGE gel immediately.

A 10% or 12.5% SDS-PAGE gel was used to resolve the proteins. The gels were run at room temperature at 110 V for ~2 hours and 15 minutes in 1X SDS-PAGE Running buffer (25 mM Tris,192 mM Glycine, 0.1% SDS). The proteins were then transferred to a 0.2 μM nitrocellulose membrane (Bio-Rad, #1620097) using a Mini-Trans Blot Cell (Bio-Rad). The proteins were transferred for one hour at 110 V using ice-cold 1X Transfer buffer (25 mM Tris, 192 mM Glycine, 20% Methanol) with the outside of the apparatus surrounded by ice to keep it cold. After transferring, the membranes were trimmed, or cut into segments to allow detection of proteins of differing size to be performed simultaneously. The trimmed blot was blocked in 5% milk in TBS (tris buffered saline - (137 mM NaCl, 2.5 mM KCl, 25 mM Tris pH 7.4) for one hour 30 minutes at room temperature. The blocking milk was discarded and the primary antibody diluted in 5% milk in TBS was added to the blot and incubated overnight at 4 °C. For information on primary antibodies used for western blots in this thesis, refer to Table 2.3.

The following day the blot was washed two times for five minutes with five mL 0.05% Tween-20 in TBS (TBST), followed by three washes with five mL TBS for five minutes. The secondary antibody diluted in 5% milk in TBS was added to the blot and incubated at room temperature for one hour and 30 minutes. For information on secondary antibodies used for western blots in this thesis, refer to Table 2.4. Following this incubation, the blot was again washed twice with five mL TBST for five minutes, followed by three washes with five mL TBS for five minutes. The membrane was then developed by chemiluminescence using Amersham ECL Select Western Blotting Detection Reagent (GE Healthcare Life Sciences, Catalog #RPN2235) using the Amersham Imager 600.

If blots were probed with more than one antibody, the signal on the blot was killed by incubating in five mL of 100 mM Sodium azide in 5% skim milk in PBS for one hour 30 minutes at room temperature. The next primary antibody diluted in 5% skim milk in PBS was added and the exact protocol described above was followed.

Western blot images were analyzed using FIJI to compare band intensities for proteins of interest (GLD-1) between genotypes. Tubulin expression was used as the loading control, with the intensity from wildtype (N2) animals treated as 100% value. The rectangle selection tool was used to draw a rectangle around the tubulin band in the control lane. Then Analyze -> Gels -> Select first lane (or CTRL 1) to set the selection as the first lane. The rectangle was then dragged over to the tubulin band in the *rack-1* mutant lane and selected using Analyze -> Gels -> Select next lane (CTRL 2). The profile

plot was then obtained by Analyze -> Gels -> plot lanes (CTRL 3). The straight line tool was used to enclose the peak (representing intensity of the band) in both lanes, allowing for the total area under the peak to be determined. This was performed using the Wand tool and selecting the area for each lane and selecting Analyze -> Gels -> Label peaks. The values obtained for each lane, area and percent, were copied into excel. The percent value from the control lane was then used to calculate the relative intensity for the tubulin band from the *rack-1* mutant lane by dividing the *rack-1* percent value by the control percent value. The relative intensity for the control was set to 1.0. This analysis was repeated for the GLD-1 bands for each genotype, and relative intensity obtained.

The relative intensities obtained from the GLD-1 bands were adjusted based upon the relative intensities of the loading control (correcting for any difference in total protein loaded). This adjusted intensity was determined by dividing the GLD-1 relative intensity obtained for the *rack-1* mutant lane by the tubulin relative intensity obtained for the *rack-1* mutant lane. As the wildtype/control lane was always set to 1 the adjusted intensity remains the same (=1). This was repeated for two independent blots. The adjusted intensities were averaged, and the standard deviation calculated and plotted as average normalized intensity ratios.

Table 2.3 – Primary antibodies used for western blot analysis

Antibody	Source	Catalog #	Species	Dilution
RACK-1	Chen Lab		Rabbit	1:5000
V5	Invitrogen	R960-25	Mouse	1:5000
Tubulin	Sigma	T6199	Mouse	1:5000
MH16 (paramyosin)[a]	DSHB	M16	Mouse	2.5 – 5 mL
GLD-1	Schedl lab		Rabbit	1:1000

[a] MH16 was deposited to the DSHB by Waterston, R.H. (DSHB Hybridoma Product MH16)

Table 2.4 – Secondary antibodies used for western blot analysis

Antibody	Source	Catalog #	Species	Dilution
HRP	Invitrogen	9186491	Mouse	1:5000
HRP	VWR	CA95017-328L	Rabbit	1:5000

2.15 Generation of the C-terminal CRISPR tagged *rack-1* alleles

To CRISPR tag the C-terminus of RACK-1, the design protocol, using double stranded DNA (dsDNA) asymmetric-hybrid donors (repair template) described by the Mello lab was followed (Dokshin et al., 2018). The guide RNAs were designed using IDT's Custom Alt-R CRISPR-Cas9 guide RNA tool (available online at idtdna.com). A guide was selected whose NGG site was located ten base pairs upstream of the desired insert site (right before the stop codon, TAA). This guide was ordered as an Alt-R CRISPR-Cas 9 crRNA (2 nmol), along with the Alt-R CRISPR-Cas9 tracrRNA (5 nmol, designed by the

company). All guide RNAs were resuspended in IDT duplex buffer to achieve a stock of 100 μM. These were further diluted to obtain a working stock of 20 μM. Both stocks were stored at -20 °C.

In order to ensure our CRISPR reagents were functioning correctly and injections were successful, the *dpy-10* gene was also targeted simultaneously (*dpy-10(cn64)* conversion) (Arribere et al., 2014; DNA Technologies, 2016). The guide RNA was ordered as an Alt-R CRISPR-Cas 9 crRNA (2 nmol) (Design ID - Ce.Cas9.DPY-10.1.AQ). The tracrRNA and *dpy-10* guide RNA (crRNA) were also pre-annealed by mixing equal volumes of the 20 μM stocks and incubating at 94 °C for two minutes. Because the *dpy-10* loci edits efficiently, the *dpy-10* guide was used at a ~1:10 ratio to the *rack-1* guide, as per the Dernburg's labs recommendation (DNA Technologies, 2016); therefore this mixture was diluted by a factor of two and used at a ratio of one μL to five μL of *rack-1* guide. This mixture was either stored at -20 °C for future use or used immediately. A single-stranded oligo repair template (AF-ZF-827) was ordered from IDT (Arribere et al., 2014).

Protein Cas-9 was used for injections (Alt-R S.p Cas9 Nuclease V3, 100 μg, from IDT). The Cas-9 protein was split into five μg aliquots (0.5 μL) and stored at -80 °C to avoid freeze thaw cycles.

The repair template was created either by ordering the full sequences as 200 base pair ultramers from IDT, or through amplification off a plasmid using both ultramers from

IDT, or regular oligos (described in detail below). The ultramers for V5::2xFLAG were resuspended in nuclease-free water (Thermofisher Scientific, Catalog #AM9939) to a concentration of one μg/μL and stored at -20 °C. The ultramers for V5::GGG::SBP were resuspended in nuclease-free water to a concentration of 100 μM and a working stock of ten μM to be used in PCR amplification.

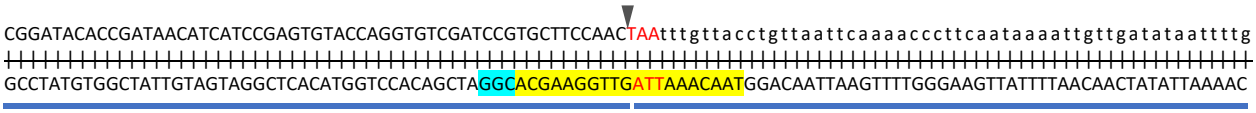

Figure 2.1 – *rack-1* CRISPR design. *rack-1* coding sequence with 55 base pair homology arm sequences marked with a blue box. The stop codon is in red. The insertion site is marked by a black triangle (▼). The 20 base pair guide RNA sequence is highlighted in yellow, and the corresponding NGG site highlighted in blue.

2.15.1 V5::2xFLAG tagging

The tracRNA and guide RNA (crRNA) were pre-annealed by mixing equal volumes (ten μL) of the 20 μM stocks and incubating at 94 °C for two minutes in a thermocycler as per the Dernburg's labs recommendation (DNA Technologies, 2016). This mixture (tracrRNA::*rack-1*crRNA) was either stored at -20 °C for future use or used immediately.

For the V5::2xFLAG tag the dsDNA asymmetric-hybrid donor was designed with 55 base pair homology arms upstream and downstream of our insertion site, not the targeted NGG site (5'HA-V5-2xFLAG-3'HA). The V5::2xFLAG insert was 90 base pairs,

and with the homology arms (55/side) was a total size of 200 base pairs. The top and bottom strands were ordered as four nmole ultramer DNA oligos from IDT (repair ultramer) (max length 200 base pairs). Additionally, the V5::2xFLAG tag alone (no homology arms or stop codon) was ordered as a four nmole Ultramer DNA oligos from IDT (repair ultramer) (top and bottom strands). This provided four oligos with which the various dsDNA asymmetric-hybrid donors can be formed form (Dokshin et al., 2018).

The injection mix was made by first complexing the Cas9 protein (0.5 μL / five μg) with the tracrRNA::*rack-1*crRNA mix (five μL of ten μM) and tracrRNA::*dpy-10*crRNA mix (one μL of five μM) for ten minutes at 37 °C. To make the repair template the *rack-1* repair ultramers were mixed in a 1:1:1:1 ratio (one μg each, total four μg) and allowed to anneal using a thermocycler, running the following protocol (obtained from Dokshin *et al.,* 2018 – '95 ºC - 2:00 min; 85ºC - 10 sec, 75 ºC - 10 sec, 65 ºC -10 sec, 55 ºC - 1:00 min, 45 ºC - 30 sec, 35 ºC- 10 sec, 25 ºC - 10 sec, 4 ºC – hold) (Dokshin et al., 2018). All four μg of dsDNA donor (four μL) was then added to the Cas9::guideRNA complex, along with the *dpy-10* ssDNA repair oligo (one μL of ten μM) and topped to 20 μL using nuclease-free water (~4.5 μL). The injection mixture was centrifuged at maximum speed (21,300 xg) for two minutes. 17 μL of the mixture was then transferred to a new tube and left on ice to be injected. All injections were performed by Dr. Dave Hansen.

Following injections, the injected worms that survived were transferred to their own plates and left for ~four to five days to produce progeny. The plates were screened for the presence of the Dumpy or Roller phenotypes, which suggests successful CRISPR at

the *dpy-10* locus. Plates with a large number of Dumpy and/or Roller worms were expanded to multiple plates by placing one Dumpy or Roller worm onto a new plate. These worms were allowed to self for one to two nights. The parental worm was then picked for worm lysis and subsequent PCR screening for editing of the *rack-1* gene (~90 bp upshift). Plates heterozygous for the CRISPR-insert were then expanded to eight plates (one progeny per plate) and allowed to self for two nights and again picked for worm lysis and PCR to look for homozygous CRISPR worms. Once homozygous worms were found, they were sent for sequencing to verify that no mutations were accumulated during CRISPR editing. Four strains, from independent CRISR insertion events, were then analyzed for wildtype expression by western blot analysis, as described above.

2.15.2 V5::SBP tagging

The same guide RNA was used to tag *rack-1* with V5::SBP (streptavidin binding protein); however, the dsDNA asymmetric-donor template (repair template) was designed differently due to the V5-GG-SBP tag used being too large to order as a 200 bp IDT ultramer. The tag consists of the V5 epitope sequence, followed by three glycine residues (short spacer) and then the SBP sequence. The SBP sequence was previously obtained by our lab from Dr. Sui-. Lam Wong and edited for optimal *C. elegans* expression (pDH475) (Wu & Wong, 2013).

To obtain the complete dsDNA donor template, two ultramers were designed as described by Dokshin *et al.,* 2018 (Dokshin et al., 2018) (5'HA-V5-GGG-SBP-3'HA). The first contained the 55 base pair upstream homology arm followed by the V5 and glycine sequences and the first 20 base pairs of the SBP sequence. The second ultramer

contained the 55 downstream homology arm (including the stop codon), followed by the last 20 base pairs of the SBP sequence. These ultramers were used to amplify the optimized SBP sequence (pDH475) creating the double stranded product 5'HA-V5-GGG-SBP-3'HA.

To amplify the tag only sequence (V5-GGG-SBP) two additional oligos were designed. The first was a 71 base pair ultramer consisting of the V5-GGG sequence followed by the first 20 base pairs of SBP sequence. The last was ordered as a regular oligo and consisted of the last 20 base pairs of the SBP sequence without a stop codon. These oligos were used to amplify the optimized SBP sequence (pDH475) creating the double stranded product sequence V5-GGG-SBP.

All PCR reactions were performed using NEB's One*Taq* as per the supplied protocol, using 30 cycles with an annealing temperature of 45 °C and elongation of 45 seconds at 68 °C. Five 50 μL reactions were performed for both (5'HA-V5-GGG-SBP-3'HA) and 5'HA-V5-GGG-SBP-3'HA). The reactions were combined and five μL ran on a gel to verify amplification (described above). The (5'HA-V5-GGG-SBP-3'HA) amplification had some faint background bands/smearing; however, the PCR product was still used. The reactions were purified and concentrated using the Qiagen MinElute PCR Purification kit (#28004) following the recommended conditions with the product being eluted in 15 μL of nuclease-free water. The two products were combined in a 1:1 ratio (two μg each) and annealed using a thermocycler, exactly as described above to create the various dsDNA asymmetric-hybrid donors (repair template) (Dokshin et al., 2018)

The injection mixture was made as described above, except the volume of water was adjusted to fit all of the of dsDNA asymmetric donor template (two μg). Following screening, and identification of homozygous strains, four strains from independent CRISR insertion events were then analyzed for wildtype expression by Western blot analysis as described above.

2.15.3 – *rack-1* CRISPR reagents sequences

rack-1 guide RNA – IDT Alt-R CRISPR-Cas 9 crRNA

5'-TAACAAATTAGTTGGAAGCA**-3'**

rack-1 HA-V5::2xFLAG-HA top strand – IDT ultramer

5'CGGATACACCGATAACATCATCCGAGTGTATCAGGTGTCGATCCGTGCTT
CCAACGGCAAGCCGATTCCGAATCCATTGCTTGGTCTCGACAGTACAGATT
ACAAAGACGATGACGACAAGGATTATAAGGACGATGATGATAAATAATTTGT
TACCTGTTAATTCAAAACCCTTCAATAAAATTGTTGATATAATTTTG**-3'**

rack-1 HA-V5::2xFLAG-HA bottom strand – IDT ultramer

5'-CAAAATTATATCAACAATTTTATTGAAGGGTTTTGAATTAACAGGTAAC
AAATTATTTATCATCATCGTCCTTATAATCCTTGTCGTCATCGTCTTTGTAATC
TGTACTGTCGAGACCAAGCAATGGATTCGGAATCGGCTTGCCGTTGGAAGC
ACGGATCGACACCTGATACACTCGGATGATGTTATCGGTGTATCCG**-3'**

V5::2xFLAG top strand – IDT ultramer

5'-GGCAAGCCGATTCCGAATCCATTGCTTGGTCTCGACAGTACAGATTACAA
AGACGATGACGACAAGGATTATAAGGACGATGATGATAAA**-3'**

V5::2xFLAG bottom strand – IDT ultramer

5'-TTTATCATCATCGTCCTTATAATCCTTGTCGTCATCGTCTTTGTAATCTGT
ACTGTCGAGACCAAGCAATGGATTCGGAATCGGCTTGCC**-3'**

rack-1 5'HA-V5::GGG::SBP first 20 bp – IDT ultramer

5'-CGGATACACCGATAACATCATCCGAGTGTACCAGGTGTCGATCCGTGCTT
CCAACGGCAAGCCGATTCCGAATCCATTGCTTGGTCTCGACAGTACAGGAG
GAGGAATGGATGAGAAGACTACTGG**-3'**

rack-1 3'HA- SBP-last 20 bp – IDT ultramer

5'-CAAAATTATATCAACAATTTTATTGAAGGGTTTTGAATTAACAGGTAACAAA
TTATGGCTCGCGTTGTCCTTGTG**-3'**

V5::GGG::SBP top – IDT ultramer

5'-GGCAAGCCGATTCCGAATCCATTGCTTGGTCTCGACAGTACAGGAGGAG
GAATGGATGAGAAGACTACTGG**-3'**

SBP reverse – DNA oligo

5'-TGGCTCGCGTTGTCCTTGTG**-3'**

dpy-10 repair template – DNA oligo

5'-CACTTGAACTTCAATACGGCAAGATGAGAATGACTGGAAACCGTACCGCA
TGCGCCTATGGTAGCGGAGCTTCACATGGCTTCAGACCAACAGCCTAT**-3'**

2.16 – Statistical Analysis

Proliferative zones were compared using an unpaired t-test when only two genotypes were present and a one-way analysis of variance (ANOVA) for comparisons when multiple genotypes were present (two single and double mutant strains). In the case of a significant main effect, a Tukey's post-hoc test was employed to determine individual differences between genotypes. A Shapiro-Wilkes test was performed to assess normal distribution of the data and a Brown-Forsythe and/or Bartlett's test to assess for homoscedasticity. In instances of violations of normality, a Kruskal-Wallis test followed by

Dunn's post-hoc test was used (*glp-1(ar202gf)* comparisons). A Brown-Forsythe and Welch's ANOVA followed by a Games-Howell's post-hoc test was used to analyze data sets with violations of homoscedasticity (*gld-1(oz264gf)* comparisons). A chi-square test was used to compare the observed versus expected proliferative zone sizes of double mutants.

For comparison of GLD-1 expression levels (determined from *in vivo* immunofluorescence) a one sample t-test was utilized to compare overall GLD-1 expression levels (total area under the curve) in the genotype of interest (*rack-1(tm2262)* and *gld-2(q497); rack-1(tm2262)*) compared to control (wildtype (N2) and *gld-2(q497)*). When comparing the maximum GLD-1 expression, peak GLD-1, an unpaired t-test was performed between genotypes of interest. A paired t-test was utilized to compare GLD-1 levels in wildtype (N2) and *rack-1(tm2262)* as determined by Western blot analysis.

An unpaired t-test was utilized to compare both the overall SYGL-1 expression levels (total area under the curve) and peak SYGL-1 (maximum SYGL-1 expression) between *rack-1(tm2262)* and control (*sygl-1(am307)*) gonads.

All statistical analysis was performed using GraphPad Prism 9.1.0 using a p-value cut-off of 0.05 to determine significance.

Chapter 3: *rack-1* influences the proliferation/differentiation balance

The GLP-1/Notch pathway has been shown to be the main regulator of the proliferation/differentiation balance in the *C. elegans* germline (Austin & Kimble, 1987; Berry et al., 1997; Seydoux & Schedl, 2001); however, the use of genetic screens has uncovered various other genes and molecular mechanisms that work to modulate GLP-1/Notch signalling or the downstream meiotic entry pathways to control the proliferation/differentiation balance. These factors/pathways include the Ubiquitin-mediated proteolysis pathway (Gupta et al., 2015; Macdonald et al., 2008; Pepper et al., 2003), and mRNA processing genes (Belfiore et al., 2004; Kerins et al., 2010; Mantina et al., 2009; Wang et al., 2012). Recent data has suggested that *rack-1* may be an additional factor influencing the proliferation/differentiation balance (Bolger, 2017; Wang, 2013).

To investigate *rack-1's* potential involvement in the stem cell proliferation decision, I characterized *rack-1's* genetic interaction with *glp-1* gain-of-function and loss-of-function mutations, as well as *rack-1's* interaction with GLP-1/Notch target genes, *lst-1 and sygl-1*. Finally, to determine if *rack-1* functions downstream of the GLP-1/Notch pathway, genetic analysis was performed with components of the GLD pathways to determine *rack-1's* impact on the entry into meiosis decision.

3.1 *rack-1(0)* enhances the over-proliferation phenotype in *glp-1* gain-of-function mutations

glp-1 gain-of-function (*glp-1(gf))* mutations are commonly used to identify, or verify, a gene's ability to impact the proliferation/differentiation balance in the *C. elegans* germline (Reviewed in: Hubbard & Schedl, 2019). Many genes involved in the

proliferation/differentiation balance do not have a phenotype on their own due to redundancy with other genes in the pathway; however, their involvement can be uncovered using sensitized genetic backgrounds, such as *glp-1(gf)*. Similarly, mutations that have subtle effects on the proliferation/differentiation balance are more easily identified in sensitized backgrounds.

glp-1(ar202gf) is a temperature sensitive allele resulting from a nonsynonymous single nucleotide mutation causing an amino acid substitution (G529E) within the LNR (LIN-12/Notch Repeats) domain of GLP-1 (Pepper et al., 2003). This mutation results in increased GLP-1 receptor activity, and therefore increased signalling (Pepper et al., 2003). This allele is categorized as a strong gain-of-function mutation (increased GLP-1/Notch signaling) as 100% of these mutant germlines have an over-proliferation phenotype at the restrictive temperature (25 °C) (Pepper et al., 2003). At the permissive temperature (20 °C) *glp-1(ar202gf)* animals possess a fairly wild-type germline that has an increase in the size, and total number of cells, in the proliferative zone, referred to as a 'late-onset tumour' (Pepper et al., 2003). Additionally, at the permissive temperature, a small percentage of these mutant germlines have proliferative cells at their most proximal end, 'protumour' / Pro (Proximal tumour), instead of developing gametes (Pepper et al., 2003).

Our lab previously demonstrated that a reduction in *rack-1* levels, by RNAi, enhances the over-proliferation phenotype in a *glp-1(ar202gf)* background at the permissive temperature (Wang, 2013); however, since RNAi has variable efficiency at

reducing gene expression, and can result in off target effects, this analysis was repeated using a presumed null allele of *rack-1* (Kamath et al., 2003; S. Qiu et al., 2005). *rack-1(tm2262)* was generated by the National BioResource Project (NBRP), and obtained from the Caenorhabditis Genetics Center (CGC) where it was outcrossed five times (Barstead et al., 2012). As seen with RNAi, *rack-1(tm2262)* enhanced the over-proliferation phenotype of *glp-1(ar202gf)* at the permissive temperature, with nearly 100% of *glp-1(ar202gf); rack-1(tm2262)* germlines having proliferating cells outside of the proliferative zone as determined by α-REC-8 and α-HIM-3 staining compared to 9% and 0% in *glp-1(ar202gf)* and *rack-1(tm2262)* respectively (Figure 3.1 and Table 3.1). A large portion of *glp-1(ar202gf); rack-1(tm2262)* germlines (57%) showed a 'Complex Tumour' phenotype, both with and without the presence of a proximal tumour (53% and 4% respectively) (Table 3.1). This phenotype has been previously associated with *glp-1* gain-of-function mutations (Pepper et al., 2003), and has more recently been defined by Hubbard and Schedl as having "cells that have entered the meiotic pathway (HIM-3 positive) in a variable pattern among the proliferating cells, either scattered within the tumor or in discrete patches" (Hubbard & Schedl, 2019).

Surprisingly, the *glp-1(ar202gf)* over-proliferation phenotype was also enhanced when combined with a *rack-1* heterozygote (*rack-1(tm2262)/nT1g; nT1g* is a balancer chromosome that contains a wildtype copy of *rack-1),* with 59% of germlines analyzed having mitotic cells outside of the proliferative zone (Table 3.1).

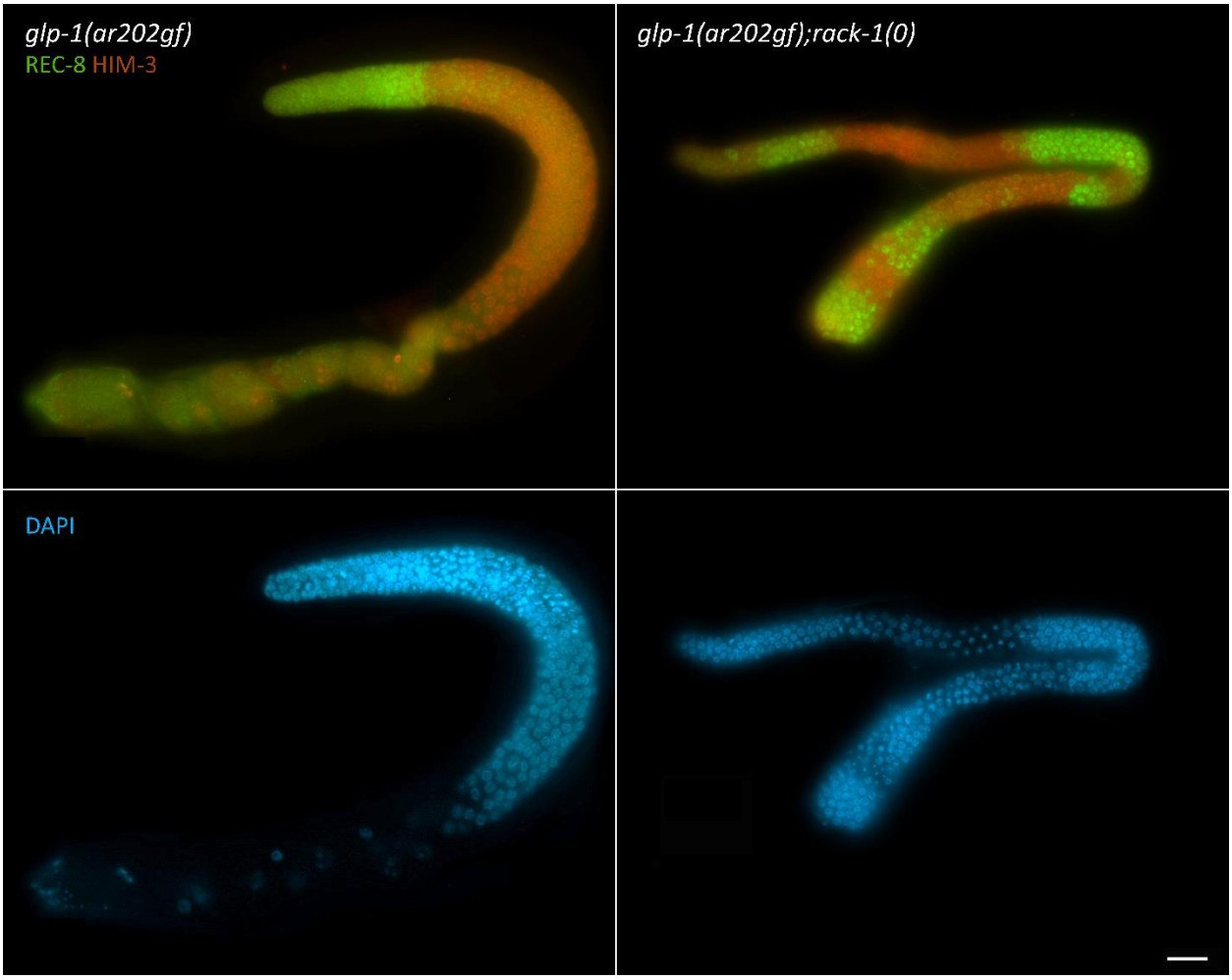

Figure 3.1 - *rack-1(0)* enhances the over-proliferation phenotype of *glp-1(ar202gf)* animals. Representative images of *glp-1(ar202gf)* and *glp-1(ar202gf); rack-1(tm2262)* young adult gonads. Animals were raised at 20 °C, dissected at one day past the L4 stage, and analyzed for ectopic proliferation using α-REC8 (proliferation marker) and α-HIM-3 (meiotic marker) antibodies. Nuclear morphology was detected using DAPI. Scale bar = 20 μm.

Table 3.1 - *rack-1(0); glp-1(ar202gf)* germline proliferation phenotype at 20 °C

	Germline Phenotype[a]				
Genotype	Wildtype (%)[b]	Complex Tumour (%)[c]	Complex Tumour + Pro (%)[d]	Pro (%)[e]	n[f]
glp-1(ar202gf)	91	2	0	7	365
rack-1(0)[g]	100	0	0	0	87
glp-1(ar202gf); rack-1(0)[h]	1	4	53	42	307
glp-1(ar202gf); rack-1(het)[i]	41	2	11	27	271

[a] Animals were dissected one day past the L4 stage, fixed and stained with DAPI, α-REC-8 and α-HIM-3 antibodies. The germline phenotype was scored based upon the presence of REC-8 positive cells outside of the proliferative zone.

[b] Wildtype refers to gonad arms with no REC-8 outside of the proliferative zone. This category includes germlines with the *glp-1(ar202gf)* late-onset tumour (increased proliferative zone size and total number of cells).

[c] Complex Tumour refers to gonad arms that had stretches of proliferative cells (REC-8 positive) outside of the proliferative zone with the most proximal end of the germline having meiotic cells determined by HIM-3 staining.

[d] Complex Tumour + Pro refers to gonad arms that had stretches of proliferative cells (REC-8 positive) outside of the proliferative zone alongside entry into meiosis (HIM-3 positive), and a pool of proliferative cells (REC-8 positive) at the most proximal end of the germline, Pro (Proximal tumour).

[e] Proximal tumour (Pro) refers to gonad arms that have relatively normal distal germlines but a pool of proliferative cells (REC-8 positive) at the most proximal end of the germline.

[f] n refers to total number of gonad arms analyzed.

[g] Actual genotype; *rack-1(tm2262).*

[h] Actual genotype; *glp-1(ar202gf); rack-1(tm2262).*

[i] Actual genotype; *glp-1(ar202gf); rack-1(tm2262)/nT1g.* nT1g is a balancer chromosome that contains a wildtype copy of *rack-1.*

In order to determine if the ability of *rack-1(tm2262)* to enhance over-proliferation is specific to the *glp-1(ar202gf)* allele, I determined if a loss of *rack-1* could enhance another *glp-1* gain-of-function mutation. *glp-1(oz264gf)* is a temperature sensitive allele resulting from a nonsynonymous single nucleotide mutation causing an amino acid substitution (G528E) within the LNR (LIN-12/Notch Repeats) domain of GLP-1, right beside the *glp-1(ar202gf)* substitution (G529E) (Kerins, 2006; Kerins et al., 2010). Similar to the *ar202* mutation, the *oz264* mutation is thought to result in slightly increased GLP-1 receptor activity, and therefore signaling (Pepper et al., 2003). *glp-1(oz264gf)* is categorized as a weak gain-of-function, as only 33% of germlines are reported to have an over-proliferation phenotype (proximal tumour) at the restrictive temperature (25 °C) (Kerins, 2006; Kerins et al., 2010). Similar to *glp-1(ar202gf), glp-1(oz264gf)* germlines have a late onset tumorous phenotype at the permissive temperature (20 °C) (Kerins, 2006; Kerins et al., 2010).

rack-1(tm2262) enhances the *glp-1(oz264gf)* over-proliferation phenotype at both 20 °C and 25 °C. At the permissive temperature, 20% of *glp-1(oz24gf); rack-1(tm2262)* had an over-proliferation phenotype as determined by α-REC-8, α-HIM-3 and DAPI staining**,** whereas neither of the single mutants showed over-proliferation alone (Figure 3.2 and Table 3.2). At the restrictive temperature, 97% of *glp-1(oz264gf); rack-1(tm2262)* displayed an over-proliferation phenotype compared to 59% *glp-1(oz264gf)* gonads (Figure 3.3 and Table 3.2). Similar to *glp-1(ar202); rack-1(tm262)*, the majority of *glp-*

1(oz264gf); rack-1(tm2262) gonads displayed a complex tumour phenotype both with and without the presence of a proximal tumour.

Taken together, the above results suggest that *rack-1* does play a role in the proliferation/differentiation balance. In the absence of *rack-1* an increase in proliferation is observed. This suggests that *rack-1* could function to directly inhibit GLP-1/Notch signaling, or that *rack-1* may be required for entry into meiosis.

Table 3.2 - *glp-1(oz264gf); rack-1(0)* germline proliferation phenotype

		Germline phenotype[a]					
Genotype	Temp (°C)	Wildtype (%)[b]	Complex tumour + embryos (%)[c]	Complex tumour (%)[d]	Complex tumour + Pro (%)[e]	Pro (%)[f]	n[g]
glp-1(oz264gf)	20	100	0	0	0	0	240
glp-1(oz264gf); rack-1(0)[h]	20	80	4	1	6	9	222
glp-1(oz264gf)	25	41	59	2	4	0	138
glp-1(oz264gf); rack-1(0)[h]	25	3	3	17	53	27	103

[a] Animals were dissected one day past the L4 stage, fixed and stained with DAPI, α-REC-8 and α-HIM-3 antibodies. The germline phenotype was scored based upon the presence of REC-8 positive cells outside of the proliferative zone.
[b] Wildtype refers to gonad arms with no REC-8 outside of the proliferative zone. This category includes germlines with the *glp-1(ar202gf)* late-onset tumour (increased proliferative zone size and total number of cells).
[c] Complex tumour + embryos refers to gonad arms that had stretches of proliferative cells (REC-8 positive) outside of the proliferative zone alongside entry into meiosis (HIM-3 positive), but with embryos present at the most proximal end of the germline.
[d] Complex Tumour refers to gonad arms that had stretches of proliferative cells (REC-8 positive) outside of the proliferative zone alongside entry into meiosis (HIM-3 positive), but with the most proximal end of the germline having meiotic cells (HIM-3 positive).
[e] Complex Tumour + Pro refers to gonad arms that had stretches of proliferative cells (REC-8 positive) outside of the proliferative zone alongside entry into meiosis (HIM-3 positive) with a pool of proliferative cells (REC-8 positive) at the most proximal end of the germline, Pro (Proximal tumour).
[f] Protumour (Pro) refers to gonad arms that have normal entry into meiosis (HIM-3) but a pool of proliferative cells (REC-8 positive) at the most proximal end of the germline.
[g] n refers to total number of gonad arms analyzed.
[h] Actual genotype; *glp-1(oz264gf); rack-1(tm2262).*

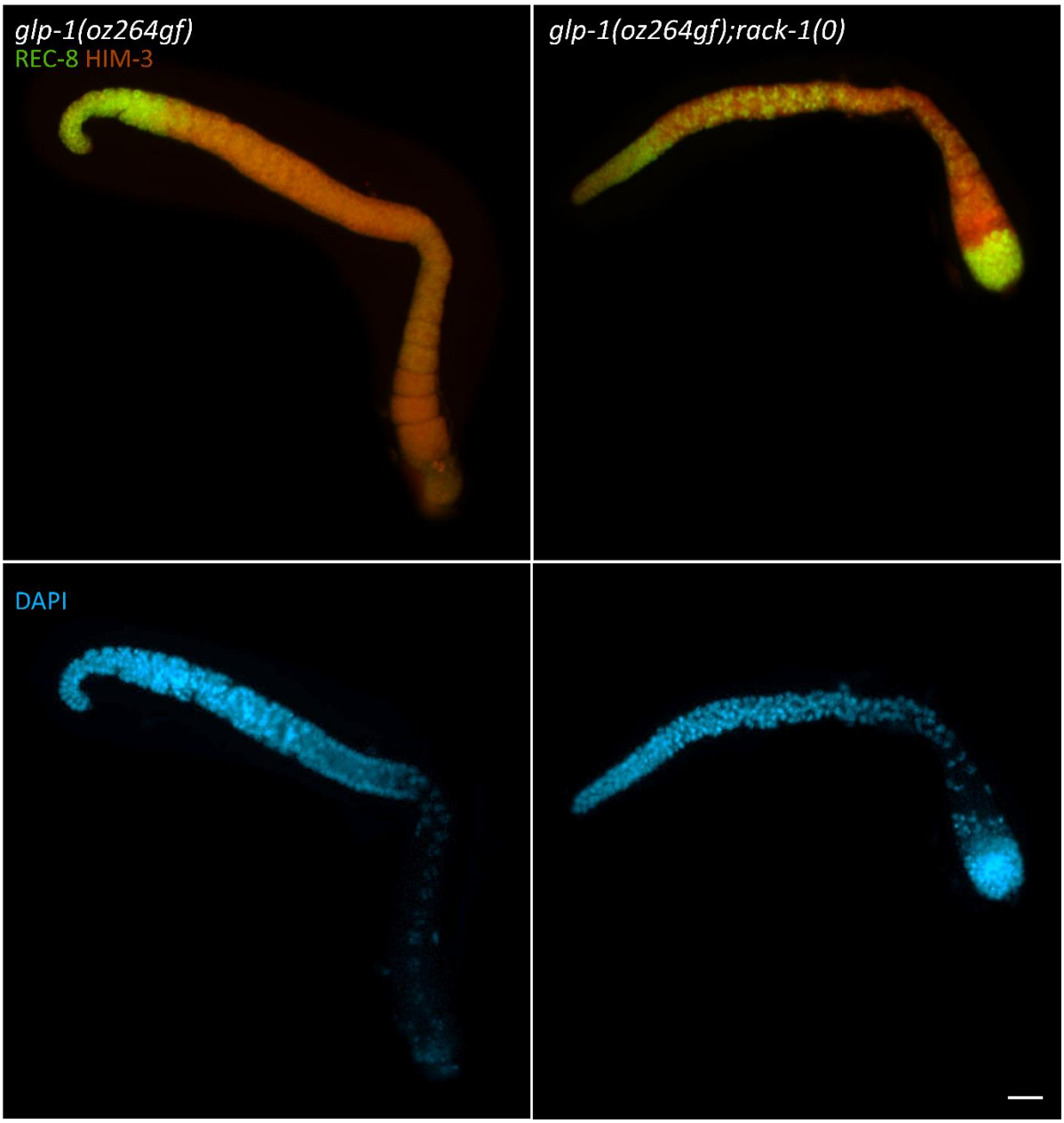

Figure 3.2 - *rack-1(0)* enhances the over-proliferation phenotype of *glp-1(oz264gf)* at 20 °C. Representative images of *glp-1(oz264gf)* and *glp-1(oz264gf); rack-1(tm2262)* young adult gonads. Animals were raised at 20 °C, dissected at one day past the L4 stage, and analyzed for ectopic proliferation using α-REC8 (proliferation marker) and α-HIM-3 (meiotic marker) antibodies. Nuclear morphology was detected using DAPI. Scale bar = 20 μm.

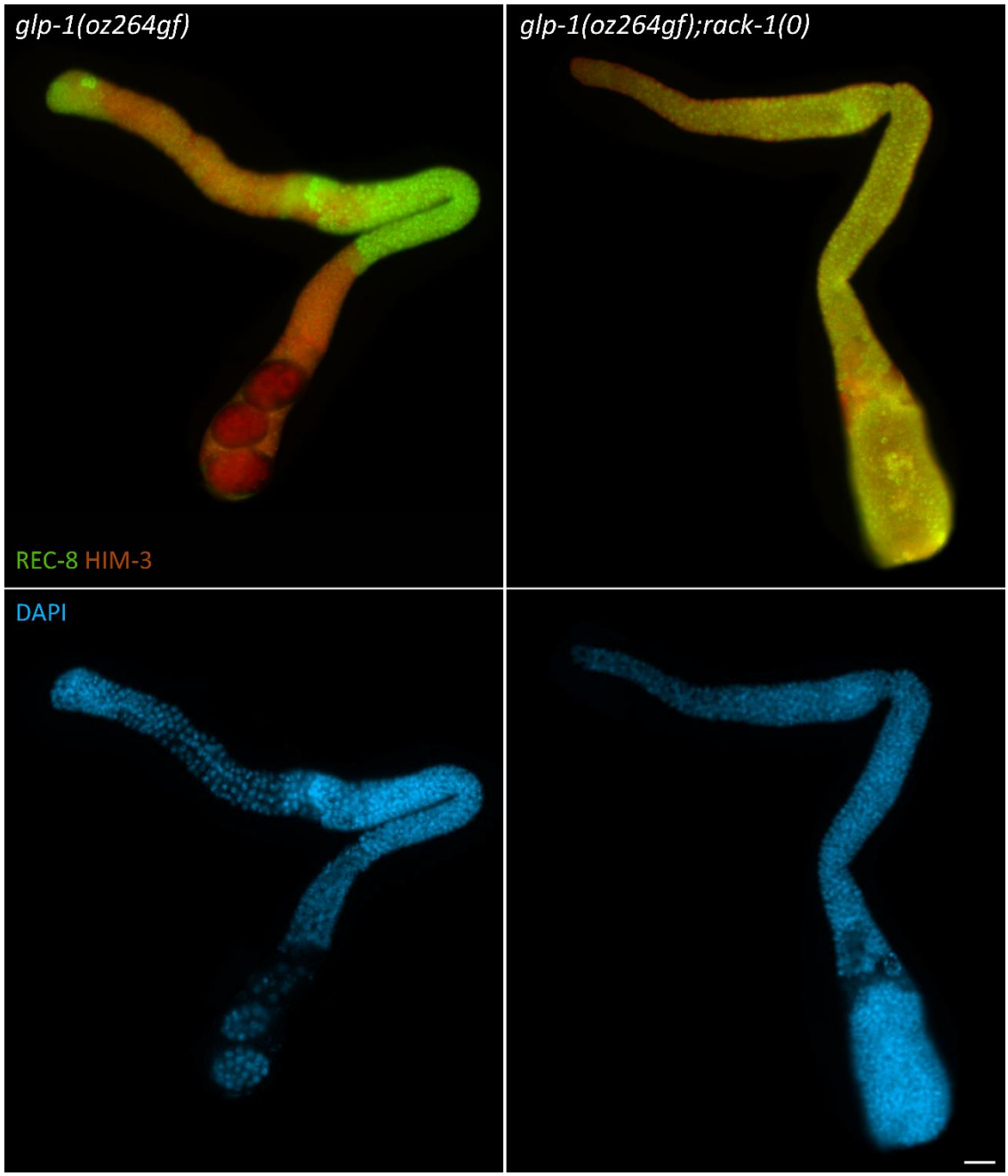

Figure 3.3 - *rack-1(0)* enhances the over-proliferation phenotype of *glp-1(oz264gf)* at 25 °C. Representative images of *glp-1(oz264gf)* and *glp-1(oz264gf); rack-1(tm2262)* young adult gonads. Animals were raised at 25 °C, dissected at one day past the L4 stage, and analyzed for ectopic proliferation using α-REC8 (proliferation marker) and α-HIM-3 (meiotic marker) antibodies. Nuclear morphology was detected using DAPI. Scale bar = 20 μm

3.2 *rack-1(0)* cannot suppress reduced proliferation associated with the loss of GLP-1/Notch signalling

As described above, a loss of *rack-1* strongly enhanced the over-proliferation phenotype in *glp-1* gain-of-function mutants. This suggests that a loss/reduction of *rack-1* may also be able to rescue a loss of GLP-1/Notch signaling. The loss of GLP-1/Notch signaling, from ablation of the DTC (Kimble, 1981) or complete loss of GLP-1 function (Austin & Kimble, 1987), results in the germ cells prematurely entering meiosis due to a lack of the mitotic signal. This premature differentiation results in a loss of the stem cell population due to all stem cells prematurely differentiating as sperm (Glp phenotype) (Austin & Kimble, 1987). To determine if loss of *rack-1* can suppress a lack of GLP-1/Notch signalling I analyzed *rack-1(tm2262)'s* interaction with two *glp-1* loss-of-function alleles, *glp-1(q175)* and *glp1(bn18ts).*

glp-1(q175) contains a nonsense mutation (R191X) that results in a truncated non-functional protein and is categorized as a true null allele (Kodoyianni et al., 1992). Loss of *rack-1(0)* was unable to suppress the Glp phenotype as 100% of g*lp-1(q175); rack-1(tm2262)* germlines were found to be Glp as determined by whole-mount analysis with DAPI (nuclear morphology) (Table 3.3). It is possible that *rack-1's* influence on the proliferation/differentiation balance is not strong enough to overcome a complete loss of *glp-1;* therefore, I next examined *rack-1's* ability to supress a *glp-1* weak loss-of-function allele.

glp-1(bn18ts) is a temperature sensitive allele resulting from a nonsynonymous point mutation causing an amino acid substitution (A1034T) within the SW16 repeat

region (Kodoyianni et al., 1992). This mutation is thought to disrupt GLP-1's ability to function as a receptor, thereby reducing signaling (Kodoyianni et al., 1992). At the permissive temperature, *glp-1(bn18ts)* animals have germlines with reduced proliferation determined by a reduction in the size, and total number of cells, in the proliferative zone (Fox & Schedl, 2015; Kodoyianni et al., 1992); however, at the restrictive temperature, these mutants display the Glp phenotype associated with a complete loss of GLP-1/Notch signaling (Kodoyianni et al., 1992). As seen with *glp-1(0), rack-1(tm2262)* was unable to supress the Glp phenotype of *glp1(bn18ts)* at the restrictive temperature (100% Glp germlines) (Table 3.4). This analysis was repeated at the permissive temperature. Similar to previous research, I found that *glp-1(bn18ts)* germlines had a smaller proliferative zone as compared to wildtype (N2) in both the extent of REC-8 expression (proliferative marker); 11 vs 18 gcd respectively, and total cell number, 126 vs 242 respectively (Unpaired t-test p-value < 0.0001) (Figure 3.4 and Table 3.5). *rack-1(tm2262)* germlines alone also had a reduction in proliferative zone size as compared to wildtype (N2); REC-8 expression 15 vs 18 gcd, and total cell number 133 vs 242 (Unpaired t-test p-value < 0.0001) (Figure 3.4 and Table 3.5). *glp-1(bn18ts);rack-1(tm2262)* germlines had a further reduced proliferative zone; REC-8 expression 11 gcd and total cell number 89 (Figure 3.4 and Table 3.3.3). This reduction was statistically significant compared to both *glp-1(bn18ts)* and *rack-1(tm2262)* alone (One-way ANOVA p-values < 0.0001). *rack-1(tm2262)'s* proliferative zone, when looking at total cell number, is reduced by 45% compared to wildtype (N2); therefore, it is anticipated that a loss of *rack-1* would reduce all other genetic backgrounds by a similar capacity, unless *rack-1(0)* works synergistically

with the other mutated gene. If the reduced proliferative zone size is due to the disruption in a mechanism independent of Notch signaling, the *glp-1(bn18ts); rack-1(tm2262)* proliferative zone size should be roughly 55% of *glp-1(bn18ts)* alone, or 69 total cells. The total number of cells in the proliferative zone of *glp-1(bn18ts); rack-1(0)* was experimentally determined to be 89, which is statistically larger than expected (69; chi-square p-value < 0.0001); therefore, the reduction in proliferative zone size is most likely due to the additive reduction found in the two single mutants alone. This suggests that loss of *rack-1* does not suppress the reduction in stem cell proliferation seen in *glp-1(bn18ts)*.

GLP-1/Notch is a membrane-bound receptor expressed on the surface of stem cells within the proliferative zone (Crittenden et al., 1994). The current model is that upon interaction with LAG-2 and APX-1 expressed on the surface of the DTC, GLP-1/Notch undergoes two cleavage events, releasing the intracellular portion, Notch Intracellular domain (NICD) (Kopan et al., 1996). NICD then translocates into the nucleus where it interacts with transcription factors, LAG-1 and SEL-8/LAG-3, to form a transcriptional activation complex (Christensen et al., 1996; Doyle et al., 2000; Petcherski & Kimble, 2000). Only two direct GLP-1/Notch target genes have been identified, *lst-1* and *sygl-1* (Chen et al., 2020; Kershner et al., 2014). These genes work redundantly to regulate stem cell proliferation within the proliferative zone (Kershner et al., 2014). Loss of both *sygl-1* and *lst-1* phenocopies a loss of GLP-1/Notch resulting in a loss of GSC proliferation and a Glp phenotype (Kershner et al., 2014). In agreement with loss of *rack-1* being unable to suppress the Glp phenotype associated with loss of GLP-1/Notch, loss of *rack-1* was

unable to suppress the loss of proliferation in *lst(ok814) sygl-1(tm5040)* null mutants (Table 3.6).

rack-1(tm2262)'s inability to suppress the proliferation defects in *glp-1* loss-of-function and *lst-1(ok814) sygl-1(tm5040)* mutants could be due to *rack-1's* influence on the proliferation/differentiation balance not being strong enough to overcome a decrease, or loss, in GLP-1/Notch signaling. Enhancement of *glp-1(gf)* mutant phenotypes without the ability to rescue the proliferation defects in *glp-1(lf)* mutants has been seen for other modulators, specifically *kin-10* (Wang, 2013; Wang et al., 2014); therefore, *glp-1(gf)* mutants may be more sensitive to changes in the activity of modulators.

Table 3.3 - *rack-1(0)* cannot suppress *glp-1(0)* Glp phenotype

Analysis at 20 °C	Genotype	Glp (%)[a]	n[b]
	glp-1(0)[c]	100	152
	glp-1(0); rack-1(0)[d]	100	138
Analysis at 25 °C			
	glp-1(0)[c]	100	156
	glp-1(0); rack-1(0)[d]	100	152

[a] Germline proliferative defective (Glp); A gonad arm was scored as Glp if only sperm was present in the gonad arm when analyzed at one day past the L4 as determined by whole mount DAPI (nuclear morphology) analysis.
[b] n refers to total number of gonad arms analyzed.
[c] Actual genotype; *glp-1(q175).*
[d] Actual genotype; *glp-1(q175); rack-1(tm262).*

Table 3.4 - *rack-1(0)* cannot suppress *glp-1(bn18ts)* Glp phenotype at 25 °C

Genotype	Glp (%)[a]	n[b]
glp-1(bn18ts)[c]	100	156
glp-1(bn18ts); rack-1(0)[d]	100	152

[a] Germline proliferative defective (Glp); A gonad arm was scored as Glp if only sperm was present in the gonad arm when analyzed at one day past the L4 with whole mount DAPI staining (nuclear morphology).
[b] n refers to total number of gonad arms analyzed.
[c] Actual genotype; *glp-1(q175).*
[d] Actual genotype; *glp-1(bn18lf); rack-1(tm2262).*

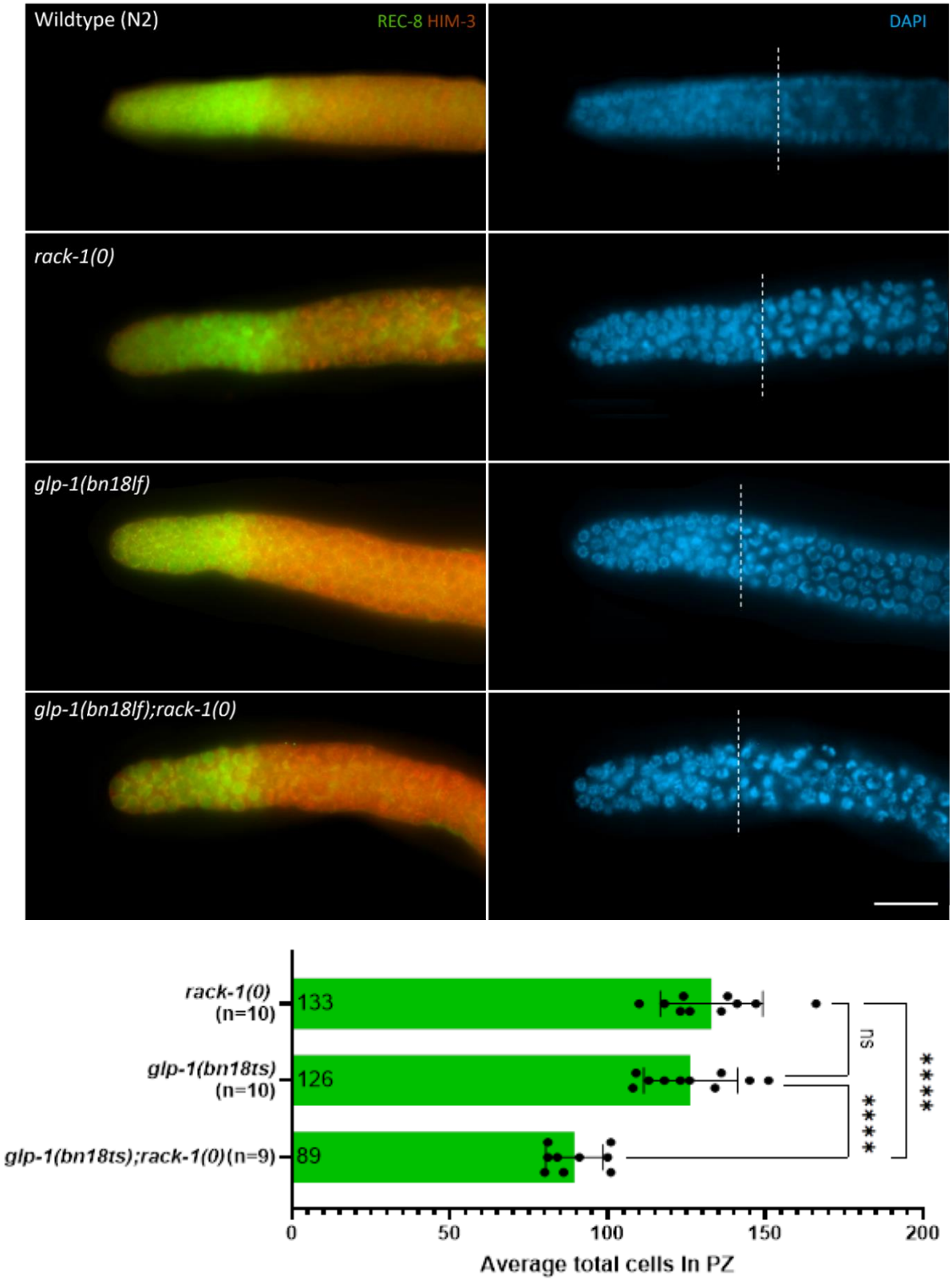
Wildtype (N2)
REC-8 HIM-3
DAPI
rack-1(0)
glp-1(bn18lf)
glp-1(bn18lf);rack-1(0)
rack-1(0)
(n=10)
133
glp-1(bn18ts)
(n=10)
126
glp-1(bn18ts);rack-1(0)(n=9)
89
ns
****
****
0
50
100
150
200
Average total cells in PZ

Figure 3.4 – *rack-1(0)* does not rescue the proliferation defect in *glp-1(bn18ts)* mutants at 20 °C. Top - Representative images of the proliferative zone of wildtype (N2), *glp-1(bn18ts), rack-1(tm2262)* and *glp-1(bn18ts); rack-1(tm2262)* young adult gonads. Animals were raised at 20 °C, dissected at one day past the L4 stage, stained with α-REC8 (proliferation marker) and α-HIM-3 (meiotic marker) antibodies to determine the size of the proliferative zone. Nuclear morphology was detected using DAPI. The dashed line represents the transition into meiosis Scale bar = 20 μm. Bottom – Average number of cells in the proliferative zone (PZ) (x-axis) is depicted in the bar graph for the given genotype (y-axis). Each point represents an individual gonad. Error bars represent ± standard deviation (S.D). Asterisks represent statistical differences determined by a one-way ANOVA with Tukey HSD *post hoc* test. ns = not significant, ****p<0.0001.

Table 3.5 - *rack-1(0)* cannot suppress the proliferation defect in *glp-1(bn18ts)*

Analysis at 20 °C Genotype	Average length of PZ (gcd) (S.D.; range)[a]	Average total cells in PZ (S.D.; range)[b]	n[c]
Wildtype (N2)	18 (2; 16-20)	242(35; 183-307)	14
rack-1(0)[d]	15 (2; 11-19)	133(16; 110-160)	10
glp-1(bn18ts)	11 (2; 8-15)	126 (15; 108-151)	10
glp-1(bn18ts); rack-1(0)[e]	11 (2; 7-13)	89(9; 80-101)	9

[a] Animals were dissected one day past the L4 stage, fixed and stained with DAPI, α-REC-8 and α-HIM-3 antibodies. The length of the proliferative zone (PZ) was determined by counting the extent (germ cell diameter) of REC-8 expression and averaged from a minimum of 14 animals. S.D. = Standard Deviation; Range = minimum-maximum values obtained.
[b] The average total number of cells in the proliferative zone (PZ) was determined using DAPI staining (nuclear morphology). Cells were counted until the transition zone, marked by crescent-shaped nuclei (DAPI staining (nuclear morphology)). S.D. = Standard Deviation; Range = minimum-maximum values obtained.
[c] n refers to total number of gonad arms analyzed for average total of cells in the PZ.
[d] Actual genotype; *rack-1(tm2262).*
[e] Actual genotype; *glp-1(bn18lf); rack-1(tm2262).*

Table 3.6 - *rack-1(0)* cannot suppress *lst-1(0) sygl-1(0)* Glp phenotype

Analysis at 20 °C Genotype	Glp (%)[a]	n[b]
lst-1(0) sygl-1(0)[c]	100	80
lst-1(0) sygl-1(0); rack-1(0)[d]	100	72
Analysis at 25 °C		
lst-1(o) sygl-1(0)[c]	100	101
lst-1(0) sygl-1(0); rack-1(0)[d]	100	68

[a] Germline proliferative defective (Glp); A gonad arm was scored as Glp if only sperm was present in the gonad arm when analyzed at one day past the L4 with whole mount DAPI staining (nuclear morphology).
[b] n refers to total number of gonad arms analyzed.
[c] Actual genotype; *lst-(ok814) sygl-1(tm5040).*
[d] Actual genotype; *lst-(ok814) sygl-1(tm5040); rack-1(tm2262).*

3.3 Loss of *rack-1* does not increase GLP-1/Notch activity

The enhancement of the over-proliferation phenotype seen with *glp-1* gain-of-function mutants upon loss of *rack-1(0)* suggests that RACK-1 could function to inhibit GLP-1/Notch activity directly. Alternatively, RACK-1 could function to promote entry into meiosis. To determine if *rack-1* functions to directly inhibit GLP-1/Notch signaling the expression profile of SYGL-1::3xFLAG, a direct GLP-1/Notch target gene was analyzed in the absence of *rack-1* (Kershner et al., 2014).

As discussed in the previous section, GLP-1/Notch is a transmembrane receptor that undergoes proteolytic cleavage when activated, resulting in the release of NICD (Reviewed (Hubbard & Schedl, 2019)). NICD translocates into the nucleus where it functions within a transcriptional activation complex to activate the expression of two direct target genes *lst-1* and *sygl-1* (Christensen et al., 1996; Doyle et al., 2000; Kershner et al., 2014; Lambie et al., 1991; Petcherski & Kimble, 2000). These genes work redundantly to regulate stem cell proliferation within the proliferative zone. SYGL-1 expression alone is correlated with the size of the proliferative zone (Shin et al., 2017); therefore, SYGL-1 expression extent and levels can be used as a read out of active GLP-1/Notch.

SYGL-1 expression can be detected using a CRISPR tagged allele of *sygl-1,* (*sygl-1(am307[sygl-11::3XFLAG*]) (Kocsisova et al., 2019). SYGL-1 has been previously shown to be expressed from the distal end to approximately 10 – 14 gcd from the DTC (Kocsisova et al., 2019; Shin et al., 2017). SYGL-1 was expressed ~11 gcd in *rack-1(tm2262)* versus ~13 gcd in control germlines (*sygl-1(am307)*) (Figure 3.5). Although,

SYGL-1 expression in *rack-1(tm2262)* was within the previously reported range for wildtype SYGL-1 expression, it was determined to be significantly different from control germlines [*sygl-1(am307)*] (Unpaired t-test p-value = 0.0015) (Figure 3.5). The overall level of SYGL-1 expression, as determined by measuring the intensity across the proliferative zone, is slightly reduced in *rack-1(tm2262)* gonads as compared to control gonads (Figure 3.6). This reduction is statistically significant (*rack-1(tm2262)* = 6769305 a.u x μm, control = 9496664 a.u x μm; Unpaired t-test p-value = 0.0147); however peak SYGL-1, or the maximum value obtained, was not statistically different between control and *rack-1(tm2262)* gonads (1651 a.u vs 1395 a.u respectively; Unpaired t-test p-value = 0.1754). This is opposite to what was expected if wild-type *rack-1* were to inhibit GLP-1/Notch signaling – that loss of *rack-1* would result in increased GLP-1/Notch signaling. *rack-1* mutant animals have a reduction in the number of GSCs within the proliferative zone (Table 3.5); therefore, a reduction in GLP-1/Notch signaling is in agreement with the smaller GSC pool. Taken together, this data suggests that *rack-1* does not function to inhibit GLP-1/Notch signaling; however, *rack-1* may have two opposing roles within the germline – functioning within the PZ to maintain the GSC pool and outside of the PZ to inhibit proliferation and/or promote meiosis. Future experiments will be needed to determine *rack-1's* role within the GSC pool and if this role is GLP-1/Notch dependent or independent.

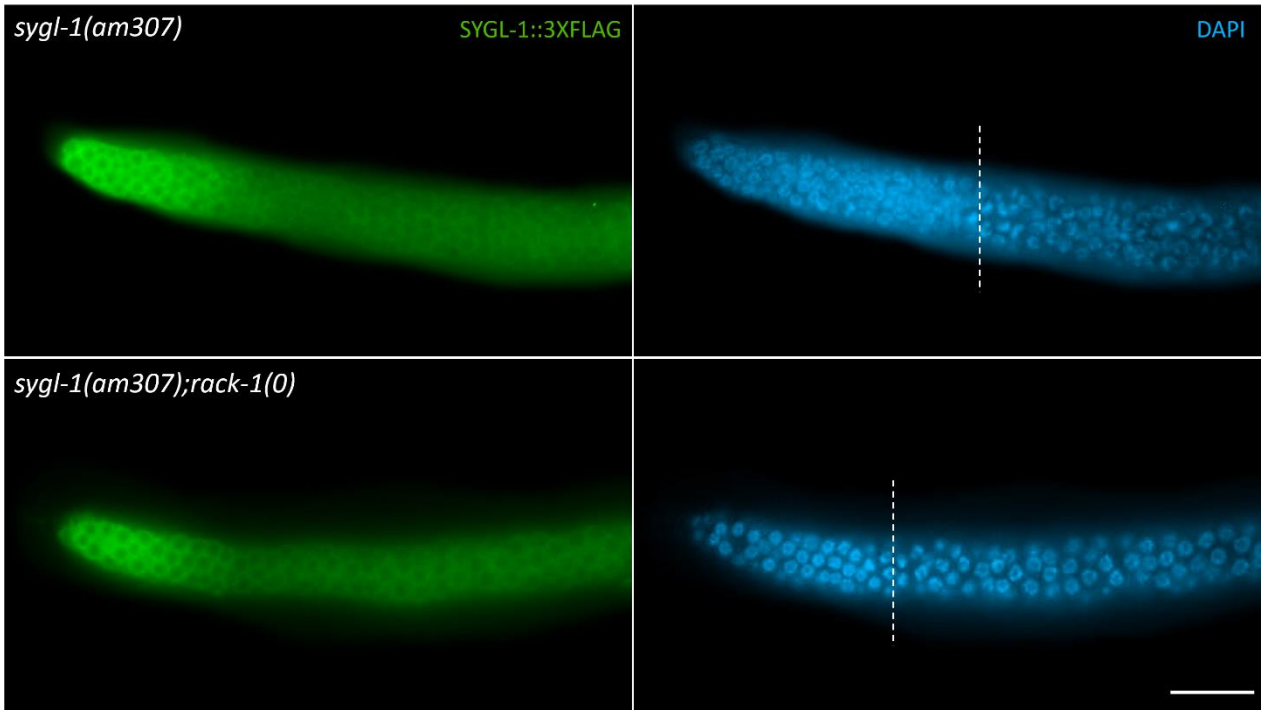

Figure 3.5 - Loss of *rack-1* does not enhance the extent of SYGL-1 expression. Representative images of the proliferative zone of *sygl-1(am307)* (control), *sygl-1(am307); rack-1(tm2262)* young adult gonads. Animals were raised at 20 °C, dissected at one day past the L4 stage, stained with α-FLAG (detect SYGL-1::3xFLAG) and DAPI (nuclear morphology). The dashed line represents the transition into meiosis. Scale bar = 20 μm.

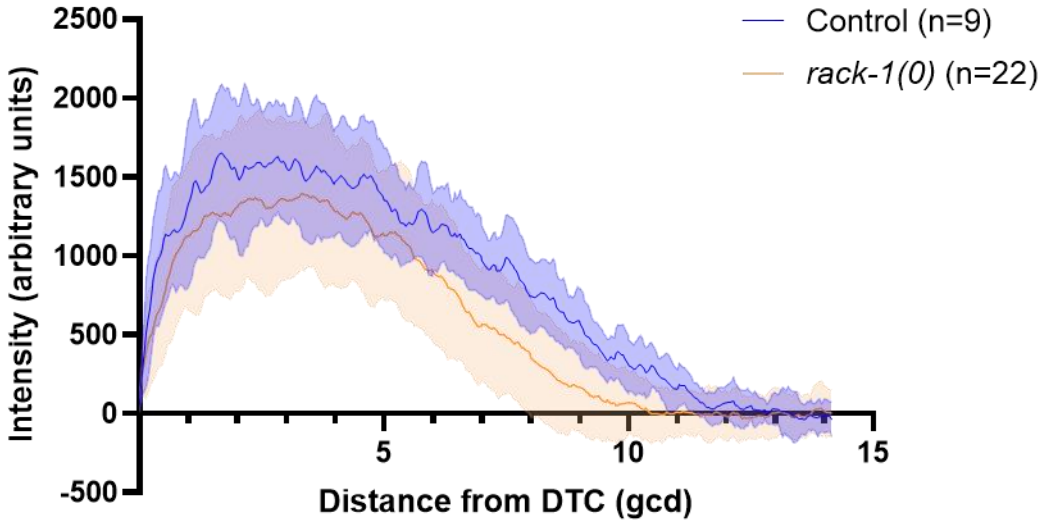

Figure 3.6 – SYGL-1 expression is lowered in *rack-1(tm2262)* germlines. Graphs depicting the average SYGL-1 accumulation profiles in control (*sygl-1(am307)*) and *sygl-1(am307); rack-1(tm2262)* germlines raised at 20 °C. SYGL-1's expression was determined using SYGL-1::3xFLAG transgene and α-FLAG antibodies. The x-axis is distance in germ cell diameters (gcd). The y-axis is the intensity of antibody staining in arbitrary units.

3.4 *rack-1* does not regulate the entry into meiosis decision

To determine if *rack-1* functions to promote meiotic entry I evaluated the entry into meiosis decision in the absence of *rack-1.* This transition is regulated by two opposing signaling gradients, GLP-1/Notching signaling (mitosis) and GLD pathways (meiosis). Active GLP-1/Notch signaling in the proliferative zone inhibits the downstream GLD-1 and GLD-2 pathways, including preventing GLD-1 accumulation (Hansen, Wilson-Berry, et al., 2004). These pathways function redundantly to promote entry into meiosis, with the activity of one of the two pathways being sufficient for normal meiotic entry; however, when both pathways are mutated, most germ cells fail to enter meiosis, resulting in the formation of a germline tumour (proliferative cells) with very little meiotic entry (Eckmann et al., 2004; Hansen et al., 2004; Kadyk & Kimble, 1998). To determine if *rack-1* functions in either of the GLD pathways, I analyzed meiotic entry in animals lacking *rack-1* and a core component of either the GLD-1 (*gld-1* and *nos-3*) or GLD-2 pathways (*gld-2* and *gld-3*). Interestingly, none of the double mutant combinations [*gld-1(q485); rack-1(tm2262)*, *nos-3(oz231); rack-1(tm2262)*, *gld-2(q497); rack-1(tm2262),* or *gld-3(q730); rack-1(tm226)*] formed strong germline tumours as would be expected if both GLD-1 and GLD-2 pathway function is disrupted; however, other proliferative phenotypes were observed (Discussed in Chapter 6).

To investigate if a loss of *rack-1* has a more subtle effect on the entry into meiosis decision the size of the proliferative zone was measured by analyzing the extent of REC-8 expression (proliferative marker) and total cell number, in the double mutant animals. If *rack-1* plays a role in the GLD-1 pathway, an increase in the proliferative zone size (meiotic entry defect), in combination with mutants of the GLD-2 pathway (*gld-2, gld-3),*

would be expected. If *rack-1* is involved in the GLD-2 pathway, an increase in the proliferative zone size (meiotic entry defect), in combination with mutants of the GLD-1 pathway (*gld-1, nos-3),* would be expected. Interestingly, no double mutant combination displayed meiotic entry defects and instead a statistically significant reduction in the proliferative zone size, as compared to the GLD pathway single mutants alone, was observed (One-way ANOVA all p-values < 0.0001); *gld-1(q485); rack-1(tm2262)* - 95 cells, REC-8 12 gcd; *gld-1(q485)* - 187 cells, REC-8 15 gcd; *nos-3(oz231); rack-1(tm2262)* - 113 cells, REC-8 15 gcd; nos-3(oz231) – 271 cells, REC-8 18 gcd; *gld-2(q497); rack-1(tm2262)* - 170 cells, REC-8 21 gcd; *gld-2(q497)* – 343 cells, REC-8 25 gcd; *gld-3(q730); rack-1(tm2262)* – 195 cells REC-8 20 gcd; *gld-3(q730)* 302 cells, REC-8 24 gcd (Figure 3.7, Figure 3.8 and Table 3.7). The size of the proliferative zone in *gld-1(q485); rack-1(tm2262), gld-2(q497); rack-1(tm2262),* and *gld-3(q730); rack-1(tm2262)* was determined to be statistically different compared to *rack-1(tm2262)* gonads alone (One-way ANOVA all p-values < 0.05).

The GSC pool in *rack-1* mutants is reduced compared to wildtype (45% reduction); therefore, it is anticipated that loss of *rack-1* would reduce all other genetic backgrounds by a similar capacity, unless *rack-1* works synergistically with the other mutated gene (See Table 3.7 for expected values). The reduction in the PZ size observed in *gld-1(q485);rack-1(tm2262),* 95 cells, was significantly different from the expected reduction, 103 cells (chi-square p-value < 0.05). The reduction in the PZ size observed in *gld-2(q497); rack-1(tm2262)*, 170 cells, was statistically different from the expected reduction (188 cells) (chi-square p-value < 0.0001). The PZ size observed in *gld-3(q730); rack-*

1(tm2262) was larger than anticipated, 195 vs 166 (chi-square p-value < 0.0001) (Table 3.7). Although the difference in the proliferative zone size is statistically significant in most of the double mutants, and greater than expected in *gld-1(q485); rack-1(tm2262) and gld-2(q497);rack-1(tm2262),* these results were opposite to what was anticipated if wildtype *rack-1* functions redundantly with GLD-1 or GLD-2 pathways to promote meiotic entry – that loss of *rack-1* would cause a meiotic entry defect and result in an increase in the proliferative zone (GSC pool).

This analysis was repeated at 25 °C for *nos-3(oz231);rack-1(tm2262), gld-2(q497);rack-1(tm2262)* and *gld-3(q730);rack-1(tm2262)* as these animals displayed additional germline phenotypes at this temperature (Discussed in Chapter 6); however, as with the analysis at 20 °C, all double mutants displayed a statistically significant reduction in proliferative zone size as compared to the GLD pathway single mutants alone (One-way ANOVA all p-values < 0.0001); *nos-3(oz231); rack-1(tm2262)* - 84 cells, REC-8 15 gcd; nos-3(oz231) – 172 cells, REC-8 13 gcd; *gld-2(q497); rack-1(tm2262)* - 131 cells, REC-8 20 gcd; *gld-2(q497)* – 348 cells, REC-8 20 gcd; *gld-3(q730); rack-1(tm2262)* – 136 cells, REC-8 13 gcd; *gld-3(q730)* 252 cells, REC-8 19 gcd (Figure 3.9 and Table 3.7). The reduction in proliferative zone size in *gld-2(q497); rack-1(tm2262)* and *gld-3(q730); rack-1(tm2262)* double mutants was statistically different from *rack-1(t2262)* mutants (One-way ANOVA all p-values < 0.01). The PZ was larger than expected in *gld-3(q730); rack-1(tm2262)* double mutants (136 vs 104 cells; chi-square p-value < 0.0001). In *gld-2(q497)*;*rack-1(tm2262)* the PZ was reduced more than the expected 45% reduction (130 vs 144 cells; chi-square p-value < 0.0001) (Table 3.5).

Again, these results were still opposite to what was anticipated – that loss of *rack-1* would cause a meiotic entry defect and result in an increase in the proliferative zone (GSC pool).

Interestingly, this reduction in proliferative zone size was also seen in double mutants with both *glp-1* gain-of-function mutations (Figure 3.10 and Table 3.8); *glp-1(ar202gf); rack-1(tm2262)* - 204 cells, REC-8 25 gcd; *glp-1(ar202gf)* – 371, REC-8 29 gcd; *glp-1(oz24);rack-1(tm2262)* – 296, REC-8 29 gcd; *glp-1(oz264gf)* – 321, REC-8 24 gcd. The PZ size in *gld-1(ar202gf);rack-1(tm2262)* was statistically different from *glp-1(ar202gf)* but not *rack-1(tm2262)* (Kruskal-Wallis p-value < 0.05) whereas the PZ size in *glp-1(oz264gf)* was only statistically different from *rack-1(tm2262)* but not *glp-1(oz264)* (Welch's ANOVA p-value < 0.0001). This result was surprising as it suggests that loss of *rack-1* may slightly reduce proliferation within the proliferative zone but enhance proliferation throughout the germline.

The reduction in the proliferative zone size in the absence of *rack-1,* even in the presence of GLP-1/Notch gain-of-function mutations that increase GSC proliferation, suggests that *rack-1* may have an additional role in the proliferative zone that is required to maintain the GSC pool. *rack-1* mutants displayed a slight reduction in SYGL-1 expression extent and levels (Figure 3.5 and 3.6); therefore, this role could be GLP-1/Notch dependent. Future experiments are needed to further characterize *rack-1's* role in maintaining the GSC pool. *rack-1's* requirement within the proliferative zone complicates the ability to conclusively determine if *rack-1* functions in either of the GLD pathways; however, *rack-1* does not appear to function to regulate the entry into meiosis decision, as no meiotic entry defects were observed with GLD pathway mutants.

Table 3.7 - Loss of *rack-1* does not cause meiotic entry defects in combination with GLD pathway mutants

Genotype	Average length of PZ (gcd) (S.D.; range)[a]	Average total cells in PZ (S.D.; range)[b]	Expected total cells in PZ[c]	n[d]
Analysis at 20 °C				
Wildtype (N2)	18 (2; 16-20)	242 (35; 183-307)		14
rack-1(0)[e]	15 (2; 11-19)	133 (16; 110-160)		10
gld-1(0)[f]	16 (2; 13-20)	187 (31; 135-240)		10
gld-1(0); rack-1(0)[g]	12 (2; 10-17)	95 (12; 83-121)	103	10
nos-3(0)[h]	18 (2; 15-21)	271 (33; 221-323)		10
nos-3(0); rack-1(0)[i]	15 (2; 11-18)	113 (20; 86-146)	149	10
gld-2(0)[j]	25 (4; 17-32)	343 (41; 303-421)		10
gld-2(0); rack-1(0)[k]	21 (1; 19-24)	170 (21; 135-205)	188	10
gld-3(0)[l]	24 (3; 20-27)	302 (41; 234-396)		10
gld-3(0); rack-1(0)[m]	20 (2; 17-21)	195 (23; 158-241)	166	10
Analysis at 25 °C				
Wildtype (N2)	16 (2; 12-20)	208 (26; 180-256)		10
rack-1(0)[d]	15 (2; 11-19)	86 (13; 71-108)		10
nos-3(0)[g]	13 (2; 10-17)	172 (30; 135-222)		10
nos-3(0); rack-1(0)[h]	15 (2; 11-18)	84 (14; 68-110)	71	10
gld-2(0)[i]	22 (3; 16-28)	348 (39; 305-424)		10
gld-2(0); rack-1(0)[j]	20 (2; 16-24)	131 (31; 92-184)	144	10
gld-3(0)[k]	19 (3; 15-27)	252 (29; 214-298)		10
gld-3(0); rack-1(0)[l]	13 (2; 10-16)	136 (28; 112-203)	104	10

[a] Animals were dissected one day past the L4 stage, fixed and stained with DAPI, α-REC-8 and α-HIM-3 antibodies. The length of the proliferative zone (PZ) was determined by counting the extent (germ cell diameter) of REC-8 expression and averaged from a minimum of 14 germlines. S.D. = Standard Deviation; Range = minimum-maximum values obtained.

[b] The average total number of cells in the proliferative zone (PZ) was determined using DAPI staining (nuclear morphology). Cells were counted until the transition zone, marked by crescent-shaped nuclei (DAPI staining (nuclear morphology)). S.D. = Standard Deviation; Range = minimum-maximum values obtained.

[c] The expected total cells in the proliferative zone were calculated by multiplying each single mutant by the percent reduction seen between *rack-1(tm2262)* compared to N2 alone (20 °C = 55%, 25 °C = 41%). Single mutant x % reduction = expected PZ size.

[d] n refers to total number of gonad arms for average total of cells in the PZ.

[e] Actual genotype; *rack-1(tm2262).*

[f] Actual genotype; *gld-1(q485).*
[g] Actual genotype; *gld-1(q485); rack-1(tm2262).*
[h] Actual genotype; *nos-3(oz231).*
[i] Actual genotype; *nos-3(oz231); rack-1(tm2262).*
[j] Actual genotype; *gld-2(q497).*
[k] Actual genotype; *gld-2(q497); rack-1(tm2262).*
[l] Actual genotype; *gld-3(q730).*
[m] Actual genotype; *gld-3(q730); rack-1(tm2262).*

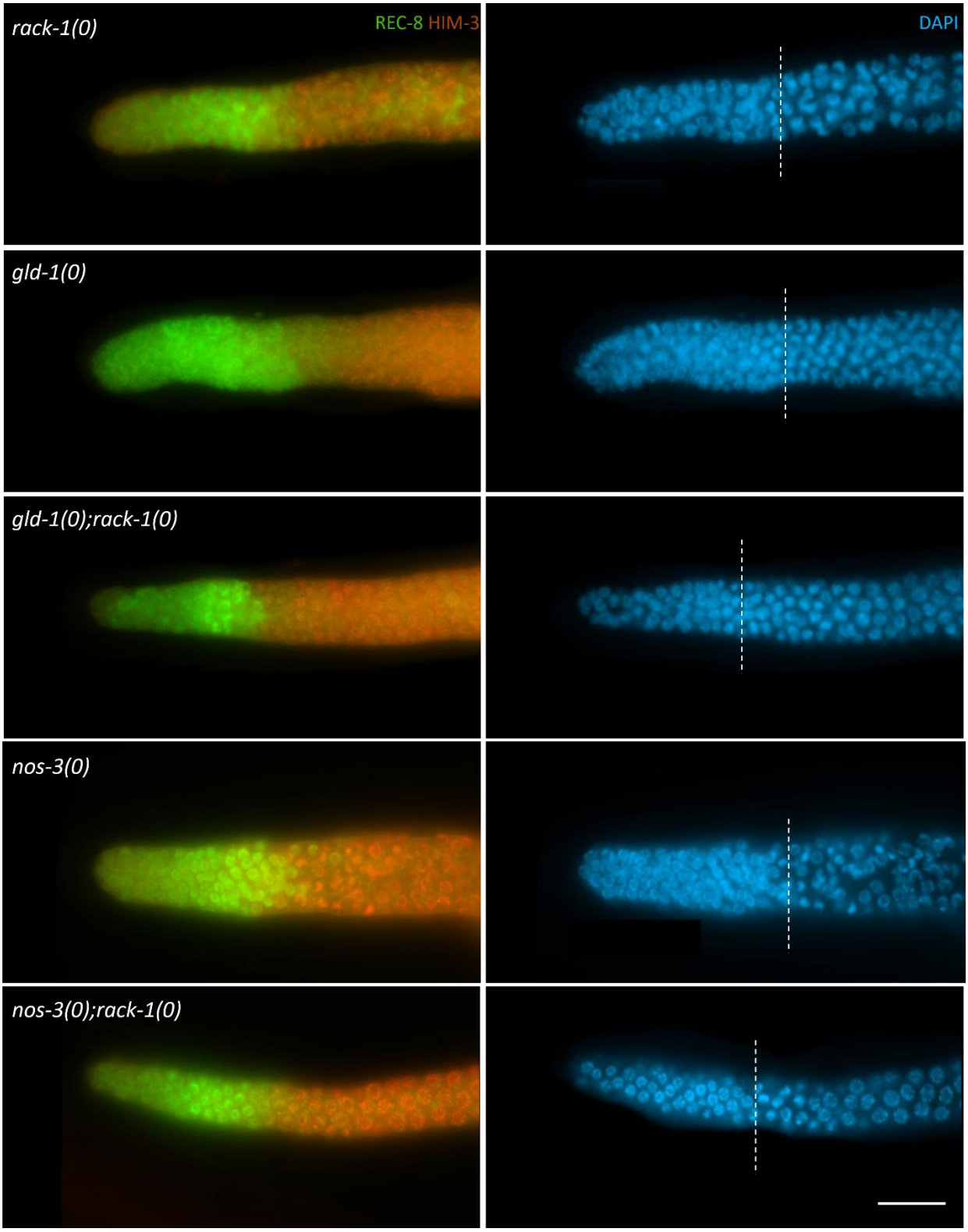
rack-1(0)
REC-8 HIM-3
DAPI
gld-1(0)
gld-1(0);rack-1(0)
nos-3(0)
nos-3(0);rack-1(0)

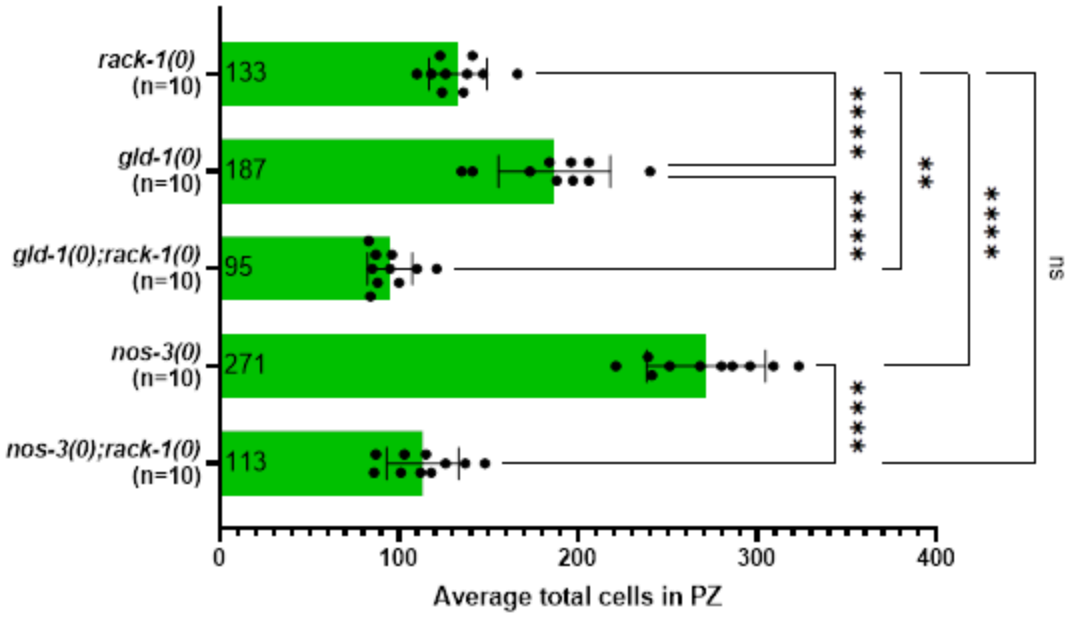

Figure 3.7 - Loss of *rack-1* does not cause meiotic entry defects in combination with GLD-1 pathway mutants at 20 °C. Top - Representative images of the proliferative zone of *rack-1(tm2262), gld-1(q485), gld-1(q485); rack-1(tm2262), nos-3(oz231) and nos-3(oz231); rack-1(tm2262)* young adult gonads. Animals were raised at 20 °C, dissected at one day past the L4 stage, stained with α-REC8 (proliferation marker) and α-HIM-3 (meiotic marker) antibodies to determine the size of the proliferative zone. Nuclear morphology was detected using DAPI. The dashed line represents the transition into meiosis. Scale bar = 20 μm. Bottom - Average number of cells in the proliferative zone (PZ) (x-axis) is depicted in the bar graph for the given genotype (y-axis). Each point represents an individual gonad. Error bars represent ± standard deviation (S.D). Asterisks represent statistical differences determined by a one-way ANOVA with Tukey HSD *post hoc* test. ns = not significant, **p=0.0014 ****p<0.0001.

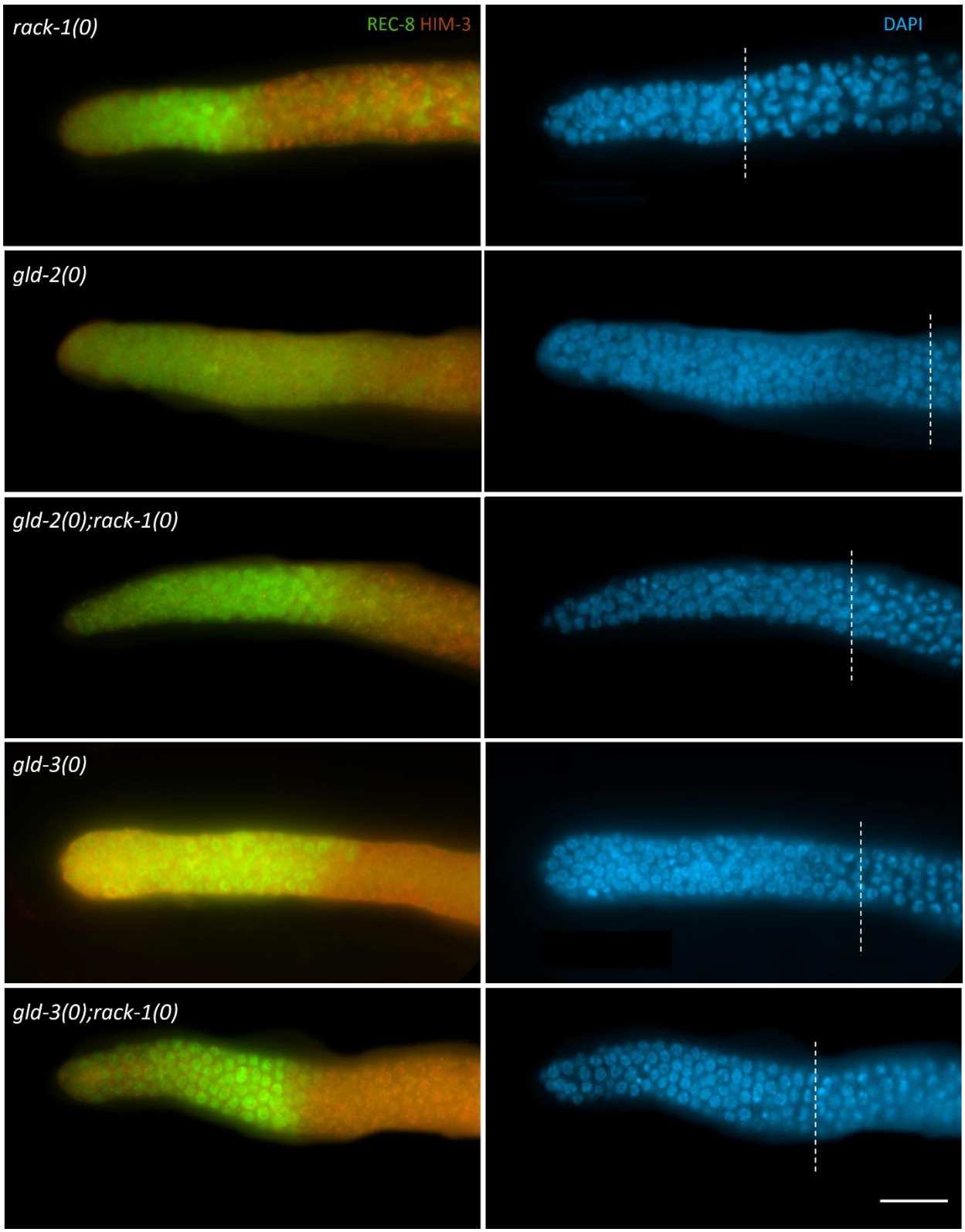
rack-1(0)
REC-8 HIM-3
DAPI
gld-2(0)
gld-2(0);rack-1(0)
gld-3(0)
gld-3(0);rack-1(0)

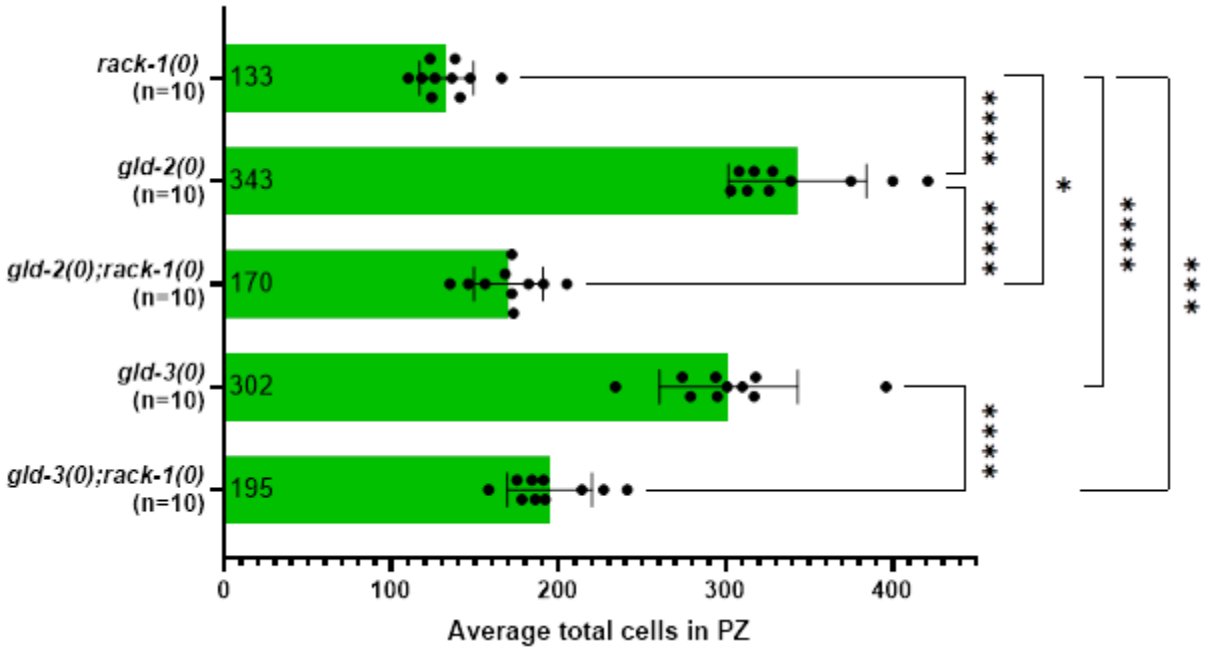

Figure 3.8 - Loss of *rack-1* does not cause meiotic entry defects in combination with GLD-2 pathway mutants at 20 °C. Top - Representative images of the proliferative zone of *rack-1(tm2262), gld-2(q497), gld-2(q497); rack-1(tm2262), gld-3(q730) and gld-3(q730); rack-1(tm2262)* young adult gonads. Animals were raised at 20 °C, dissected at one day past the L4 stage, stained with α-REC8 (proliferation marker) and α-HIM-3 (meiotic marker) antibodies to determine the size of the proliferative zone. Nuclear morphology was detected using DAPI. The dashed line represents the transition into meiosis. Scale bar = 20 μm. Bottom - Average number of cells in the proliferative zone (PZ) (x-axis) is depicted in the bar graph for the given genotype (y-axis). Each point represents an individual gonad. Error bars represent ± standard deviation (S.D). Asterisks represent statistical differences determined by a one-way ANOVA with Tukey HSD *post hoc* test. *p=0.0176 ***p=0.0002 ****p<0.0001.

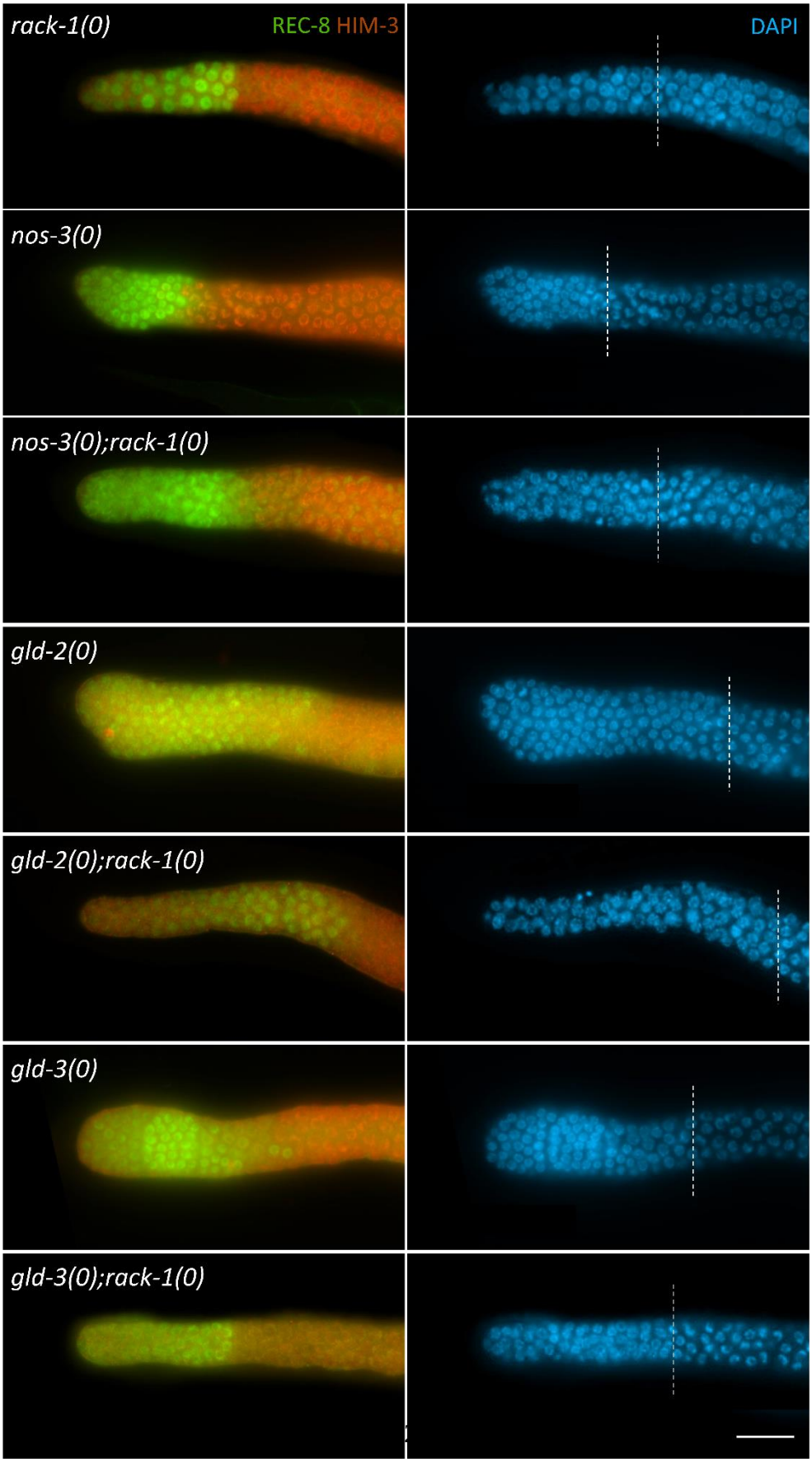
rack-1(0)
REC-8 HIM-3
DAPI
nos-3(0)
nos-3(0);rack-1(0)
gld-2(0)
gld-2(0);rack-1(0)
gld-3(0)
gld-3(0);rack-1(0)

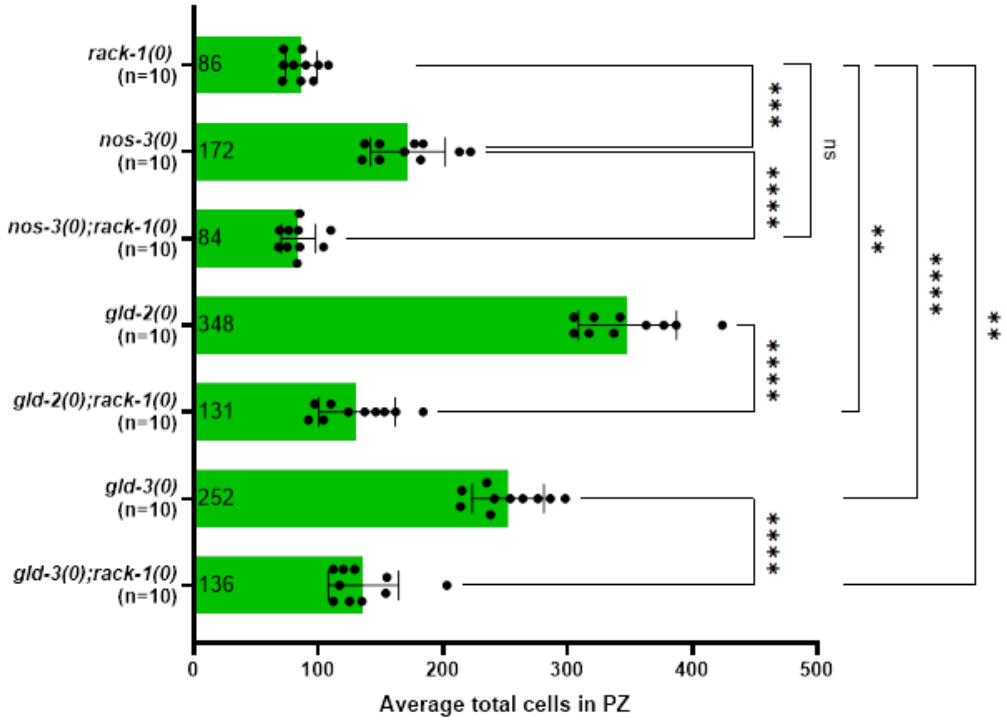

Figure 3.9 - Loss of *rack-1* does not cause meiotic entry defects in combination with GLD pathway mutants at 25 °C. Top - Representative images of the proliferative zone of *rack-1(tm2262), nos-3(oz231), nos-3(oz231); rack-1(tm2262), gld-2(q497), gld-2(q497); rack-1(tm2262), gld-3(q730) and gld-3(q730); rack-1(tm2262)* young adult gonads. Animals were raised at 25 °C, dissected at one day past the L4 stage, stained with α-REC8 (proliferation marker) and α-HIM-3 (meiotic marker) antibodies to determine the size of the proliferative zone. Nuclear morphology was detected using DAPI. The dashed line represents the transition into meiosis. Scale bar = 20 μm. Bottom - Average number of cells in the proliferative zone (PZ) (x-axis) is depicted in the bar graph for the given genotype (y-axis). Each point represents an individual gonad. Error bars represent ± standard deviation (S.D). Asterisks represent statistical differences determined by a

one-way ANOVA with Tukey HSD *post hoc* test. ns = not significant **p<0.01 ***p=0.001 ****p<0.0001.

Table 3.8 - *rack-1(0)* does not enhance the proliferative zone size of *glp-1* gf mutants

Analysis at 20 °C

Genotype	Average length of PZ (gcd) (S.D.; range)[a]	Average total cells in PZ (S.D.; range)[b]	n[c]
Wildtype (N2)	18 (2; 16-20)	242(35; 183-307)	14
rack-1(0)[d]	15 (2; 11-19)	133(16; 110-160)	10
glp-1(ar202gf)[e]	29 (6; 17-44)	371 (93; 277-579)	10
glp-1(ar202gf); rack-1(0)[f]	25 (16; 12-93)	204 (109; 113-462)	10
glp-1(oz264gf)[g]	24 (2; 20-26)	321 (40; 267-281)	10
glp-1(oz264gf); rack-1(0)[h]	29 (4; 22-36)	296 (69; 197-402)	10

[a] Animals were dissected one day past the L4 stage, fixed and stained with DAPI and α-REC-8 and α-HIM-3 antibodies. The length of the proliferative zone (PZ) was determined by counting the extent (germ cell diameter) of REC-8 expression and averaged from a minimum of 14 animals. S.D. = Standard Deviation; Range = minimum - maximum values obtained.

[b] The average total number of cells in the proliferative zone (PZ) was determined using DAPI staining (nuclear morphology). Cells were counted until the transition zone, marked by crescent-shaped nuclei (DAPI staining (nuclear morphology). S.D. = Standard Deviation; Range = minimum-maximum values obtained.

[c] n refers to total number of gonad arms analyzed for average total of cells in the PZ.

[d] Actual genotype; *rack-1(tm2262).*

[e] Actual genotype; *glp-1(ar202gf).*

[f] Actual genotype; *glp-1(ar202gf); rack-1(tm2262).*

[g] Actual genotype; *glp-1(oz264gf).*

[h] Actual genotype; *glp-1(oz264gf); rack-1(tm2262).*

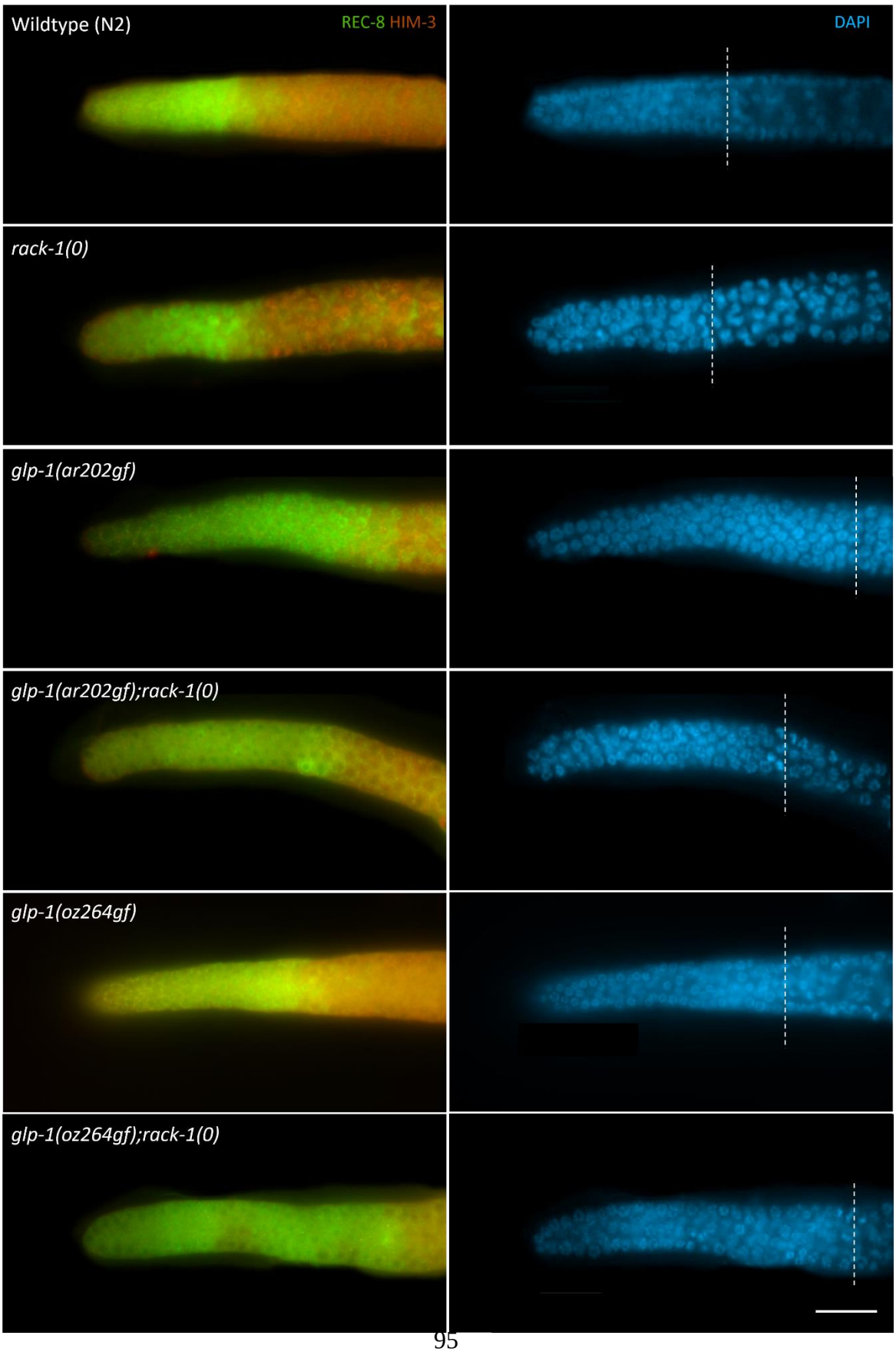
Wildtype (N2)
REC-8 HIM-3
DAPI
rack-1(0)
glp-1(ar202gf)
glp-1(ar202gf);rack-1(0)
glp-1(oz264gf)
glp-1(oz264gf);rack-1(0)

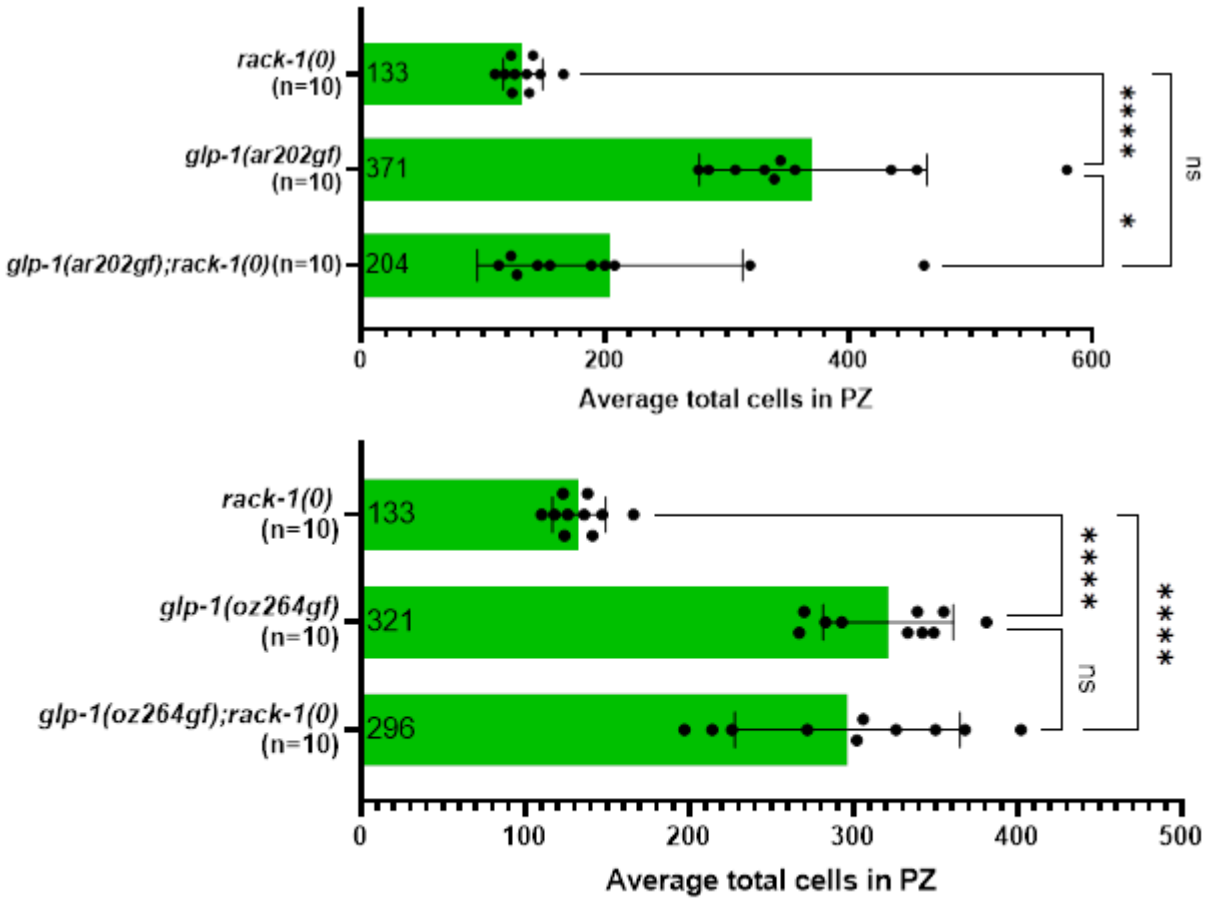

Figure 3.10 Loss of *rack-1* does not increase the proliferative zone size in GLP-1/Notch gain-of-function mutants. Top - Representative images of the proliferative zone of wildtype (N2), *rack-1(tm2262), glp-1(ar202gf), glp-1(ar202gf); rack-1(tm2262), glp-1(oz262), glp-1(oz264); rack-1(tm2262)* young adult gonads. Animals were raised at 20 °C, dissected at one day past the L4 stage, stained with α-REC8 (proliferation marker) and α-HIM-3 (meiotic marker) antibodies to determine the size of the proliferative zone. Nuclear morphology was detected using DAPI. The dashed line represents the transition into meiosis. Scale bar = 20 μm. Bottom - Average number of cells in the proliferative zone (PZ) (x-axis) is depicted in the bar graph for the given genotype (y-axis). Each point

represents an individual gonad. Error bars represent ± standard deviation (S.D). For *glp-1(ar202gf)* graph asterisks represent statistical differences determined by a Kruskal-Wallis analysis with Dunn's *post hoc* test. ns = not significant *p<0.0320 ****p<0.0001. For *glp-1(oz264gf)* asterisks represent statistical differences determined by a Welch's one-way ANOVA followed by Games-Howell's *post hoc* test. ns = not significant ****p<0.0001.

Chapter 4 – Characterization of RACK-1 in the germline

In Chapter 3, I established a potential role for RACK-1 in the proliferation/differentiation balance in the germline of *C. elegans;* however, it is unclear where, downstream of GLP-1/Notch activation, RACK-1 functions. In order to elucidate *rack-1's* influence on this pathway, I investigated the germline phenotypes associated with a loss of *rack-1* activity, and RACK-1's germline expression using CRISPR tagged alleles of *rack-1*.

4.1 *rack-1* null mutants do not display germline proliferation defects

glp-1(ar202gf)'s over-proliferation phenotype was enhanced when *rack-1* was knocked out through the use of a genetic mutant allele, *rack-1(tm2262).* The strain carrying *rack-1(tm2262)*, generated by the National BioResource Project (NBRP), was obtained from the Caenorhabditis Genetics Center (CGC) where it was outcrossed five times (Barstead et al., 2012). This allele contains a 331 bp deletion, removing the majority of the second and third exon of *rack-1* (Figure 4.1). This is an in-frame deletion that may result in a truncated protein being produced; however, *rack-1* RNAi did not enhance *rack-1(tm2262)* associated phenotypes, and therefore is considered a true null allele (Demarco & Lundquist, 2010). This allele is the primary mutant allele used throughout this thesis; however, another allele, *rack-1(ok3676),* was used to ensure phenotypes observed were due to a loss of *rack-1* and not any uncharacterized background mutations present in the strain. A strain carrying *rack-1(ok3676)*, generated by the NBRP, was obtained from the CGC, where it was outcrossed once (Barstead et al., 2012). This allele contains a 591 bp deletion, removing half of exon 2 and 4, and all of exon 3 (Figure 4.1). This deletion results

in a frameshift of the remaining portion of exon four; however, no premature stop codon is formed. Worms carrying either allele did not express a protein detectable at the expected size (35.8 kDa) as determined by western blot analysis of whole-worm lysate utilizing a RACK-1 C-terminal specific antibody generously provided by Dr. Shih-Peng Chan at National Taiwan University (Figure 4.1) (Chu et al., 2014). This antibody would have been able to detect the truncated protein that may be produce in *rack-1(tm2262)*; however, no such protein was detected by western blot analysis (~25 kDa).

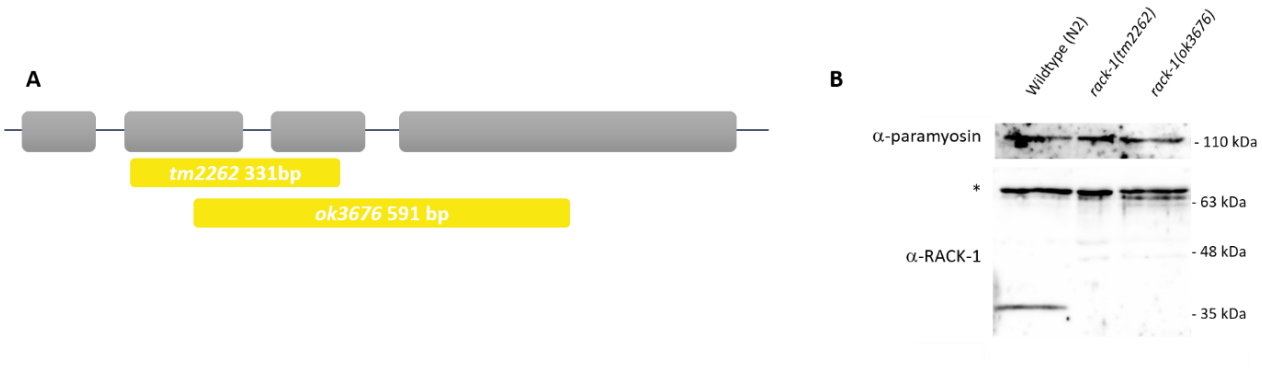

Figure 4.1 – Genetic mutations for *rack-1* A) Schematic of the *rack-1* deletion mutants *tm2262* and *ok3676.* B) Analysis of RACK-1 expression on whole worm lysate from 100 young adult wildtype (one day past the L4 stage), *rack-1(tm2262),* and *rack-1(ok3676)* worms. RACK-1 was detected just above 35 kDa in the wildtype lane. Paramyosin was used as a loading control. * represents non-specific band.

Both mutant alleles are homozygous viable; however, these animals were significantly delayed in development compared to wildtype, and other mutant genotypes. Strains carrying *rack-1(tm2262) or rack-1(ok2676)* take about a day longer to develop from arrested L1 larva into L4 larva at 20 °C. This is consistent with previously reported descriptions of *rack-1(tm2262)* (Demarco & Lundquist, 2010). Additionally, animals carrying either *rack-1* mutant allele had significantly reduced brood sizes at 20 °C compared to wildtype worms; wildtype (N2) – 239; *rack-1(tm2262)* – 19; *rack-1(ok3676)* – 12. This reduction in brood size was previously reported for *rack-1(tm2262)* and *rack-1* RNAi (Ai et al., 2009; Demarco & Lundquist, 2010) (Table 4.1). *rack-1* RNAi had been previously reported to result in sterility at 25 °C (Ai et al., 2009). I confirmed this sterility with both *rack-1(tm2262)* and *rack-1(ok3676)* producing no viable progeny when grown at 25 °C (Table 4.1).

To determine if the reduction in brood size, and sterility, was a result of a decrease in the production of embryos, an embryonic viability assay was performed. This assay compares the number of embryos to the number of hatched worms produced (progeny) to determine embryo viability. Wildtype (N2) animals have almost 100% embryonic viability at 20 °C, whereas *rack-1(tm2262)* and *rack-1(ok3676)* had 45% and 43% embryonic viability, respectively (Table 4.1). This highlights that *rack-1* mutant animals produce fewer embryos compared to wildtype (92 - 95% reduction), and that roughly half of the embryos produced are not viable. At 25 °C, these mutants still produced fewer

embryos compared to wildtype (90 - 99% reduction); however, none of these embryos were viable (0 progeny produced) (Table 4.1).

This temperature sensitive phenotype of sterility has been previously reported for other genes, specifically *pgl-1* and *deps-1*, whose proteins localize to germ granules (P granules) (Kawasaki et al., 1998; Spike et al., 2008). These studies demonstrated that maternal contribution of the protein of interest was sufficient to rescue the sterility found in mutant animals (Kawasaki et al., 1998; Spike et al., 2008). To determine if a maternal contribution of RACK-1 was sufficient to rescue the reduction in embryos, and/or embryonic viability, an embryonic viability assay was performed on maternal + zygotic – animals (m^+z^-) at 25 °C. These animals were non-balanced (*rack-1(tm2262)* homozygotes) F1 progeny from animals heterozygous for *rack-1(tm2262).* Half of the m^+z^- animals analyzed were sterile (5 out of 10 animals) and the other half of the animals gave rise to at least one progeny with a slight increase in the number of embryos produced (Table 4.1); therefore, maternal contribution is not sufficient to rescue the sterility and embryonic viability, although there appears to be some contribution.

Table 4.1 - Embryonic viability assay of *rack-1* mutants and *rack-1* CRISPR-tagged alleles

Genotype	Average number of embryos laid (S.D.; range)[a]	Average number of progeny hatched (S.D.; range)[b]	Embryonic viability (%)[c]	n[d]
Analysis at 20 °C				
Wildtype (N2)	242 (47; 144-299)	239(47; 140-290)	99	14
rack-1(tm2262)	42 (40; 0-113)	19(16; 0-42)	45	14
rack-1(ok3676)	28 (22; 0-58)	12 (14; 0-38)	43	11
rack-1(ug12)[e]	115 (25; 67-164)	166 (22; 127-207)	100	12
rack-1(ug17)[f]	134 (21; 103-163)	181 (20; 149-206)	100	13
Analysis at 25 °C				
Wildtype (N2)	90 (31; 36-133)	106 (36; 52-153)	100	14
rack-1(tm2262)	11 (17; 0-54)	0 (0; 0-0)	0	13
m^+z^- rack-1(tm2262)[g]	17 (9; 8-36)	1 (1; 0-3)	6	10
rack-1(ok3676)	1(2; 0-6)	0 (0; 0-0)	0	10
rack-1(ug12)[d]	71 (17; 48-100)	84 (24; 44-123)	100	15
rack-1(ug17)[e]	85 (19; 56-119)	85 (18; 57-123)	100	15

[a] Single animals were put on individual plates and allowed to lay eggs for 24 hours at which point the were moved to a new plate. This was repeated until egg laying ceased, approximately 6 days. S.D. = Standard Deviation; Range = minimum-maximum values obtained.

[b] The average number of progeny hatched was counted 48-72 hours after the parental worm was removed from the plate. S.D. = Standard Deviation; Range = minimum-maximum values obtained.

[c] Embryonic viability was determined by dividing the average number of progeny hatched by the average number of embryos laid for each genotype.

[d] n refers to total number of individual animals analyzed for each genotype.

[e] Actual genotype; *rack-1(ug12[rack-1::V5:2XFLAG]).*

[f] Actual genotype; *rack-1(ug17[rack-1::V5::SBP]).*

[g] *m^+z^-rack-1(tm2262)* worms were obtained by picking non-balanced F1 progeny from *rack-1(tm2262)* heterozygous mothers (*rack-1(tm2262)/nT1g; nT1g is a balancer chromosome that contains a wildtype copy of rack-1).*

The reduction in viable embryos in *rack-1* mutants is likely due to *rack-1's* requirement in cytokinesis in the early embryo, as previously discussed in Chapter 1 (Ai et al., 2009; Nilsson et al., 2004); however, the reduction in the number of embryos produced could be due to a disruption in the stem cell proliferation/ differentiation balance resulting in a decreased ability to produce gametes (sperm and/or oocytes). To determine if a loss of *rack-1* alone disrupts stem cell proliferation, as seen in *glp-1* gain-of-function mutant backgrounds, the germline phenotypes of both null mutants, *tm2262 and ok3676* were analyzed. The majority of the animals for both mutants had no ectopic proliferation as determined by α-REC-8 (proliferation marker) and α-HIM-3 (meiotic marker) staining or by whole mount DAPI (nuclear staining) (Table 4.2). *rack-1* mutant germlines were smaller and had a decrease in the number of developing oocytes at both 20 °C and 25 °C (Figure 4.2). Some of the animals analyzed had germlines that lacked the presence of developing oocytes and instead had only a small number of developing spermatocytes and mature sperm at the proximal end of the germline. These were referred to as 'defective oogenesis' because they appeared to have failed to, or were delayed in, switching from spermatogenesis to oogenesis. Additionally, a very small percentage (less than 2% at 20 °C, and less than 6% at 25 °C) of germlines analyzed had proximal proliferation in the germline, suggesting that loss of *rack-1* alone does not obviously disrupt the proliferation/differentiation balance, and/or that *rack-1's* effect is masked due to redundancy with other genes within this pathway (Table 4.2).

Table 4.2 - Germline phenotypes associated with a loss of *rack-1*

	Germline Phenotype[a]				
Genotype	Wildtype (%)[b]	Pro (%)[c]	Defective oogenesis (%)[d]	Empty or underdeveloped (%)[e]	n[f]
Analysis at 20 °C					
rack-1(tm2262)	96	1	2	1	442
rack-1(ok3676)	93	2	2	3	204
Analysis at 25 °C					
rack-1(tm2262)	85	0	9	6	334
rack-1(ok3676)	85	6	9	0	82

[a] Animals were either dissected one day past the L4 stage, fixed and stained with DAPI, α-REC-8 and α-HIM-3 antibodies, or analyzed by whole mount DAPI.
[b] Wildtype refers to gonad arms with no proliferative cells outside of the proliferative zone and visible sperm and oocytes present.
[c] Protumour (Pro) refers to gonad arms that have normal entry into meiosis but a pool of proliferative cells at the most proximal end of the germline.
[d] Defective oogenesis refers to gonad arms that lack the presence of developing oocytes and have developing spermatocytes and sperm present at the proximal end of the germline.
[e] Empty or underdeveloped refers to animals where no germline arm was detectable by whole-mount DAPI, or it was severely underdeveloped (very few cells).
[f] n refers to total number of gonad arms analyzed.

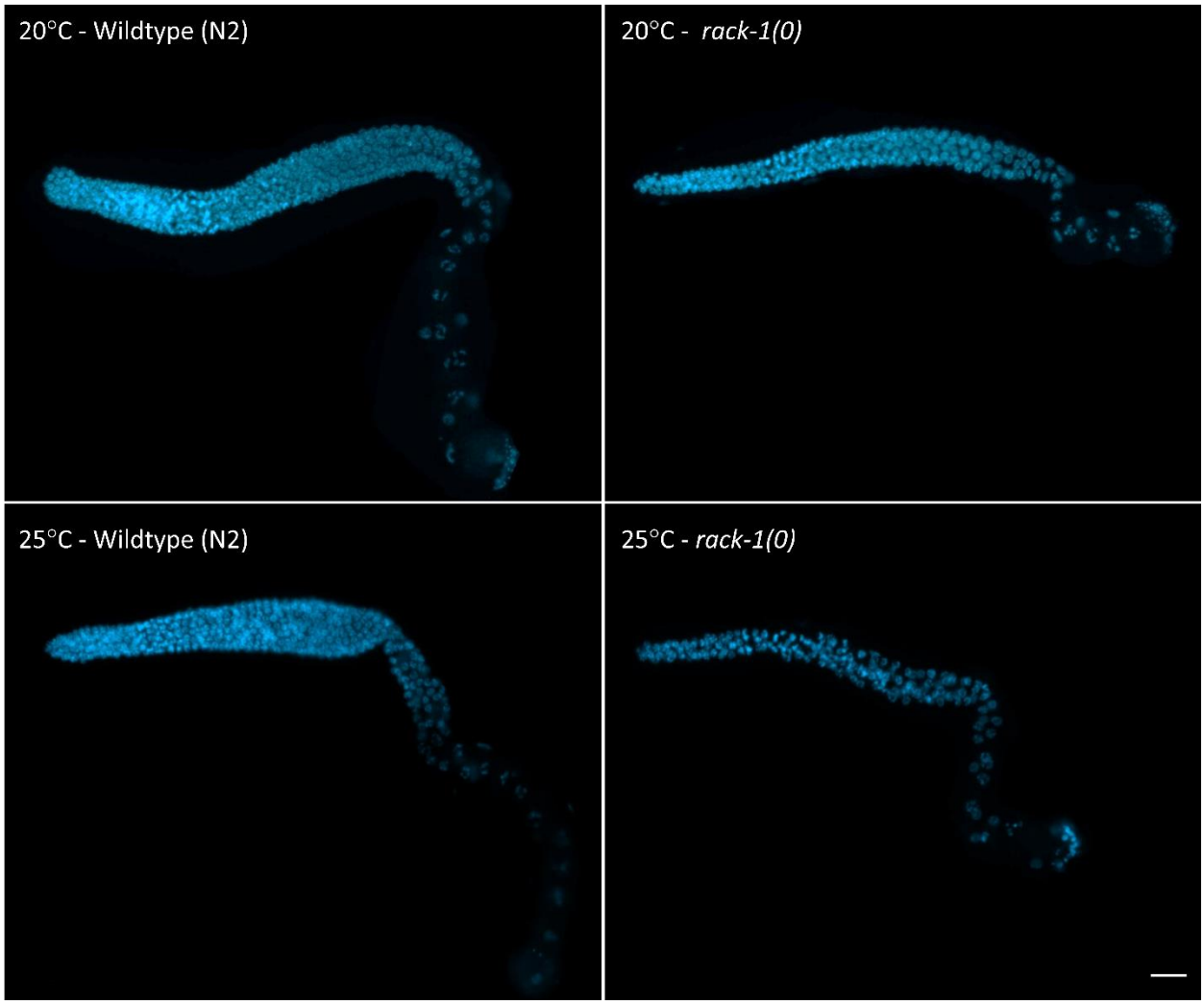

Figure 4.2 - *rack-1(0)* germlines are smaller and have reduced oogenesis. Representative images of wildtype (N2) and *rack-1(tm2262)* young adult gonads at 20 °C and 25 °C. Animals were raised at 20 °C or 25 °C, dissected at one day past the L4 stage, and analyzed with DAPI (nuclear morphology). Scale bar = 20 μm.

4.2 RACK-1's expression in the germline

Previous research on *rack-1* in *C. elegans* primarily focused on its role in the developing embryo and neurons (Ai et al., 2009, 2011; Demarco & Lundquist, 2010). RACK-1's expression in these cells was determined using either a polyclonal antibody generated against mammalian RACK1 (sc-10775) or tagged transgenes of *rack-1* [*IqEx463*(*rack-1::GFP* + *lin-15(+))* and *IqIs126*(*rack-1::MYC* + *osm-6::GFP)).* The polyclonal antibody utilized in previous publications, SC-10775, had been discontinued and replaced with a monoclonal antibody raised against the same C-terminal epitope of mammalian RACK1 (SC-17754) (Ai et al., 2009). Transgenes, both extrachromosomal (*IqEx463)* or integrated (*IqIs126),* are known to be formed from multiple copies of the construct, resulting in overexpression of the gene of interest, and are often silenced in the germline (Kelly et al., 1997; Praitis et al., 2001); therefore, I compared the expression pattern of the transgenes to that of the monoclonal antibody. Although strong expression of both transgenes was identifiable in the DTC, as previously reported, the expression pattern in the germline was very different from the pattern detected with the antibody. The *Iqis126* transgene showed an expression pattern reminiscent of cytoplasmic/membrane expression, whereas the antibody showed punctate/aggregated expression throughout cells of the germline, similar to the published results with the polyclonal antibody (Ai et al., 2009) (Figure 4.3); however, the antibody gave the same expression pattern in *rack-1(tm2262)* and control worms (N2) (Figure 4.3). The western blot analysis from Section 4.1 suggests that *rack-1(tm2262)* most likely does not produce a detectable truncated protein; therefore, this immunostaining is likely non-specific. As the expression profiles

were inconsistent between the two reagents, and from previously published *in vivo* expression in the germline, I generated two independent CRISPR tagged alleles as CRISPR editing efficiency in *C. elegans* had been greatly improved (See Chapter 2 for details) (Dokshin et al., 2018).

Previous characterization of the C-terminal tagged transgenes (*IqEx463* and *IqIs126*) showed that the transgenes rescued both the neuronal defects and lowered brood size associated with *rack-1(tm2262),* suggesting that the inserted tag did not disrupt the function of RACK-1 (Demarco & Lundquist, 2010); therefore, CRISPR editing was designed to create two independent tagged alleles with either V5::2xFLAG tag (*rack-1(ug12)*) or a V5::SBP tag (Streptavidin Binding Peptide) (*rack-1(ug17)*) inserted immediately before the stop codon at the end of exon four. Both the V5::2xFLAG, and V5::SBP tags were codon optimized to increase the likelihood of proper expression in the *C. elegans* germline. The expression of both tagged alleles was verified by western blot analysis of whole worm lysates (Figure 4.4).

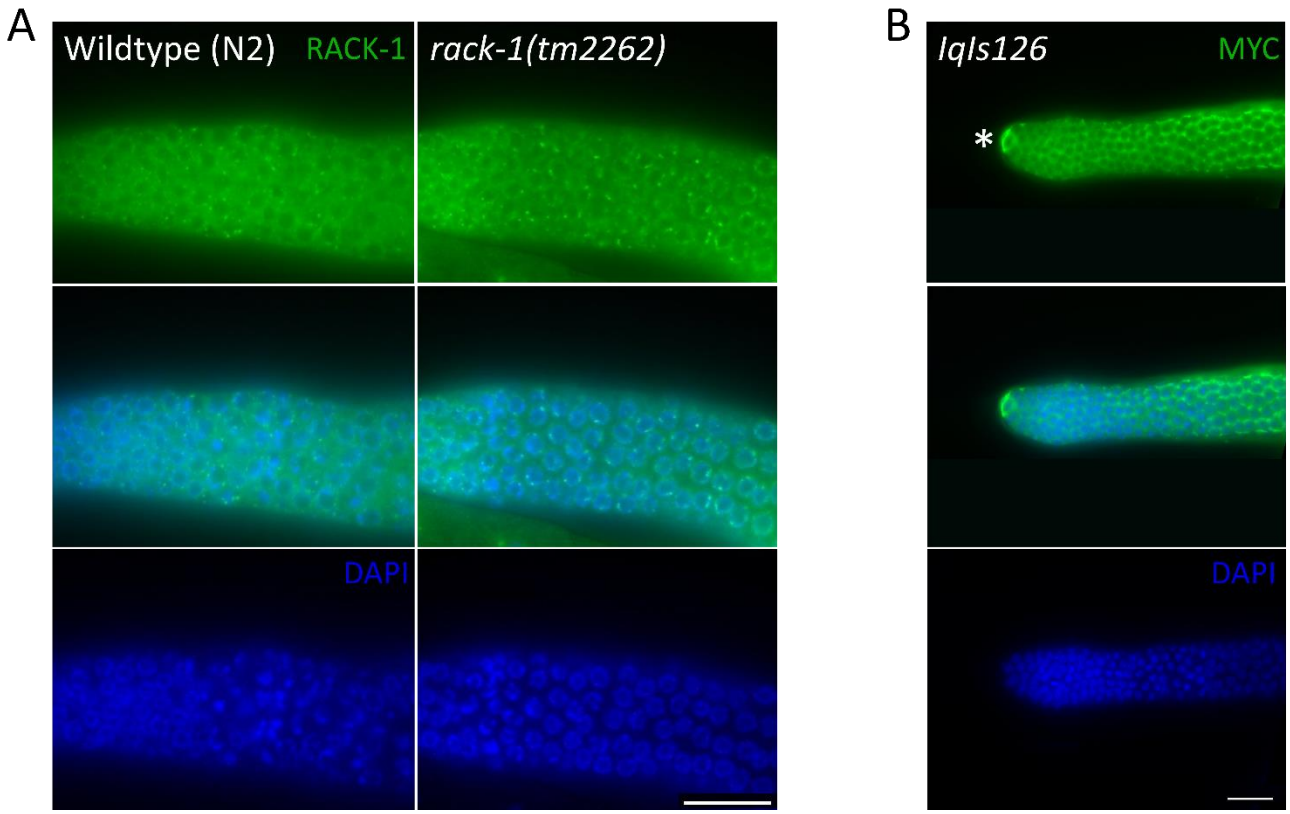

Figure 4.3 - RACK-1's *in vivo* expression using available reagents. Representative images of RACK-1 expression within the germline. A) RACK-1's *in vivo* expression in wildtype (N2) and *rack-1(tm2262)* gonads. The area depicted is the transition zone with the distal end on the left-hand side. Animals were raised at 20 °C, dissected at one day past the L4 stage, and RACK-1's expression analyzed using the mammalian RACK1 antibody (SC-17754) and DAPI (nuclear morphology). B) RACK-1's *in vivo* expression determined utilizing the *lqIs126* transgene (*rack-1::MYC + osm-6::GFP).* Animals were raised at 20 °C, dissected at one day past the L4 stage, and RACK-1::MYC was detected with α-MYC antibodies. The strong intensity at the distal most end (left, marked by *) of the germline represents expression in the DTC. Scale bar = 20 μm.

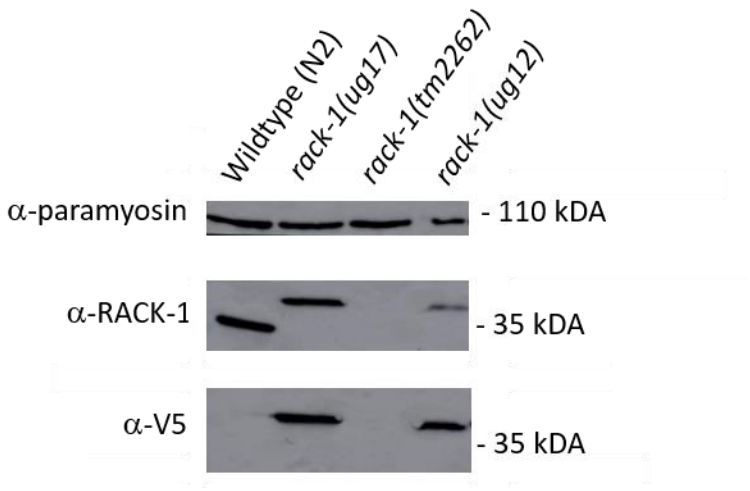

Figure 4.4 - Expression of RACK-1 CRISPR tagged alleles. Expression of RACK-1::V5::SBP (*rack-1(ug17)*) and RACK-1::V5::2xFLAG (*rack-1(ug12)*) was confirmed through western blot analysis on 100 young adult worms (one day past the L4 stage). Expression of the upshifted transgenes, and wildtype RACK-1 was detected using α-RACK-1 antibodies. Expression of the transgenes only was detected using α-V5 antibodies. Paramoysin was used as a loading control.

In order to determine if the tagged alleles had any impact on RACK-1's function, I performed an embryonic viability assay for *rack-1(ug12)* and *rack-1(ug17)*. At 20 °C both tagged alleles had 100% embryonic viability, producing 166 and 181 progeny respectively (Table 4.1) At 25 °C none of the animals analyzed for either *ug12* or *ug17* were sterile, and instead had 100% embryonic viability, producing approximately 84 progeny (Table 4.1); therefore, both tagged alleles appear to produce functional RACK-1 protein. The number of progeny produced was lower than that of wildtype; therefore, there may be some reduced function.

To further determine if tagging *rack-1* interfered with proper RACK-1 function, the size of the proliferative zone was determined for both *rack-1(ug12)* and *rack-1(ug17)*. *rack-1(tm2262)* alone, as mentioned previously, had a 45% reduction in the size of the proliferative zone compared to wildtype animals (as determined by total cell count) (Table 4.5). *rack-1(ug12)* had an average of 162 cells and 143 cells at 20 °C and 25 °C respectively; a reduction of 33% and 31% compared to wildtype (Table 4.5). *rack-1(ug17)* had an average of 168 cells and 135 cells at 20 °C and 25 °C respectively; a reduction of 31% and 36% compared to wildtype (Table 4.5). The PZ size in *rack-1(ug12)* and *rack-1(ug17)* at both 20 and 25 °C was statistically different than in *rack-1(tm2262)* animals (One-way ANOVA all p-values < 0.05). Although these alleles still had a reduction in the proliferative zone size compared to wildtype, the stability of the proliferative zone size between 20 °C and 25 °C is more reminiscent of wildtype than *rack-1(tm2262),* which gave a larger reduction between the two temperatures (Table 4.5). Taken together with

the embryonic viability assay, this data suggests that the CRISPR tagged *rack-1* alleles may have some disrupted function but are still highly functional and similar to wildtype RACK-1.

Table 4.3 - *rack-1(ug12)* and *rack-1(ug17)* proliferative zone analysis

Genotype	Average length of PZ (gcd) (S.D.; range)[a]	Average total cells in PZ (S.D.; range)[b]	n[c]
Analysis at 20 °C			
Wildtype (N2)	18 (2; 16-20)	242 (35; 183-307)	14
rack-1(0)[d]	15 (2; 11-19)	133 (16; 110-160)	10
rack-1(ug12)[e]	17 (1; 15-20)	162 (23; 123-194)	10
rack-1(ug17))[f]	16 (1; 14-18)	168 (24; 130-196)	10
Analysis at 25 °C			
Wildtype (N2)	16 (2; 12-20)	208 (26; 180-256)	14
rack-1(0)[d]	15 (2; 11-19)	86 (13; 71-108)	10
rack-1(ug12)[e]	16 (1; 13-19)	143 (21; 106-168)	10
rack-1(ug17)[f]	14 (1; 11-16)	134 (19; 103-165)	10

[a] Animals were dissected one day past the L4 stage, fixed and stained with DAPI and α-REC-8 antibodies. The length of the proliferative zone (PZ) was determined by counting the extent (germ cell diameter) of REC-8 expression and averaged from a minimum of 10 animals. S.D. = Standard Deviation; Range = minimum-maximum values obtained.

[b] The average total number of cells in the proliferative zone (PZ) was determined using DAPI staining (nuclear morphology). Cells were counted until the transition zone, marked by crescent-shaped nuclei (DAPI staining (nuclear morphology)).

[c] n refers to total number of gonad arms analyzed.

[d] Actual genotype; *rack-1(tm2262).*

[e] Actual genotype; *rack-1(ug12[rack-1::V5::2xFLAG]).*

[f] Actual genotype; *rack-1(ug17[rack-1::V5::SBP]).*

4.3 RACK-1's germline expression

Key regulators in the GLP-1/Notch pathway, such as SYGL-1 and GLD-1, are expressed in distinct patterns in the germline that reflects their function within the proliferation/differentiation balance. SYGL-1 is expressed within the proliferative zone, reflective of its role in promoting proliferation, whereas GLD-1 is expressed at low levels in the proliferative zone and instead has much higher levels as cells enter into meiosis, consistent with its requirement for entry into and progression through meiosis (Jones et al., 1996; Kocsisova et al., 2019; Shin et al., 2017); therefore, RACK-1's expression profile could provide an insight into its role in regulating the proliferation/differentiation balance. I analyzed RACK-1's *in vivo* expression pattern in the germline utilizing the CRISPR tagged alleles, *rack-1(ug12(rack-1::V5::2XFLAG)* and *rack-1(ug17(rack-1::V5::SBP)* and α-V5 antibodies.

RACK-1 was expressed throughout the distal and proximal germline, with no obvious change in levels throughout (Figure 4.5). RACK-1 was excluded from the nuclei of cells in the distal end; however, low levels appeared to be present in the nucleus of developing oocytes; therefore, low levels distally cannot be conclusively ruled out (Figure 4.6). RACK-1 appeared to be enriched in the cellular membrane, with lower levels within the cytoplasm, which is more apparent in developing oocytes (Figure 4.6). Interestingly, this expresion profile is similar to that detected with the *Iqis126* transgene (Figure 4.3); however, in contrast to the *IqIs126* transgene, no obvious enrichment of RACK-1 was detected in the DTC with *rack-1(ug12)* or *rack-1(ug17)*. It is possible that the high levels

detected in the DTC with *IqIs126* is due to the overexpression of RACK-1, as is common with transgenes.

In order to validate that RACK-1's expression is enriched at the cellular membrane of germ cells, *rack-1(ug12)* and *rack-1(ug17)* were crossed into a background containing a transgene expressing the pleckstrin homology domain (PH) of rat PLC1δ1, fused to the mCherry fluorscent-tag (*Itis44[*pie-1p::mCherry::PH(PLC1δ1)]), generated in Dr. Dave Pilgrim's laboratory. PH(PLC1δ1) localizes to plasma membranes through its binding of phosphatidylinosoitol 4,5-bisphosphatase and can therefore be used to vizualize the cellular membrane (Kachur et al., 2008). This trangene has been demonstrated to be expressed within the *C. elegans* germline. Co-localization experiments demonstrated that RACK-1 does strongly co-localize with PH-mCherry expression throughout the germline (Figure 4.7). Additionaly, the germ cell membranes were the expected hexagonal shape, as seen in wildtype germlines, in contrast to the disrupted membrane organization phenotype previously associated with *rack-1* RNAi. This further supports that that *rack-1(ug12),* and *rack-1(ug17)* produce functional RACK-1 protein (Ai et al., 2009).

The generation of tagged *rack-1* alleles at the endogenous loci, which are expressed at endogenous levels, will be a useful reagent for future biochemical experiments focused on RACK-1; however, the uniform expression of RACK-1 throughout the germline did not provide any clarity on where in the genetic pathway controlling the proliferation/differentation decision RACK-1 functions. This data does support the

possibility of a role for *rack-1* within the cells of the germline, as opposed to *rack-1* only acting in somatic cells, such as the DTC, to impact the proliferation/differenation balance.

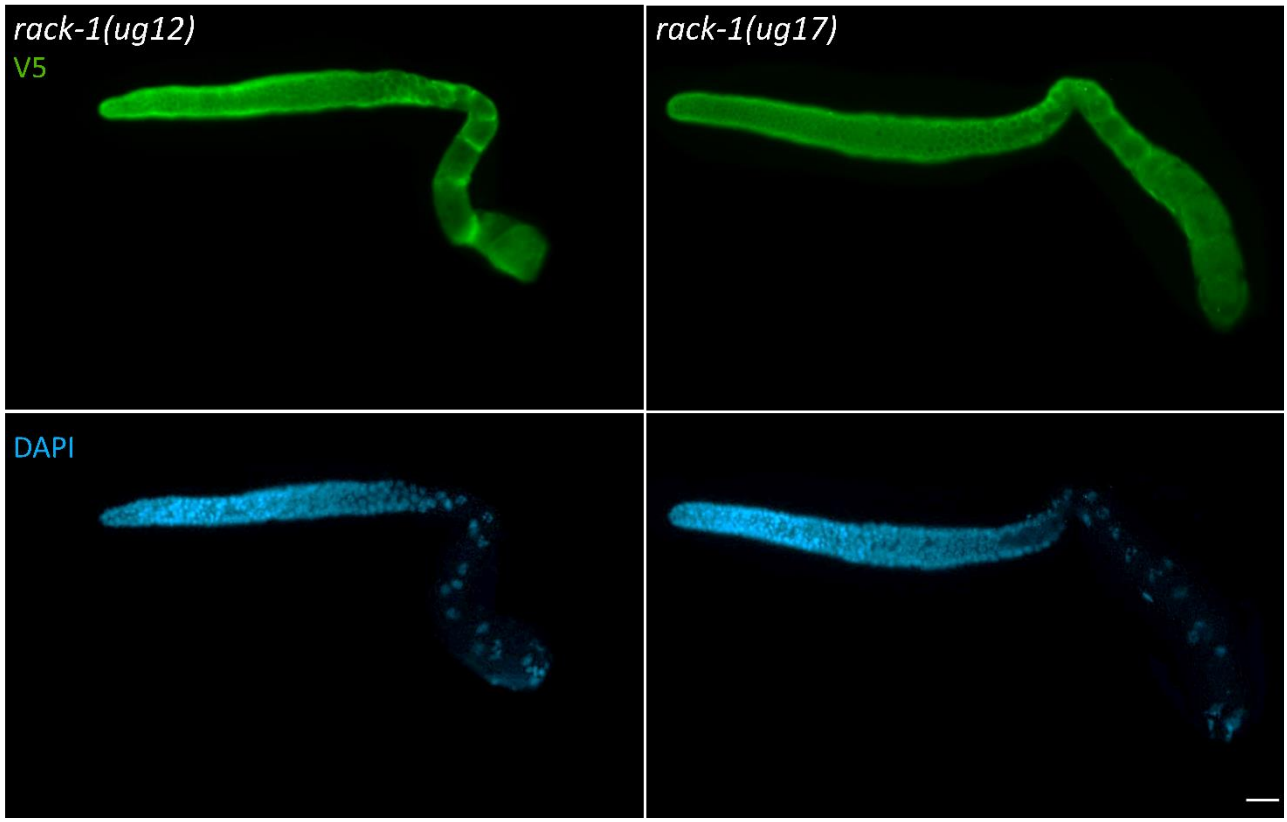

Figure 4.5 - RACK-1's *in vivo* expression using the CRISPR-tagged alleles. Representative images of *rack-1(ug12[rack-1:V5::2xFLAG]*) and *rack-1(ug17[rack-1::V5::SBP)]* young adult gonads. Animals were raised at 20 °C, dissected at one day past the L4 stage, and analyzed for RACK-1 expression using α-V5 antibodies. Nuclear morphology was detected using DAPI. Scale bar = 20 μm.

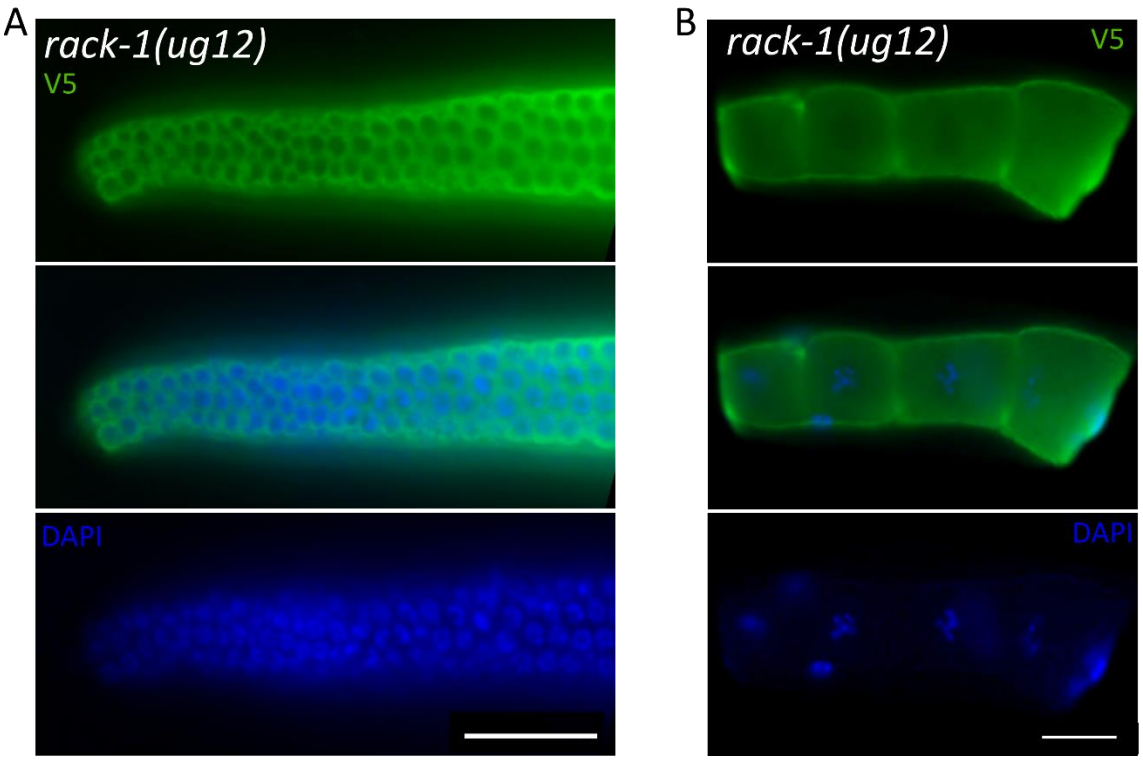

Figure 4.6 - RACK-1's expression in the distal end of the germline and developing oocytes. Representative images of *rack-1(ug12[rack-1::V5::2xFLAG]*) young adult gonadss. Animals were raised at 20 °C, dissected at one day past the L4 stage, and analyzed for RACK-1 expression using α-V5 antibodies. Nuclear morphology was detected using DAPI. Scale bar = 20 μm. A) A magnified image of RACK-1::V5::2XFLAG's expression in the proliferative zone B) A magnified image of RACK-1::V5::2XFLAG's expression in developing oocytes as determined. The distal-most oocyte is located on the left, and the more proximal/mature oocyte is on the right. Scale bar = 20 μm.

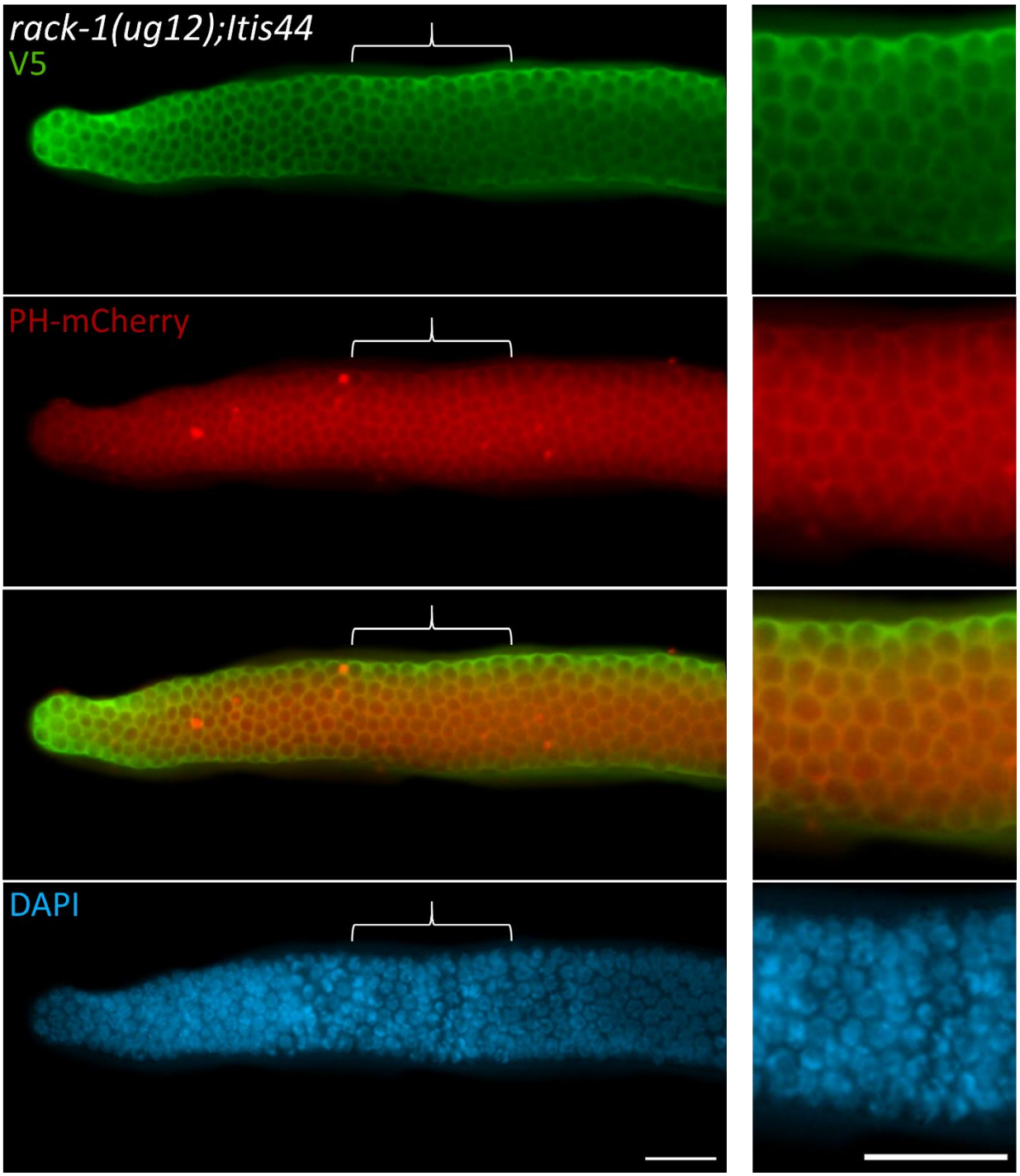

Figure 4.7 - RACK-1 is enriched at the cellular membrane of germ cells. Representative germline images from animals expressing both *rack-1(ug12(rack-*

1::V5::2XFLAG)) and *ltIs44[*pie-1p::mCherry::PH(PLC1δ1)]). Animals were raised at 20 °C, dissected at one day past the L4 stage, and analyzed for co-localization of RACK-1 and PH::mCherry. RACK-1::V5::2xFLAG was detected with α-V5 antibodies, PH::mCherry was detected based on endogenous mCherry expression. Nuclear morphology was detected using DAPI. The white bracket represents the area of the germline that is blown up in the righthand panel. The red spots present in the PH::mCherry panel is debris from the dissected animals stuck onto the germline. Scale bar = 20 μm.

Chapter 5: *rack-1* is required for proper GLD-1 cellular localization and levels

The over-proliferation phenotype associated with a loss of *rack-1* in *glp-1* gain-of-function backgrounds suggests that *rack-1* could function to inhibit proliferation or promote entry and/or progression through meiosis. As previously discussed, *rack-1* does not appear to directly inhibit GLP-1/Notch signaling as a loss of *rack-1* failed to expand the expression of SYGL-1, a direct GLP-1/Notch target (Figure 3.5 and 3.6). In addition, it remains unclear if *rack-1* functions in the GLD meiotic pathways as no clear defect in meiotic entry was identified in various mutant backgrounds (Table 3.7). Previous research uncovered the potential for a protein-protein interaction between GLD-1 and RACK-1 through IP-MS experiments (Akay et al., 2013). To investigate the possibility that *rack-1* may regulate GLD-1's activity, GLD-1's expression and localization was analyzed in *rack-1* mutants using available antibodies. In *rack-1* mutants, GLD-1's overall germline expression pattern resembled that of wildtype, low in the distal and proximal germline, and high in the meiotic zone of the germline until the loop region; however, GLD-1's subcellular localization was dramatically disrupted in the absence of *rack-1,* with the formation of perinuclear GLD-1 aggregates. Using transgenes and available antibodies, I determined that the GLD-1 aggregates localized to P granules, sites of RNA metabolism, throughout the germline. The mislocalization of GLD-1 does not require GLD-1's ability to bind RNA. GLD-1 levels were also found to be reduced in *rack-1* mutant animals as compared to wildtype. I further demonstrate that *rack-1* and *gld-2* function independently to regulate GLD-1's expression. This data highlights a potential mechanism where loss of *rack-1* results in a disruption to GLD-1 (levels and localization), which likely reduces

GLD-1 function and disrupts the balance between proliferation and differentiation in the germline in sensitized backgrounds.

5.1 RACK-1 is required for proper GLD-1 localization

GLD-1, a translational repressor, is required for the entry and progression through meiosis (Francis et al., 1995; Jones et al., 1996; Kadyk & Kimble, 1998). In the absence of GLD-1 germ cells enter meiosis normally, since GLD-2 is present, but fail to progress through meiotic prophase, reverting to mitosis and forming a proximal tumour (Francis et al., 1995). The germline accumulation pattern of GLD-1, low distally with increasing levels as the GSCs enter meiosis, has been shown to be required for proper germline organization (Figure 5.1) (Hansen, Wilson-Berry, et al., 2004; Jones et al., 1996). Interestingly, GLD-1's overall germline accumulation pattern of being low in the distal end then increasing with high levels as cells enter meiosis, was similar to wildtype in *rack-1* mutant germlines; however, its subcellular localization pattern was significantly altered (Figure 5.1). In the absence of *rack-1,* GLD-1 formed perinuclear aggregates throughout the germline at 20 °C (Figure 5.1). This mislocalization phenotype was also seen in *rack-1(tm2262)* and *rack-1(ok3676)* mutants at 25 °C (Figure 5.2). Surprisingly, GLD-1's subcellular localization in *rack-1* mutants at 15 °C resembled that of wildtype germlines (Figure 5.3). This may help to explain the increase in germline phenotypes (sterility, decreased production of oocytes and embryos) associated with *rack-1* mutants at higher temperatures.

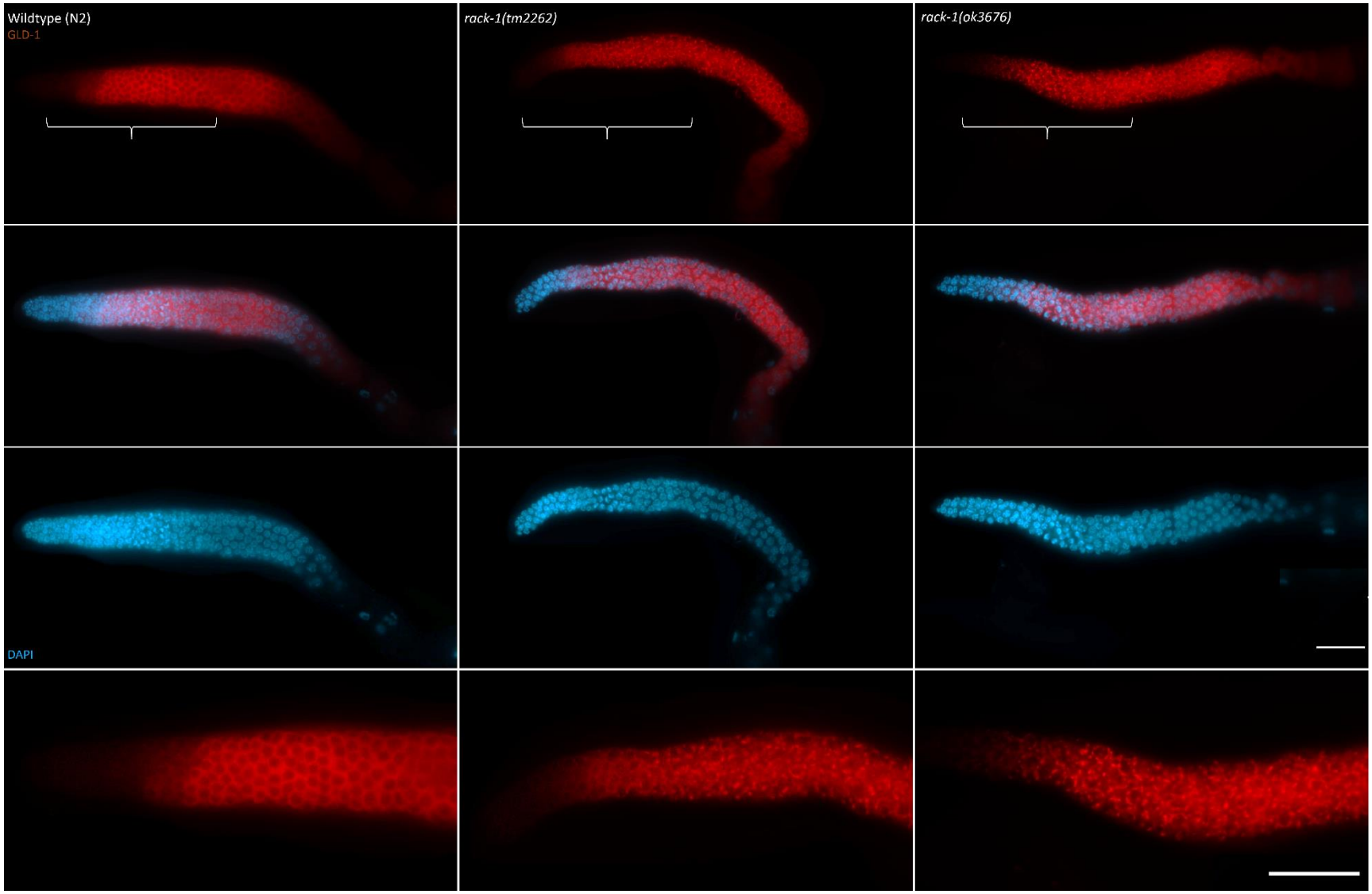
Wildtype (N2)
GLD-1
rack-1(tm2262)
rack-1(ok3676)
DAPI

Figure 5.1 - GLD-1 is mislocalized in *rack-1* mutant germlines at 20 °C. Representative images of the GLD-1 expression in wildtype (N2), *rack-1(tm2262),* and *rack-1(ok3676)* young adult germlines. Animals were raised at 20 °C, dissected at one day past the L4 stage, stained with α-GLD-1 antibodies. Nuclear morphology was detected using DAPI. The white bracket represents the area of the germline that has been blown up in the bottom panel of the image. Scale bar = 20 μm.

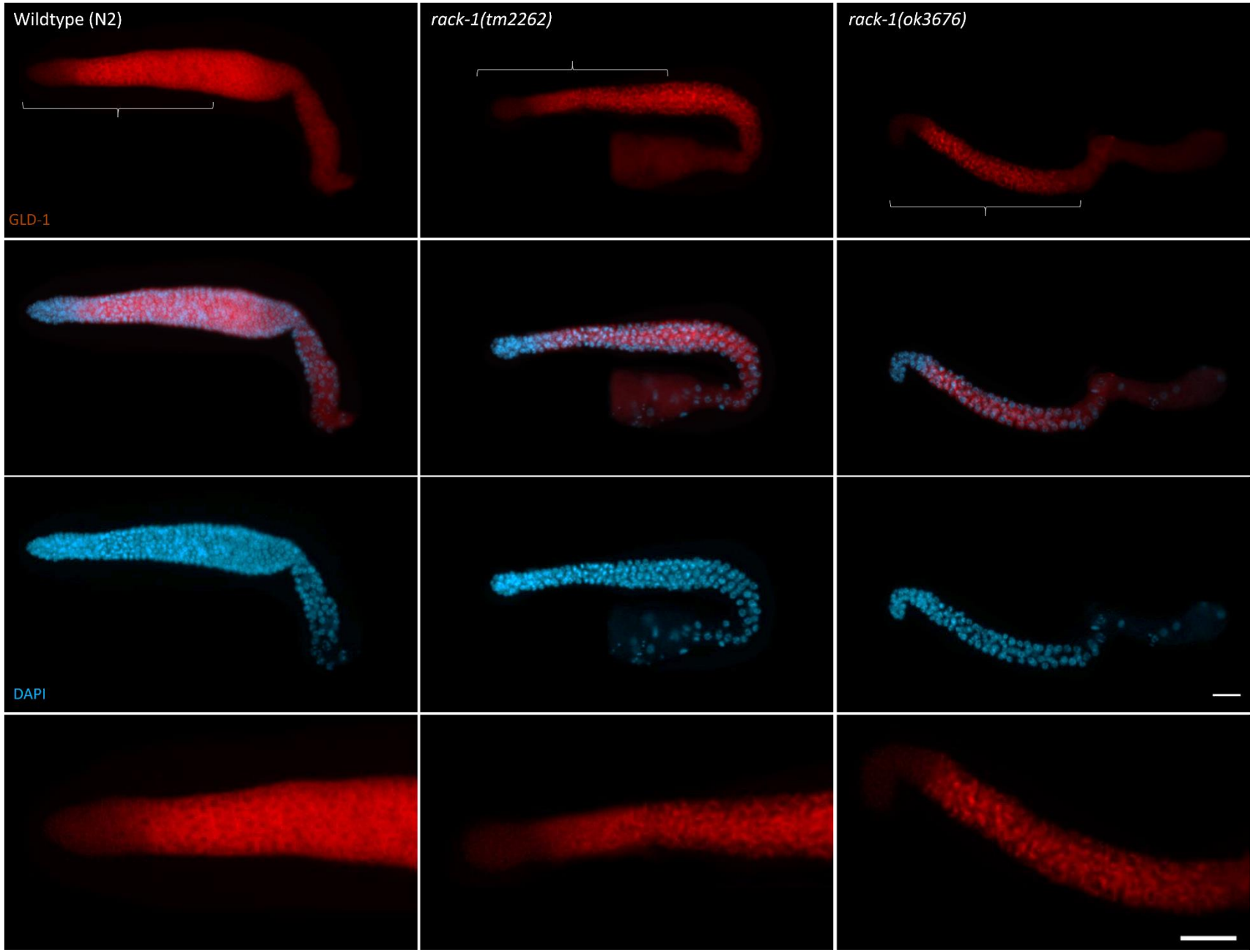
Wildtype (N2)
rack-1(tm2262)
rack-1(ok3676)
GLD-1
DAPI

Figure 5.2 - GLD-1 is mislocalized in *rack-1* mutant germlines at 25 °C. Representative images of the GLD-1 expression in wildtype (N2), *rack-1(tm2262),* and *rack-1(ok3676)* young adult germlines. Animals were raised at 25 °C, dissected at one day past the L4 stage, stained with α-GLD-1 antibodies. Nuclear morphology was detected using DAPI. The white bracket represents the area of the germline that has been blown up in the bottom panel of the image. Scale bar = 20 μm.

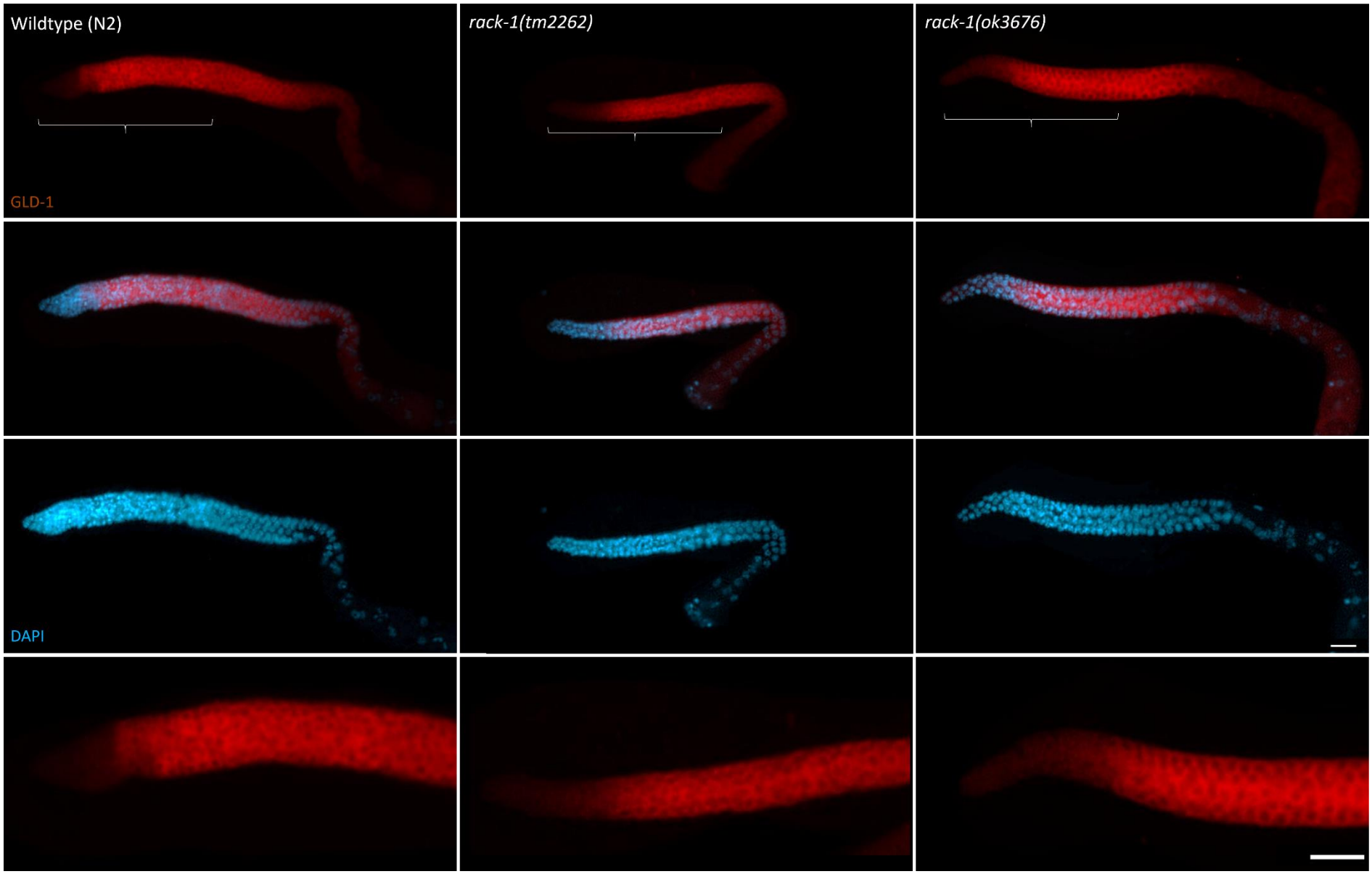
Wildtype (N2)
rack-1(tm2262)
rack-1(ok3676)
GLD-1
DAPI

Figure 5.3 – GLD-1 has wildtype localization in *rack-1* mutant germlines at 15 °C. Representative images of the GLD-1 expression in wildtype (N2), *rack-1(tm2262),* and *rack-1(ok3676)* young adult germlines. Animals were raised at 15 °C, dissected at one day past the L4 stage, stained with α-GLD-1 antibodies. Nuclear morphology was detected using DAPI. The white bracket represents the area of the germline that has been blown up in the bottom panel of the image. Scale bar = 20 μm.

5.2 GLD-1 localizes to P granules in *rack-1* mutant germlines

The GLD-1 aggregates that are formed in *rack-1* mutants appeared to be peri-nuclear, reminiscent of the patterning of *C. elegans* germ granules, P granules, in the germline. P granules are ribonucleoprotein granules (RNP) that become restricted to the cell lineage responsible for germline development, the P cell lineage (Strome & Wood, 1982). P granules are present throughout both embryonic and germline development at all stages, in both mitotic and meiotic cells, including developing oocytes (Strome & Wood, 1982). As mentioned in Chapter 1, these RNPs contain a wide array of proteins and maternally contributed mRNAs (Reviewed by: (Updike & Strome, 2010)). One core protein required for P granule assembly is PGL-1 (Kawasaki et al., 1998). PGL-1 is associated with P granules at all developmental stages, and therefore, is a good marker to visualize P granules (Kawasaki et al., 1998). Interestingly, GLD-1 has been shown to localize to P granules, through PGL-1 co-localization experiments, in developing embryos (Jones et al., 1996) and more recently, a portion of wildtype GLD-1 has been shown to be present in P granules within the adult germline (Ellenbecker et al., 2019). To investigate the possibility of GLD-1 localizing to P granules in *rack-1* mutants, co-localization experiments were performed using a monomeric RFP tagged transgene of PGL-1 (Chihara & Nance, 2012). This experiment demonstrated that GLD-1 co-localizes with PGL-1 when mislocalized in *rack-1(tm2262)* germlines (Figure 5.4). This co-localization data supports the hypothesis that a substantial fraction of GLD-1 localizes to P granules in the absence of *rack-1.* Future analysis should be performed to quantify and

compare the levels of cytoplasmic GLD-1 versus P granule aggregated GLD-1 in *rack-1* mutants as there may still be low levels within the cytoplasm.

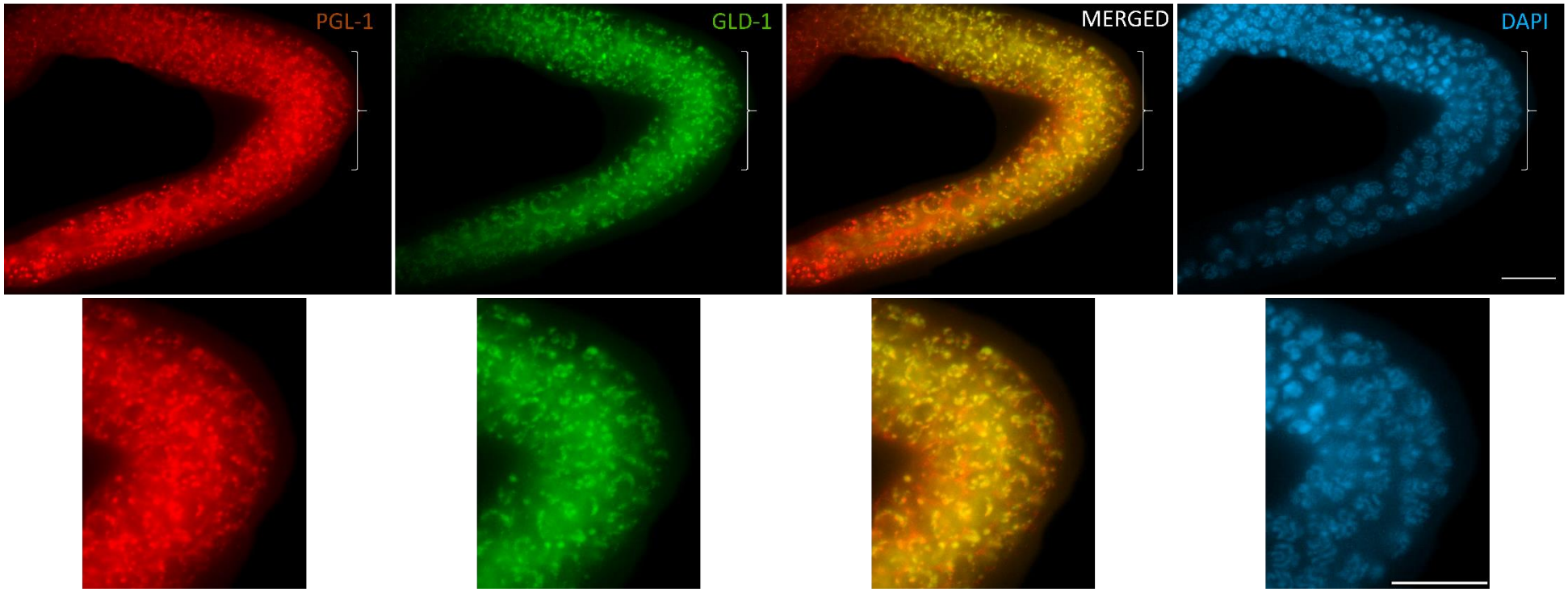

Figure 5.4 - GLD-1 co-localizes with the P granule component PGL-1 in *rack-1(tm2262)* germlines. Representative images of animals expressing both *rack-1(tm2262)* and *zuIs244[nmy-2p::PGL-1::RFP].* Animals were raised at 20 °C, dissected at one day past the L4 stage, dissected and stained with α-GLD-1 antibodies (green). PGL-1's expression was detected based on endogenous RFP expression (red). Nuclear morphology (blue) was detected using DAPI. The distal end of the germline is on the top left of the image. The white bracket represents the area of the germline that has been blown up in the lower panel of the image. Scale bar = 20 μm.

5.3 The mislocalization of GLD-1 to P granules in *rack-1* mutants does not require RNA binding

Many P granule associated proteins are RNA-binding proteins, in agreement with the role of P granules in RNA metabolism and processing (Reviewed in: (Updike & Strome, 2010); therefore, it is possible that the sub-cellular mislocalization of GLD-1 to P granules is dependent on GLD-1's ability to bind mRNA. A mutant *gld-1* allele, *gld-1(q361)*, was used in combination with *rack-1(tm2262)*, to determine if this mislocalization depends on GLD-1's RNA binding ability. The *gld-1(q361)* allele, obtained from EMS mutagenesis, contains a nonsynonymous point mutation within the KH domain (RNA binding domain) of GLD-1 (G227D), resulting in the expression of a full-length protein that is unable to bind to mRNA and is considered a null allele (Chen et al., 1997; Francis et al., 1995; Jan et al., 1999; Lee & Schedl, 2001). GLD-1 still displayed subcellular mislocalization in *gld-1(q361); rack-1(tm2262)* germlines, suggesting GLD-1 mislocalization in the absence of RACK-1 activity does not depend on GLD-1's ability to bind to mRNA (Figure 5.5). This indicates that protein-protein interactions may be required for GLD-1's mislocalization in *rack-1* mutants. This may also hold true for the subset of GLD-1 that is enriched in P granules in wildtype germlines (Ellenbecker et al., 2019).

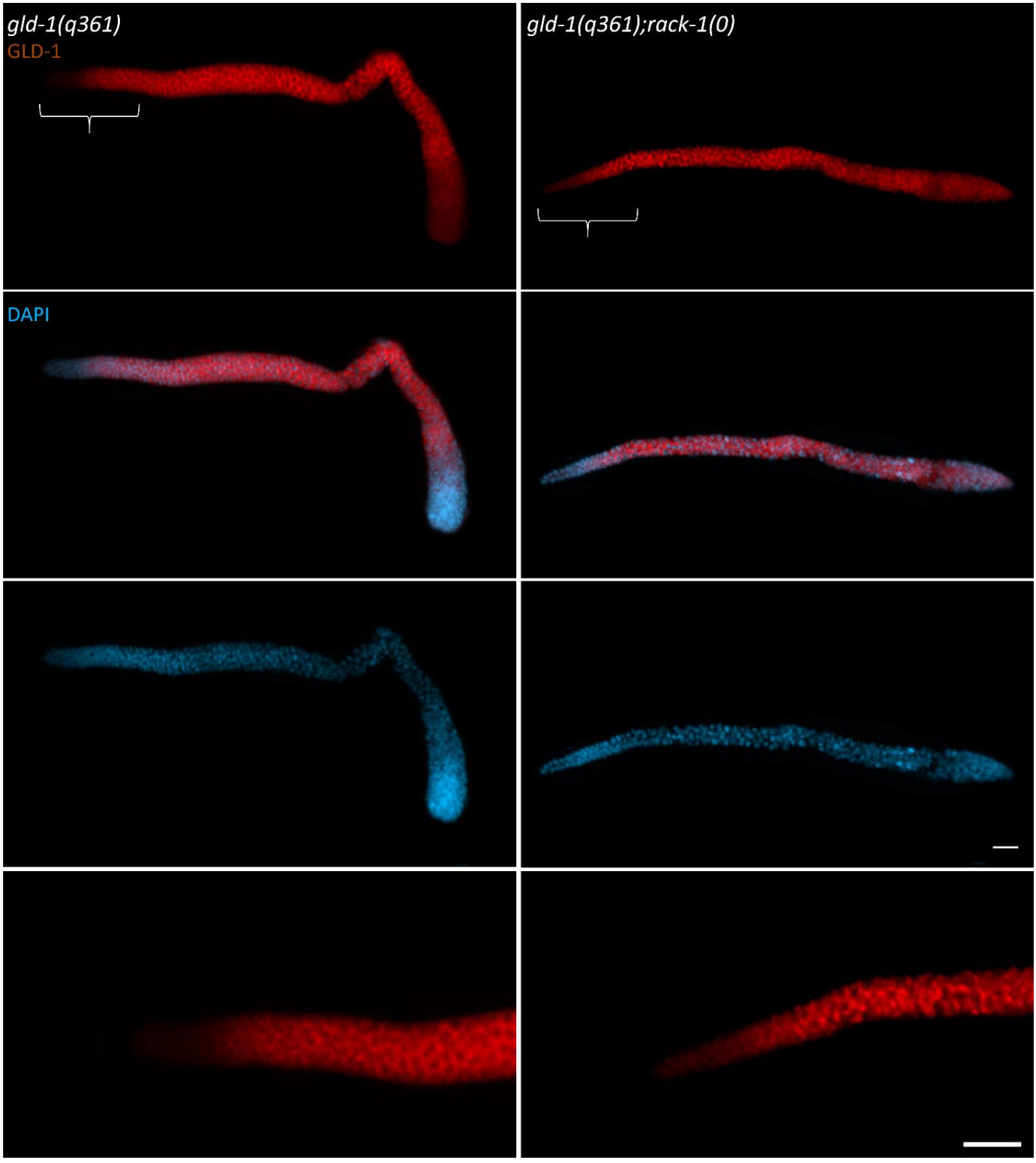
gld-1(q361)
GLD-1
gld-1(q361);rack-1(0)
DAPI

Figure 5.6 - GLD-1 is mislocalized in gld-1(q361); rack-1 mutant germlines at 20 °C. Representative images of the GLD-1 expression in *gld-1(q361) and gld-1(q361); rack-1(tm2262)* young adult germlines. Animals were raised at 20 °C, dissected at one day past the L4 stage, stained with α-GLD-1 antibodies. Nuclear morphology was detected using DAPI. The white bracket represents the area of the germline that has been blown up in the bottom panel of the image. Scale bar = 20 μm.

5.4 RACK-1 is required for proper GLD-1 levels

Immunofluorescent analysis of GLD-1 in *rack-1* mutants suggested that GLD-1 is mislocalized in the absence of *rack-1(0).* To determine if GLD-1 levels are also affected in the absence of *rack-1,* GLD-1 accumulation was compared between wildtype and *rack-1(tm2262)* animals. Interestingly, GLD-1's overall levels were lowered, as compared to wildtype, at all temperatures – 15 °C – 24% reduction; 20 °C – 19% reduction; 25 °C 33% reduction (Figure 5.6). This reduction in GLD-1 levels was statistically significant at all three temperatures (One sample t-test p-values < 0.0001). *rack-1(tm2262)* gonads appear smaller (shorter) than wildtype gonads; therefore, the maximum GLD-1 level measured, or peak GLD-1, was compared between the two genotypes at all three temperatures. At 15 °C *rack-1(tm2262)* peak GLD-1 was reduced by 17% (wildtype = 2017 a.u.; *rack-1(tm2262)* = 1683 a.u.; Unpaired t-test p-value < 0.0001). At 20 °C peak GLD-1 was reduced by 17% (wildtype = 1862 a.u.; *rack-1(tm2262)* = 1552 a.u.; Unpaired t-test p-value < 0.0001). At 25 °C peak GLD-1 was reduced by 28% (wildtype = 1773 a.u.; *rack-1(tm2262)* = 1274 a.u.; Unpaired t-test p-value < 0.0001). This demonstrates that GLD-1's expression is reduced in *rack-1* mutants, independently of the reduction in gonad size.

Interestingly, GLD-1 levels were lowered in *rack-1(tm2262)* mutants at 15 °C even though the localization of GLD-1 remains relatively wildtype (Figure 5.3). This suggests that the mislocalization seen at higher temperatures is not simply due to a loss of cytoplasmic GLD-1, making GLD-1 localized within P-granules more apparent. This supports the hypothesis that *rack-1* is required to prevent the majority of GLD-1, either

directly or indirectly, from localizing to P granules. It also suggests that *rack-1* may play a role in stabilizing or protecting GLD-1 from degradation, allowing for proper accumulation within the germline.

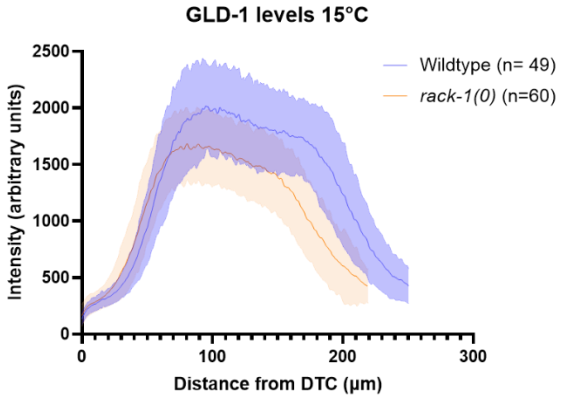

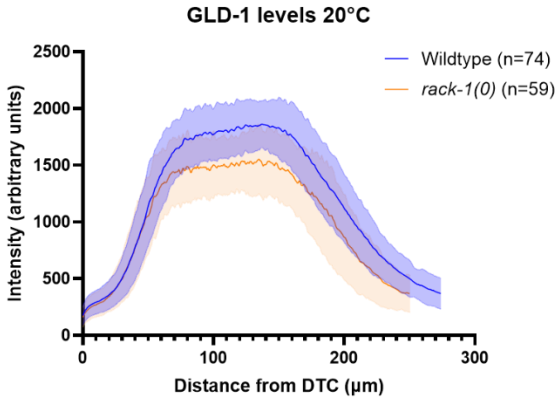

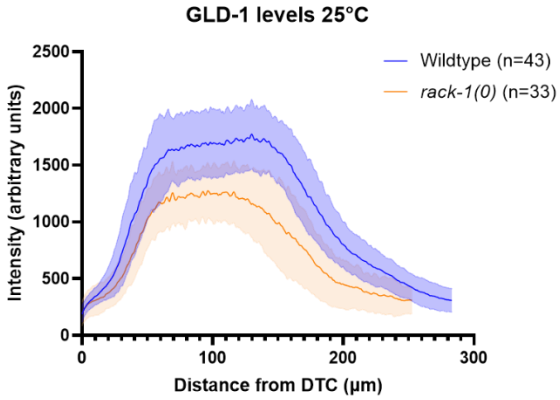

Analysis at 15°C	Genotype	Area under curve (a.u*µm)	Percent reduction
	Control	3066891	24
	rack-1(0)	2317357	

Analysis at 20°C	Genotype	Area under curve (a.u*µm)	Percent reduction
	Control	3093566	19
	rack-1(0)	2496372	

Analysis at 25°C	Genotype	Area under curve (a.u*µm)	Percent reduction
	Control	2903367	33
	rack-1(0)	1906099	

Figure 5.7 - GLD-1 levels are reduced in *rack-1(tm2262).* Graphs depicting the average GLD-1 accumulation profiles in Wildtype (blue) and *rack-1(tm2262)* (orange) germlines raised at 15 °C (left) 20 °C (center) and 25 °C (right). GLD-1's expression was determined using α-GLD-1 antibodies. The x-axis is distance in µm from the distal tip cell (DTC) to the loop region of the germline. The y-axis is the intensity of antibody staining in arbitrary units. The area under the curve, representing total GLD-1, was calculated and supplied in the tables underneath the graphs.

To verify the reduction in GLD-1 levels, western blot analysis of whole protein lysate was performed on wildtype and *rack-1* animals. GLD-1 is present in both the germline and developing embryos (Jones et al., 1996); therefore, to restrict the analysis to only germline expressed GLD-1, L4 animals were used as they have not begun producing fertilized embryos. In agreement with the *in vivo* analysis, western blot analysis also showed a reduction in GLD-1 levels in *rack-1(tm2262)* animals compared to wildtype (Normalized Ratio of GLD-1 in *rack-1(tm2262)* compared to wildtype= 0.17, n=2) (Figure 5.7); however, the percent reduction calculated between the two experiments is very different – *in vivo* ~19% reduction vs western blot ~83%. The exact reduction of GLD-1 levels in *rack-1(tm2262)* germlines remains unclear; however, the trend is that GLD-1 is lowered in the absence of *rack-1.*

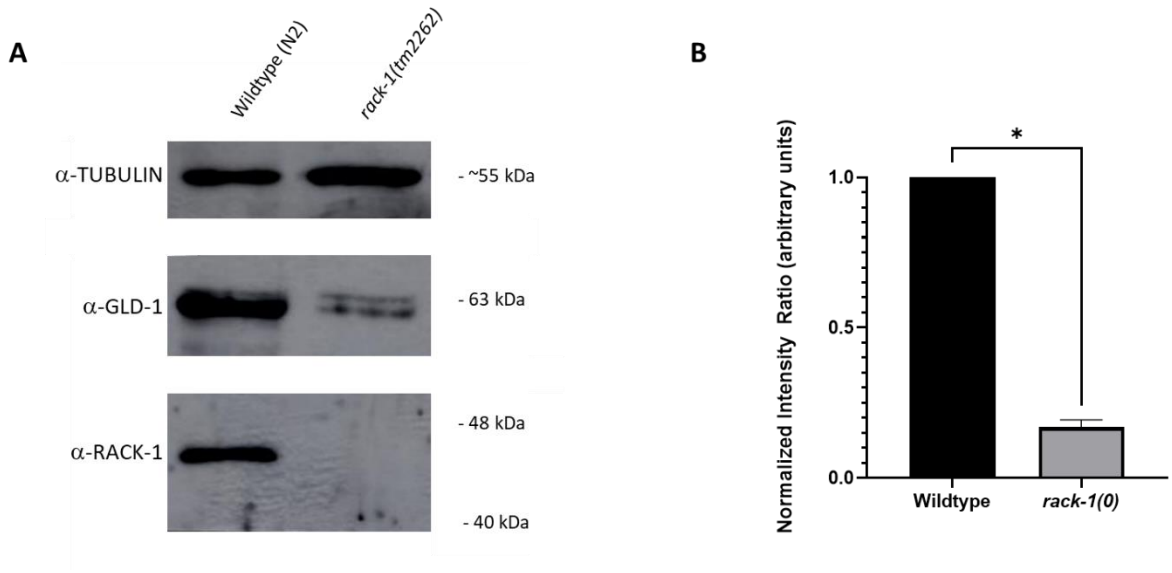

Figure 5.8 - GLD-1 levels are reduced in rack-1(tm2262) as determined by western blot analysis. GLD-1 levels were determined through western blot analysis of 100 L4 worms of each genotype [wildtype and *rack-1(tm2262)*]. GLD-1 expression was detected using α-GLD-1 antibodies, RACK-1 expression was detected using α-RACK-1 antibodies. α-TUBULIN was used as a loading control A) A Representative image of western blot analysis of GLD-1 in wildtype versus *rack-1(tm2262)* B) The normalized intensity ratio (arbitrary units) of GLD-1 between *rack-1(tm2262)* (0.17 ± 0.02) and wildtype (1.0 ± 0), n=2. Error bars represent ± standard deviation (S.D). The asterisk represents the statistical difference determined by a paired t-test *p-value = 0.0130.

5.5 *rack-1* functions independently from *gld-2* to regulate GLD-1 expression

GLD-1's germline accumulation pattern, and expression levels, are known to be regulated by two opposing mechanisms; FBF-1 and FBF-2 function in the proliferative zone to repress *gld-1* expression, while GLD-2 functions to promote *gld-1* expression for entry into meiosis (Hansen, Wilson-Berry, et al., 2004; Hansen & Schedl, 2013; Jiang & Hui, 2008; Suh et al., 2006, 2009). The data presented above suggests that *rack-1* may function to promote the accumulation of GLD-1, as a loss of *rack-1* results in a decrease in GLD-1 levels. To investigate the possibility that *rack-1* functions with *gld-2* to promote GLD-1 accumulation, GLD-1 levels were analyzed in *gld-2(q497); rack-1(tm2262)*.

GLD-2, a catalytic subunit of a poly(A) polymerase, promotes the accumulation of target mRNAs through stabilization upon the addition of a poly(A) tail (Wang et al., 2002). *gld-2(q497)* mutant animals have been shown to have reduced *gld-1* mRNA and protein levels (Suh et al., 2006). If *rack-1* functions with *gld-2* to regulate GLD-1 levels, there should be no measurable difference in GLD-1 accumulation between *gld-2(q497)* and *gld-2(q497); rack-1(tm2262)* mutants. Interestingly, *gld-2(q497); rack-1(tm2262)* had statistically significant reduction in total overall GLD-1 levels (33%; One sample t-test p-value < 0.0001), and a 27% reduction of peak GLD-1 as compared to *gld-2(q497)* alone (*gld-2(q497)* = 1801 a.u.; *gld-2(q497); rack-1(tm2262)* = 1311 a.u.; Unpaired t-test p-value < 0.0001) (Figure 5.8). This suggests that *rack-1* functions independently of *gld-2* to promote GLD-1 expression within the germline.

As yeast and mammalian RACK-1 orthologs have been shown to be required for ribosome function and protein translation, it is possible that *rack-1* is required for proper

translation of *gld-1* (Gallo et al., 2018; Gerbasi et al., 2004); however, another possibility is that there is a protein-protein interaction between GLD-1 and RACK-1 that influences GLD-1's stability and localization. Further research will be required to determine if the reduction of GLD-1 accumulation in the absence of *rack-1* occurs at the translational or protein level.

The data in this chapter demonstrates that a loss of *rack-1* has an impact on both the levels and subcellular localization of GLD-1. This data provides a possible mechanism by which the proliferation/differentiation balance is disrupted upon the loss of *rack-1* in sensitized backgrounds; GLD-1 levels are lowered, and sub-cellular localization disrupted, resulting in a decrease in function of GLD-1, which in turn disrupts the proliferation/differentiation balance.

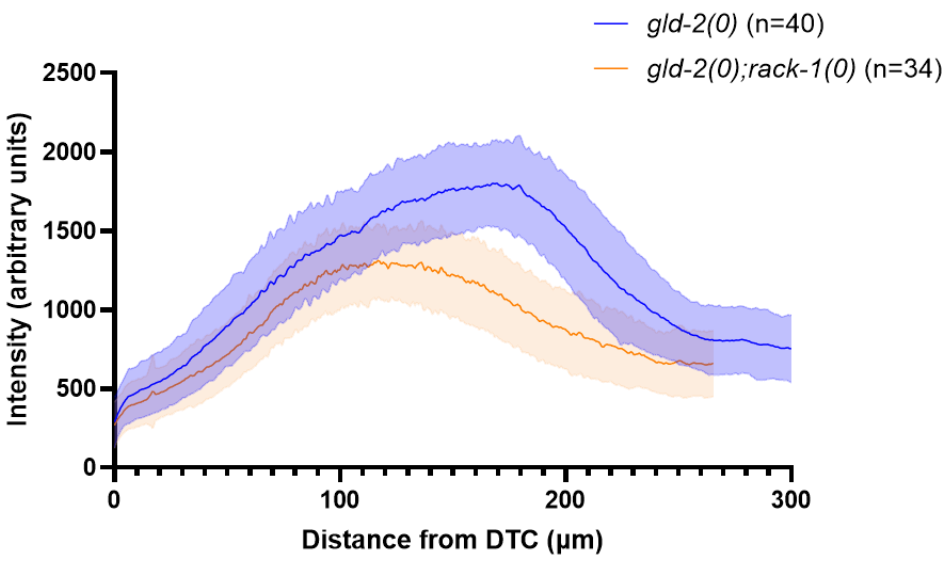

Analysis at 20°C	Genotype	Area under curve (a.u*µm)	Percent reduction
	gld-2(0)	3447194	33
	gld-2(0);rack-1(0)	2315848	

Figure 5.9 - GLD-1 levels are reduced in *gld-2(q497); rack-1(tm2262)* compared to *gld-2(q497)*. A Graph depicting the average GLD-1 accumulation profiles in *gld-2(q497)* and *gld-2(q497); rack-1(tm2262)* germlines raised 20 °C. GLD-1's expression was determined using α-GLD-1 antibodies. The x-axis is distance in µm from the distal tip cell (DTC) to the loop region of the germline. The y-axis is the intensity of antibody staining in arbitrary units. The area under the curve, representing total GLD-1, was calculated and supplied in the table below the graph.

Chapter 6 – *rack-1* is required for proper GLD-1 function

The data presented in Chapters 3-5 have demonstrated that RACK-1 is expressed in the germline, where it is required to maintain proper homeostasis of germline stem cell proliferation and differentiation. Additionally, *rack-1* is required for the proper localization and levels of GLD-1, a core protein required for entry and progression through meiosis (Jones et al., 1996). Taken together, this data indicates that *rack-1* may influence the proliferation/differentiation balance by modulating GLD-1's activity. Using the data presented in this chapter I will demonstrate that loss of *rack-1* disrupts the proliferation/differentiation balance by reducing, but not abolishing, GLD-1's activity.

By comparing the germline phenotypes of *gld-1* and *gld-1; rack-1* null mutants, I demonstrate that a loss of *rack-1* does not enhance *gld-1(0)* germline proliferation defects. Furthermore, *rack-1* mutant germlines do not phenocopy *gld-1(0)* mutant germlines. This data highlights that GLD-1's activity is reduced, not completely abolished, in the absence of *rack-1.* Additionally, using genetic analysis I demonstrate that loss of *rack-1* and GLD-2 pathway function results in a disruption of germline proliferation/differentiation balance, without impacting the entry into meiosis decision. I demonstrate that a partial reduction of *gld-1* in the absence of GLD-2 pathway function results in over-proliferation similar to what was seen with *rack-1(0).* I determined that the over-proliferation phenotype observed in the absence of *gld-2* and *rack-1* is Glp-1/Notch dependent. This agrees with GLD-1's activity being reduced, but not abolished. Additionally, I demonstrate that a loss of *rack-1* enhances germline defects associated with a *gld-1* partial loss-of-function allele, *gld-1(op236).* Finally, I demonstrate that a loss

of *rack-1* phenocopies a partial reduction of *gld-1* in a *fbf-1 fbf-2* mutant background. This data supports the model that *rack-1* functions to modulate GLD-1's activity through regulating GLD-1's subcellular localization and overall levels.

6.1 *rack-1(0)* does not enhance *gld-1(0)* germline over-proliferation phenotype but slightly enhances germline defects in *gld-1* heterozygotes

These data presented above indicates that *rack-1* may exert its influence on the proliferation/differentiation balance by controlling GLD-1's activity by regulating GLD-1's sub-cellular localization and levels (Chapter 5). As mentioned previously, GLD-1 is a translational repressor required for the entry and progression through meiosis (Francis et al., 1995; Jones et al., 1996; Kadyk & Kimble, 1998). In the absence of *gld-1,* cells are able to enter into meiosis, as the redundant GLD-2 pathway is present; however, the cells are unable to progress through meiotic prophase and revert back to mitosis, resulting in the formation of a proximal tumour (de-differentiation) (Figure 6.1) (Francis et al., 1995). *gld-1(q485)* is a frameshift mutation resulting from an ~82 bp deletion within exon 2, causing no detectable protein to be produced, and is therefore considered a true null allele (Francis et al., 1995; Jones et al., 1996; Jones & Schedl, 1995). If the mislocalization of GLD-1 in *rack-1* mutants completely disrupts GLD-1's activity, then *rack-1(tm2262)* germlines should display similar germline defects as *gld-1(q485)* animals. Approximately 1% of *rack-1(tm2262)* germlines analyzed had proximal tumours, whereas 100% of *gld-1(q485)* germlines display proximal tumours as determined by whole mount DAPI (nuclear staining), α-REC-8 (proliferation marker) and α-HIM-3 (meiotic marker) staining (Table 6.1). This data demonstrates that the mislocalized GLD-1 in *rack-1*

mutants retains some wildtype function as *rack-1(tm2262)* germlines do not phenocopy *gld-1(q485).* Moreover, *gld-1(q485); rack-1(tm2262)* germlines displayed normal entry into meiosis, with ectopic proliferation being restricted to the proximal germline, with no apparent difference from *gld-1(q485)* germlines, as determined by α-REC-8 (proliferation marker) and α-HIM-3 (meiotic marker) staining (Figure 6.1). This suggests that loss of *rack-1* does not enhance the over-proliferation phenotype of *gld-1(q485).* This data supports the model that the lower levels of GLD-1, and mislocalization of GLD-1, in *rack-1* mutants reduces, but does not eliminate, GLD-1 function.

Table 6.1 - Loss of *rack-1* does not enhance *gld-1(q485)* germline phenotypes

Analysis at 20 °C	Germline Phenotype[a]			
Genotype	Wildtype[b] (%)	Pro[c] (%)	Other[d] (%)	n[e]
gld-1(0)[f]	0	100	0	117
rack-1(0)[g]	96	1	3	442
gld-1(0); rack-1(0)[h]	0	100	0	111
Analysis at 25 °C				
gld-1(0)[f]	0	100	0	104
rack-1(0)[g]	85	0	15	334
gld-1(0); rack-1(0)[h]	0	100	0	112

[a] Animals were dissected one day past the L4 stage, fixed and stained with DAPI, and α-REC-8 and α-HIM-3 antibodies. The germline phenotype was scored based upon the presence of REC-8 positive cells outside of the proliferative zone.
[b] Wildtype refers to gonad arms with no REC-8 outside of the proliferative zone.
[c] Proximal tumour (Pro) refers to gonad arms that have normal relatively normal distal germline but a pool of proliferative cells (REC-8 positive) at the most proximal end of the germline.
[d] Other includes germlines classified as defective oogenesis and Empty or underdeveloped (See Table 4.1.2 for full description and numbers).
[e] n refers to total number of gonad arms analyzed.
[f] Actual genotype; *gld-1(q485).*
[g] Actual genotype; *rack-1(tm2262).*
[h] Actual genotype; *gld-1(485); rack-1(tm2262).*

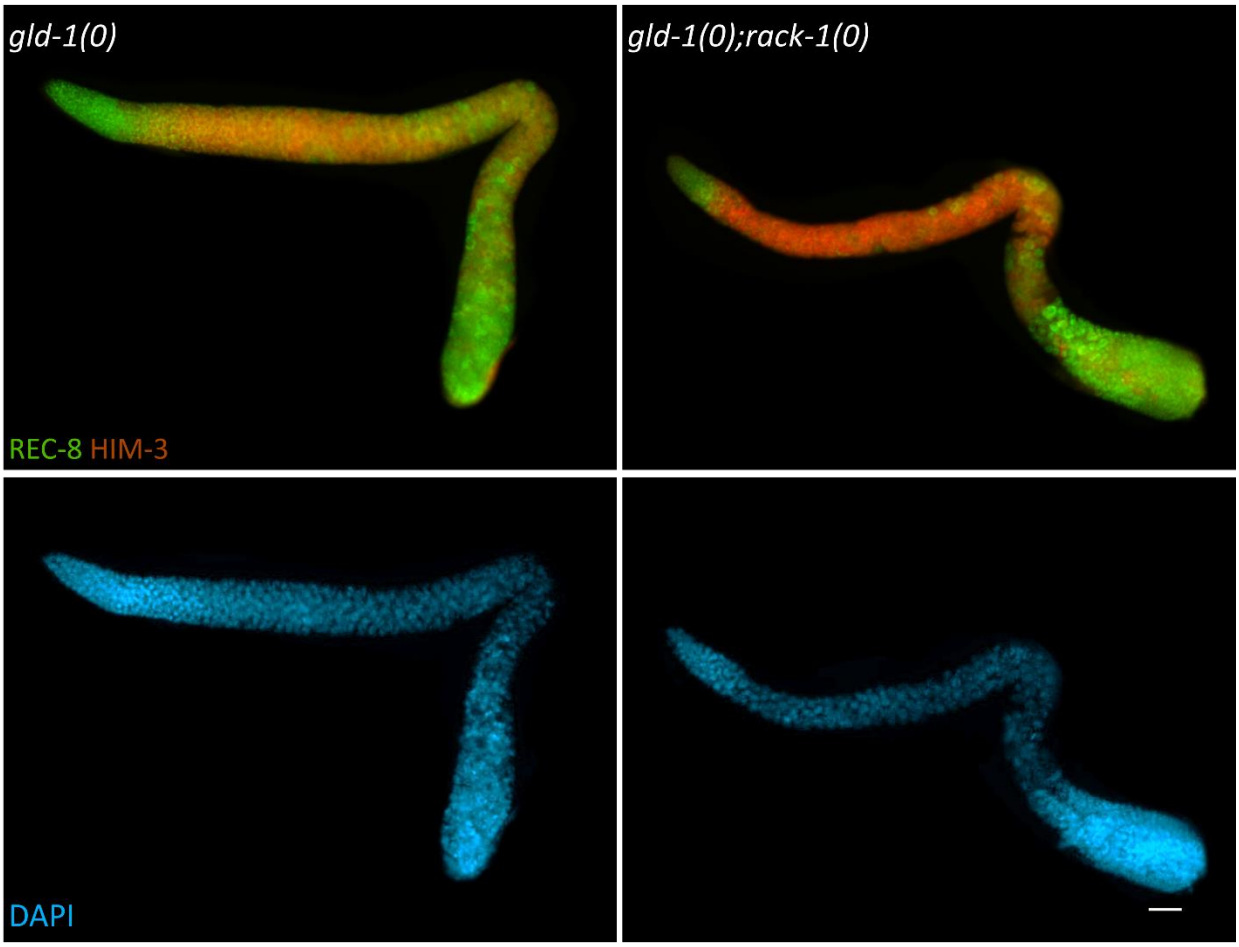

Figure 6.1 – Loss of *rack-1* does not enhance *gld-1(0)* germline phenotype. Representative images of *gld-1(q485)* and *gld-1(q485); rack-1(tm2262)* young adult gonads. Animals were raised at 20 °C, dissected at one day past the L4 stage, and analyzed for ectopic proliferation using α-REC8 (proliferation marker) and α-HIM-3 (meiotic marker) antibodies. Nuclear morphology was detected using DAPI. Scale bar = 20 μm.

Complete loss of *gld-1* results in cells failing to progress through meiosis and instead returning to the mitotic cell cycle (Francis et al., 1995); however, *gld-1* heterozygote animals do not display any germline defects at 20 °C or 25 °C (Table 6.2 and Figure 6.2). If loss of *rack-1* does reduce GLD-1's activity, then *rack-1(tm2262)* may enhance *gld-1* mutant phenotypes in *gld-1* heterozygote animals (*gld-1(q485/tmC18--tmC18* is a balancer chromosome that contains a wildtype copy of *gld-1*). Interestingly, 4% of *gld-1(+/q485); rack-1(tm2262)* germlines analyzed at 20 °C and 25 °C displayed proximal tumours compared to less than 1% in *rack-1(tm2262)* determined by α-REC-8 and α-HIM-3 staining (Table 6.2). *gld-1(+/q485); rack-1(tm2262)* germlines displayed reduced oogenesis similar to *rack-(tm2262)* germlines (Figure 6.2). Additionally, a portion of *gld-1(+/q485); rack-1(tm2262)* germlines analyzed displayed a delay in pachytene progression, with cells in pachytene being present past the loop, where developing oocytes (diplotene/diakinesis cells) are normally located (20 °C = 41% n=110; 25 °C = 24% n=153) (Table 6.3 and Figure 6.2). This delayed meiotic progression was not observed in *gld-1(q485/tmC18)* animals (20 °C n = 65; 25 °C n = 124) or *rack-1(tm2262)* animals (20 °C n= 60; 25 °C n = 43) (Table 6.3). This data demonstrates that loss of *rack-1* enhances *gld-1* mutant phenotypes, delayed meiotic progression and ectopic proliferation, in *gld-1* heterozygous animals.

Table 6.2 - Loss of *rack-1* enhances germline defects in *gld-1* heterozygous animals

Analysis at 20 °C	Germline Phenotype[a]		
Genotype	Wildtype (%)[b]	Pro (%)[c]	n[d]
gld-1(het)[e]	100	0	117
rack-1(0)[f]	99[g]	1	442
gld-1(het); rack-1(0)[h]	96	4	110
Analysis at 25 °C			
gld-1(het)[f]	100	0	104
rack-1(0)[g]	100	0	334
gld-1(het); rack-1(0)[h]	96	4	153

[a] Animals were dissected one day past the L4 stage, fixed and stained with DAPI, and α-REC-8 and α-HIM-3 antibodies. The germline phenotype was scored based upon the presence of REC-8 positive cells outside of the proliferative zone.
[b] Wildtype refers to gonad arms with no REC-8 outside of the proliferative zone.
[c] Proximal tumour (Pro) refers to gonad arms that have normal relatively normal distal germline but a pool of proliferative cells (REC-8 positive) at the most proximal end of the germline.
[d] n refers to total number of gonad arms analyzed.
[e] Actual genotype; *gld-1(q485/tmC18).*
[f] Actual genotype; *rack-1(tm2262).*
[g] This includes other *rack-1(tm2262)* germline defects that did not have ectopic proliferation (defective oogenesis and Empty or underdeveloped (See Table 4.1.2 for full description and numbers).
[h] Actual genotype; *gld-1(q485/tmC18); rack-1(tm2262).*

Table 6.3 - Loss of *rack-1* delays meiotic progression in *gld-1* heterozygous animals

Analysis at 20 °C	Germline Phenotype[a]		
Genotype	Wildtype[b] (%)	Extended Pachytene[c] (%)	n[d]
gld-1(het)[e]	100	0	65
rack-1(0)[f]	100	0	60
gld-1(het); rack-1(0)[g]	59	41	110
Analysis at 25 °C			
gld-1(het)[e]	100	0	124
rack-1(0)[f]	100	0	43
gld-1(het); rack-1(0)[g]	76	24	153

[a] Animals were dissected one day past the L4 stage, fixed and stained with DAPI. The germline phenotype was scored based upon nuclear morphology as determined by DAPI staining.
[b] Wildtype refers to gonad arms where cells progressed from pachytene into diplotene/diakinesis at the loop of the gonad arm.
[c] Extended pachytene refers to gonad arms where cells did not progress into diplotene/diakinesis at the loop, and instead had an extended region of pachytene with late-pachytene staged nuclei past the loop.
[d] n refers to total number of gonad arms analyzed.
[e] Actual genotype; *gld-1(q485/tmC18).*
[f] Actual genotype; *rack-1(tm2262).*
[g] Actual genotype; *gld-1(q485/tmC18); rack-1(tm2262).*

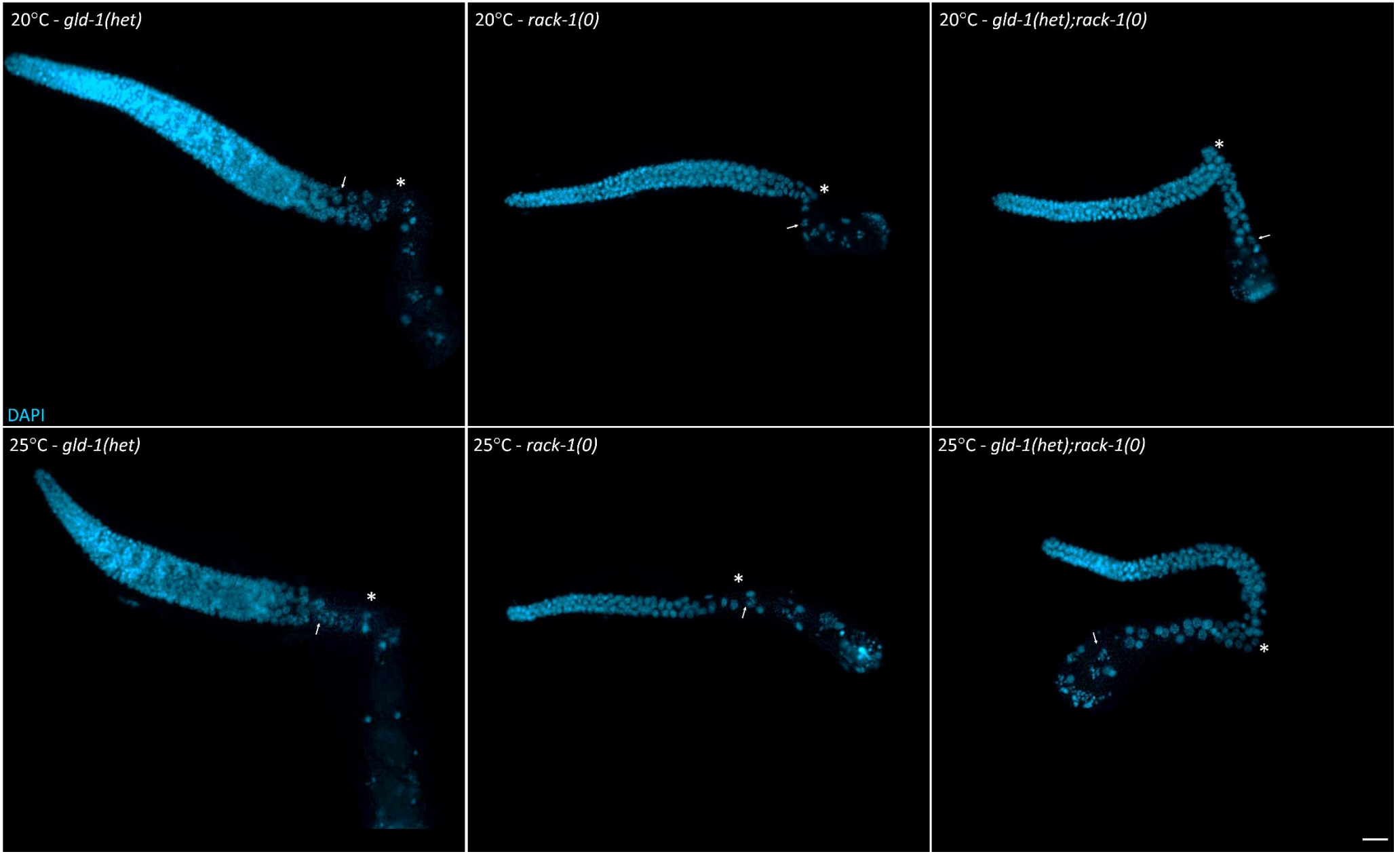
20°C - gld-1(het)
20°C - rack-1(0)
20°C - gld-1(het);rack-1(0)
DAPI
25°C - gld-1(het)
25°C - rack-1(0)
25°C - gld-1(het);rack-1(0)

Figure 6.2 - Loss of *rack-1* results in delayed meiotic progression in *gld-1* heterozygous animals. Loss of *rack-1* does not enhance *gld-1(0)*. Representative images of *gld-1(q485/tmC18)*, *rack-1(tm2262)* and *gld-1(q485/tmC18); rack-1(tm2262)* young adult gonads. Animals were raised at 20 °C (top) and 25 °C (bottom), dissected at one day past the L4 stage and analyzed for delayed transition from pachytene to diplotene/diakinesis using DAPI to determine nuclear morphology. Arrow (→) represents first visible diplotene nuclei indicating progression through pachytene. * represents the loop of the germline. Scale bar = 20 μm.

6.2 Loss of *rack-1* in GLD-2 pathway mutant backgrounds results in a germline over-proliferation phenotype

The GLD-1 and GLD-2 meiotic pathways function redundantly to promote entry into meiosis (Eckmann et al., 2004; Hansen et al., 2004; Kadyk & Kimble, 1998). Genetic analysis between *rack-1* and core GLD pathway components, discussed in Chapter 3, demonstrated that loss of *rack-1* does not completely disrupt GLD-1 activity and/or pathway function, as no impact on the entry into meiosis decision was observed when combined with core GLD-2 pathway mutants, *gld-2(q497)* and *gld-3(q730)* (Table 3.7). It is possible that GLD-1's activity is not reduced enough in *rack-1* mutants for GLD-1 pathway function to be disrupted, resulting in normal entry into meiosis. Although the entry into meiosis decision was not disrupted in *rack-1(0)* GLD-2 pathway double mutants, these animals displayed disrupted germline organization with the formation of proximal tumours.

GLD-2, a catalytic subunit of a poly(A) polymerase, functions redundantly with GLD-1 to promote entry into meiosis. In the absence of *gld-2* cells are able to enter into meiosis, as the redundant GLD-1 pathway is present; however, cells arrest in an abnormal pachytene state and gametogenesis fails to occur (Kadyk & Kimble, 1998). The *gld-2* null allele, *gld-2(q497),* contains a single nucleotide mutation that results in a premature stop codon with no detectable protein produced (Wang et al., 2002). At 20 °C *gld-2(q497)* animals have a low penetrance of proximal tumour formation (~2%) (Kadyk & Kimble, 1998); however at 25 °C 33% of *gld-2(q497)* animals display proximal tumour formation (two days past the L4 stage) (Park et al., 2020). At 25 °C young adult *gld-*

2(q497) animals (one day past the L4 stage) displayed 3% proximal tumour formation (Table 6.4 and Figure 6.3). The difference in the penetrance of Pro germlines may be attributable to the age difference between animals analyzed. Interestingly, at 25 °C *gld-2(q497); rack-1(tm2262)* germlines displayed an increase in the formation of proximal tumours (67%) compared to *gld-2(q497)* (3%) or *rack-1(tm2262)* (0%) alone as determined by α-REC-8 and α-HIM-3 staining (Table 6.4 and Figure 6.3). This over-proliferation phenotype was not observed when animals were raised at 20 °C.

Table 6. 4 - Loss of *rack-1* enhances proximal tumour formation in *gld-2(0)* animals

Analysis at 20 °C Genotype	Germline Phenotype[a] Wildtype (%)[b]	Pro (%)[c]	n[d]
gld-2(0)[e]	99[f]	1	173
rack-1(0)[g]	99[h]	1	442
gld-2(0); rack-1(0)[i]	100[j]	0	147
Analysis at 25 °C			
gld-2(0)[e]	97[f]	3	154
rack-1(0)[g]	100[h]	0	334
gld-2(0); rack-1(0)[i]	33[j]	67	142

[a] Animals were dissected one day past the L4 stage, fixed and stained with DAPI, and α-REC-8 and α-HIM-3 antibodies. The germline phenotype was scored based upon the presence of REC-8 positive cells outside of the proliferative zone.
[b] Wildtype refers to gonad arms with no REC-8 outside of the proliferative zone.
[c] Proximal tumour (Pro) refers to gonad arms that have normal relatively normal distal germline but a pool of proliferative cells (REC-8 positive) at the most proximal end of the germline.
[d] n refers to total number of gonad arms analyzed.
[e] Actual genotype; *gld-2(q497).*
[f] This includes *gld-2(0)* germline defects that did not have ectopic proliferation (arrested meiotic cells and gametogenesis failure).
[g] Actual genotype; *rack-1(tm222)*
[h] This includes other *rack-1(tm2262)* germline defects that did not have ectopic proliferation (defective oogenesis and empty or underdeveloped (See Table 4.1.2 for full description and numbers).
[i] Actual genotype; *gld-2(q497); rack-1(tm2262)*
[j] This includes *gld-2(0)* germline defects that did not have ectopic proliferation (arrested meiotic cells and gametogenesis failure). No germlines displayed known *rack-1(0)* germline defects.

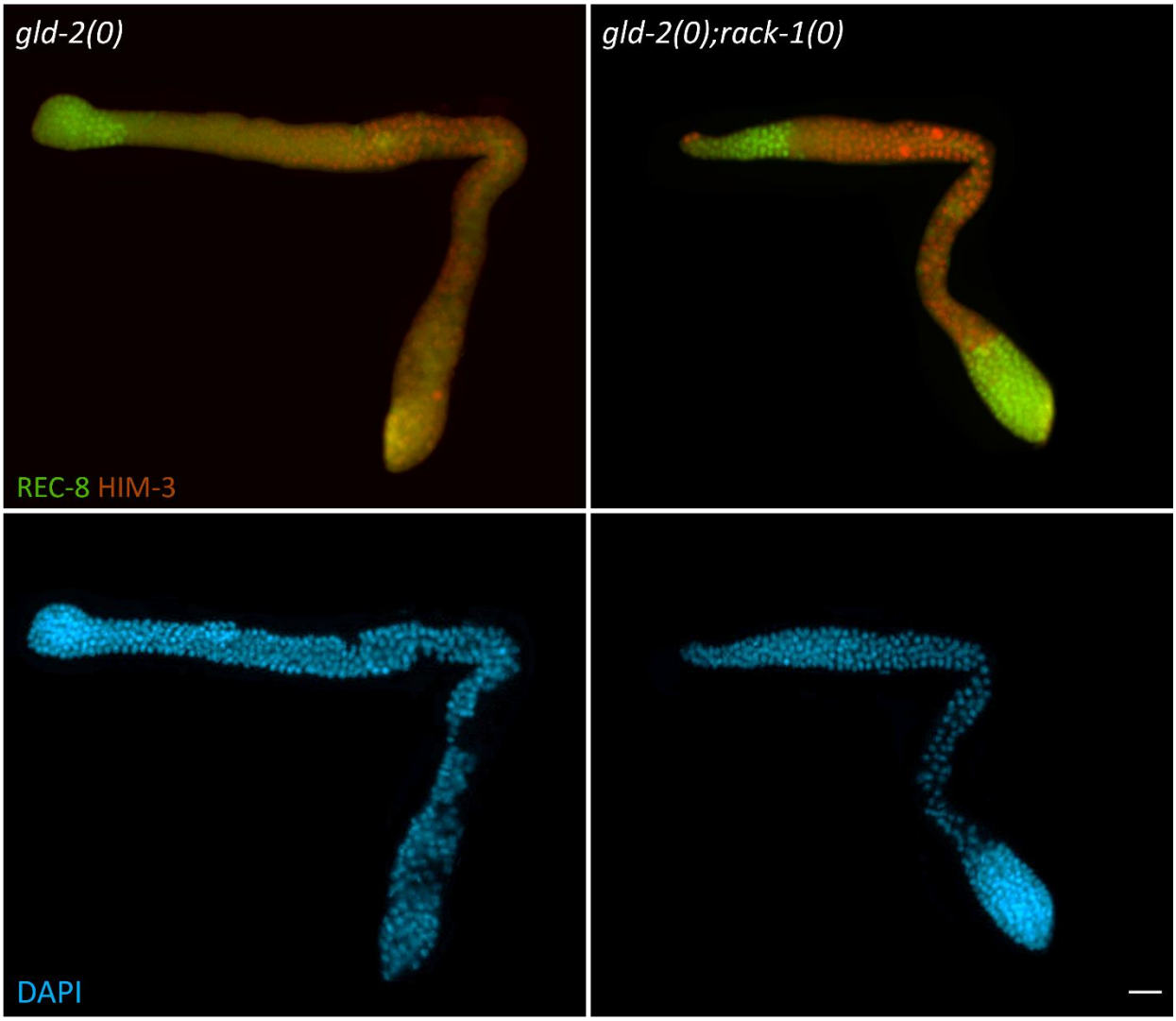

Figure 6.3 - Loss of *rack-1* results in ectopic proliferation in *gld-2(0)* animals raised at 25 °C. Representative images of *gld-2(q497)* and *gld-2(q497); rack-1(tm2262)* young adult gonads. Animals were raised at 25 °C, dissected at one day past the L4 stage, and analyzed for ectopic proliferation using α-REC8 (proliferation marker) and α-HIM-3 (meiotic marker) antibodies. Nuclear morphology was detected using DAPI. Scale bar = 20 μm.

GLD-3, a bicaudal-C homolog, is another core component of the GLD-2 pathway (Eckmann et al., 2002). GLD-3 complexes with GLD-2 to form active poly-A polymerase heterodimers (Eckmann et al., 2002; Wang et al., 2002). In the absence of *gld-3* cells are able to enter into meiosis, as the redundant GLD-1 pathway is present; however, spermatogenesis is defective resulting in abnormal or stacked oocytes (Eckmann et al., 2002). The *gld-3* null allele, *gld-3(q730),* contains a 876 bp deletion resulting in a frameshift mutation with no detectable protein produced (Eckmann et al., 2004). Since loss of *rack-1* resulted in proximal over-proliferation in *gld-2(0)* germlines, I predicted loss of *rack-1* would have a similar impact on *gld-3(0)* germlines; therefore, *gld-3(0); rack-1(0)* animals were analyzed for germline defects. At 20 °C *gld-3(q730)* and *gld-3(q730); rack-1(tm2262)* animals did not display any proliferation/differentiation defects as determined by α-REC-8 and α-HIM-3 staining (Table 6.5); however, at 25 °C 75% of *gld-3(q730); rack-1(tm2262)* germlines analyzed displayed a proximal proliferation phenotype versus 4% for *gld-3(q730)* and 0% for *rack-1(tm2262)* alone (Table 6.5 and Figure 6.4).

Table 6.5 - Loss of *rack-1* enhances proximal tumour formation in *gld-3(0)* animals

Analysis at 20 °C	Germline Phenotype[a]		
Genotype	Wildtype (%)[b]	Pro (%)[c]	n[d]
gld-3(0)[e]	100[f]	0	138
rack-1(0)[g]	99[h]	1	442
gld-3(0); rack-1(0)[i]	100[j]	0	112
Analysis at 25 °C			
gld-3(0)[e]	96[f]	4	135
rack-1(0)[g]	100[h]	0	334
gld-3(0); rack-1(0)[i]	28[j]	72	89

[a] Animals were dissected one day past the L4 stage, fixed and stained with DAPI, α-REC-8 and α-HIM-3 antibodies. The germline phenotype was scored based upon the presence of REC-8 positive cells outside of the proliferative zone.
[b] Wildtype refers to gonad arms with no REC-8 outside of the proliferative zone.
[c] Proximal tumour (Pro) refers to gonad arms that have normal relatively normal distal germline but a pool of proliferative cells (REC-8 positive) at the most proximal end of the germline.
[d] n refers to total number of gonad arms analyzed.
[e] Actual genotype; *gld-3(q730).*
[f] This includes *gld-3(0)* germline defects that did not have ectopic proliferation (abnormal or stacked oocytes).
[g] Actual genotype; *rack-1(tm2262).*
[h] This includes other *rack-1(tm2262)* germline defects that did not have ectopic proliferation (defective oogenesis and empty or underdeveloped (See Table 4.1.2 for full description and numbers).
[i] Actual genotype; *gld-3(q730); rack-1(tm2262).*
[j] This includes *gld-3(0)* germline defects that did not have ectopic proliferation (abnormal or stacked oocytes). No germlines displayed known *rack-1(0)* germline defects.

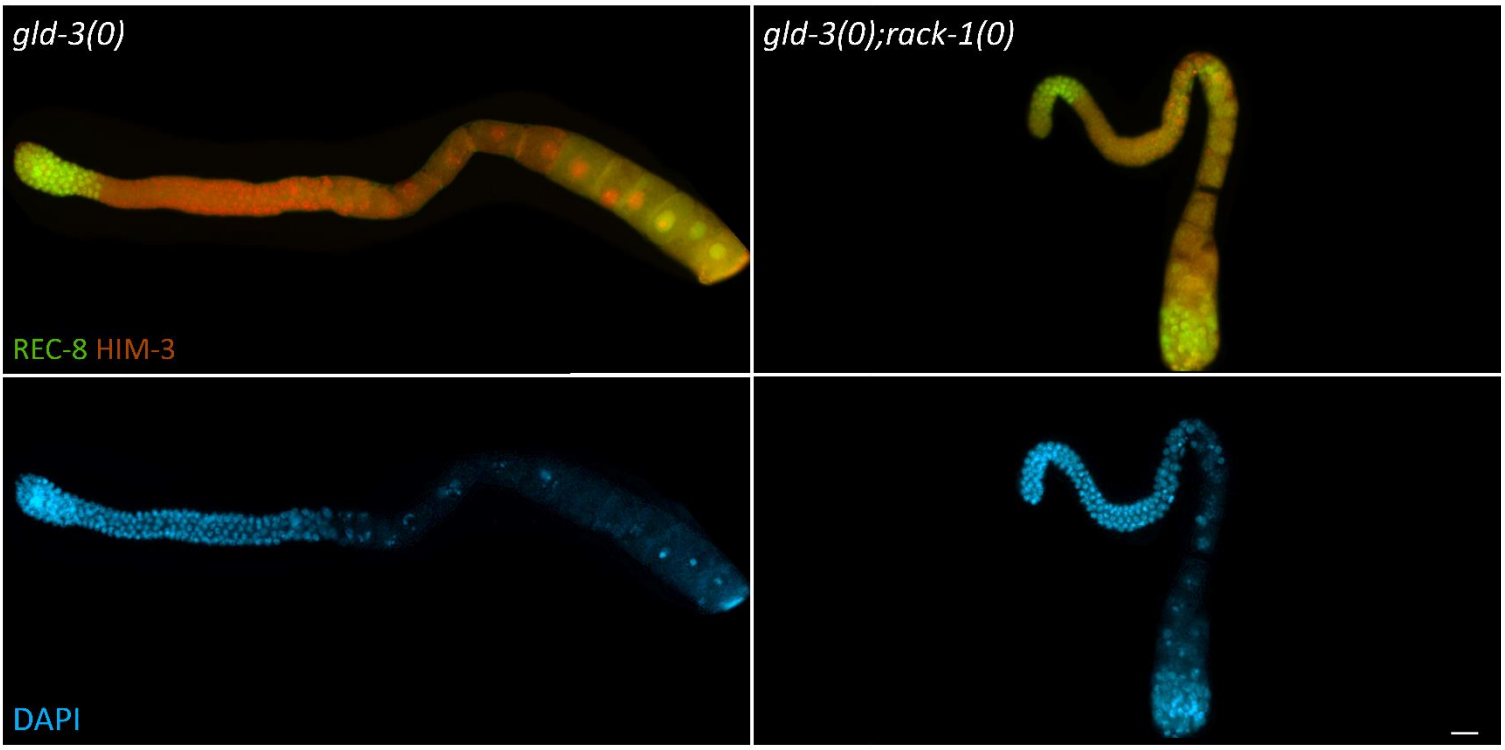

Figure 6.4 - Loss of *rack-1* enhances proximal tumour formation in *gld-3(0)* germlines at 25 °C. Representative images of *gld-3(q730)* and *gld-3(q730); rack-(tm2262)* young adult gonads. Animals were raised at 25 °C, dissected at one day past the L4 stage, and analyzed for ectopic proliferation using α-REC8 (proliferation marker) and α-HIM-3 (meiotic marker) antibodies. Nuclear morphology was detected using DAPI. Scale bar = 20 μm.

How loss of *rack-1* in *gld-2(q497)* and *gld-3(q730)* backgrounds results in germline over-proliferation in the proximal end remains unclear. One possibility is that the over-proliferation observed in these double mutants is due to the proposed reduction in GLD-1 activity upon loss of *rack-1.* Complete loss of *gld-1* alongside *gld-2(0) or gld-3(0)* results in the formation of meiotic-entry defect tumours, with little meiotic entry detected (Eckmann et al., 2004; Hansen, Hubbard, et al., 2004; Kadyk & Kimble, 1998). The extent of ectopic proliferation observed in *gld-2(q497); rack-1(tm2262)* or *gld-3(q730); rack-1(tm2262)* germlines is significantly reduced from what is observed in *gld-2(q497) gld-1(485)* or *gld-1(485); gld-3(q730)* (Figure 6.5 and Figure 6.6); however, since the loss of *rack-1* only partially reduces GLD-1 function this is not surprising. Additionally, the meiotic entry defect tumour in *gld-2(q497) gld-1(485)* or *gld-1(485); gld-3(q730)* germlines would mask any downstream germline defect; therefore, it is still possible that this over-proliferation may be related to a disruption of GLD-1 function in *rack-1* mutants. It cannot yet be ruled out that the over-proliferation observed is due to a function of *rack-1* that is independent of its control of GLD-1. Importantly, the formation of proximal tumours in *gld-2(q497); rack-1(tm2262)* and *gld-3(q730); rack-1(tm2262)* germlines supports the idea that loss of *rack-1* disrupts the proliferation/differentiation balance in sensitized backgrounds, further demonstrating a role for *rack-1* in modulating the proliferation/differentiation balance in the germline of *C. elegans.*

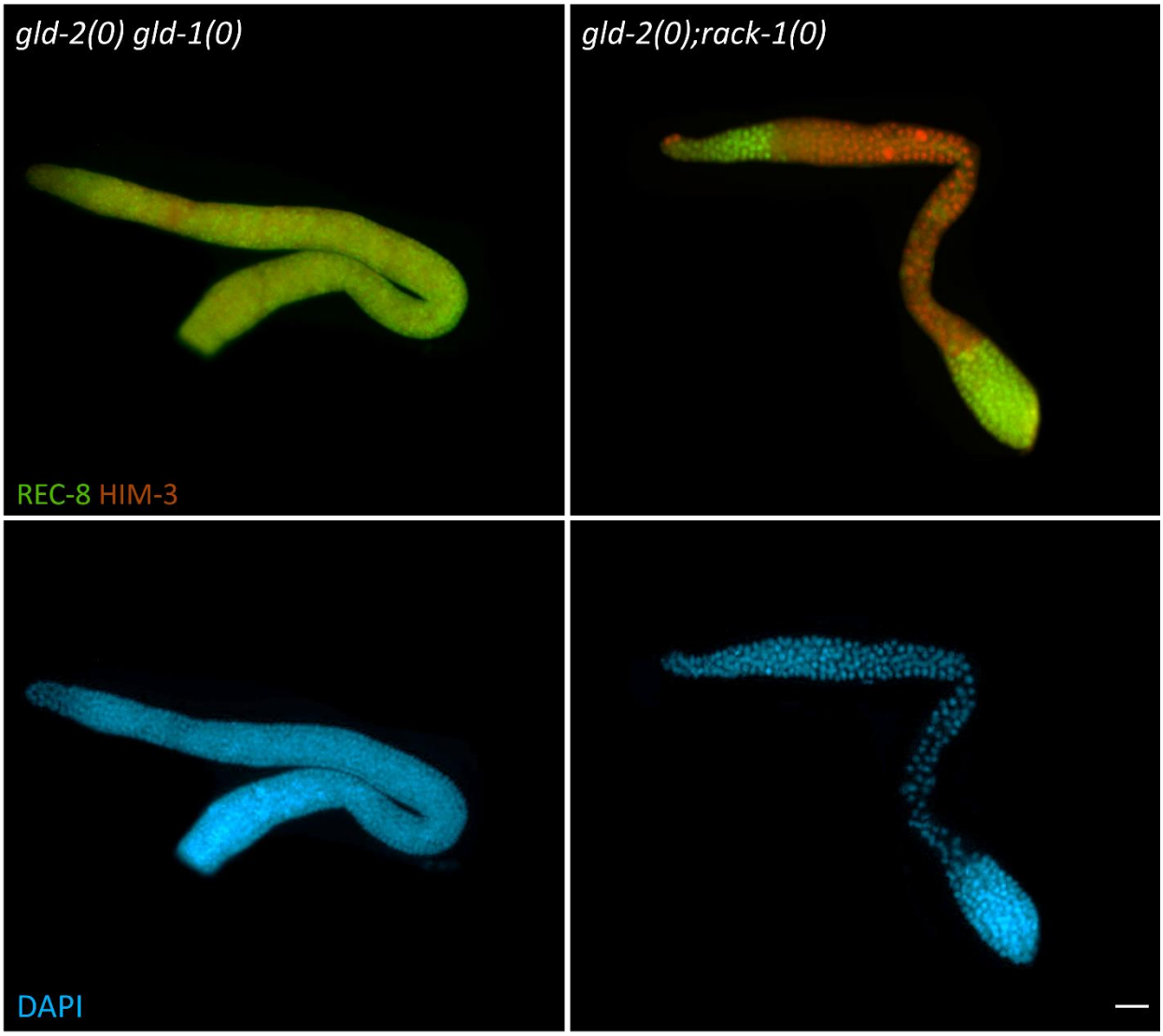

Figure 6.5 – *gld-2(0); rack-1(0)* germlines do not phenocopy *gld-2(0) gld-1(0).* Representative images of young adult gonads from *gld-2(q497); rack-1(tm2262)* (25 °C) and *gld-2(q497) gld-1(q485)* (20 °C). Animals were dissected at one day past the L4 stage and analyzed for ectopic proliferation using α-REC8 (proliferation marker) and α-HIM-3 (meiotic marker) antibodies. Nuclear morphology was detected using DAPI. Scale bar = 20 μm.

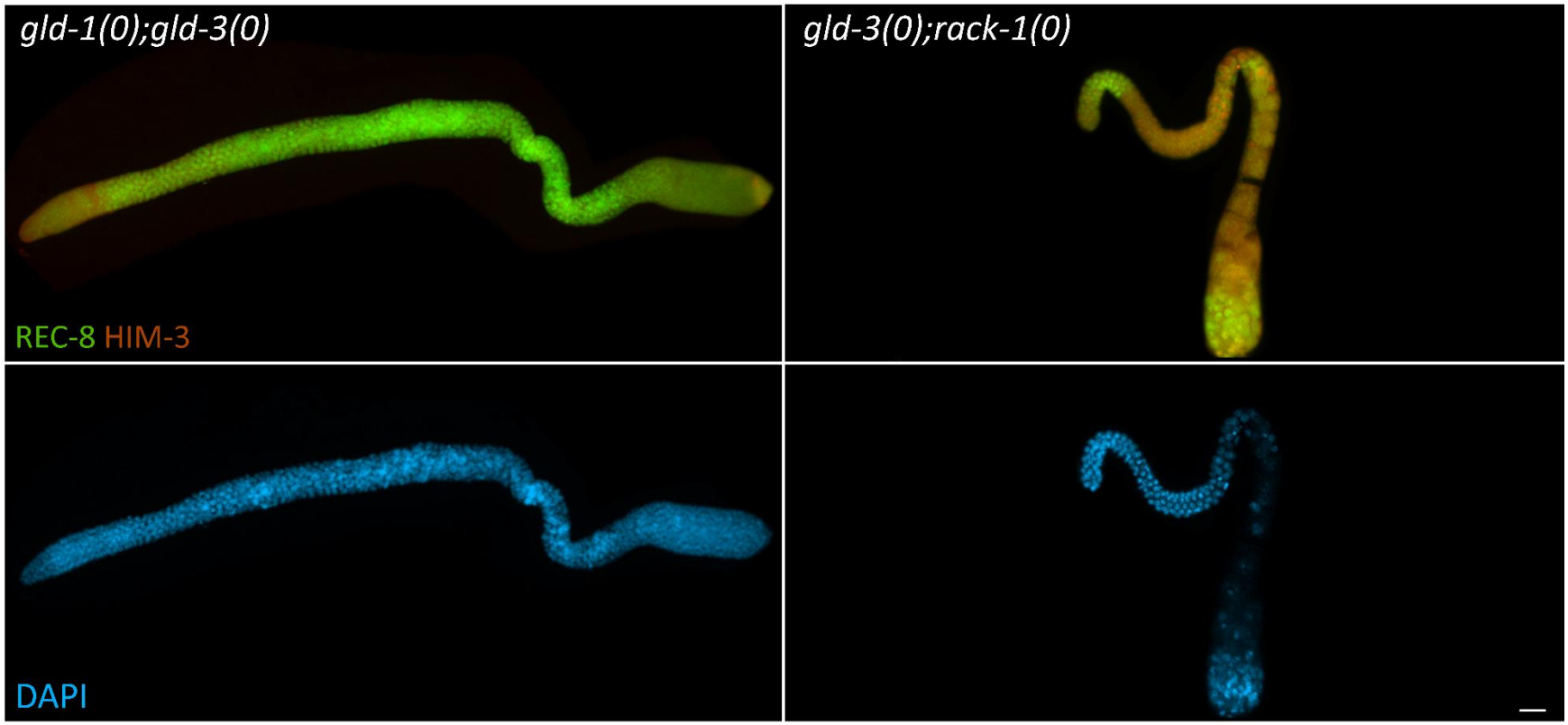

Figure 6.6 - *gld-3(0); rack-1(0)* germlines do not phenocopy *gld-1(0); gld-3(0).* Representative images of young adult gonads from *gld-1(q485); gld-3(q730)* (20 °C) and *gld-3(q730); rack-1(tm2262)* (25 °C). Animals were dissected at one day past the L4 stage and analyzed for ectopic proliferation using α-REC8 (proliferation marker) and α-HIM-3 (meiotic marker) antibodies. Nuclear morphology was detected using DAPI. Scale bar = 20 μM

6.3 A reduction of GLD-1 phenocopies a loss of *rack-1* in a *gld-3* mutant background

As mentioned above, it remains unclear how the loss of *rack-1* in *gld-2(0)* and *gld-3(0)* animals results in germline over-proliferation. One possibility is that this over-proliferation phenotype is due to a function of *rack-1* that is independent of its effect on GLD-1; however, it is also possible that the over-proliferation phenotype is due to a reduction in GLD-1 activity when it is lowered and mislocalized in *rack-1* mutants. To determine if the over-proliferation phenotypes observed in *gld-3(q730); rack-1(tm2262)* at 25 °C might be due to a reduction in GLD-1 activity in *rack-1* mutants, germline phenotypes in *gld-1(het); gld-3(0)* animals were analyzed (*gld-1(q485/tmC18); gld-3(q730)* - tmC18 is a balancer chromosome carrying a wildtype copy of *gld-1).*

At 25 °C 4% of *gld-3(q730)* germlines displayed proximal over-proliferation, whereas no proximal proliferation was detected in *gld-1(q485/tmC18)* germlines alone (Table 6.6). Interestingly, 75% of *gld-1(q485/tmC18); gld-3(q730)* animals displayed proximal over-proliferation as determined by α-REC-8 and α-HIM-3 staining (Table 6.6 and Figure 6.7). This suggests that a partial reduction of GLD-1 activity (*gld-1(het)*) in a *gld-3* mutant background results in proximal over-proliferation. This demonstrates that a reduction in GLD-1 activity leads to a disruption in the proliferation/differentiation balance in GLD-2 pathway mutants. Loss of *rack-1* in a GLD-2 pathway mutant (*gld-2(0)* or *gld-3(0)*) resulted in proximal over-proliferation as well. This supports the proposed model that GLD-1's activity is reduced when it is mislocalized and lowered in *rack-1* mutants.

Table 6.6 - A partial reduction in *gld-1* enhances proximal tumour formation in *gld-3(0)* animals

Analysis at 25 °C	Germline Phenotype[a]		
Genotype	Wildtype (%)[b]	Pro (%)[c]	n[d]
gld-3(0)[e]	96[f]	4	135
gld-1(het)[g]	100	0	124
gld-1(het); gld-3(0)[h]	25[i]	75	98

[a] Animals were dissected one day past the L4 stage, fixed and stained with DAPI, and α-REC-8 and α-HIM-3 antibodies. The germline phenotype was scored based upon the presence of REC-8 positive cells outside of the proliferative zone.
[b] Wildtype refers to gonad arms with no REC-8 outside of the proliferative zone.
[c] Proximal tumour (Pro) refers to gonad arms that have normal relatively normal distal germline but a pool of proliferative cells (REC-8 positive) at the most proximal end of the germline.
[d] n refers to total number of gonad arms analyzed.
[e] Actual genotype; *gld-3(q730).*
[f] This includes *gld-3(0)* germline defects that did not have ectopic proliferation (abnormal or stacked oocytes).
[g] Actual genotype; *gld-1(q485/tmC18) – tmC18* is a balancer chromosome carrying a wildtype copy of *gld-1.*
[h] Actual genotype; *gld-1(q485/tmC18); gld-3(q730) – tmC18* is a balancer chromosome carrying a wildtype copy of *gld-1.*
[i] This includes *gld-3(0)* germline defects that did not have ectopic proliferation (abnormal or stacked oocytes).

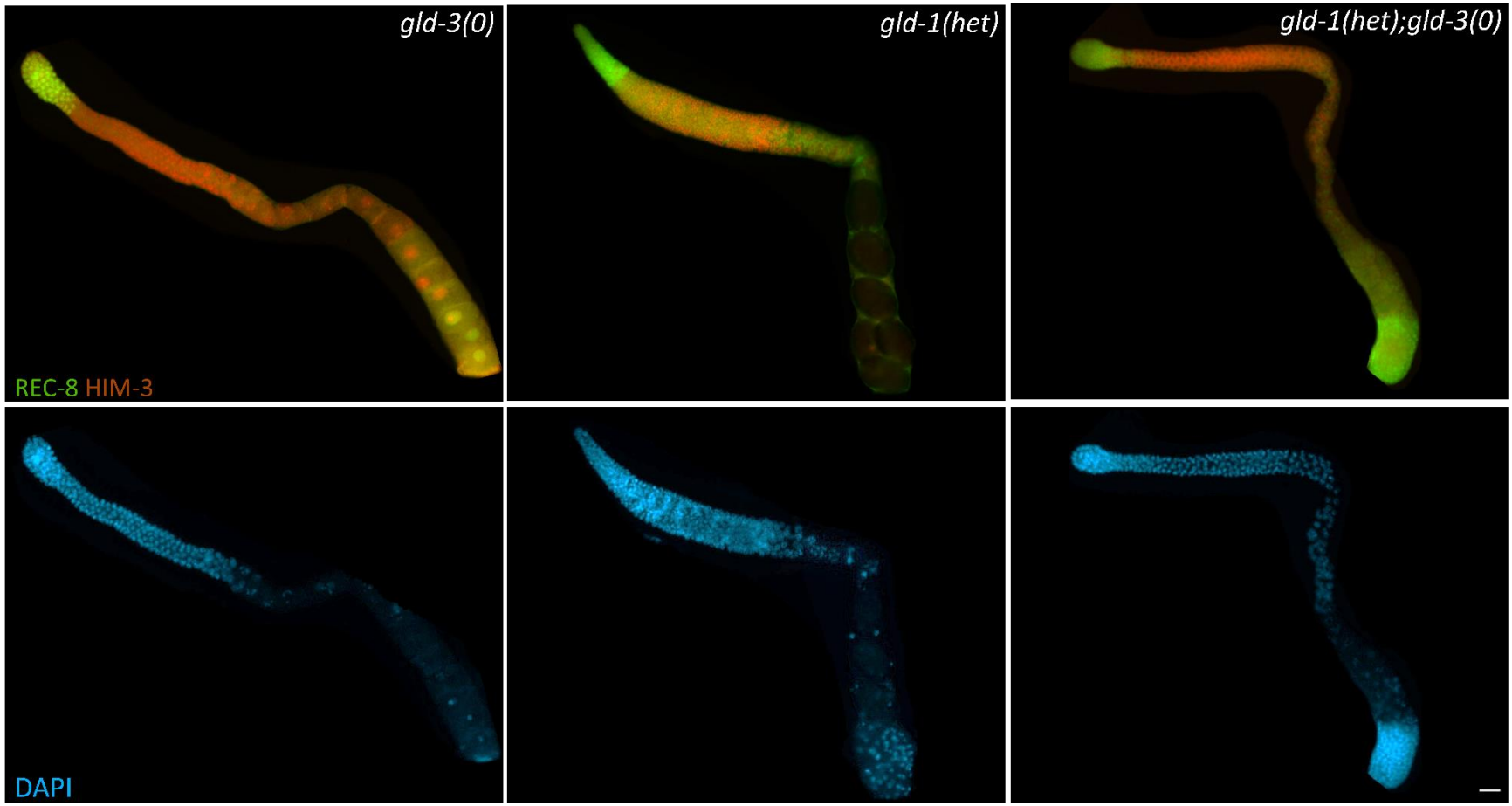

Figure 6.7 - A partial reduction of *gld-1* enhances proximal tumour formation in *gld-3(0)* at 25 °C. Representative images of *gld-3(q730), gld-1(q485/tmC18), gld-1(q485/tmC18); gld-3(q730)* young adult gonads. Animals were raised at 25 °C, dissected at one day past the L4 stage, and analyzed for ectopic proliferation using α-REC-8 (proliferation marker) and α-HIM-3 (meiotic marker) antibodies. Nuclear morphology was detected using DAPI. Scale bar = 20 μm.

As *rack-1* does not disrupt the entry into meiosis decision in *gld-3(0)* or *gld-2(0)* germlines, meiotic entry-defects in the adult germline may not account for the over-proliferation phenotype observed; however, proximal tumours can form due to a delay in the initial switch from mitosis to meiosis during early development (L3 stage), referred to as latent-niche dependent proliferation (McGovern et al., 2009). Conversely, proximal proliferation can form due to cells failing to progress through meiosis and re-entering the mitotic cell cycle. This de-differentiation phenotype is the cause of proximal proliferation in *gld-1* null germlines (Francis et al., 1995). Further research investigating when in development these ectopic proliferative cells develop will be necessary to understand the mechanism underlying proximal tumour formation in these double mutant animals.

6.4 The over-proliferation phenotype observed in *gld-2(0); rack-1(0)* is GLP-1/Notch dependent

As previously mentioned, the GLD-1 and GLD-2 pathways function redundantly to promote entry into meiosis. When both pathways are disrupted, as in a *gld-2(q497) gld-1(485)* animals, meiotic entry is severely disrupted, resulting in the formation of a tumorous germline with little meiotic entry detected (Hansen, Hubbard, et al., 2004; Kadyk & Kimble, 1998). Interestingly, this meiotic entry-defective tumour was found to be GLP-1/Notch-independent, with *gld-2(q730) gld-1(q485);glp-1(q175)* germlines still displaying robust over-proliferation (Kadyk & Kimble, 1998), To determine if the ectopic proliferation observed upon loss of *rack-1* with core GLD-2 pathway mutants forms independently of Glp-1/Notch, *gld-2(q497);glp-1(q175);rack-1(tm2262)* animals were analyzed.

Interestingly, all *gld-2(q497); glp-1(q175); rack-1(tm2262)* germlines analyzed were Glp with no detectable ectopic proliferation as determined by whole-mount DAPI staining (nuclear morphology) (Table 6.7). This data suggests that the over-proliferation observed in *gld-2(q730); rack-1(tm2262)* is GLP-1/Notch-dependent. The data presented in the previous sections supports that GLD-1 activity is reduced, not abolished, in *rack-1(0)* mutants; therefore, the over-proliferation phenotype in *gld-2(q730); rack-1(tm2262)* being GLP-1/Notch-dependent is not overly surprising as GLD-1 activity and GLD-1 pathway function are not completely disrupted.

Table 6.7 - Proximal tumour formation in *gld-2(0); rack-1(0)* animals is GLP-1/Notch-dependent

Analysis at 20 °C Genotype	Glp (%)[a]	n[b]
gld-2(0); glp-1(0)[c]	100	135
gld-2(0); glp-1(0); rack-1(0)[d]	100	184
Analysis at 25 °C		
gld-2(0); glp-1(0)[c]	100	146
gld-2(0); glp-1(0); rack-1(0)[d]	100	169

[a] Germline proliferative defective (Glp); A gonad arm was scored as Glp if only sperm was present in the gonad arm when analyzed at one day past the L4 as determined by whole mount DAPI (nuclear morphology) analysis.
[b] n refers to total number of gonad arms analyzed.
[c] Actual genotype; *gld-2(q497); glp-1(q175).*
[d] Actual genotype; *gld-2(q497); glp-1(q175); rack-1(tm2262).*

6.5 Loss of *rack-1(0)* enhances mutant phenotypes of a *gld-1* partial loss-of-function allele *gld-1(op236)*

The data presented above supports a model where the mislocalized and reduced GLD-1 in *rack-1(0)* germlines has reduced activity leading to dysregulation of the balance between proliferation and differentiation in sensitized backgrounds. *rack-1(0)* germline phenotypes, sterility at 25 °C and reduced oogenesis, are reminiscent of a partial loss-of-function allele of *gld-1*, *gld-1(op236),* suggesting that the reduction of GLD-1 function may be similar in these two genetic backgrounds.

The *gld-1(op236)* allele contains a nonsynonymous point mutation (V276F) within the KH domain (RNA binding domain) (Schumacher et al., 2005). This allele has relatively wildtype function at 20 °C, but at the restrictive temperature (25 °C) the germlines exhibit increased apoptosis due to the reduced ability to bind and repress *cep-1* mRNA (Schumacher et al., 2005). The germlines of this mutant display no obvious defect in entry into meiosis but have meiotic progression defects with the germlines displaying an extended pachytene stage region with little to no diplotene/diakinesis nuclei (Schumacher et al., 2005). To determine if *rack-1(0)* does reduce GLD-1 activity, I analyzed *rack-1(0)'s* ability to enhance *gld-1(op236)* germline defects.

I first analyzed the pachytene to diplotene/diakinesis transition in *gld-1(op236); rack-1(tm2262)* germlines at the permissive temperature (20 °C). In wildtype germlines cells transition from pachytene stage to diplotene/diakinesis at the loop of the gonad arm (Hubbard & Greenstein, 2005). This transition is marked by both a reorganization of germline cells and chromatin reorganization. As germ cells enter diplotene the

chromosomes become condensed allowing the six individual bivalents to be observed (Hubbard & Greenstein, 2005). As chromosomal re-arrangement is occurring, the cells also rearrange into a single-file linear progression through oogenesis, with cell volume increasing as cells progress through diplotene forming mature oocytes (Hubbard & Greenstein, 2005). *rack-1(tm2262)* germlines do not display any delayed transition from pachytene to diplotene stage; however, they do show reduced oogenesis (Figure 4.2, Figure 6.8 and Table 6.8). No extended pachytene was observed in *gld-1(op236)* germlines as determined by DAPI staining (nuclear morphology), in agreement with previous reports (Schumacher et al., 2005), nor did they display reduced oogenesis as seen in *rack-1(tm2262)* (Figure 6.8 and Table 6.8). Interestingly, 31% of *gld-1(op236); rack-1(tm2262)* germlines analyzed displayed extended pachytene with reduced oogenesis (Figure 6.8 and Table 6.8). This result indicates that the loss of *rack-1* enhances the meiotic progression defect of the partial loss-of-function allele *gld-1(op236).*

Table 6.8 - Loss of *rack-1* enhances delayed pachytene exit in *gld-1(op236)* germlines at the permissive temperature

Analysis at 20 °C	Germline Phenotype[a]		
Genotype	Wildtype[b] (%)	Extended Pachytene[c] (%)	n[d]
gld-1(op236)	100	0	60
rack-1(0)[e]	100	0	60
gld-1(op236); rack-1(0)[f]	69	31	59

[a] Animals were dissected one day past the L4 stage, fixed and stained with DAPI. The germline phenotype was scored based upon nuclear morphology as determined by DAPI staining.
[b] Wildtype refers to gonad arms where cells progressed from pachytene into diplotene/diakinesis at the loop of the gonad arm.
[c] Extended pachytene refers to gonad arms where cells did not progress into diplotene/diakinesis at the loop, and instead had an extended region of pachytene with late-pachytene staged nuclei past the loop.
[d] n refers to total number of gonad arms analyzed.
[e] Actual genotype; *rack-1(tm2262).*
[f] Actual genotype; *gld-1(op236); rack-1(tm2262).*

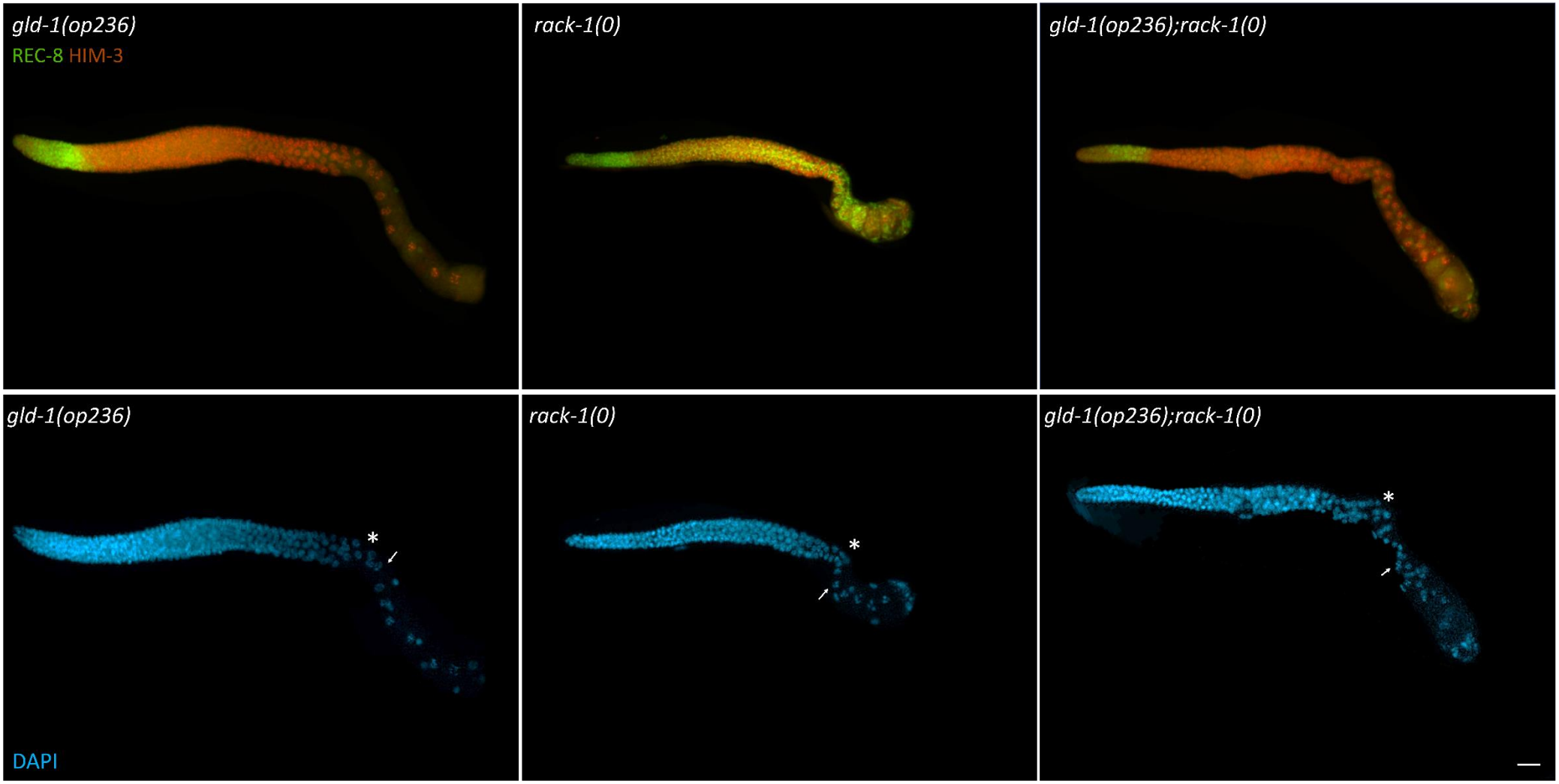

Figure 6.8 - **Loss of *rack-1* enhances meiotic progression delay in *gld-1(op236)* germlines at the permissive temperature.** Representative images of *gld-1(op236)*, *rack-1(tm2262)* and *gld-1(op236); rack-1(tm2262)* young adult

gonads. Animals were raised at 20 °C, dissected at one day past the L4 stage and analyzed for delayed transition from pachytene to diplotene/diakinesis using α-REC-8 and α-HIM-3 antibodies. DAPI staining was used to determine nuclear morphology. Arrow (→) represents first visible diplotene nuclei indicating progression through pachytene. * represents the loop of the germline. Scale bar = 20 μm

At the restrictive temperature, *gld-1(op236)* germlines produce little to no oocytes as germ cells are unable to progress through pachytene. This germline defect leads to *gld-1(op236)* animals being sterile at the restrictive temperature (25 °C) (Schumacher et al., 2005). To further characterize enhancement of *gld-1(op236)* in the absence of *rack-1*, I conducted an embryonic viability assay and analyzed the brood size of *gld-1(op236); rack-1(tm2262)* animals at 20 °C to see if loss of *rack-1* can result in sterility of *gld-1(op236)* at the permissive temperature.

I first examined the number of embryos produced in *gld-1(op236)* and *rack-1(tm2262)* animals and found that both mutants had a reduction in the number of embryos produced compared to wildtype (Table 6.9). *gld-1(op236)* animals produced on average 139 embryos; a 43% reduction compared to wildtype (avg = 241). *rack-1(tm2262),* as previously mentioned, produced 42 embryos on average, an 82% reduction compared to wildtype (Table 6.9). *gld-1(op236); rack-1(tm2262)* animals produced on average 12 embryos; a 95% reduction compared to wildtype (Table 6.9).

Additionally, *gld-1(op236)* and *rack-1(tm2262)* had a reduction in the number of viable progeny produced compared to wildtype (Table 6.9). *gld-1(op236)* animals produced on average 137 viable progeny; a 43% reduction compared to wildtype (avg = 239) (Table 6.9). *rack-1(tm2262),* as previously mentioned, produced on average 19 viable progeny, a 92% reduction compared to wildtype (Table 6.9). *gld-1(op236); rack-1(tm2262)* animals produced on average 2 viable progeny; a 99% reduction compared to wildtype (Table 6.9). It is important to note that 6 out of 14 *gld-1(op236); rack-1(tm2262)*

animals analyzed (43%) did not give rise to any viable progeny, with only 1 of the 14 *rack-1(tm2262)* animals analyzed (7%) having no progeny. All *gld-1(op236)* animals produced viable progeny (n=13).

Table 6.9 - Embryonic viability assay of *rack-1(0), gld-1(op236) and gld-1(op236); rack-1(tm2262)* animals at 20 °C.

Genotype	Average number of embryos laid (S.D.; range)[a]	Average number of progeny hatched (S.D.; range)[b]	Embryonic viability (%)[c]	n[d]
Wildtype (N2)	242 (47; 144-299)	239 (47; 140-290)	99	14
rack-1(0)[e]	42 (40; 0-113)	19 (16; 0-42)	45	14
gld-1(op236)	139 (36; 53-193)	137 (37; 51-193)	99	13
gld-1(op236); rack-1(0)[f]	12 (5; 1-21)	2 (2; 0-8)	17	14

[a] Single animals were put on individual plates and allowed to lay eggs for 24 hours at which point the were moved to a new plate. This was repeated until egg laying ceased, approximately 6 days. S.D. = Standard Deviation; Range = minimum-maximum values obtained.
[b] The average number of progeny hatched was counted 48-72 hours after the parental worm was removed from the plate. S.D. = Standard Deviation; Range = minimum-maximum values obtained.
[c] Embryonic viability was determined by dividing the average number of progeny hatched by the average number of embryos laid for each genotype.
[d] n refers to total number of individual animals analyzed for each genotype.
[e] Actual genotype; *rack-1(tm2262).*
[f] Actual genotype; *gld-1(op236); rack-1(tm2262).*

It is possible that the reduction seen in *gld-1(op236); rack-1(tm2262)* animals, on both the number of embryos and viable progeny produced, is simply the additive effect of the reduction seen with the two mutant alleles alone. If these alleles were acting additively, it is anticipated the double mutant would have produced approximately 23 embryos and 11 progeny; however, *gld-1(op236); rack-1(tm2262)* produced only 12 embryos and 2 progeny. This suggests that these two genes are working synergistically, and not additively, and suggests that the loss of *rack-1* enhances the phenotypes associated with a *gld-1* partial loss-of-function allele, *gld-1(op236).* This is in agreement that mislocalized and reduced GLD-1, in *rack-1* mutant animals, has reduced, but not abolished, GLD-1 activity.

The reduction in the number of embryos produced by *gld-1(op236); rack-1(tm2262)* animals is not surprising due to the meiotic progression failure and reduced number of oocytes produced within their germlines; however, the reduction in progeny produced when *rack-1* is lost in combination with *gld-1(op236)* was interesting. I previously demonstrated that *rack-1(tm2262)* animals have low embryonic viability, 45% (average number of progeny produced divided by the average number of embryos produced), which can be attributed to its known role in cytokinesis in the early embryo (Ai et al., 2009; Nilsson et al., 2004). *gld-1(op236)* animals had 99% embryonic viability, similar to wildtype animals; however, *gld-1(op236); rack-1(tm2262)* animals had only 17% embryonic viability (Table 6.9). Moreover, the few progeny produced from *gld-1(op236); rack-1(tm2262)* animals appeared to arrest during an early larval stage but this observation was not measured in detail. Taken together this data suggests that a genetic

interaction between *gld-1* and *rack-1* may be required within the embryo for proper development to occur. Further research will need be conducted to uncover how these genes function synergistically during early development.

6.6 Loss of *rack-1* phenocopies a partial reduction in *gld-1* in a *fbf-1(0) fbf-2(0)* genetic background

The data presented above suggests that GLD-1's activity is partially reduced in *rack-1(0)* animals. To further test this hypothesis, I compared the phenotypes associated with a partial reduction of *gld-1* to a loss of *rack-1.*

Active GLP-1/Notch signaling promotes proliferation within the distal end of the germline, in part, through the repression of GLD-1. This repression is achieved through the activation of two nearly identical translational repressors, FBF-1 and FBF-2*,* referred to collectively as FBF (Crittenden et al., 2002; Lamont et al., 2004; Zhang et al., 1997)*. fbf-1* functions to prevent meiotic entry and *fbf-2* functions to promote cell division (Wang et al., 2020). The combined effect allows for proper regulation of the GSC pool (Wang et al., 2020); therefore, in the absence of both *fbf-1* and *fbf-2* germ cells lose their ability to proliferate, and all cells enter meiosis by the L4 stage, resulting in the adult germline being completely filled with mature sperm (Glp) (Crittenden et al., 2002). This premature meiotic entry was found to be dependent on FBF's regulation of GLD-1, as a partial reduction of *gld-1, gld-1(+/q485),* was sufficient to rescue the proliferative zone in *fbf-1(0) fbf-2(0)* germlines, and a complete loss of *gld-1, gld-1(q485)* resulted in proliferating cells throughout the germline in *fbf-1(0) fbf-2(0)* animals (Crittenden et al., 2002).

If loss of *rack-1* does partially reduce GLD-1 activity, then *fbf-1(0) fbf-2(0); rack-1(0)* mutants may phenocopy *gld-1(+/q485); fbf-1(0) fbf-2(0),* with a suppression of the premature meiotic entry phenotype resulting in a rescue of the proliferative zone. At 20 °C all *fbf-1(ok91) fbf-2(q704); rack-1(tm2262)* germlines analyzed had proliferating cells present at the distal end of the germline in contrast to *fbf-1(ok91) fbf-1(q704)* germlines analyzed, which were completely Glp (n=35) as determined by α-REC-8, α-HIM-3 and DAPI staining (Table 6.10 and Figure 6.9). Interestingly, 'young adult' (one day past the L4 stage) *fbf-1(ok91) fbf-2(q704); rack-1(tm2262)* germlines analyzed appeared slightly delayed, with the proximal end of the germline housing primary spermatocytes and not mature sperm as would be expected at this stage (Figure 6.9). As *rack-1* mutant animals are developmentally delayed compared to wildtype, it is possible that this proliferative zone rescue could be a result of delayed germline development (this thesis and (Demarco & Lundquist, 2010)). To rule out this possibility, *fbf-1(ok91) fbf-2(q704); rack-1(tm2262)* animals were analyzed as 'old adults' (3 days past the L4 stage). All *fbf-1(ok91) fbf-2(q704); rack-1(tm2262)* old adult germlines analyzed displayed a rescue of the proliferative zone, suggesting that the suppression of premature meiotic entry is not likely due to developmental delay in *rack-1* mutants (Table 6.10 and Figure 6.9). This data demonstrates that in a *fbf-1(ok91) fbf-2(q704)* mutant background loss of *rack-1* phenocopies a partial reduction of *gld-1.* This further supports the hypothesis that GLD-1's activity is reduced in *rack-1* mutants.

The data presented in this chapter supports the hypothesis that loss of *rack-1(0)* results in GLD-1 mislocalization and reduced levels, leading to a decrease, but not complete loss, of GLD-1 activity. This reduction in GLD-1 activity is the likely cause of the disruption in the proliferation/differentiation balance in the various genetic backgrounds analyzed in this thesis.

Table 6.10 - Loss of *rack-1* rescues the proliferative defects in *fbf-1(0) fbf-2(0)* germlines

Young Adults[a]	**Genotype[b]**	**Proliferative Zone[c] (%)**	**Glp[d] (%)**	**n[e]**
	fbf-1(0) fbf-2(0)[f]	0	100	35
	fbf-1(0) fbf-2(0); rack-1(0)[g]	100	0	45
Old Adults[h]				
	fbf-1(0) fbf-2(0)[f]	0	100	65
	fbf-1(0) fbf-2(0); rack-1(0)[g]	100	0	84

[a] Young adult animals were analyzed one day past the L4 stage.
[b] Animals were dissected, fixed and stained with α-REC-8 and α-HIM-3 antibodies. Nuclear morphology was determined by DAPI staining. The germline phenotype was scored based upon α-REC-8 positive cells present in the distal most are of the germline.
[c] Proliferative Zone refers to germlines that had proliferating cells (α-REC-8 positive) in the distal most end of the germline.
[d] Germline proliferative defective (Glp); A gonad arm was scored as Glp if only sperm was present in the gonad arm when analyzed.
[e] n refers to total number of gonad arms analyzed.
[f] Actual genotype; *fbf-1(ok91) fbf-2(q704)*
[g] Actual genotype; *fbf-1(ok91) fbf-2(q704); rack-1(tm2262)*
[h] Old adult animals were analyzed 3 days past the L4 stage.

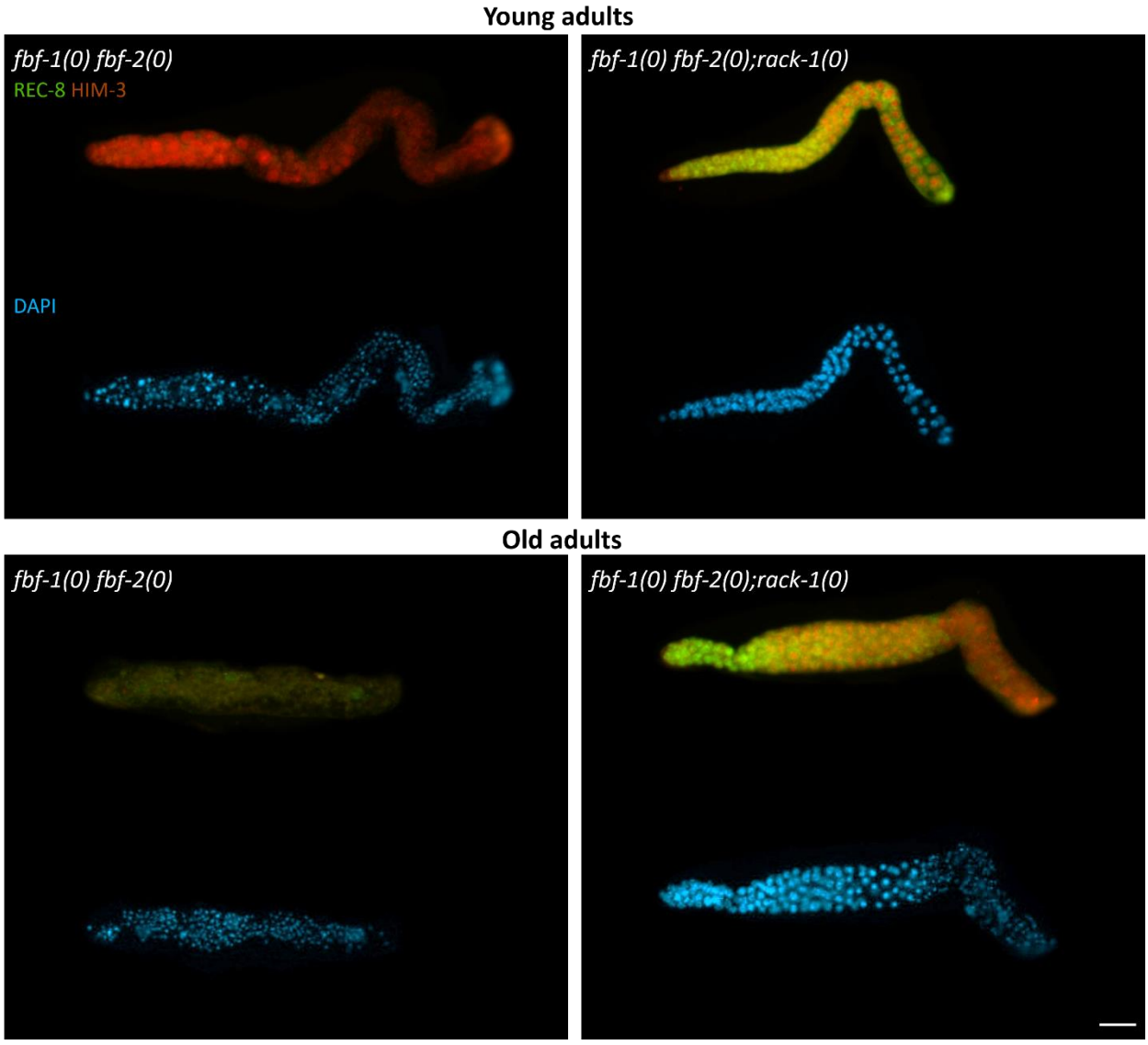

Figure 6.9 - Loss of *rack-1* rescues the proliferation defect in *fbf-1(0) fbf-2(0)* germlines. Representative images of *fbf-1(ok91) fbf-2(q704), fbf-1(ok91) fbf-2(q704); rack-1(tm2262)* gonads. Animals were raised at 20 °C, dissected at one day past the L4 stage (young adult, top panel), or at 3 days past the L4 stage (old adult, lower panel), and analyzed for proliferating cells within the distal end of the germline using α-REC-8, α-HIM-3 antibodies. DAPI staining was used to determine nuclear morphology. Scale bar = 20 μm.

Chapter 7 – Discussion

Stem cells are unspecified cells that are central to the development and tissue homeostasis of multi-cellular organisms, including *C. elegans* and humans. Stem cells possess the ability to self-renew through cellular divisions (proliferation/mitosis), or to develop into other more specialized cells (differentiation). Proper development requires a balance between stem cell proliferation and differentiation. Understanding how this balance is regulated provides information on normal development and tissue maintenance, and also provides insight on how cell proliferation becomes dysregulated leading to diseases such as cancer. In this thesis I describe the characterization of *rack-1* as a novel factor involved in controlling stem cell fate in the germline of *C. elegans.* Genetic and molecular analyses have uncovered *rack-1*'s role in promoting differentiation through regulating the subcellular localization and levels of a core meiotic protein, GLD-1. GLD-1's role in the proliferation/differentiation balance has been well researched (Brenner & Schedl, 2016; Doh et al., 2013; Francis et al., 1995; Jones et al., 1996); however, this study is the first to demonstrate that GLD-1's activity is dependent upon its subcellular localization.

7.1 *rack-1* is involved in regulating the proliferation/differentiation balance within the *C. elegans* germline

The balance between stem cell proliferation and differentiation in the germline of *C. elegans* is regulated by GLP-1/Notch signaling, *lst-1 sygl-1* PUF hub, and the downstream meiotic entry pathways (GLD-1, GLD-2 and SCF^{PROM-1}); however, other molecular mechanisms have been uncovered that function alongside of this core genetic pathway (Gupta et al., 2015; Kerins et al., 2010; Mohammad et al., 2018; Wang et al.,

2012). In this thesis I describe the identification of RACK-1 as an additional factor that influences the proliferation/differentiation balance within the germline.

Using *glp-1(ar202gf)* as a sensitized background, loss of *rack-1* was found to cause germline over-proliferation (Figure 3.1 and Table 3.1). This over-proliferation phenotype was also observed with a weaker gain-of-function allele, *glp-1(oz264),* demonstrating that this is not an allele-specific effect (Figure 3.2 and Table 3.2). *glp-1* gain-of-function mutations disrupt the proliferation/differentiation balance by increasing GLP-1/Notch signaling to promote proliferation; however, mutations that affect the entry and progression through meiosis can also disrupt the proliferation/differentiation balance. Interestingly, loss of *rack-1* resulted in an over-proliferation phenotype in mutant animals of core meiotic genes, *gld-2* (Figure 6.3), *gld-3* (Figure 6.3) and *nos-3* (Appendix B). Loss of *rack-1* alone had little impact on stem cell proliferation (Table 3.7 and Table 3.8). Taken together these findings are consistent with *rack-1* functioning as a modulator of the core genetic pathway regulating the balance between proliferation and differentiation, as loss of *rack-1* in combination with a disruption in these pathway results in an over-proliferation phenotype.

The ability of *rack-1(0)* to enhance proliferation in the presence of increased GLP-1/Notch signaling suggested that loss of *rack-1* may also rescue a loss of or decrease in GLP-1/Notch signaling; however, *rack-1(0)* was unable to rescue a complete loss of *glp-1* (Table 3.3), or reduced GLP-1/Notch signaling, *glp-1(bn18ts)* (Table 3.4) A loss of GLP-1/Notch signaling, *glp-1(0),* results in a failure of the primordial germ cells to proliferate

during germline development in the early larval stages, causing premature meiotic entry and the formation of only 4-8 mature sperm (Kershner et al., 2014; Kimble & White, 1981). The failure of *rack-1(0)* to rescue the proliferation defect in these backgrounds suggest that loss of *rack-1* is not strong enough to overcome a loss of GLP-1/Notch signaling. Alternatively, *rack-1* may function redundantly with other components in the germline, such that loss of one factor alone is not sufficient to have an impact. *rack-1(0)* was able to rescue the proliferation defect in *fbf-1(0) fbf-2(0)* germlines (Figure 6.10). *fbf-1* and *fbf*-2 function downstream of *glp-1,* and *lst-1 sygl-1,* and are required for primordial germ cell proliferation during the L4 stage (Crittenden et al., 2002). Rescue of proliferation in this genetic background may indicate that *rack-1* functions downstream of GLP-1/Notch signaling.

Analysis of RACK-1's germline expression, using the C-terminal CRISPR-tagged alleles *rack-1(ug12)* and *rack-1(ug17)*, demonstrated that RACK-1 is expressed throughout the germline, consistent it with playing a role in regulating the proliferation/differentiation balance. RACK-1 was previously detected in the distal tip cell (Demarco & Lundquist, 2010); however, no obvious DTC enrichment was identified using *rack-1(ug12)* or *rack-1(ug17).* Previous research demonstrated that knocking down *rack-1* expression in the germline by RNAi enhanced *glp-1(ar202gf)*'s over-proliferation phenotype, indicating that *rack-1* is required within the germline cells to modulate the proliferation/differentiation balance (Wang, 2013). RACK-1's germline expression did not provide any insight into how it functions to modulate the proliferation/differentiation

balance as it was uniformly expressed throughout the germline in both mitotic and meiotic cells, as well as developing oocytes (Figure 4.5 and 4.6).

The over-proliferation/rescue of proliferation phenotypes observed upon loss of *rack-1* in various genetic backgrounds, combined with RACK-1's germline expression, suggests that wildtype *rack-1* could function to directly inhibit GLP-1/Notch signaling and/or promote differentiation. Loss of *rack-1* did not result in increased GLP-1/Notch signaling, as determined using SYGL-1 expression (Figure 3.5 and Figure 3.6), and the stem cell pool size (proliferative zone) as read outs of GLP-1/Notch activity (Table 3.8). Interestingly, SYGL-1 expression, and the stem cell pool, were reduced in the absence of *rack-1,* opposite to what was expected (See Section 7.4.1).

Germline over-proliferation upon loss of *rack-1* requires sensitized backgrounds to be observed; therefore, it is possible that the background utilized to examine SYGL-1 expression was not "sensitized enough" to observe a change; however, loss of *rack-1* did not increase the size of the stem cell pool size in *glp-1(ar202gf),* or *glp-1(oz264gf)* sensitized germlines even though over-proliferation was observed throughout the germline. Taken together, this data suggests that *rack-1* does not function to directly inhibit GLP-1/Notch signaling.

7.2 *rack-1* is required for the proper levels and subcellular localization of the core meiotic protein GLD-1

RACK-1, and its orthologs, have no known enzymatic activity on their own, and instead function as scaffold proteins mediated through their highly conserved WD-repeat domains (Reviewed in: (Gandin et al., 2013)). The tertiary structure of WD-repeats have

been shown to form β-propellor structures that serve to facilitate protein-protein and protein-DNA interactions [(Wall et al., 1995) and Reviewed in (C. Xu & Min, 2011)]. Mammalian RACK1 is known to be involved in a number of diverse processes including protein translation and cell death, and has over 100 proposed interacting proteins (direct or in complex) (Gandin et al., 2013). Previous research using Immunoprecipitation-Mass Spectrometry (IP-MS) in *C. elegans* identified a potential interaction between RACK-1 and GLD-1 (Akay et al., 2013). I found that GLD-1's subcellular localization was dramatically altered in *rack-1(0)* germlines (Figure 5.1.1). In wildtype germlines GLD-1's expression is relatively uniform throughout the cytoplasm in meiotic germ cells up until the loop region (Jones et al., 1996); however, in *rack-1(0)* germlines GLD-1 formed large perinuclear aggregates within the meiotic cells which I refer to as sub-cellular mislocalization (Figure 5.1). These aggregates were found to co-localize with P granules (Figure 5.4). GLD-1 was recently found to be slightly enriched at P granules in wildtype adult germlines (Ellenbecker et al., 2019); however, unlike the aggregation of GLD-1 in *rack-1(0)* which is quite obvious, the enrichment of GLD-1 in P granules in wildtype is more subtle.

The dramatically increased localization of GLD-1 to P granules in the absence of *rack-1* did not require GLD-1's ability to interact with mRNA (Figure 5.5). This indicates that the subset of GLD-1 that is found associated with P granules in the adult germline may depend on protein-protein interactions. One possibility is that RACK-1 directly interacts with GLD-1, throughout the cytoplasm, and prevents the majority of GLD-1 from

localizing to P-granules. The identification of the protein-protein interaction between GLD-1 and RACK-1 supports this possibility (Akay et al., 2013). Future co-immunoprecipitation experiments, using CRISPR-tagged alleles of *rack-1,* should be performed to further characterize this interaction. Additionally, proximity ligation assays (PLA) can be performed to detect interactions between GLD-1 and RACK-1 *in situ,* which would provide subcellular information on where this potential interaction occurs (Day et al., 2020).

WD-proteins, like RACK-1, are known to facilitate complex formation; therefore, it is possible that RACK-1 and GLD-1 do not directly interact, but instead are part of a larger protein complex (Gandin et al., 2013). The microRNA Induced Silencing Complex (miRISC) is one potential complex containing both RACK-1 and GLD-1. Previous research has identified both RACK-1 and GLD-1 interacting with miRISC components, specifically ALG-1 and VIG-1 (Akay et al., 2013; Dallaire et al., 2018; Jannot et al., 2011; Zhang et al., 2007). Co-IP or IP-MS experiments, pulling down both RACK-1 and GLD-1, and comparing the interacting proteins detected, may help determine if RACK-1 and GLD-1 interact through the miRISC, or another complex. The possibility exists that interaction with miRISC may be required for GLD-1's proper localization. Future experiments investigating GLD-1's localization in the absence of miRISC components, such as ALG-1 and VIG-1, will help determine if a miRISC interaction plays a role in GLD-1's localization. It is also possible that RACK-1 and GLD-1 do not interact directly, or through a shared complex, and instead RACK-1 influences an intermediate protein that functions to directly regulate GLD-1's localization. IP-MS data from GLD-1 in wildtype and *rack-1*

mutant animals may help identify candidates that could function as the intermediate protein.

RACK-1 has been found to interact with proteins involved in other small RNA pathways that localize to P granules within the germline (CSR-1, PRG-1 (PIWI) and WAGO-1) (Barucci et al., 2020; Batista et al., 2008; Claycomb et al., 2009; Gu et al., 2009). This suggests that a portion of RACK-1 may localize to P granules; however, no obvious aggregation was detected when analyzing RACK-1's *in vivo* germline expression (Figure 4.5 and Figure 4.6). This does not rule out the possibility of RACK-1 being present within P granules, as it may be present at similar levels to its cytoplasmic expression. If RACK-1 is present in P granules, this suggests that it may function to prevent or block GLD-1's accumulation within the granules; however, it is possible that RACK-1 interacts with a small portion of these P granule localized proteins within the cytoplasm. In-depth analysis, such as co-localization experiments or PLAs, with P granule components, such as PGL-1, or potential interactors (CSR-1, PRG-1, or WAGO-1) will be necessary to determine if RACK-1 is present within P granules. This data will help determine how RACK-1 exerts its influence on GLD-1's localization pattern within the cells of the germline.

rack-1 mutants also have reduced GLD-1 levels throughout the germline as determined by western blot and immunofluorescence analyses (Figure 5.6 and 5.7). This suggests that the interaction between RACK-1 and GLD-1, or the potential intermediate proteins, may help stabilize GLD-1 and/or protect GLD-1 from degradation or that *rack-1*

regulates GLD-1's expression post-transcriptionally, as is the main form of regulation in the germline (Merritt et al., 2008). RACK-1 orthologs in yeast and mammalian systems have been well-established as components of the 40s ribosome, where they function to promote ribosome assembly. RACK1 recruits PKCβII, allowing for the phosphorylation and release of eIF6, facilitating the proper assembly of the 80S ribosomal subunit (Ceci et al., 2003). In *C. elegans,* RACK-1 has been shown to inhibit translation by recruiting miRISC to active ribosomes (Jannot et al., 2011); therefore, one possibility is that *rack-1* regulates GLD-1's expression by facilitating miRISC-ribosome interactions. Although miRNAs have been demonstrated to regulate *gld-1's* expression, a loss of RACK-1, and decreased miRISC-ribosome interactions, would be predicted to increase GLD-1 expression, an opposite result to what is seen in *rack-1(0)* (Liu et al., 2011; Theil et al., 2019). To determine how *rack-1* regulates GLD-1 levels, quantitative PCR analysis of *gld-1* mRNA in *rack-1* mutants should be performed to confirm that the reduction in GLD-1 is due to post-transcriptional regulation, where RACK-1 is known to function. Additionally, GLD-1 protein levels in *rack-1(0)* animals can be measured in a background with reduced proteasome function. If *rack*-1 functions to protect GLD-1 from degradation, then GLD-1 levels should increase in the absence of *rack-1* when proteasome function is reduced. This data would provide insight into how *rack-1* may regulate GLD-1 levels.

gld-1's expression is known, in part, to be regulated by the poly-A polymerase subunit GLD-2. GLD-2 has been shown to be required to promote translation of *gld-1* as cells begin to enter meiosis, with GLD-1 levels being reduced throughout the germline of

gld-2(0) animals (Hansen, Wilson-Berry, et al., 2004; Suh et al., 2006). Analysis of *gld-2(0); rack-1(0)* germlines indicated that *rack-1* does not function with *gld-2* to regulate GLD-1 levels, as GLD-1 was further reduced in *gld-2(0); rack-1(0)* double mutant germlines compared to *gld-2(0)* germlines alone (Figure 5.8). GLD-1 expression is also regulated by the PUF proteins, FBF-1 and FBF-2 (FBF collectively). FBF functions to translationally repress *gld-1* in the proliferative zone (mitotic cells) (Crittenden et al., 2002; Merritt et al., 2008; Suh et al., 2009; Zhang et al., 1997). Interestingly, RACK-1 has been detected interacting with both FBF-1 and FBF-2 (Friend et al., 2012; Wang et al., 2016). The possibility exists that the potential interaction between FBF and RACK-1 may function to reduce or modulate FBF's ability to repress *gld-1* expression; therefore, in the absence of *rack-1* more FBF is available to repress *gld-1*, leading to a decrease in overall GLD-1 levels; however, GLD-1 levels only appear to increase within the distal most region of the proliferative zone in *fbf-1(0) fbf-2(0)* germlines, not as cells transition into meiosis (Suh et al., 2009). The levels of GLD-1 throughout the proliferative zone in *rack-1(0)* germlines is relatively wildtype, with reduced GLD-1 levels becoming evident after the transition zone and throughout the meiotic region (Figure 5.4). This suggests that RACK-1 may not interact with FBF to control *gld-1's* expression.

How GLD-1's interaction with RACK-1 or a shared complex, like miRISC, controls GLD-1's subcellular localization, and influences GLD-1 levels, remains unclear but will be an interesting topic for future research as this implies a novel mechanism by which GLD-1, a core meiotic protein, is regulated.

7.3 *rack-1* is required for proper GLD-1 function

The data described in this thesis has identified *rack-1* as a modulator of stem cell proliferation/differentiation. Moreover, my data demonstrates that *rack-1* is required for proper GLD-1 levels and subcellular localization. Taken together, this data has led to the proposed model where RACK-1 functions either directly or indirectly to regulate GLD-1's subcellular localization and levels. In the absence of *rack-1,* GLD-1 levels are reduced, and GLD-1 becomes mislocalized to perinuclear aggregates (P granules). This leads to a decrease, but not a complete loss, of GLD-1 activity, resulting in a disruption in the proliferation/differentiation balance, visible as over-proliferation in sensitized backgrounds (Figure 7.1).

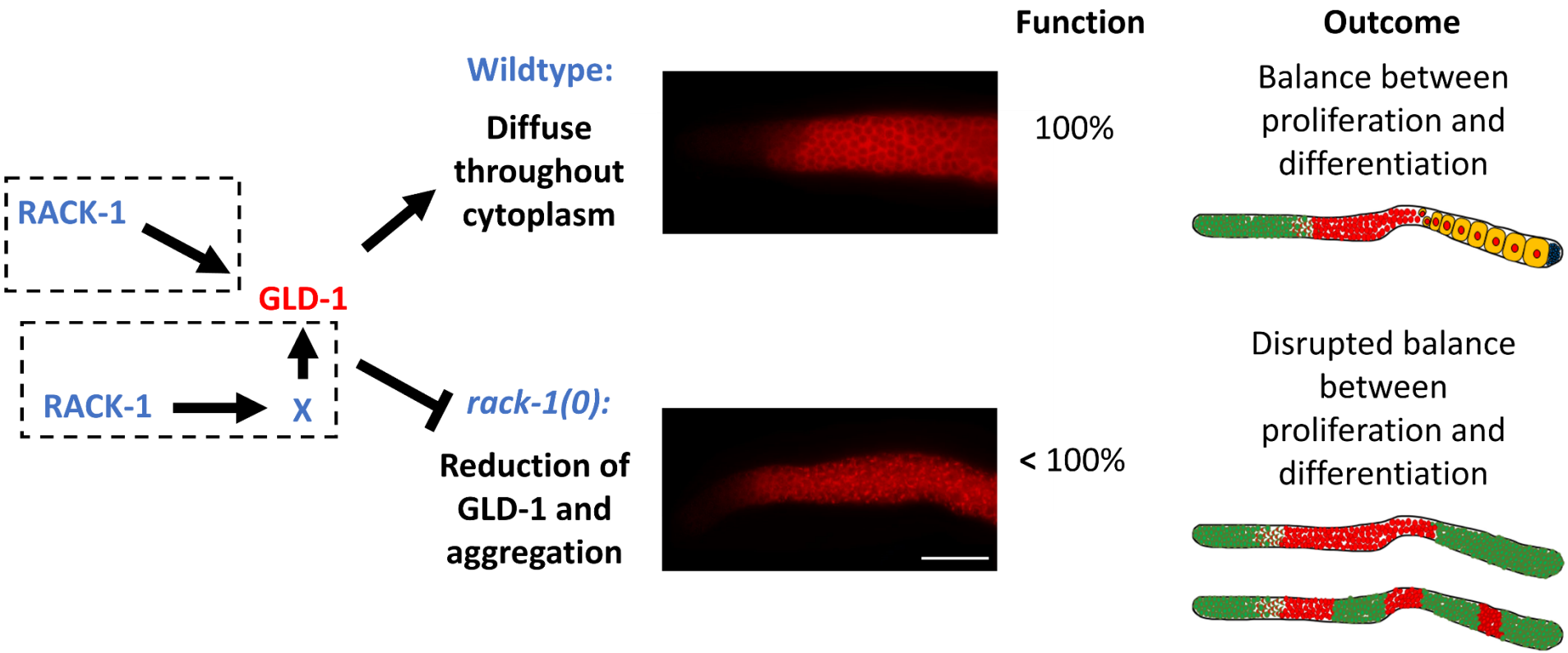

Figure 7.1 – Proposed model. RACK-1 functions either directly or indirectly (through protein or protein complex X) to regulate GLD-1's activity. This interaction allows for proper localization and levels of GLD-1 resulting in 100% function. Proper GLD-1 function allows for a precise balance between GSC proliferation/differentiation resulting in a functional

germline. In the absence of *rack-1,* GLD-1 levels are reduced, and GLD-1 becomes mislocalized. This results in less than 100% function and disruptions to the proliferation/differentiation balance in sensitized backgrounds.

A complete loss of *gld-1* leads to the formation of proximal tumours as cells are unable to progress through meiosis and revert to the mitotic cell cycle (de-differentiation), whereas complete loss of *rack-1* has little germline ectopic proliferation on its own (Table 4.2) (Francis et al., 1995). This highlights that loss of *rack-1* does not phenocopy a loss of *gld-1,* indicating that the mislocalized GLD-1 retains some function. When GLD-1 is absent, as in *gld-1(0),* the loss of *rack-1* had no impact on germline proliferation as *gld-1(0); rack-1(0)* animals displayed the *gld-1(0)* de-differentiation phenotype; however, loss of *rack-1* in *gld-1* heterozygous animals subtly enhanced germline defects (Table 6.2 and Table 6.3). This supports the model of *rack-1* exerting its influence on the proliferation/differentiation balance through regulation of GLD-1.

GLD-1 functions downstream of the GLP-1/Notch signaling pathway to promote entry into meiosis. GLD-1's role in the proliferation/differentiation balance has been characterized mainly through the use of the *gld-1* null allele, *gld-1(q485)*; therefore, little has been reported about the effect of a reduction in GLD-1 activity, as opposed to a complete loss, on the proliferation/differentiation balance. One reported effect associated with a reduction in GLD-1 was characterized in an FBF mutant background. Loss of FBF results in germ cells entering meiosis prematurely, and a complete loss of the proliferative stem cell pool (Crittenden et al., 2002); however, Crittenden *et al.* determined that a partial reduction in *gld-1,* through the use of a *gld-1* heterozygote (*gld-1(+/q485)*), suppressed the premature meiotic entry defect in *fbf* mutant germlines (Crittenden et al., 2002). Loss of *rack-1* was able to rescue the proliferation defect in *fbf* mutants, phenocopying the

rescue observed with a partial reduction of GLD-1 (Table 6.10). This rescue strongly supports the model that GLD-1 has reduced activity in *rack-1* mutant germlines.

gld-1 functions redundantly with the GLD-2 pathway (*gld-2* and *gld-3*) to regulate the entry into meiosis decision (Eckmann et al., 2002; Hansen, Hubbard, et al., 2004; Kadyk & Kimble, 1998). Loss of *gld-1* in combination with a GLD-2 pathway mutant results in the majority of germ cells failing to enter meiosis, and the germline containing mostly proliferative cells (Eckmann et al., 2004; Hansen, Hubbard, et al., 2004; Kadyk & Kimble, 1998). This entry into meiosis defect was not observed in animals lacking *rack-1* in combination with a GLD-2 pathway mutant (Table 3.7). Meiotic entry defects were also not observed in *glp-1* gain-of-function backgrounds upon loss of *rack-1* (Table 3.8). This was not surprising, as GLD-1 activity is only partially reduced in *rack-1* mutants.

This data indicates that there may be a certain threshold of GLD-1 activity that is required for normal entry into meiosis, and that GLD-1 activity does not fall below that threshold in *rack-1(0)* germlines. *gld-1* functions redundantly with multiple other genes to regulate entry into meiosis; therefore, it is possible that low levels are sufficient for normal meiotic entry. This is supported by *gld-2* mutants having significantly reduced GLD-1 levels without any severe defects in meiotic entry (Suh et al., 2006). Alternatively, it could suggest that GLD-1 requires different ‘co-factors’ to translationally repress the subset of target genes involved in each process; therefore, the expression of some but not all GLD-1 targets would be disrupted. Lastly, it is possible that the failure to see changes in meiotic

entry, could be a result of a GLD-1-independent function of *rack-1*, within the proliferative zone.

Although an obvious entry into meiosis defect was not observed in *gld-3(0); rack-1(0)* and *gld-2(0); rack-1(0)* adult germlines, these animals did display proximal over-proliferation (Table 6.4 and 6.5). To determine if this over-proliferation phenotype could be due to a reduction in GLD-1 activity, *gld-1(+/-); gld-3(0)* animals were analyzed (Table 6.6). This experiment demonstrated that a reduction in GLD-1 activity alongside of a loss of GLD-2 pathway mutants causes proximal over-proliferation similar to that observed in animals' mutant for *rack-1* and a GLD-2 pathway gene (Table 6.4).

How a reduction in GLD-1 activity results in over-proliferation in these genetic backgrounds remains unclear. Proximal proliferation can form due to a number of reasons including mitotic re-entry, and delayed "initial meiosis" leading to latent niche-dependent proliferation (Reviewed by: (Hubbard & Schedl, 2019)). In *gld-1(0)* germlines, proximal tumour formation occurs due to cells failing to progress through the meiotic cell cycle and re-entering the mitotic cell cycle (de-differentiation) (Francis et al., 1995). Both *gld-2(0)* and *gld-3(0)* have germline defects associated with disruptions in gametogenesis, and/or meiotic progression (Eckmann et al., 2002; Kadyk & Kimble, 1998); therefore, it is possible that the combination of lowered GLD-1 activity, through loss of *rack-1,* and loss of *gld-2* or *gld-3* may exacerbate the meiotic progression defects in these backgrounds, resulting in mitotic re-entry. To investigate if the proximal tumours form due to this 'de-differentiation' mechanism, future experiments analyzing a reduction in GLD-1 activity

[*gld-1(+/-)* and *rack-1(0)*] in combination with a loss of *gld-2(0) or gld-3(0)* should be analyzed throughout the L4 stage. Meiotic pachytene nuclei are detectable during the early L4 stage, with no differentiated spermatocytes detectable until later in L4 development (Barton & Kimble, 1990; Francis et al., 1995). The presence of proliferating cells in these backgrounds at a late L4/young adult stage, but not during early L4 development, would suggest that the proximal proliferation forms because the germ cells fail to progress through meiosis and re-enter the cell cycle. If proximal proliferation is detected prior to the onset of differentiation (early L4 stage), this would indicate that another mechanism, such as latent-niche dependent proliferation, is responsible for the ectopic proliferation phenotype.

Latent niche-dependent proliferation, occurs when the switch from mitosis to meiosis ("initial meiosis") is delayed during germline development (McGovern et al., 2009). This delayed initial meiosis results in cells competent to respond to GLP-1/Notch signaling being located next to somatic cells expressing GLP-1/Notch ligands (McGovern et al., 2009). These somatic cells function as a "latent niche" by providing ectopic GLP-1/Notch activation, promoting proliferation. Both *gld-2(0)* and *gld-3(0)* mutant germlines display delayed initial meiosis (Eckmann et al., 2004); therefore, it is possible that reducing GLD-1 activity, through loss of *rack-1,* could impact initial entry into meiosis and lead to latent niche-dependent proximal tumours; however, this model is inconsistent with the observation that the complete loss of *gld-1(0)* does not disrupt initial meiotic entry on its own (Francis et al., 1995). A combined loss of *gld-1 and gld-2/gld-3* results in defective entry into meiosis; therefore, it is possible that a partial reduction in GLD-1 activity, in the

presence of *gld-2/gld-3* mutants, could increase the delay in initial meiosis or disrupt early entry into meiosis, and result in a latent niche-dependent proximal tumour. Analyzing these mutant backgrounds throughout the larval stages, during the initial switch into meiosis (L3 stage), similar to the experiment describe above, will provide insight into how proximal proliferation develops in *gld-2(0); rack-1(0), gld-3(0); rack-1(0) and gld-1(+/-); gld-3(0)* animals.

Initial identification and characterization of *gld-1* mutants uncovered roles for *gld-1* in the entry into meiosis decision, progression through meiosis and germline sex determination (Francis et al., 1995). The discovery of multiple loss-of-function and separation-of-function alleles allowed these functions of *gld-1* to be identified and uncoupled from each other (Francis et al., 1995). It is thought that *gld-1* regulates these developmental processes through translationally repressing its diverse range of target genes (Jan et al., 1999; Lee & Schedl, 2004; Lee & Schedl, 2001; Marin & Evans, 2003; Mootz et al., 2004; Xu et al., 2001). The data presented in this thesis suggests that a loss of *rack-1* disrupts *gld-1's* activity, resulting in germline over-proliferation and defective progression through meiosis.

In support of *rack-1* impacting *gld-1's* function in promoting progression through meiosis, loss of *rack-1* was able to subtly enhance proximal proliferation in *gld-1* heterozygous animals (Table 6.2). Moreover, *gld-1(+/-); rack-1(0)* germlines displayed an extended pachytene region (Table 6.3). Loss of *rack-1* in combination with a *gld-1* partial loss-of-function allele, (*gld-1(op236)*), which is defective for meiotic progression at

elevated temperatures, resulted in disrupted meiotic progression at the permissive temperature with very few detectable oocytes (diakinesis/diplotene staged nuclei). This phenotype is similar to the phenotype of *gld-1(op236)* animals grown at the restrictive temperature. Additionally, *gld-1(op236);rack-1(0)* animals produced very few embryos (avg = 12) (Table 6.9), with 43% of *gld-1(op236);rack-1(0)* animals analyzed being sterile (Akay et al., 2013; Schumacher et al., 2005). This data supports the model that loss of *rack-1* leads to a decrease in GLD-1's activity and disruption in GSC progression through meiosis.

In addition to *gld-1(op236),* the *gld-1(q93oz50)* and *gld-1(oz116)* separation-of-function alleles of *gld-1* have also been identified as having pachytene progression defects. *gld-1(q93oz50)* carries a mutation within the KH domain, *q93* allele (G248R), and may have reduce RNA binding capabilities (Jones et al., 1996; Jones & Schedl, 1995). *gld-1(oz116)* possess a 3' splice acceptor variant for exon 8, with no disruption to the KH domain (Jones et al., 1996; Jones & Schedl, 1995). Future experiments can be performed to determine if loss of *rack-1* enhances pachytene progression defects in animals heterozygous for *gld-1(q93oz50)* and *gld-1(oz116),* as was demonstrated with *gld-1(q485/+)* animals (Table 6.3).

7.4 Can disrupting GLD-1's aggregation in P granules rescue its function?

In the absence of *rack-1,* GLD-1 is mislocalized at the sub-cellular level, and GLD-1 levels appear to be reduced. The model proposed attributes the over-proliferation in various sensitized backgrounds to a reduction in GLD-1 activity upon mislocalization and/or reduced levels in the absence of *rack-1* (Figure 7.1). This suggests that restoring

GLD-1 localization or levels would be anticipated to rescue the germline defects observed. As mentioned in Section 7.2, *rack-1* may function to promote GLD-1 stabilization and/or protect GLD-1 from degradation. Analyzing GLD-1 levels in *rack-1(0)* mutants alongside a reduction in proteasome function, may result in a rescue of GLD-1 levels. If GLD-1 levels are increased in *rack-1(0)* proteasome reduced animals, backgrounds that showed over-proliferation in the absence of *rack-1,* such as *glp-1* gain-of-function mutants or GLD-2 pathway mutants, should be analyzed alongside of reduced proteasome activity to see if a rescue in GLD-1 levels is sufficient to rescue GLD-1 activity.

GLD-1 is mislocalized to P granules upon loss of *rack-1;* therefore, experiments should also be performed to disrupt P granule formation/stabilization to determine if there is a rescue of GLD-1's wildtype cytoplasmic expression. Knocking down four core P granule factors simultaneously (*pgl-1, pgl-3, glh-1, and glh-4)* disrupts P granule formation and results in cytoplasmic localization of proteins that normally localize in P granules (Updike et al., 2014). This quadruple knockdown could be performed in *rack-1(0)* mutant animals to determine if GLD-1 localization can be rescued. This would further validate GLD-1's mislocalization to P granules in *rack-1(0).* Moreover, if GLD-1 localization can be rescued, this experiment could be performed on other mutant backgrounds, such as *glp-1* gain-of-function mutants or GLD-2 pathway mutants, which displayed over-proliferation when combined with *rack-1(0).* These experiments would determine if restoring GLD-1 localization is sufficient to rescue the over-proliferation in these

backgrounds. This data would support the model that the mislocalization of GLD-1 results in decreased activity.

Loss of P granules results in sterility and loss of germ cell identity as cells begin expressing somatic markers (Updike et al., 2014). These phenotypes may mask the ability to detect a rescue in GLD-1 function in the various mutant backgrounds; therefore, knockdown of individual P granule components may need to be performed to look for rescue of GLD-1 localization, while minimizing germline defects. Additionally, various proteins that localize to P granules (CGH-1, CAR-1, CEY-1, CEY-3 and CEY-4) have been identified to interact with GLD-1 (Akay et al., 2013; Scheckel et al., 2012; Theil et al., 2019). RACK-1 may function to prevent the majority of GLD-1 from interacting with these proteins. In the absence of *rack-1,* GLD-1 may be able to interact more freely with these proteins, resulting in increased GLD-1 P granule localization. If true, knockdown of these GLD-1 interacting proteins may rescue GLD-1's mislocalization in *rack-1* mutants. If knockdown of these components restores GLD-1's cytoplasmic localization, rescue of GLD-1 activity should be investigated in mutant backgrounds that displayed over-proliferation upon loss of *rack-1,* such as *glp-1* gain-of-function mutants and GLD-2 pathway mutants.

7.5 GLD-1 as a translational repressor

GLD-1 is well characterized as a translational repressor with the identification of many target genes, including *glp-1* and *mex-3* (meiotic entry decision), *cep-1* (apoptotic pathway), *spn-4* (embryogenesis) and *puf-5* (oogenesis) (Ariz et al., 2009; Ellenbecker et al., 2019; M.-H. Lee & Schedl, 2004; Lublin & Evans, 2007; Marin & Evans, 2003; Merritt

et al., 2008; Mootz et al., 2004; Schumacher et al., 2005). How GLD-1 functions to repress expression of its target mRNAs remains unclear. Target specific GLD-1 'co-factors' have been previously identified (Clifford et al., 2000; Ellenbecker et al., 2019); therefore it is possible that RACK-1 may serve as a target specific co-factor or RACK-1 may facilitate GLD-1 co-factor interactions.

GLD-1 has been identified to be a miRISC interacting component in the germline (Akay et al., 2013; Dallaire et al., 2018; Zhang et al., 2007). This suggests that GLD-1 targets, or a subset of its targets, may be translationally silenced via miRNAs (Dallaire et al., 2018). As RACK-1 is a miRISC interacting protein, one possibility is that RACK-1 facilitates GLD-1's association with miRISC. Loss of RACK-1 disrupts GLD-1 function through reduced association with miRISC, which may be why GLD-1 becomes mislocalized (See section 7.5). If RACK-1 exerts control on GLD-1's activity through association with the miRISC, then in the absence of RACK-1, GLD-1 miRISC interactions should decrease. Immunoprecipitation of GLD-1 in *rack-1(0)* and wildtype animals, followed by western blot analysis to identify known miRISC interactors (ALG-1, VIG-1, GLH-1) could suggest if this is true; however, more information could be obtained from comparisons of GLD-1 IP:MS data from *rack-1(0)* and wildtype animals. It is possible that *rack-1's* impact on GLD-1's function is disrupted through a miRISC-independent mechanism, which could be uncovered through further investigation into how *rack-1* controls GLD-1 localization (Section 7.5).

As GLD-1 is a translational repressor, the reduction in GLD-1 activity, upon loss of *rack-1,* is anticipated to result in changes in expression of *gld-1* target genes. Initial analysis of *rack-1(0)* germlines did not reveal increased expression of three GLD-1 target genes, *mex-3, spn-4* and *puf-5* (Appendix C); however, it is possible that only a subset of GLD-1 target genes are mis-expressed in the absence of *rack-1*. As germline defects identified upon loss of *rack-1* in combination with mutants of the core genetic regulatory pathway (*glp-1, gld-2, gld-3, gld-1(+/-)*) may be a result of disruptions in meiotic progression (de-differentiation, pachytene arrest), GLD-1 targets involved in these decisions should be examined.

gld-1(op236) was identified in a screen looking for negative regulators of the p53 apoptotic pathway (Schumacher et al., 2005). This study characterized the *C. elegans* p53 ortholog, *cep-1,* as a GLD-1 target, with both *gld-1(op236) and gld-1(0)* germlines having increased CEP-1 expression (Schumacher et al., 2005); however, only *gld-1(op236)* germlines, not *gld-1(0),* display meiotic progression defects. Schumacher *et al.,* suggested that increased apoptosis and meiotic progression defects are not observed in *gld-1(0)* germlines, even though expression of *cep-1* is increased, because the germ cells do not reach late pachytene when apoptosis is known to occur, and instead re-enter the mitotic cell cycle form an early pachytene stage (Schumacher et al., 2005). Interestingly, initial analysis of apoptosis in *rack-1(0)* germlines indicated a reduction in apoptosis compared to control germlines (Appendix D). This result is opposite to what was expected – that loss of *rack-1* would result in increased apoptosis - based on the ability of *rack-1(0)* to enhance *gld-1(op236)* mutant phenotypes (Table 6.8 and 6.9). *rack-1(0)* germlines do

not have an extended pachytene region, suggesting that apoptosis may not be increased; however, *rack-1(0)* germlines do have reduced oogenesis. This could indicate that there are fewer cells progressing into late pachytene and therefore, fewer cells are capable to undergo apoptosis or develop into oocytes. Future analysis characterizing apoptosis and CEP-1 expression in *rack-1* mutants should be performed. It is also possible that *gld-1* activity is not reduced enough in *rack-1(0)* animals to detect changes in the expression of GLD-1 targets; therefore, more sensitized backgrounds, such as *gld-1(+/-); rack-1* and *gld-1(op236); rack-1(0)* (at the permissive temperature), may be required to detect changes. These genetic analyses will be helpful to further characterize *rack-1's* role in regulating GLD-1's ability to promote meiotic progression.

Changes in CEP-1 expression would account for the failure to progress through pachytene but would not account for the proximal over-proliferation detected with GLD-2 pathway mutants; therefore, other targets are likely disrupted. *lin-45* has been identified as a GLD-1 target (Lee & Schedl, 2001). Moreover, loss of *lin-45,* or *mpk-1,* a downstream component of the ERK MAP kinase pathway, cause germ cells to arrest in pachytene in *gld-1(q485)* germlines, preventing the re-entry into the mitotic cell cycle (Lee et al., 2007; Lee & Schedl, 2001). If the ectopic proliferation in *gld-2(0); rack-1(tm2262)* and *gld-3(0); rack-1(tm2262)* are found to be due to de-differentiation, then *lin-45* would be another candidate GLD-1 target whose expression may be disrupted upon loss of *rack-1.* Additionally, knockdown of *lin-45* and *mpk-1* can be used to help determine how the proximal over-proliferation forms when *rack-1* is lost in *glp-1(gf), gld-2(0), gld-3(0)* animals.

7.6 *rack-1* has additional roles within the *C. elegans* germline

This thesis aimed to characterize *rack-1's* role in modulating the proliferation/differentiation balance within the germline of *C. elegans*, with a focus on *rack-1*'s control of GLD-1. The ubiquitous expression of RACK-1 throughout the germline, combined with RACK-1 and its orthologs having a number of diverse interaction partners suggests that *rack-1* may have additional functions within the germline, independent of *gld-1* (Gandin et al., 2013).

7.6.1 *rack-1* may be required within the proliferative zone

Analysis of the proliferative zone in *rack-1* mutants demonstrated a 45% decrease in the number of proliferating cells as compared to wildtype. This decrease was unexpected as a loss of r*ack-1* enhanced ectopic proliferation throughout the germline in sensitized backgrounds, specifically with *glp-1* gain-of-function mutations (Section 7.1); therefore, *rack-1* may be required within the proliferative zone to maintain the GSC pool. GLP-1/Notch activity was slightly reduced in *rack-1(tm2262)* germlines compared to control as determined by the extent of SYGL-1 expression (11 gcd vs 13 gcd; p=0.001) (Figure 3.5 and Figure 3.6). Moreover, the overall level of SYGL-1 expression, as determined by measuring the intensity across the proliferative zone, is slightly reduced in *rack-1(tm2262)* compared to control germlines (Figure 3.5 and Figure 3.6). This data suggests that *rack-1* may be involved to promote GLP-1/Notch signaling within the proliferative zone. Further characterization of active GLP-1/Notch signaling, through another known direct target *lst-1*, may help elucidate if *rack-1* impacts GLP-1/Notch activity.

Analysis of SYGL-1 expression and the proliferative zone size were performed in *rack-1(0)* animals. RACK-1 expression in the DTC has been previously reported (Demarco & Lundquist, 2010). It is possible that RACK-1 expression in the DTC may be required to maintain the GSC pool (PZ size), as was previously shown for ALG-1, a miRISC component and RACK-1 interacting protein (Akay et al., 2013; Bukhari et al., 2012). A mutant strain is available that restricts RNAi to the DTC only (Linden et al., 2017; Martynovsky et al., 2012). This strain can be used to analyze GLP-1/Notch activation and the proliferative zone size in the presence and absence of RACK-1 expression in the DTC. This experiment will demonstrate if *rack-1* is required cell-autonomously (within the germline) or non-autonomously (within the DTC) to regulate the stem cell pool. Furthermore, this data would help characterize the role of miRISC in regulating the stem cell pool, as has been previously demonstrated using *alg-1* mutants (Bukhari et al., 2012)

Alternatively, *rack-1* may influence the stem cell pool independently of any component of the core genetic regulatory pathway (GLP-1/Notch, *lst-1 sygl-1,* PUF hub, meiotic entry pathways). One possibility is that *rack-1* functions to regulate the cell cycle through promoting cell divisions or inhibiting entry into meiosis, a disruption in either would result in a decrease in the stem cell pool. Interestingly, research has demonstrated a role for mammalian RACK1 in controlling the cell cycle at various checkpoints including G2/M (Mamidipudi et al., 2007; McLeod et al., 2000; Núñez et al., 2010). Analysis of the cell cycle in *rack-1(0)* would determine if *rack-1* is required to promote proper cell cycle timing (Fox et al., 2011; Fox & Schedl, 2015; Kocsisova et al., 2019). Alternatively, *rack-1* may be required to prevent meiotic entry, such that in the absence of *rack-1* the rate of

meiotic entry may be increased resulting in a decrease in the stem cell pool, as was previously shown for *fbf-1(0)* (Wang et al., 2020). These experiments could uncover a conserved role for *rack-1* in regulating the mitotic cell cycle.

Analysis of *gld-2 gld-1; rack-1* germlines supports the possibility of *rack-1* functioning to regulate meiotic entry. GLD-1 and GLD-2 function redundantly to promote entry into meiosis, with *gld-2 gld-1* germlines having little to no entry into meiosis (Eckmann et al., 2004; Hansen et al., 2004; Kadyk & Kimble, 1998). Small patches (less than 10 gcd in length) of meiotic cells are detectable in *gld-2 gld-1* germlines at 20 °C; however, the majority of cells are mitotic as determined by α-REC-8 and α-HIM-3 staining (Figure A.1). Although *gld-2(0) gld-1(0); rack-1(0)* germlines display over-proliferation, particularly in the proximal germline, large clear stretches of meiotic entry, more than what is observed in *gld-2(0) gld-1(0)* double mutants (10 gcd in length), was observed following the proliferative zone (Figure A.1 and Table A.1). How *rack-1(0)* increases the amount of meiotic entry in *gld-2(0) gld-1(0)* mutants remains unclear; however, identification of a role for *rack-1* in regulating the cell cycle may help explain this increase in meiotic entry in the *gld-2(0) gld-1(0); rack-1(0)* triple mutant as compared to the *gld-2(0) gld-1(0)* double mutant.

7.6.2 *rack-1* may be required in the sex determination pathway

Analysis of loss of *rack-1* in various mutant backgrounds suggested that *rack-1* may play a role in germline sex determination. In the hermaphrodite germline, both spermatogenesis and oogenesis occur. Several players have been identified as being involved in regulating sex determination that also are involved in regulating the balance

between proliferation and differentiation, including *gld-1* and *nos-3.* In addition to promoting meiotic entry and progression, *gld-1* is required to promote the male germ cell fate in hermaphrodite germlines, with *gld-1(q485)* germlines having little to no detectable sperm (Francis et al., 1995; Jones et al., 1996; Jones & Schedl, 1995). Interestingly, *gld-1(q485); rack-1(tm2262)* and *gld-1(q361); rack-1(tm2262)* animals displayed increased spermatogenesis compared to *gld-1(q485)* or *gld-1(q361)* alone (Table B.1). This suggests that *rack-1* may function to inhibit spermatogenesis and/or promote oogenesis independently of its regulation of GLD-1. The potential involvement in the sex determination pathway may help explain the reduction in oocytes observed in *rack-1(0)* germlines (Figure 4.2).

nos-3 has been shown to be involved in promoting the female fate through regulating the spermatogenesis to oogenesis switch; however, loss of *nos-3* alone is relatively wildtype with a low penetrance of germline masculinization (Mog) (Figure B.1 and Table B.2) (This thesis and Kraemer et al., 1999). All *nos-3(0); rack-1(0)* animals analyzed at 20 °C and 25 °C had no detectable oocytes, and appeared to be Mog, although exact sperm numbers were not analyzed (Figure B.1 and Table B.2). This is in agreement with the possibility of *rack-1* playing a role in the hermaphrodite sex determination pathway. Genetic analysis with genes involved in the sex determination pathway should be performed to solidify *rack-1's* role in germline sex determination and determine where in the pathway *rack-1* might function.

Chapter 8 - Conclusion

GLD-1 is a translational repressor that is involved in many processes in the germline including entry into meiosis, progression through meiosis and germline sex determination (Francis et al., 1995; Jones et al., 1996; Jones & Schedl, 1995; Schumacher et al., 2001). Specifically, complete loss of *gld-1* results in meiotic cells de-differentiating, resulting in proximal over-proliferation (Francis et al., 1995). Some partial loss-of-function alleles of *gld-1* cause delayed progression through the meiotic pachytene stage (Francis et al., 1995; Schumacher et al., 2001). Loss of *gld-1,* in combination with loss of GLD-2 pathway function or SCF^{PROM-1} pathway function, results in an over-proliferative germline as GSC entry into meiosis is disrupted (Eckmann et al., 2004; Hansen, Hubbard, et al., 2004; Kadyk & Kimble, 1998; Mohammad et al., 2018). Additionally, a partial reduction of *gld-1* (*gld-1(+/-)* in combination with loss of GLD-2 pathway function (*gld-3(0)*) results in proximal over-proliferation (this thesis).

The genetic analyses described in this thesis support the model that *rack-1* is required, either directly or indirectly, to regulate GLD-1's subcellular localization and/or levels. In the absence of *rack-1,* GLD-1 is mislocalized at the sub-cellular level, and GLD-1 levels are reduced. This leads to a reduction of GLD-1 function, resulting in phenotypes associated with a disruption in GLD-1 function. Specifically, loss of *rack-1* resulted in germline over-proliferation in combination with *glp-1* gain-of-function mutants (*glp-1(ar202gf), glp-1(oz264gf))* and GLD-2 pathway mutants (*gld-2(q497), gld-3(q730)*). Loss of *rack-1* rescued the proliferation defects of *fbf-1(ok91) fbf-2(q704)*, similar to the rescue observed when GLD-1 function is partially reduced (Crittenden et al., 2002). Finally, loss

of *rack-1* enhanced the defective progression through meiosis phenotype associated with reduced GLD-1 activity (*gld-1(q485/+)* and *gld-1(op236)*).

GLD-1's expression is spatially regulated within the germline to ensure proper GLD-1 function (Brenner & Schedl, 2016; Hansen, Wilson-Berry, et al., 2004; Haupt et al., 2020; Kisielnicka et al., 2018; Shin et al., 2017; Suh et al., 2006). *rack-1's* regulation of GLD-1's subcellular localization identifies a novel mechanism that functions to control GLD-1's activity. This highlights that multiple layers, transcriptional control, protein degradation and protein localization, are required to ensure proper GLD-1 activity and therefore proper germline function (maintenance of GSC pool and development of gametes). How exactly GLD-1's mislocalization disrupts, but does not abolish, GLD-1's activity remains unclear but will be important to investigate further as it may uncover how GLD-1 functions as a translational repressor.

A small fraction of GLD-1 is found in P granules in wildtype adult germlines and has been shown to interact with multiple P granule associated proteins (Akay et al., 2013; Ellenbecker et al., 2019; Scheckel et al., 2012; Theil et al., 2019). These interactions may be required for GLD-1 to locate and bind its target mRNAs. P granules are estimated to be associated with ~75% of all nuclear pores; therefore, it is thought that most, if not all, mRNAs transit through P granules (Pitt et al., 2000). If GLD-1 in P granules is still fully active, then aggregation of GLD-1 at P granules in *rack-1* mutant germlines should not have resulted in reduced *gld-1* activity. The data in this thesis implies a requirement for

diffuse expression of GLD-1 (cytoplasmic and P granules) within GSCs for optimal function.

RACK-1 orthologs are required to stabilize interacting proteins in ‘active’ or ‘inactive’ states, as is the case for PKCβII (Ron et al., 1994, 1999; Stebbins & Mochly-Rosen, 2001)**;** therefore, it is possible that RACK-1 is required to maintain GLD-1 in an active state. Sam68, the mammalian ortholog of GLD-1, is known to be post-translationally modified including through methylation, phosphorylation, SUMOylation and acetylation (Frisone et al., 2015). These modifications function to regulate Sam68 function (Frisone et al., 2015). GLD-1 is known to be phosphorylated in *C. elegans*, with western blot analysis of GLD-1 showing a faint upshifted band (phosphorylated GLD-1); however, this phosphorylation results in the destabilization of GLD-1 (Jeong et al., 2011). Currently, no other post-translational modifications of GLD-1 have been identified; therefore, it is more likely for RACK-1 to be required to promote GLD-1 activity through regulating protein-protein interactions. Although GLD-1 was identified and characterized over 25 years ago, many aspects of its function as a translational repressor remain unclear, including where within the cell GLD-1 functions, what co-factors are required for GLD-1 translational repression, and by what mechanisms GLD-1 represses its targets (miRNA pathway, stabilization, translation initiation/elongation). The identification of target specific co-factors and the stabilization of some, but not all, target mRNAs implies that GLD-1 may regulate its targets through diverse mechanisms (Clifford et al., 2000; Ellenbecker et al., 2019; M.-H. Lee & Schedl, 2004).

RACK-1's requirement for proper GLD-1 activity and localization is consistent with known functions of RACK-1 orthologs in other systems (Ron et al., 1994, 1999; Stebbins & Mochly-Rosen, 2001); however, how exactly RACK-1 regulates GLD-1's localization and activity (indirectly/directly) remains unclear. In addition to regulating GLD-1, the data presented in this thesis suggests that *rack-1* may be involved in other processes within the germline, including maintenance of the GSC pool and germline sex determination. Interestingly, the requirement of *rack-1* in maintaining the GSC pool may be conserved as loss of *RACK1* in *Drosophila* results in a decrease or loss of the GSC pool (Kadrmas et al., 2007). The identification of additional RACK-1 interacting proteins in *C. elegans* will help elucidate its function within the germline.

The identification of RACK-1 as a modulator of the proliferation/differentiation balance adds to the growing list of factors, including those involved in mRNA splicing and protein degradation, that function alongside the core genetic pathway to regulate this balance (Hubbard & Schedl, 2019). It is interesting to note that many of the factors identified appear to be involved in the GLD-1 pathway, including various splicing factors (*prp-17*, *teg-4,* and *teg-1*), as well as other modulators including CK2/*kin-10* and *dlc-1* (Belfiore et al., 2004; Ellenbecker et al., 2019; Kerins et al., 2010; Mantina et al., 2009; Wang et al., 2012; Wang, 2013; Wang et al., 2014). Identification of these factors demonstrates that multiple mechanisms are required to ensure proper regulation of GSC proliferation and differentiation. This redundancy creates an optimum balance between the maintenance of GSCs and production of gametes, thereby ensuring the fitness/reproductive success of the animal. Furthermore, research using model

organisms, such as *C. elegans,* has allowed the regulation of stem cells to be studied *in vivo.* Specifically, it has allowed for the identification and characterization of genetic, physiological, and environmental factors that function to regulate GSC development and maintenance within an organism over its lifespan, contributing to the overall understanding of stem cell behaviour.

Appendix A - *rack-1* may function in the sex determination pathway

The GLD-1 and GLD-2 pathways function redundantly to promote entry into meiosis (Eckmann et al., 2004; Hansen et al., 2004; Kadyk & Kimble, 1998). When both pathways are mutated the majority of germ cells fail to enter into meiosis, resulting in proliferating cells throughout the germline (Eckmann et al., 2004; Hansen, Hubbard, et al., 2004; Kadyk & Kimble, 1998); however, the presence of some meiotic cells suggested that other mechanisms/pathways function redundantly to the GLD pathways to promote meiotic entry (Hansen et al., 2004). A third pathway, SCF^{PROM-1}, was identified that further reduced the meiotic entry in *gld-2(0) gld-1(0)* germlines but did not completely abolish it, with low levels of meiotic cells still detectable in *gld-2(0) gld-1(0) prom-1(0)* germlines (Mohammad et al., 2018). This result highlighted that there must be additional mechanisms that regulate entry into meiosis along with the three identified pathways. To test the model that *rack-1* exerts its influence on the germline proliferation/differentiation balance through regulating GLD-1's activity I analyzed *gld-2(q497) gld-1(q485);rack-1(tm2262)*. If *rack-1* functions solely by regulating GLD-1's activity, there should be no change in the germline phenotype of *gld-2(q497) gld-1(q485)* compared to *gld-2(q497) gld-1(q485); rack-1(tm2262)* germlines. Interestingly, all *gld-2(q497) gld-1(q485); rack-1(tm2262)* germlines had clear stretches of meiotic entry (> 10 gcd in length) immediately following the proliferative zone (Figure A.1 and Table A.1). The germlines displayed over-proliferation; however, it was restricted to the more proximal portion of the germline (Figure A.1); whereas *gld-2(q497) gld-1(q485)* germlines displayed small patches (< 10 gcd in length) of meiotic cells randomly interspersed with proliferating cells throughout the

germline (Figure A.1 and Table A.1). This result demonstrated *gld-2(q497) gld-1(q485); rack-1(tm2262)* germlines display increased meiotic entry compared to *gld-2(q497) gld-1(q485)* alone. This result is opposite to what was expected – that a loss of *rack-1* would have no impact on meiotic entry in *gld-2(q497) gld-1(q485)*. This suggests that loss of *rack-1* partially suppresses the entry into meiosis defect. This is reminiscent of the reduction in the proliferative zone observed upon loss of *rack-1* in combination with GLD-1 or GLD-2 pathway mutants (Table 3.7). As this reduction in the size of the proliferative zone, or partial suppression of the meiotic entry defect, was seen in the presence and absence of *gld-1* it suggests that *rack-1* may play an additional role in the proliferation/differentiation balance that is *gld-1*-independent. *rack-1* could normally function to inhibit meiotic entry within the stem cell pool or could be required for proper cell cycle regulation or cell division.

If *rack-1* is required in the third redundant meiotic entry pathway, SCF^{PROM-1}, a loss of *rack-1* in a *gld-2(q497) gld-1(q485)* background should result in a decrease in the number of meiotic cells present within the germline, resembling the loss of SCF^{PROM-1} pathway components in this background (Mohammad et al., 2018). The increase in meiotic entry in *gld-2(q497) gld-1(q485); rack-1(tm2262)* is opposite to what is expected if *rack-1* functions to positively regulate the SCF^{PROM-1} pathway. To further verify that *rack-1* does not function in the SCF^{PROM-1} pathway additional analysis should be performed with loss of *rack-1* in combination with SCF^{PROM-1} pathway components.

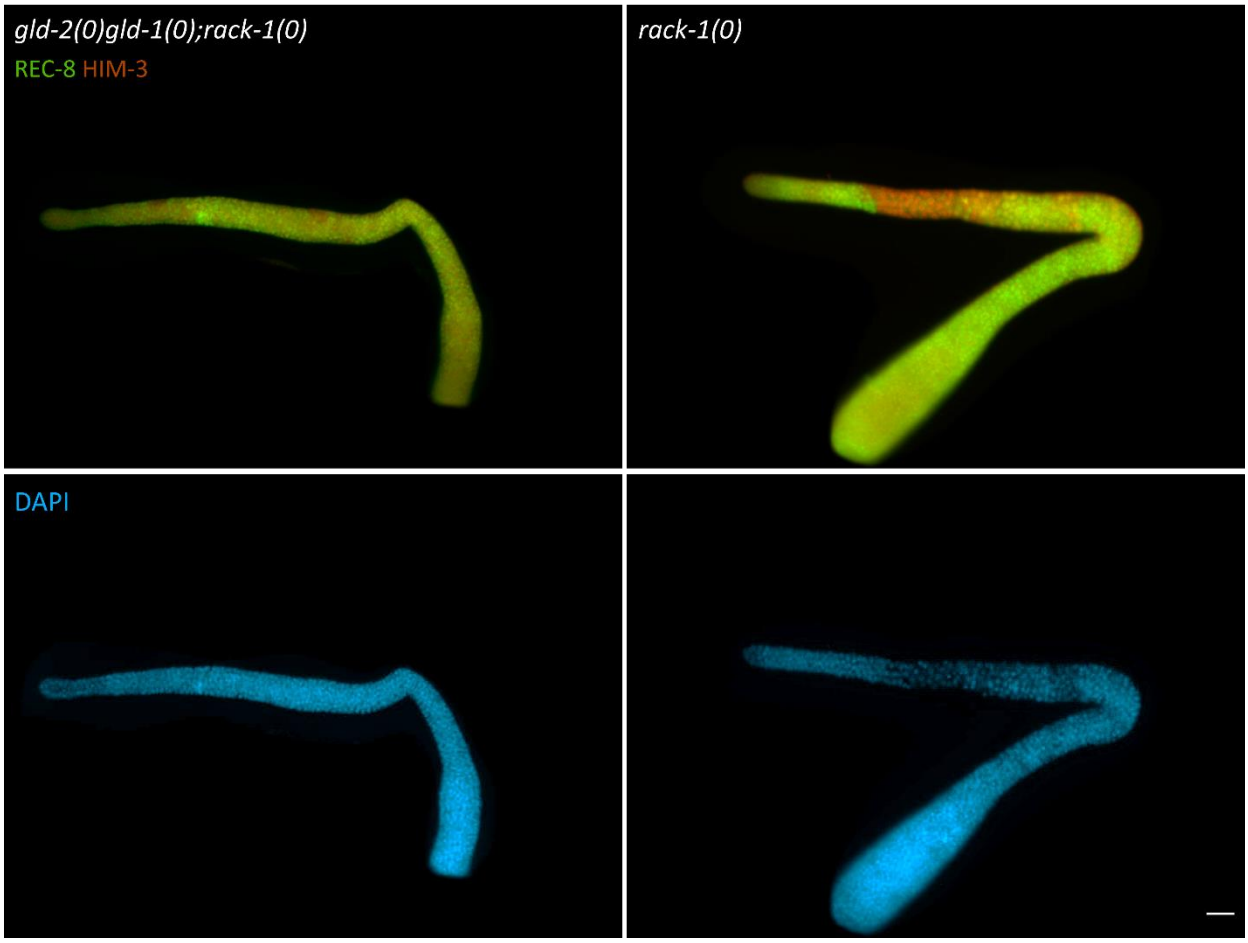

Figure A.1 – Loss of *rack-1* rescues the meiotic entry defect in *gld-2(0) gld-1(0)* germlines. Representative images of *gld-2(q497) gld-1(q485)*, *gld-2(q497)gld-1(q485); rack-1(tm2262)* young adult gonads. Animals were raised at 20 °C, dissected at one day past the L4 stage, and analyzed for meiotic entry using α-REC8 (proliferation marker) and α-HIM-3 (meiotic marker) antibodies. Nuclear morphology was detected using DAPI. Scale bar = 20 μM

Table A.1 - *rack-1(0)* rescues meiotic entry in *gld-2(0) gld-1(0)* germlines

Analysis at 20 °C	Meiotic Entry[a]		
Genotype	> 10 gcd (%)[b]	< 10 gcd (%)[c]	n[d]
gld-2(0) gld-1(0)[e]	0	100	127
gld-2(0) gld-1(0); rack-1(0)[f]	100	0	132

[a] Animals were dissected one day past the L4 stage, fixed and stained with DAPI, and α-REC-8 and α-HIM-3 antibodies. The meiotic entry was scored based upon the presence of HIM-3 positive cells outside within the germline.

[b] > 10 gcd refers to germlines where the patches of meiotic cells were larger than 10 germ cell diameters in length (*i.e.,* large stretch of meiotic entry).

[c] < 10 gcd refers to germlines where the patches of meiotic cells were smaller than 10 germ cell diameters in length (*i.e.,* small amount of meiotic entry).

[d] n refers to total number of gonad arms analyzed.

[e] Actual genotype; *gld-2(q497) gld-1(q485).*

[f] Actual genotype; *gld-2(q497) gld-1(q485); rack-1(tm2262).*

Appendix B - *rack-1* may function in the sex determination pathway

Gamete production (meiotic progression) in the *C. elegans* hermaphrodite begins with the development of sperm during the L4 stage (Hirsh et al., 1976). At the L4 to adult molt there is a switch from spermatogenesis to oogenesis, with oocytes being continually produced throughout the adult's lifespan (Hirsh et al., 1976). This switch is controlled by a complex regulatory network that functions to ensure proper ratios of spermatogenesis and oogenesis promoting genes (Reviewed in: (Ellis & Schedl, 2007)). Disruptions to this regulatory network can result in masculinization of the germline, continuous production of sperm throughout a hermaphrodite's life, as the switch to oogenesis does not occur (Ellis & Schedl, 2007). Alternatively, disruptions can result in feminization of the germline where all germ cells differentiate into oocytes, and the hermaphrodite is no longer self-fertile as no sperm is produced (Ellis & Schedl, 2007).

Many of the genes that function in the proliferation/differentiation balance in the germline also play a role in germline sex determination, such as *gld-1* and *nos-3.* GLD-1 has been shown to translationally repress *tra-2* which is responsible for promoting oogenesis (Crittenden et al., 2002; Francis et al., 1995; Hargitai et al., 2009; Jan et al., 1999); therefore, in the absence of *gld-1* little to no sperm is produced (Francis et al., 1995; Jones et al., 1996). Loss of *rack-1* in *gld-1(q485)* hermaphrodite germlines rescued the spermatogenesis defect with 97% of animals having sperm detectable using an antibody against the major sperm protein (α-MSP) (Table B.1). 70% of g*ld-1(q485)* animals had detectable sperm, which was surprising since *gld-1(q485)* was originally characterized as having no sperm (Francis et al., 1995) (Table B.1). To ensure this

observation was not caused by an unknown accumulated background mutation two other independent strains were used to isolate and analyze *gld-1(q485)* for the presence of sperm. Sperm was detectable in 69% an 81% of germlines analyzed (Table B.1)

To confirm the ability of loss of *rack-1* to rescue the spermatogenic defect in *gld-1* mutants I analyzed *gld-1(q361); rack-1(tm2262)* germlines for the presence of sperm. 100% of *gld-1(q361); rack-1(tm2262)* animals had detectable sperm compared to 16% of *gld-1(q361)* alone (Table B.1). Taken together this suggested that *rack-1* may function to repress spermatogenesis, or maybe required to promote oogenesis.

Table B.1 – Loss of *rack-1* rescues spermatogenesis in *gld-1* mutant germlines

Analysis at 20 °C	Germline Phenotype[a]		
	Sperm		
Genotype	Yes (%)[c]	No (%)[d]	n[b]
gld-1(q485)[e]	67	33	156
gld-1(q485)[f]	69	31	90
gld-1(q485)[g]	81	19	96
gld-1(q485); rack-1(tm2262)	97	3	93
gld-1(q361)	16	84	82
gld-1(q361); rack-1(tm2262)	100	0	63

[a] Animals were dissected one day past the L4 stage, fixed and stained with α-MSP antibodies and DAPI.
[b] n refers to total number of gonad arms analyzed.
[c] Yes refers to the percent of germlines that had sperm detectable detected by α-MSP antibodies.
[d] No refers to the percent of germlines that did not have any sperm detectable (no α-MSP staining).
[e] *gld-1(q485)* was isolated from XB478 strain.
[f] *gld-1(q485)* was isolated from BS3680.
[g] *gld-1(q485)* was isolated from XB152.

nos-3 is also involved in the germline sex determination pathway; however, *nos-3* functions to inhibit spermatogenesis, and promote oogenesis, through the suppression of *fem-3* (Kraemer et al., 1999). *C. elegans* has three nanos orthologs that are thought to function redundantly to repress *fem-3* (Kraemer et al., 1999). Germlines from *nos-3* mutant animals are wildtype with a very low penetrance of Mog (~0.2% - masculinization of the germline); however, when *nos-3* is lost in combination with *nos-1* or *nos-2* mutants the penetrance of Mog increases (12% and 24% respectively) (Kraemer et al., 1999). *nos-3(oz231)* allele carries a 139 base pair deletion resulting in a frameshift and premature stop codon, with no protein product being detectable and is considered a null allele (Hansen, Wilson-Berry, et al., 2004). At 20 °C *nos-3(oz231)* germlines were completely wildtype, with no Mog detected, whereas 100% of *nos-3(oz231); rack-1(tm2262)* germlines appeared Mog with only spermatogenic nuclei present (no detectable oocytes) (Figure B.1 and Table B.2). At 25 °C *nos-3(oz231); rack-1(tm2262)* germlines were still Mog; however, 74% of germlines displayed proximal proliferation (Figure B.1 and Table B.2). At 25 °C the majority of *nos-3(oz231)* germlines analyzed were wildtype This data highlights that *rack-1* is likely involved in both the germline sex determination pathway and the proliferation/differentiation balance.

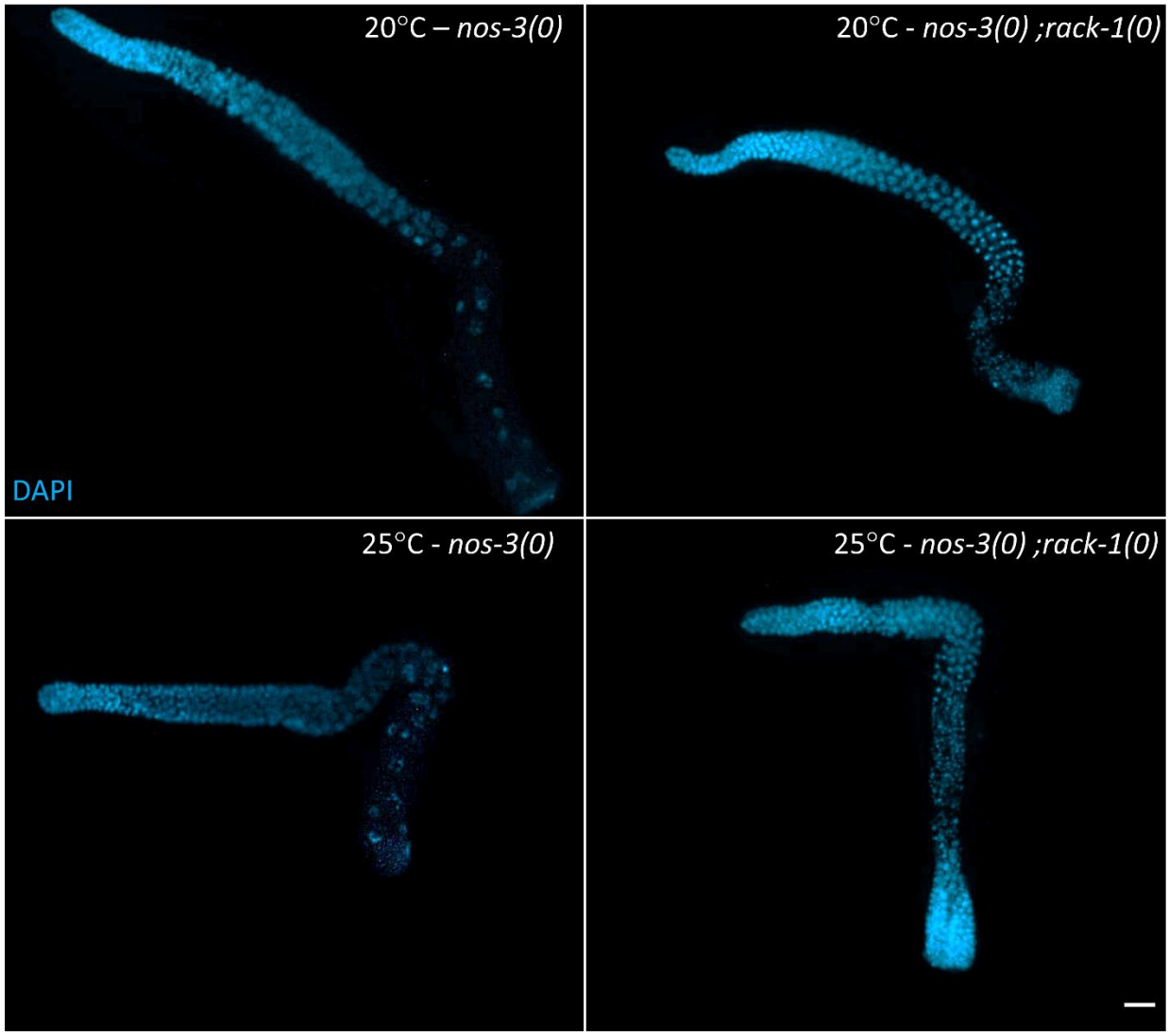

Figure B.1 – Loss of *rack-1* masculinizes *nos-3(oz231)* germlines. Representative DAPI images of *nos-3(o231)* and *nos-3(oz231); rack-1(tm2262)* germlines. Animals were raised at 20 °C and 25 °C, dissected at one day past the L4 stage and analyzed for germline defects using α-REC-8, α-HIM-3 antibodies and DAPI staining (nuclear morphology). Scale bar = 20 μm.

Table B.2 – Loss of *rack-1* masculinizes the germlines of *nos-3(0)* animals

	Germline Phenotype[a]					
Genotype	Wildtype (%)[b]	Mog (%)[c]	Mog + Pro (%)[d]	Defective oogenesis (%)[e]	Other (%)[f]	n[g]
Analysis at 20 °C						
rack-1(tm2262)	96	0	0	2	3[h]	442
nos-3(oz231)	100	0	0	0	0	150
nos-3(oz331); rack-1(tm2262)	0	100	0	0	0	138
Analysis at 25 °C						
rack-1(tm2262)	85	0	0	9	6	334
nos-3(oz231)	86	0	0	0	14[i]	102
nos-3(oz331); rack-1(tm2262)	0	26	74	0	0	88

[a] Animals were either dissected one day past the L4 stage, fixed and stained with DAPI and α-REC-8 and α-HIM-3 antibodies.
[b] Wildtype refers to gonad arms with no proliferative cells outside of the proliferative zone and visible sperm and oocytes present.
[c] Masculinization of the germline (Mog) refers to gonad arms where only spermatogenesis occurs, with primary spermatocytes and sperm continuously being over-produced.
[d] Mog + Pro (Protumour) refers to gonad arms that have only spermatogenesis occurring (over-production of sperm, no oocytes present), with a pool of proliferative cells (REC-8 positive) at the most proximal end of the germline.
[e] Defective oogenesis refers to gonad arms that lack the presence of developing oocytes, or have extremely reduced numbers of oocytes, with developing spermatocytes and sperm present at the proximal end of the germline.
[f] Other refers to animals where no germline arm was detectable by whole-mount DAPI, or it was severely underdeveloped (very few cells).
[g] n refers to total number of gonad arms analyzed.
[h] This number contains the 1% of *rack-1(tm2262)* germlines that displayed a Pro phenotype (See Table 4.2.1)
[i] This number contains *nos-3(oz231)* gonads that appeared to have reduced oogenesis (not fully measured) with no embryos detectable.

Appendix C - Loss of *rack-1* does not disrupt the expression of known GLD-1 targets

GLD-1 has many functions within the germline, including roles in entry into meiosis decision, apoptosis pathway, and the sex determination pathway. It contributes to these diverse mechanisms through its activity as a translational repressor (Jan et al., 1999; M.-H. Lee & Schedl, 2004; M. H. Lee & Schedl, 2001; Marin & Evans, 2003; Mootz et al., 2004; L. Xu et al., 2001). Many GLD-1 mRNA targets have been identified, including *glp-1* and *mex-3 (*mitosis-meiosis decision)*, cep-1* (apoptotic pathway)*, spn-4 (embryogenesis) and puf-5* (oogenesis) (Ariz et al., 2009; Ellenbecker et al., 2019; M.-H. Lee & Schedl, 2004; Lublin & Evans, 2007; Marin & Evans, 2003; Merritt et al., 2008; Mootz et al., 2004; Schumacher et al., 2005). To test the possibility that GLD-1's activity as a translational repressor is disrupted in *rack-1* mutants*,* I analyzed the expression of three known GLD-1 targets, MEX-3, SPN-4, and PUF-5 in *rack-1(tm2262)* germlines using fluorescently tagged alleles, *mex-3(tn1753[gfp::3xflag::mex-3]), spn-4(tn1699[spn-4::gfp::3xflag]), and puf-5(tn1728[gfp::3xflag::puf-5]),* generated by Dr. David Greenstein's lab (Tsukamoto et al., 2017).

If GLD-1's activity as a translational repressor is reduced in *rack-1(0)* animals then the protein levels of GLD-1 targets (*mex-3, spn-4, puf-4)* are expected to increase in meiotic cells/areas of the germline where GLD-1 is normally active; therefore, I hypothesized that I would see increased levels of GLD-1 targets in *rack-1(tm2262)* germlines.

At 20 °C MEX-3 was expressed at similar levels in *mex-3(tn1753); rack-1(tm2262)* and control (*mex-3(tn1753)* alone) germlines, with no increase in MEX-3 expression in the meiotic region of the germline where GLD-1 is active (to the right of the black line) (Figure C.1). Interestingly, at 25 °C, MEX-3's expression was reduced in both the proliferative zone and meiotic region in *mex-3(tn1753); rack-1(tm2262)* germlines compared to control germlines (*mex-3(tn1753)* alone) (Figure C.1).

At 20 °C SPN-4 expression was slightly decreased in *spn-4(tn1699); rack-1(tm2262)* germlines compared to control germlines (*spn-4(tn1699)* alone), in both the proliferative zone and distal meiotic region (to the right of the black line) (Figure C.1). This slight decreased in SPN-4 expression was also seen at 25 °C (Figure C.1).

At 20 °C PUF-5 expression was slightly higher in developing oocytes of *puf-5(tn1728); rack-1(tm2262)* compared to control germlines (*puf-5(tn1728)* alone); however, in the meiotic region (to the right of the black line), where GLD-1 is active, there was no difference in PUF-5 expression (Figure C.1). Interestingly, at 25 °C PUF-5 expression was reduced in both the developing oocytes and proximal meiotic region (Figure C.1).

This data suggests that GLD-1's repression of these targets is not disrupted upon loss of *rack-1.* This could indicate that loss of *rack-1* may only disrupt GLD-1's ability to regulate a subset of its targets. It is possible that different thresholds of GLD-1 activity are required to regulate the expression of GLD-1 target genes; therefore, some GLD-1 targets may be more sensitive to a change in GLD-1 function than others. Since *rack-1* mutants

have reduced, but not abolished, GLD-1 function it is possible that the three target genes analyzed (*mex-3, spn4, puf-5)* require low levels of GLD-1 activity for proper expression and are therefore unaffected in *rack-1* mutants. Additional GLD-1 targets should be analyzed to determine which, if any, GLD-1 targets are mis-expressed in *rack-1* mutant germlines.

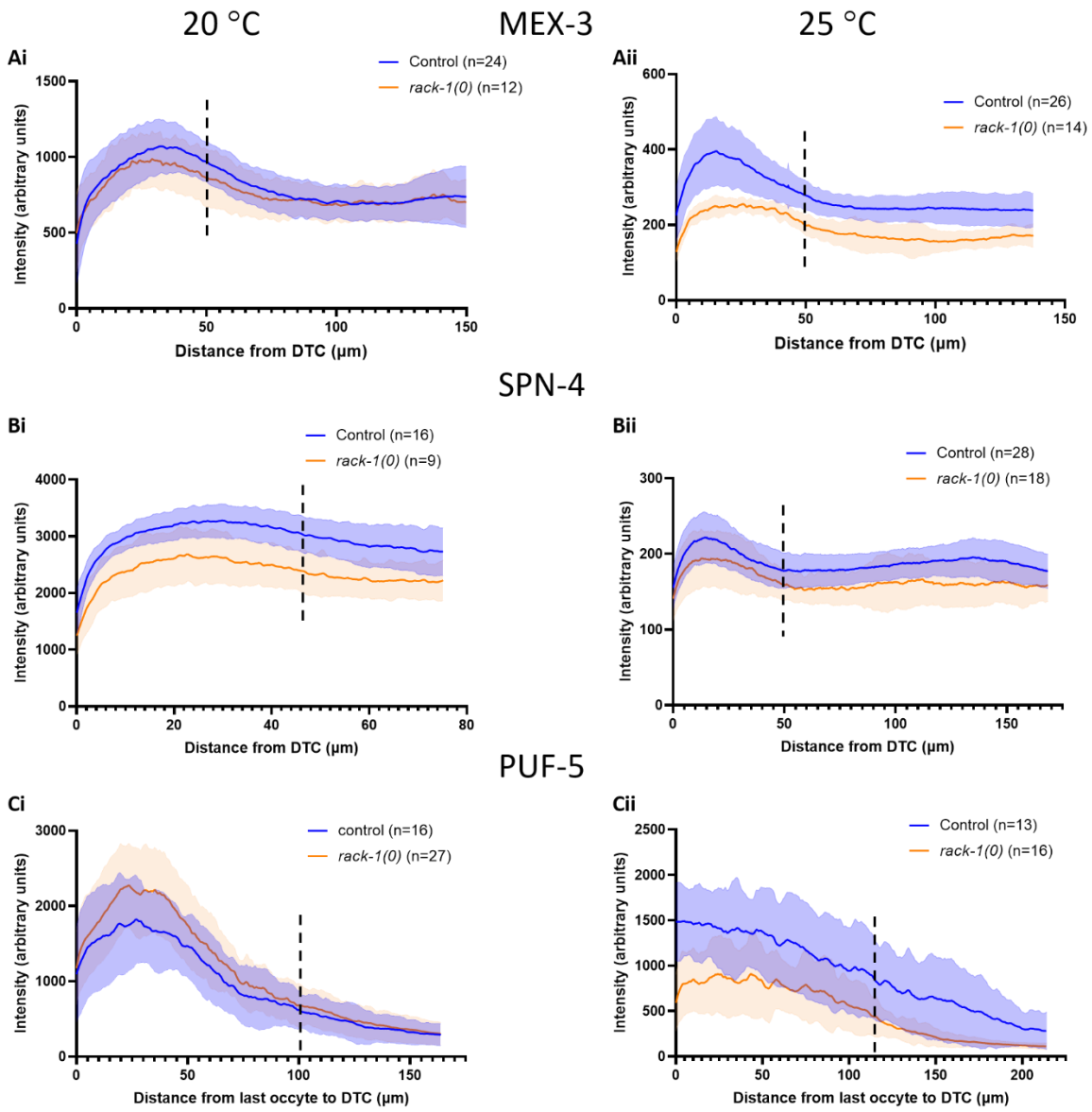

Figure C.1 – Loss of *rack-1* does not increase the expression of known GLD-1 targets. Graphs depicting the average expression levels of three GLD-1 targets, MEX-3(A), SPN-4(B), and PUF-5 (C), in *rack-1(0)* germlines compared to control at 20 °C (left, i) and 25 °C (right, ii). A) MEX-3 expression was determined using endogenous expression of GFP::3XFLAG::MEX-3 [*mex-3(tn1753)*] alone as control or in combination

with *rack-1(tm2262) [mex-3(tn1753); rack-1(t2262)].* The x-axis is distance in μm from DTC towards the loop as far as was measurable. The y-axis is the intensity (arbitrary units) of endogenous GFP expression, representing MEX-3 levels. The dotted line represents approximately where GLD-1 beings to be expressed, with the right-hand side representing where GLD-1 is expressed. B) SPN-4 expression was determined using endogenous expression of SPN-4::GFP::3xFLAG [*spn-4(1699)*] alone as control or in combination with *rack-1(tm2262) [spn-4(1699);rack-1(t2262)].* The x-axis is distance in μm from DTC towards the loop as far as was measurable. The y-axis is the intensity of endogenous GFP expression, representing SPN-4 levels. The dotted line represents approximately where GLD-1 beings to be expressed, with the right-hand side representing where GLD-1 is expressed. C) PUF-5 expression was determined using endogenous expression of GFP::3XFLAG::PUF-5 [*puf-5(tn178)*] alone as control or in combination with *rack-1(tm2262) [puf-5(tn178);rack-1(t2262)].* The x-axis is distance in μm from the last oocyte past the loop as far as was measurable. The loop was used to align the intensity measurement between the two strains. The y-axis is the intensity of endogenous GFP expression, representing SPN-4 levels. The dotted line represents approximately where GLD-1 beings to be expressed, with the right-hand side representing where GLD-1 is expressed.

Appendix D - Loss of *rack-1* decrease CED-1 expression in somatic sheath cells

Apoptosis occurs within the germline during normal oogenesis in order to reduce the number of germ cells that differentiate into mature oocytes (Gumienny et al., 1999). The apoptotic cells become cellularized and reduced in size as their cytoplasmic content remains in the rachis to be taken up by mature oocytes; therefore, these apoptotic cells are thought to function as nurse cells (Gumienny et al., 1999). Increased apoptosis in *gld-1(op236)* was identified by analysing CEP-1 and CED-1 expression (Schumacher et al., 2005). CEP-1/p53 is a pro-apoptotic marker that is expressed within germ cells (Schumacher et al., 2001). CED-1 is a phagocytic receptor expressed in somatic sheath cells, with CED-1 detectable surrounding the apoptotic corpses in the germline during engulfment (Yu et al., 2008; Zhou et al., 2001); therefore CED-1 expression can be used to estimate the extent of apoptosis within the germline (Schumacher et al., 2001). CED-1 expression within the germline of *gld-1(op236)* animals was expanded compared to wildtype controls (Schumacher et al., 2005). Since my model is that GLD-1 activity is reduced in *rack-1* mutants, I hypothesized that CED-1 expression may be expanded in *rack-1* mutants, similar to what is observed in animals carrying the *gld-1(op236)* partial loss-of-function allele. This would suggest that *rack-1* mutants had increased apoptosis, similar to *gld-1(op236)* animals. I analyzed the extent of CED-1 expression using a CED-1::GFP transgene *(bcIs39*). CED-1 expression was decreased in *rack-1(tm2262)* animals compared to control (Figure D.1). This was opposite to what was expected that CED-1 expression would increase in *rack-1* mutant germlines similar to *gld-1(op236)*. This preliminary result could suggest that *rack-1(0)* has defects within sheath cells resulting in

a failure to appropriately recognize and engulf apoptotic germ cells, or that *rack-1(tm2262)* may not have increased CED-1 expression and/or apoptosis. It is important to note that control animals appeared to have a larger CED-1 expression domain than anticipated based on previous reports for CED-1 expression (Schumacher et al., 2005); however, the difference in CED-1 expression levels between control and *rack-1(tm2262)* germlines was consistent between independent experiments. This analysis should be repeated using CEP-1 and CED-1 as read outs of apoptosis alongside in-depth analysis such as counting engulfed apoptotic cells per germline and the number of cells expressing CEP-1 to obtain reliable data reflecting levels of apoptosis in *rack-1* mutant germlines. Additionally, acridine orange or SYTO12 dyes that incorporate, and stain apoptotic nuclei can also be used to measure apoptosis in *rack-1(tm2262)* germlines. *rack-1(tm2262)* germlines appear relatively wildtype; therefore, more sensitized backgrounds may be required to detect increased apoptosis, such as *gld-1(op236)* or *gld-1(+/q485).*

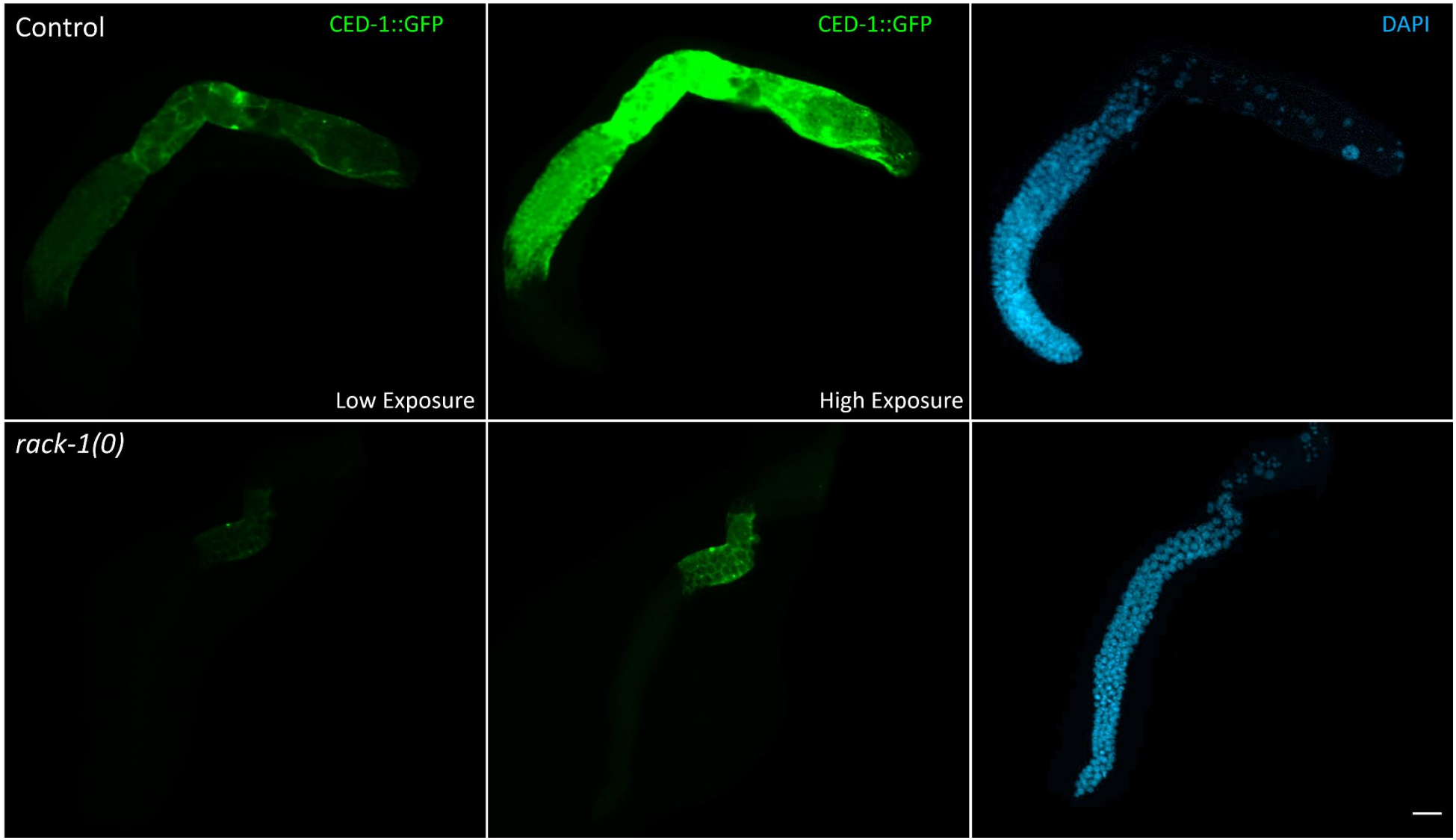
Control
CED-1::GFP
Low Exposure
CED-1::GFP
High Exposure
DAPI
rack-1(0)

Figure D.1 - CED-1 expression is decreased in *rack-1(0)* germlines. Representative images of CED-1::GFP expression in control (*bcIs39*[*lim-7p::ced-1::GFP* + *lin-15(+)]*) and *rack-1(tm2262)* young adult gonads. Animals were raised at 20 °C dissected at one day past the L4 stage and analyzed for endogenous CED-1::GFP expression using the integrated transgene *bcIs39*[*lim-7p::ced-1::GFP* + *lin-15(+)]*. DAPI staining was used to determine nuclear morphology. Low exposure = 100 ms. High exposure = 500 ms. Scale bar = 20 μm.

Appendix E – List of primers used in this thesis

Hansen lab primer name	Primer name	Sequence (5'-3')
T21	*glp-1(ar202) fwd*	GAGCCACTTGGAGTATAATG
T22	*glp-1(ar202) rvs*	CCACATCCAATGAAACTGC
T23	*glp-1(ar202) seq*	GCTGGGCATCGAAATAACTC
HD52	*rack-1(ok3676) rack-1(tm2262) fwd*	TCACACCGGATGGGTTACCC
HD54	*rack-1(ok3676) rack-1(tm2262) rvs*	TGATGTTATCGGTGTATCCGGCG
T21	*glp-1(oz264) fwd*	GAGCCACTTGGAGTATAATG
T22	*glp-1(oz264) rvs*	CCACATCCAATGAAACTGC
T23	*glp-1(oz264) seq*	GCTGGGCATCGAAATAACTC
D51	*glp-1(q175) fwd*	TCCTGACTGCAAAACTCCTC
D52	*glp-1(q175) rvs*	CCTGAAGGACACTCAATCTC
D53	*glp-1(q175) seq*	CTCGCAATACTTTCCAGCGT
S13	*glp-1(bn18) fwd*	CAACAGAGGCAATTCGATGC
S15	*glp-1(bn18) rvs*	CCTTATTAGAGCTTCGTCGG
S14	*glp-1(bn18) seq*	CTTCGTGAAGGAGCTAATCC
R58	*gld-1(q485) fwd*	TGCCGTCGTGCACCACTCCAA
U59	*gld-1(q485) rvs*	GATCAGCCAAGTACTCGACAG
R27	*nos-3(oz231) fwd*	GGACAGTATAGGGGTCCACAAG
R28	*nos-3(oz231) rvs*	CCTGCACGTGAGCTAACTGG

T52	*gld-2(q497) fwd and seq*	TCTCGTTTTCTTTATTTAGTC
T53	*gld-2(q497) rvs*	AACAGTTATATCATCAAAAGGTG
L43	*gld-3(q730) fwd*	CGTCGATGGATCCTTTGGTG
L69	*gld-3(q730) rvs*	GTCTAGATCCCAACGAAGAC
hd14	*lst-1(ok814) fwd*	GAGCGGCTTCGATTAATGGG
HD15	*lst-1(ok814) rvs*	GAATTGTAGTGTGTCGGGCG
HD16	*sygl-1(tm5040) fwd*	CATTGTGTGACACCGCCAC
HD17	*sygl-1(tm5040) rvs*	GACTGCGAAAATCAGGCT
HA35	*syg-1(am307) fwd*	ATCTACCCGCCGATTTTCTAAT
HA36	*syg-1(am307) rvs*	ATCTCCAAGTGTTGCACATAACC
HC57	*rack-1(ug12) rack-1(ug17) fwd and seq*	CAAGCACTTGTACACCCTTCC
HC58	*rack-1(ug12) rack-1(ug17) rvs*	GGCTAGTTGAGTAATGCTAGG
HC79	*gld-1(q361) fwd and seq*	TCGAGTACTTGGCTGATCTGG
HC80	*gld-1(q361) rvs*	AGGAGTTGGCGACATCAAAAC
HC69	*gld-1(op236) fwd*	CTGTCGAGTACTTGGCTGATC
HC70	*gld-1(op236) rvs*	CAAGATCGATCCTCCAAATGTCG
HC71	*gld-1(op236) seq*	CTTCGTCGGTAGAATTCTCGG
I66	*fbf-(ok91) fwd*	CGTCTTGAATGATTCATGTC
I67	*fbf-1(ok91) rvs*	CAATCAAAAATGCGCTATAC

Appendix F – List of strains used in thesis in order of how they appear in the chapters.

Strain name	Genotype
BS3148	*glp-1(ar202) III*
LE1837	*rack-1(tm2262) IV*
XB730	*glp-1(ar202) III; rack-1(tm2262)/nT1g IV*
XB184	*glp-1(oz264) III*
XB872	*glp-1(oz264) III; rack-1(tm2262)/tmC5 IV*
XB380	*glp-1(q175)/hT2g III*
XB883	*glp-1(q175)/hT2g III; rack-1(tm2262)/tmC5 IV*
BS121	*glp-1(bn18) III*
XB731	*glp-1(bn18) III; rack-1(tm2262)/nT1g IV*
JK4774	*lst-1(ok814) sygl-1(tm5040)/hT2g I*
XB859	*lst-1(ok814) sygl-1(tm5040)/tmC27 I; rack-1(tm2262)/tmC5 IV*
WU1770	*sygl-1(am307[3XFLAG::sygl-1) I*
XB767	*sygl-1(am307) I; rack-1(tm2262)/nT1g IV*
XB478	*gld-1(q485)/hT2g I*
XB750	*gld-1(q485)/tmC20 I; rack-1(tm2262)/tmC5 IV*
BS5272	*nos-3(oz231) II*
XB879	*nos-3(oz231)/mC6g II; rack-1(tm2262)/tmC5 IV*

XB482	*gld-2(q497)/hT2g I*
XB768	*gld-2(q497)/tmC20 I; rack-1(tm2262)/tmC5 IV*
XB397	*gld-3(q730)/mC6g*
XB860	*gld-3(q730)/mC6g III; rack-1(tm2262)/tmC5 IV*
VC3013	*rack-1(ok3676) IV*
XB790	*rack-1(ug12[rack-1::V5::2xFLAG) IV*
XB805	*rack-1(ug17[rack-1::V5::SBP) IV*
LE2290	*lqIs126 [rack-1::MYC + osm-6::GFP]*
OD70	*ltIs44 [pie-1p::mCherry::PH(PLC1delta1) + unc-119(+)] V*
XB890	*rack-1(ug12) IV/tmC5; ltis44 V*
JJ2204	*zuIs244[nmy-2::PGL-1::RFP; unc-119(ed3)*
XB733	*zuIs244[nmy-2::PGL-1::RFP; unc-119(ed3); rack-1(tm2262)/nT1g IV*
XB896	*gld-1(q361)/hT2g I*
XB826	*gld-1(q361)/tmC20 I; rack-1(tm2262)/tmC5 IV*
XB897	*gld-1(q485)/tmC18 I*
XB895	*gld-1(q485)/tmC18 I; rack-1(tm2262)/tmC5 IV*
XB487	*gld-2(q497) gld-1(q485)/hT2g I*
XB875	*gld-1(q485)/tmC18 I; gld-3(q730)/mC6g II*
XB636	*gld-2(q497)/hT2g I; glp-1(q175)/hT2g III*
XB884	*gld-2(q497)/hT2g I; glp-1(q175)/hT2g III; rack-1(tm2262) IV*

TG34	*gld-1(op236) I*
XB825	*gld-1(op236)/tmC20 I; rack-1(tm2262)/tmC5 IV*
BS3548	*fbf-1(ok91) fbf-2(q704)/mC6g II*
XB813	*fbf-1(ok91) fbf-2(q704)/mC6g II; rack-1(tm2262)/tmC5 IV*
XB876	*gld-2(q497) gld-1(q485)/tmC20 I; rack-1(tm2262)/tmC5 IV*
BS3680	*gld-1(q485)/ccIs4251 unc-13(e51) I*
XB152	*gld-1(q485)/nc-29(e193) dpy-24(s71) I*
DG4158	*spn-4(tn1699[spn-4::gfp::3xflag]) V*
XB802	*rack-1(tm2262)/tmC5 IV; spn-4(tn1699[spn-4::gfp::3xflag]) V*
DG4215	*puf-5(tn1726[gfp::3xflag::puf-5]) II*
XB801	*puf-5(tn1726[gfp::3xflag::puf-5]) II; rack-1(tm2262)/tmC5 IV*
DG4269	*mex-3(tn1753[gfp::3xflag::mex-3]) I*
XB800	*mex-3(tn1753[gfp::3xflag::mex-3]) I; rack-1(tm2262)/tmC5 IV*

References

Adams, D. R., Ron, D., & Kiely, P. A. (2011). RACK1, A multifaceted scaffolding protein: Structure and function. *Cell Communication and Signaling*, *9*(1), 22. https://doi.org/10.1186/1478-811X-9-22

Ai, E., Poole, D. S., & Skop, A. R. (2009). RACK-1 Directs Dynactin-dependent RAB-11 Endosomal Recycling during Mitosis in *Caenorhabditis elegans*. *Molecular Biology of the Cell*, *20*(6), 1629–1638. https://doi.org/10.1091/mbc.e08-09-0917

Ai, E., Poole, D. S., & Skop, A. R. (2011). Long Astral Microtubules and RACK-1 Stabilize Polarity Domains during Maintenance Phase in Caenorhabditis elegans Embryos. *PLoS ONE*, *6*(4), e19020. https://doi.org/10.1371/journal.pone.0019020

Akay, A., Craig, A., Lehrbach, N., Larance, M., Pourkarimi, E., Wright, J. E., Lamond, A., Miska, E., & Gartner, A. (2013). RNA-binding protein GLD-1/quaking genetically interacts with the *mir-35* and *the let-* 7 miRNA pathways in *Caenorhabditis elegans*. *Open Biology*, *3*(11), 130151. https://doi.org/10.1098/rsob.130151

Alessi, A. F., Khivansara, V., Han, T., Freeberg, M. A., Moresco, J. J., Tu, P. G., Montoye, E., Yates, J. R., Karp, X., & Kim, J. K. (2015). Casein kinase II promotes target silencing by miRISC through direct phosphorylation of the DEAD-box RNA helicase CGH-1. *Proceedings of the National Academy of Sciences of the United States of America*, *112*(52), E7213-22. https://doi.org/10.1073/pnas.1509499112

Ambros, V., & Ruvkun, G. (2018). Recent Molecular Genetic Explorations of Caenorhabditis elegans MicroRNAs. *Genetics*, *209*(3), 651–673. https://doi.org/10.1534/genetics.118.300291

Amiri, A., Keiper, B. D., Kawasaki, I., Fan, Y., Kohara, Y., Rhoads, R. E., & Strome, S. (2001). An isoform of eIF4E is a component of germ granules and is required for spermatogenesis in C. elegans. *Development (Cambridge, England)*, *128*(20), 3899–3912.

Ariz, M., Mainpal, R., & Subramaniam, K. (2009). C. elegans RNA-binding proteins PUF-8 and MEX-3 function redundantly to promote germline stem cell mitosis. *Developmental Biology*, *326*(2), 295–304. https://doi.org/10.1016/j.ydbio.2008.11.024

Arribere, J. A., Bell, R. T., Fu, B. X. H., Artiles, K. L., Hartman, P. S., & Fire, A. Z. (2014). Efficient marker-free recovery of custom genetic modifications with CRISPR/Cas9 in Caenorhabditis elegans. *Genetics*, *198*(3), 837–846. https://doi.org/10.1534/genetics.114.169730

Austin, J., & Kimble, J. (1987). glp-1 Is required in the germ line for regulation of the decision between mitosis and meiosis in C. elegans. *Cell*, *51*(4), 589–599. https://doi.org/10.1016/0092-8674(87)90128-0

Barstead, R., Moulder, G., Cobb, B., Frazee, S., Henthorn, D., Holmes, J., Jerebie, D., Landsdale, M., Osborn, J., Pritchett, C., Robertson, J., Rummage, J., Stokes, E., Vishwanathan, M., Mitani, S., Gengyo-Ando, K., Funatsu, O., Hori, S., Imae, R., … Zapf, R. (2012). Large-scale screening for targeted knockouts in the caenorhabditis elegans genome. *G3: Genes, Genomes, Genetics*, *2*(11), 1415–1425. https://doi.org/10.1534/g3.112.003830

Barton, M. K., & Kimble, J. (1990). fog-1, a regulatory gene required for specification of spermatogenesis in the germ line of Caenorhabditis elegans. *Genetics*, *125*(1), 29–39. https://doi.org/10.1093/genetics/125.1.29

Barucci, G., Cornes, E., Singh, M., Li, B., Ugolini, M., Samolygo, A., Didier, C., Dingli, F., Loew, D., Quarato, P., & Cecere, G. (2020). Small-RNA-mediated transgenerational silencing of histone genes impairs fertility in piRNA mutants. *Nature Cell Biology*, *22*(2), 235–245. https://doi.org/10.1038/s41556-020-0462-7

Batista, P. J., Ruby, J. G., Claycomb, J. M., Chiang, R., Fahlgren, N., Kasschau, K. D., Chaves, D. A., Gu, W., Vasale, J. J., Duan, S., Conte, D., Luo, S., Schroth, G. P., Carrington, J. C., Bartel, D. P., Mello, C. C., & Mello, C. C. (2008). PRG-1 and 21U-RNAs interact to form the piRNA complex required for fertility in C. elegans. *Molecular Cell*, *31*(1), 67–78. https://doi.org/10.1016/j.molcel.2008.06.002

Becker, A. J., McCulloch, E. A., & Till, J. E. (1963). Cytological Demonstration of the Clonal Nature of Spleen Colonies Derived from Transplanted Mouse Marrow Cells. *Nature*, *197*(4866), 452–454. https://doi.org/10.1038/197452a0

Belfiore, M., Pugnale, P., Saudan, Z., Puoti, A., Kohler, R., Brunschwig, K., Tobler, H., & Müller, F. (2004). Roles of the C. elegans cyclophilin-like protein MOG-6 in MEP-1 binding and germline fates. *Development (Cambridge, England)*, *131*(12), 2935–2945. https://doi.org/10.1242/dev.01154

Berry, L. W., Westlund, B., & Schedl, T. (1997). Germ-line tumor formation caused by activation of glp-1, a Caenorhabditis elegans member of the Notch family of receptors. *Development (Cambridge, England)*, *124*(4), 925–936.

Bezler, A., Braukmann, F., West, S. M., Duplan, A., Conconi, R., Schütz, F., Gönczy, P., Piano, F., Gunsalus, K., Miska, E. A., & Keller, L. (2019). Tissue- and sex-specific small RNAomes reveal sex differences in response to the environment. *PLOS Genetics*, *15*(2), e1007905. https://doi.org/10.1371/journal.pgen.1007905

Biedermann, B., Wright, J., Senften, M., Kalchhauser, I., Sarathy, G., Lee, M.-H., & Ciosk, R. (2009). Translational repression of cyclin E prevents precocious mitosis and embryonic gene activation during C. elegans meiosis. *Developmental Cell*, *17*(3), 355–364. https://doi.org/10.1016/j.devcel.2009.08.003

Bolger, G. B. (2017). The RNA-binding protein SERBP1 interacts selectively with the signaling protein RACK1. *Cellular Signalling*, *35*, 256–263.

https://doi.org/10.1016/j.cellsig.2017.03.001

Braydich-Stolle, L., Kostereva, N., Dym, M., & Hofmann, M.-C. (2007). Role of Src family kinases and N-Myc in spermatogonial stem cell proliferation. *Developmental Biology*, *304*(1), 34–45. https://doi.org/10.1016/j.ydbio.2006.12.013

Brenner, J. L., & Schedl, T. (2016). Germline Stem Cell Differentiation Entails Regional Control of Cell Fate Regulator GLD-1 in Caenorhabditis elegans. *Genetics*, *202*(3), 1085–1103. https://doi.org/10.1534/genetics.115.185678

Brenner, S. (1974). The genetics of Caenorhabditis elegans. *Genetics*, *77*(1), 71–94.

Brinster, R. L. (2002). Germline stem cell transplantation and transgenesis. In *Science* (Vol. 296, Issue 5576, pp. 2174–2176). NIH Public Access. https://doi.org/10.1126/science.1071607

Brosnan, C. A., Palmer, A. J., & Zuryn, S. (2021). Cell-type-specific profiling of loaded miRNAs from Caenorhabditis elegans reveals spatial and temporal flexibility in Argonaute loading. *Nature Communications*, *12*(1), 2194. https://doi.org/10.1038/s41467-021-22503-7

Bukhari, S. I. A., Vasquez-Rifo, A., Gagné, D., Paquet, E. R., Zetka, M., Robert, C., Masson, J.-Y., & Simard, M. J. (2012). The microRNA pathway controls germ cell proliferation and differentiation in C. elegans. *Cell Research*, *22*(6), 1034–1045. https://doi.org/10.1038/cr.2012.31

Byrd, D. T., Knobel, K., Affeldt, K., Crittenden, S. L., & Kimble, J. (2014). A DTC Niche Plexus Surrounds the Germline Stem Cell Pool in Caenorhabditis elegans. *PLoS ONE*, *9*(2), e88372. https://doi.org/10.1371/journal.pone.0088372

Ceci, M., Gaviraghi, C., Gorrini, C., Sala, L. A., Offenhäuser, N., Marchisio, P. C., & Biffo, S. (2003). Release of eIF6 (p27BBP) from the 60S subunit allows 80S ribosome assembly. *Nature*, *426*(6966), 579–584. https://doi.org/10.1038/nature02160

Chang, B Y, Conroy, K. B., Machleder, E. M., & Cartwright, C. A. (1998). RACK1, a receptor for activated C kinase and a homolog of the beta subunit of G proteins, inhibits activity of src tyrosine kinases and growth of NIH 3T3 cells. *Molecular and Cellular Biology*, *18*(6), 3245–3256. https://doi.org/10.1128/mcb.18.6.3245

Chang, Betty Y, Harte, R. A., & Cartwright, C. A. (2002). RACK1: a novel substrate for the Src protein-tyrosine kinase. *Oncogene*, *21*(50), 7619–7629. https://doi.org/10.1038/sj.onc.1206002

Chen, J., Mohammad, A., Pazdernik, N., Huang, H., Bowman, B., Tycksen, E., & Schedl, T. (2020). GLP-1 Notch—LAG-1 CSL control of the germline stem cell fate is mediated by transcriptional targets lst-1 and sygl-1. *PLOS Genetics*, *16*(3), e1008650. https://doi.org/10.1371/journal.pgen.1008650

Chen, T., Damaj, B. B., Herrera, C., Lasko, P., & Richard, S. (1997). Self-association of the single-KH-domain family members Sam68, GRP33, GLD-1, and Qk1: role of the KH domain. *Molecular and Cellular Biology*, *17*(10), 5707–5718. https://doi.org/10.1128/mcb.17.10.5707

Chihara, D., & Nance, J. (2012). An E-cadherin-mediated hitchhiking mechanism for C. elegans germ cell internalization during gastrulation. *Development*, *139*(14), 2547–2556. https://doi.org/10.1242/dev.079863

Christensen, S., Kodoyianni, V., Bosenberg, M., Friedman, L., & Kimble, J. (1996). lag-1, a gene required for lin-12 and glp-1 signaling in Caenorhabditis elegans, is homologous to human CBF1 and Drosophila Su(H). *Development (Cambridge, England)*, *122*(5), 1373–1383.

Chu, Y.-D., Wang, W.-C., Chen, S.-A. A., Hsu, Y.-T., Yeh, M.-W., Slack, F. J., & Chan, S.-P. (2014). RACK-1 regulates *let-7* microRNA expression and terminal cell differentiation in *Caenorhabditis elegans*. *Cell Cycle*, *13*(12), 1995–2009. https://doi.org/10.4161/cc.29017

Clark, J. M., & Eddy, E. M. (1975). Fine structural observations on the origin and associations of primordial germ cells of the mouse. *Developmental Biology*, *47*(1), 136–155. https://doi.org/10.1016/0012-1606(75)90269-9

Claycomb, J. M., Batista, P. J., Pang, K. M., Gu, W., Vasale, J. J., van Wolfswinkel, J. C., Chaves, D. A., Shirayama, M., Mitani, S., Ketting, R. F., Conte, D., & Mello, C. C. (2009). The Argonaute CSR-1 and its 22G-RNA cofactors are required for holocentric chromosome segregation. *Cell*, *139*(1), 123–134. https://doi.org/10.1016/j.cell.2009.09.014

Clifford, R., Lee, M. H., Nayak, S., Ohmachi, M., Giorgini, F., & Schedl, T. (2000). FOG-2, a novel F-box containing protein, associates with the GLD-1 RNA binding protein and directs male sex determination in the C. elegans hermaphrodite germline. *Development*, *127*(24), 5265–5276. https://doi.org/10.1242/dev.127.24.5265

Corsi, A. K., Wightman, B., & Chalfie, M. (2015). A Transparent Window into Biology: A Primer on Caenorhabditis elegans. *Genetics*, *200*(2), 387–407. https://doi.org/10.1534/genetics.115.176099

Coyle, S. M., Gilbert, W. V, & Doudna, J. A. (2009). Direct link between RACK1 function and localization at the ribosome in vivo. *Molecular and Cellular Biology*, *29*(6), 1626–1634. https://doi.org/10.1128/MCB.01718-08

Crews, C. (2003). Feeding the machine: mechanisms of proteasome-catalyzed degradation of ubiquitinated proteins. *Current Opinion in Chemical Biology*, *7*(5), 534–539. https://doi.org/10.1016/j.cbpa.2003.08.002

Crittenden, S. L., Bernstein, D. S., Bachorik, J. L., Thompson, B. E., Gallegos, M.,

Petcherski, A. G., Moulder, G., Barstead, R., Wickens, M., & Kimble, J. (2002). A conserved RNA-binding protein controls germline stem cells in Caenorhabditis elegans. *Nature*, *417*(6889), 660–663. https://doi.org/10.1038/nature754

Crittenden, S. L. L., Troemel, E. R. R., Evans, T. C. C., & Kimble, J. (1994). GLP-1 is localized to the mitotic region of the C. elegans germ line. *Development (Cambridge, England)*, *120*(10), 2901–2911. https://doi.org/10.1242/dev.120.10.2901

Crittenden, S. L., Leonhard, K. A., Byrd, D. T., & Kimble, J. (2006). Cellular analyses of the mitotic region in the Caenorhabditis elegans adult germ line. *Molecular Biology of the Cell*, *17*(7), 3051–3061. https://doi.org/10.1091/mbc.e06-03-0170

Dallaire, A., Frédérick, P.-M., & Simard, M. J. (2018). Somatic and Germline MicroRNAs Form Distinct Silencing Complexes to Regulate Their Target mRNAs Differently. *Developmental Cell*, *47*(2), 239-247.e4. https://doi.org/10.1016/j.devcel.2018.08.022

Day, N. J., Wang, X., & Voronina, E. (2020). In Situ Detection of Ribonucleoprotein Complex Assembly in the C. elegans Germline using Proximity Ligation Assay. *Journal of Visualized Experiments : JoVE*, *159*. https://doi.org/10.3791/60982

Demarco, R. S., & Lundquist, E. A. (2010). RACK-1 Acts with Rac GTPase Signaling and UNC-115/abLIM in Caenorhabditis elegans Axon Pathfinding and Cell Migration. *PLoS Genetics*, *6*(11), e1001215. https://doi.org/10.1371/journal.pgen.1001215

DNA Technologies, I. (2016). *C. elegans injection—Alt-R CRISPR-Cas9 System ribonucleoprotien delivery, Dernburg Lab (CRS-10052-PR)*.

Dobrikov, M. I., Dobrikova, E. Y., & Gromeier, M. (2018). Ribosomal RACK1:Protein Kinase C βII Phosphorylates Eukaryotic Initiation Factor 4G1 at S1093 To Modulate Cap-Dependent and -Independent Translation Initiation. *Molecular and Cellular Biology*, *38*(19). https://doi.org/10.1128/MCB.00304-18

Doh, J. H., Jung, Y., Reinke, V., & Lee, M.-H. (2013). *C. elegans* RNA-binding protein GLD-1 recognizes its multiple targets using sequence, context, and structural information to repress translation. *Worm*, *2*(4), e26548. https://doi.org/10.4161/worm.26548

Dokshin, G. A., Ghanta, K. S., Piscopo, K. M., & Mello, C. C. (2018). Robust Genome Editing with Short Single-Stranded and Long, Partially Single-Stranded DNA Donors in Caenorhabditis elegans. *Genetics*, *210*(3), 781–787. https://doi.org/10.1534/genetics.118.301532

Doll, M. A., Soltanmohammadi, N., & Schumacher, B. (2019). ALG-2/AGO-Dependent mir-35 Family Regulates DNA Damage-Induced Apoptosis Through MPK-1/ERK

MAPK Signaling Downstream of the Core Apoptotic Machinery in Caenorhabditis elegans. *Genetics*, *213*(1), 173–194. https://doi.org/10.1534/genetics.119.302458

Doyle, T. G., Wen, C., & Greenwald, I. (2000). SEL-8, a nuclear protein required for LIN-12 and GLP-1 signaling in Caenorhabditis elegans. *Proceedings of the National Academy of Sciences of the United States of America*, *97*(14), 7877–7881. https://doi.org/10.1073/pnas.97.14.7877

Ebersole, T. A., Chen, Q., Justice, M. J., & Artzt, K. (1996). The quaking gene product necessary in embryogenesis and myelination combines features of RNA binding and signal transduction proteins. *Nature Genetics*, *12*(3), 260–265. https://doi.org/10.1038/ng0396-260

Eckmann, C. R., Crittenden, S. L., Suh, N., & Kimble, J. (2004). GLD-3 and Control of the Mitosis/Meiosis Decision in the Germline of Caenorhabditis elegans. *Genetics*, *168*(1), 147–160. https://doi.org/10.1534/genetics.104.029264

Eckmann, C. R., Kraemer, B., Wickens, M., & Kimble, J. (2002). GLD-3, a bicaudal-C homolog that inhibits FBF to control germline sex determination in C. elegans. *Developmental Cell*, *3*(5), 697–710. https://doi.org/10.1016/s1534-5807(02)00322-2

Ellenbecker, M., Osterli, E., Wang, X., Day, N. J., Baumgarten, E., Hickey, B., & Voronina, E. (2019). Dynein Light Chain DLC-1 Facilitates the Function of the Germline Cell Fate Regulator GLD-1 in Caenorhabditis elegans. *Genetics*, *211*(2), 665–681. https://doi.org/10.1534/genetics.118.301617

Ellis, R. (2007). Sex determination in the germ linerevisedversioncorrectedfigure1. *WormBook*. https://doi.org/10.1895/wormbook.1.82.2

Evans, M. J., & Kaufman, M. H. (1981). Establishment in culture of pluripotential cells from mouse embryos. *Nature*, *292*(5819), 154–156. https://doi.org/10.1038/292154a0

Fitzgerald, K., & Greenwald, I. (1995). Interchangeability of Caenorhabditis elegans DSL proteins and intrinsic signalling activity of their extracellular domains in vivo. *Development*, *121*(12), 4275–4282. https://doi.org/10.1242/dev.121.12.4275

Fox, P. M., & Schedl, T. (2015). Analysis of Germline Stem Cell Differentiation Following Loss of GLP-1 Notch Activity in Caenorhabditis elegans. *Genetics*, *201*(September), 167–184. https://doi.org/10.1534/genetics.115.178061

Fox, P. M., Vought, V. E., Hanazawa, M., Lee, M.-H., Maine, E. M., & Schedl, T. (2011). Cyclin E and CDK-2 regulate proliferative cell fate and cell cycle progression in the C. elegans germline. *Development (Cambridge, England)*, *138*(11), 2223–2234. https://doi.org/10.1242/dev.059535

Francis, R., Barton, M. K., Kimble, J., & Schedl, T. (1995). Gld-1, a Tumor Suppressor Gene Required for Oocyte Development in Caenorhabditis Elegans. *Genetics*,

139(2), 579.

Francis, Ross, Maine, E., & Schedl, T. (1995). *Analysis of the Multiple Roles of gld-I in Germline Development: Interactions With the Sex Determination Cascade and the glP-1 Signaling Pathway*.

Friend, K., Campbell, Z. T., Cooke, A., Kroll-Conner, P., Wickens, M. P., & Kimble, J. (2012). A conserved PUF–Ago–eEF1A complex attenuates translation elongation. *Nature Structural & Molecular Biology 2012 19:2*, *19*(2), 176–183. https://doi.org/10.1038/nsmb.2214

Frisone, P., Pradella, D., Di Matteo, A., Belloni, E., Ghigna, C., & Paronetto, M. P. (2015). SAM68: Signal Transduction and RNA Metabolism in Human Cancer. *BioMed Research International*, *2015*, 1–14. https://doi.org/10.1155/2015/528954

Gallo, S., Ricciardi, S., Manfrini, N., Pesce, E., Oliveto, S., Calamita, P., Mancino, M., Maffioli, E., Moro, M., Crosti, M., Berno, V., Bombaci, M., Tedeschi, G., & Biffo, S. (2018). RACK1 Specifically Regulates Translation through Its Binding to Ribosomes. *Molecular and Cellular Biology*, *38*(23). https://doi.org/10.1128/MCB.00230-18

Gandin, V., Senft, D., Topisirovic, I., & Ronai, Z. A. (2013). RACK1 Function in Cell Motility and Protein Synthesis. *Genes & Cancer*, *4*(9–10), 369–377. https://doi.org/10.1177/1947601913486348

Gerbasi, V. R., Weaver, C. M., Hill, S., Friedman, D. B., & Link, A. J. (2004). Yeast Asc1p and mammalian RACK1 are functionally orthologous core 40S ribosomal proteins that repress gene expression. *Molecular and Cellular Biology*, *24*(18), 8276–8287. https://doi.org/10.1128/MCB.24.18.8276-8287.2004

Giansanti, M. G., Belloni, G., & Gatti, M. (2007). Rab11 is required for membrane trafficking and actomyosin ring constriction in meiotic cytokinesis of Drosophila males. *Molecular Biology of the Cell*, *18*(12), 5034–5047. https://doi.org/10.1091/mbc.e07-05-0415

Gu, W., Shirayama, M., Conte, D., Vasale, J., Batista, P. J., Claycomb, J. M., Moresco, J. J., Youngman, E. M., Keys, J., Stoltz, M. J., Chen, C.-C. G., Chaves, D. A., Duan, S., Kasschau, K. D., Fahlgren, N., Yates, J. R., Mitani, S., Carrington, J. C., & Mello, C. C. (2009). Distinct argonaute-mediated 22G-RNA pathways direct genome surveillance in the C. elegans germline. *Molecular Cell*, *36*(2), 231–244. https://doi.org/10.1016/j.molcel.2009.09.020

Guillemot, F., Billault, A., & Auffray, C. (1989). Physical linkage of a guanine nucleotide-binding protein-related gene to the chicken major histocompatibility complex. *Proceedings of the National Academy of Sciences of the United States of America*, *86*(12), 4594–4598. https://doi.org/10.1073/pnas.86.12.4594

Gumienny, T. L., Lambie, E., Hartwieg, E., Horvitz, H. R., & Hengartner, M. O. (1999). Genetic control of programmed cell death in the Caenorhabditis elegans hermaphrodite germline. *Development*, *126*(5), 1011–1022. https://doi.org/10.1242/dev.126.5.1011

Gupta, P., Leahul, L., Wang, X., Wang, C., Bakos, B., Jasper, K., & Hansen, D. (2015). Proteasome regulation of the chromodomain protein MRG-1 controls the balance between proliferative fate and differentiation in the C. elegans germ line. *Development*, *142*(2), 291–302. https://doi.org/10.1242/dev.115147

Gutnik, S., Thomas, Y., Guo, Y., Stoecklin, J., Neagu, A., Pintard, L., Merlet, J., & Ciosk, R. (2018). PRP-19, a conserved pre-mRNA processing factor and E3 ubiquitin ligase, inhibits the nuclear accumulation of GLP-1/Notch intracellular domain. *Biology Open*, *7*(7). https://doi.org/10.1242/bio.034066

Hall, D. H., Winfrey, V. P., Blaeuer, G., Hoffman, L. H., Furuta, T., Rose, K. L., Hobert, O., & Greenstein, D. (1999). Ultrastructural features of the adult hermaphrodite gonad of Caenorhabditis elegans: relations between the germ line and soma. *Developmental Biology*, *212*(1), 101–123. https://doi.org/10.1006/dbio.1999.9356

Hansen, D., Hubbard, E. J. A., & Schedl, T. (2004). Multi-pathway control of the proliferation versus meiotic development decision in the Caenorhabditis elegans germline. *Developmental Biology*, *268*(2), 342–357. https://doi.org/10.1016/J.YDBIO.2003.12.023

Hansen, D., & Schedl, T. (2013). Stem cell proliferation versus meiotic fate decision in Caenorhabditis elegans. *Advances in Experimental Medicine and Biology*, *757*, 71–99. https://doi.org/10.1007/978-1-4614-4015-4_4

Hansen, D., Wilson-Berry, L., Dang, T., & Schedl, T. (2004). Control of the proliferation versus meiotic development decision in the C. elegans germline through regulation of GLD-1 protein accumulation. *Development (Cambridge, England)*, *131*(1), 93–104. https://doi.org/10.1242/dev.00916

Hardy, R. W., Tokuyasu, K. T., Lindsley, D. L., & Garavito, M. (1979). The germinal proliferation center in the testis of Drosophila melanogaster. *Journal of Ultrastructure Research*, *69*(2), 180–190. https://doi.org/10.1016/s0022-5320(79)90108-4

Hargitai, B., Kutnyánszky, V., Blauwkamp, T. A., Steták, A., Csankovszki, G., Takács-Vellai, K., & Vellai, T. (2009). xol-1, the master sex-switch gene in C. elegans, is a transcriptional target of the terminal sex-determining factor TRA-1. *Development (Cambridge, England)*, *136*(23), 3881–3887. https://doi.org/10.1242/dev.034637

Haupt, K. A., Enright, A. L., Ferdous, A. S., Kershner, A. M., Shin, H., Wickens, M., & Kimble, J. (2019). The molecular basis of LST-1 self-renewal activity and its control of stem cell pool size. *Development (Cambridge, England)*, *146*(20).

https://doi.org/10.1242/dev.181644

Haupt, K. A., Law, K. T., Enright, A. L., Kanzler, C. R., Shin, H., Wickens, M., & Kimble, J. (2020). A PUF Hub Drives Self-Renewal in Caenorhabditis elegans Germline Stem Cells. *Genetics*, *214*(1), 147–161. https://doi.org/10.1534/genetics.119.302772

He, Z., Jiang, J., Kokkinaki, M., Golestaneh, N., Hofmann, M.-C., & Dym, M. (2008). Gdnf upregulates c-Fos transcription via the Ras/Erk1/2 pathway to promote mouse spermatogonial stem cell proliferation. *Stem Cells (Dayton, Ohio)*, *26*(1), 266–278. https://doi.org/10.1634/stemcells.2007-0436

Hirsh, D., Oppenheim, D., & Klass, M. (1976). Development of the reproductive system of Caenorhabditis elegans. *Developmental Biology*, *49*(1), 200–219. https://doi.org/10.1016/0012-1606(76)90267-0

Hofmann, M.-C., Braydich-Stolle, L., & Dym, M. (2005). Isolation of male germ-line stem cells; influence of GDNF. *Developmental Biology*, *279*(1), 114–124. https://doi.org/10.1016/j.ydbio.2004.12.006

Hubbard, E. J. A., & Schedl, T. (2019). Biology of the Caenorhabditis elegans Germline Stem Cell System. *Genetics*, *213*(4), 1145–1188. https://doi.org/10.1534/genetics.119.300238

Hubbard, E. J., & Greenstein, D. (2005). Introduction to the germ line. In *WormBook*. https://doi.org/10.1895/wormbook.1.18.1

Iino, Y., & Yamamoto, M. (1985). Negative control for the initiation of meiosis in Schizosaccharomyces pombe. *Proceedings of the National Academy of Sciences of the United States of America*, *82*(8), 2447–2451. https://doi.org/10.1073/pnas.82.8.2447

Ikenishi, K., Tanaka, T. S., & Komiya, T. (1996). Spatio-temporal distribution of the protein of Xenopus vasa homologue (Xenopus vasa-like gene 1, XVLG1) in embryos. *Development, Growth and Differentiation*, *38*(5), 527–535. https://doi.org/10.1046/j.1440-169X.1996.t01-4-00009.x

Irfan, S., Bukhari, A., Vasquez-Rifo, A., Gagné, D., Paquet, E. R., Zetka, M., Robert, C., Masson, J.-Y., & Simard, M. J. (2012). Germ cells regulation by miRNAs 1034 The microRNA pathway controls germ cell proliferation and differentiation in C. elegans. *Cell Research* |, *22*(6), 1034–1045. https://doi.org/10.1038/cr.2012.31

Ishidate, T., Ozturk, A. R., Durning, D. J., Sharma, R., Shen, E., Chen, H., Seth, M., Shirayama, M., & Mello, C. C. (2018). ZNFX-1 Functions within Perinuclear Nuage to Balance Epigenetic Signals. *Molecular Cell*, *70*(4), 639-649.e6. https://doi.org/10.1016/J.MOLCEL.2018.04.009

Jackson, R. J., Hellen, C. U. T., & Pestova, T. V. (2010). The mechanism of eukaryotic

translation initiation and principles of its regulation. *Nature Reviews Molecular Cell Biology*, *11*(2), 113–127. https://doi.org/10.1038/nrm2838

Jan, E., Motzny, C. K., Graves, L. E., & Goodwin, E. B. (1999). The STAR protein, GLD-1, is a translational regulator of sexual identity in Caenorhabditis elegans. *The EMBO Journal*, *18*(1), 258–269. https://doi.org/10.1093/emboj/18.1.258

Jannot, G., Bajan, S., Giguère, N. J., Bouasker, S., Banville, I. H., Piquet, S., Hutvagner, G., & Simard, M. J. (2011). The ribosomal protein RACK1 is required for microRNA function in both C. elegans and humans. *EMBO Reports*, *12*(6), 581–586. https://doi.org/10.1038/embor.2011.66

Jantsch, V., Tang, L., Pasierbek, P., Penkner, A., Nayak, S., Baudrimont, A., Schedl, T., Gartner, A., & Loidl, J. (2007). Caenorhabditis elegans prom-1 is required for meiotic prophase progression and homologous chromosome pairing. *Molecular Biology of the Cell*, *18*(12), 4911–4920. https://doi.org/10.1091/mbc.e07-03-0243

Jeong, J., Verheyden, J. M., & Kimble, J. (2011). Cyclin E and Cdk2 Control GLD-1, the Mitosis/Meiosis Decision, and Germline Stem Cells in Caenorhabditis elegans. *PLoS Genetics*, *7*(3), e1001348. https://doi.org/10.1371/journal.pgen.1001348

Jiang, J., & Hui, C. (2008). Hedgehog Signaling in Development and Cancer. *Developmental Cell*, *15*(6), 801–812. https://doi.org/10.1016/j.devcel.2008.11.010

Jones, A. R., Francis, R., & Schedl, T. (1996). GLD-1, a cytoplasmic protein essential for oocyte differentiation, shows stage- and sex-specific expression during Caenorhabditis elegans germline development. *Developmental Biology*, *180*(1), 165–183. https://doi.org/10.1006/dbio.1996.0293

Jones, A. R., & Schedl, T. (1995). Mutations in gld-1, a female germ cell-specific tumor suppressor gene in Caenorhabditis elegans, affect a conserved domain also found in Src-associated protein Sam68. *Genes & Development*, *9*(12), 1491–1504. https://doi.org/10.1101/gad.9.12.1491

Jungkamp, A.-C., Stoeckius, M., Mecenas, D., Grün, D., Mastrobuoni, G., Kempa, S., & Rajewsky, N. (2011). In vivo and transcriptome-wide identification of RNA binding protein target sites. *Molecular Cell*, *44*(5), 828–840. https://doi.org/10.1016/j.molcel.2011.11.009

Kachur, T. M., Audhya, A., & Pilgrim, D. B. (2008). UNC-45 is required for NMY-2 contractile function in early embryonic polarity establishment and germline cellularization in C. elegans. *Developmental Biology*, *314*(2), 287–299. https://doi.org/10.1016/J.YDBIO.2007.11.028

Kadrmas, J. L., Smith, M. A., Pronovost, S. M., & Beckerle, M. C. (2007). Characterization of RACK1 function in Drosophila development. *Developmental Dynamics*, *236*(8), 2207–2215. https://doi.org/10.1002/DVDY.21217

Kadyk, L. C., & Kimble, J. (1998). Genetic regulation of entry into meiosis in Caenorhabditis elegans. *Development (Cambridge, England)*, *125*(10), 1803–1813.

Kamath, R. S., Fraser, A. G., Dong, Y., Poulin, G., Durbin, R., Gotta, M., Kanapin, A., Le Bot, N., Moreno, S., Sohrmann, M., Welchman, D. P., Zipperlen, P., & Ahringer, J. (2003). Systematic functional analysis of the Caenorhabditis elegans genome using RNAi. *Nature*, *421*(6920), 231–237. https://doi.org/10.1038/nature01278

Kawasaki, I., Shim, Y. H., Kirchner, J., Kaminker, J., Wood, W. B., & Strome, S. (1998). PGL-1, a predicted RNA-binding component of germ granules, is essential for fertility in C. elegans. *Cell*, *94*(5), 635–645. https://doi.org/10.1016/s0092-8674(00)81605-0

Kawase, E., Wong, M. D., Ding, B. C., & Xie, T. (2004). Gbb/Bmp signaling is essential for maintaining germline stem cells and for repressing *bam* transcription in the *Drosophila* testis. *Development*, *131*(6), 1365–1375. https://doi.org/10.1242/dev.01025

Kelly, W. G., Xu, S., Montgomery, M. K., & Fire, A. (1997). Distinct Requirements for Somatic and Germline Expression of a Generally Expressed Caernorhabditis elegans Gene. *Genetics*, *146*(1).

Kerins, J. (2006). *PPR-17 and the pre-mRNA splicing pathway are preferentially required for the proliferation versus meiotic development decision and germline sex determination in Caenorhabditis elegans.* Washington University.

Kerins, J. A., Hanazawa, M., Dorsett, M., & Schedl, T. (2010). PRP-17 and the pre-mRNA splicing pathway are preferentially required for the proliferation versus meiotic development decision and germline sex determination in Caenorhabditis elegans. *Developmental Dynamics : An Official Publication of the American Association of Anatomists*, *239*(5), 1555–1572. https://doi.org/10.1002/dvdy.22274

Kershner, A. M., & Kimble, J. (2010). Genome-wide analysis of mRNA targets for Caenorhabditis elegans FBF, a conserved stem cell regulator. *Proceedings of the National Academy of Sciences of the United States of America*, *107*(8), 3936–3941. https://doi.org/10.1073/pnas.1000495107

Kershner, A. M., Shin, H., Hansen, T. J., & Kimble, J. (2014). Discovery of two GLP-1/Notch target genes that account for the role of GLP-1/Notch signaling in stem cell maintenance. *Proceedings of the National Academy of Sciences of the United States of America*, *111*(10), 3739–3744. https://doi.org/10.1073/pnas.1401861111

Kiger, A. A., Jones, D. L., Schulz, C., Rogers, M. B., & Fuller, M. T. (2001). Stem cell self-renewal specified by JAK-STAT activation in response to a support cell cue. *Science*, *294*(5551), 2542–2545. https://doi.org/10.1126/science.1066707

Kim, K. W., Nykamp, K., Suh, N., Bachorik, J. L., Wang, L., & Kimble, J. (2009).

Antagonism between GLD-2 binding partners controls gamete sex. *Developmental Cell*, *16*(5), 723–733. https://doi.org/10.1016/j.devcel.2009.04.002

Kim, K. W., Wilson, T. L., & Kimble, J. (2010). GLD-2/RNP-8 cytoplasmic poly(A) polymerase is a broad-spectrum regulator of the oogenesis program. *Proceedings of the National Academy of Sciences of the United States of America*, *107*(40), 17445–17450. https://doi.org/10.1073/pnas.1012611107

Kimble, J. E., & White, J. G. (1981). On the control of germ cell development in Caenorhabditis elegans. *Developmental Biology*, *81*(2), 208–219. https://doi.org/10.1016/0012-1606(81)90284-0

Kimble, J, & Hirsh, D. (1979). The postembryonic cell lineages of the hermaphrodite and male gonads in Caenorhabditis elegans. *Developmental Biology*, *70*(2), 396–417. https://doi.org/10.1016/0012-1606(79)90035-6

Kimble, Judith. (1981). Alterations in cell lineage following laser ablation of cells in the somatic gonad of Caenorhabditis elegans. *Developmental Biology*, *87*(2), 286–300. https://doi.org/10.1016/0012-1606(81)90152-4

Kirilly, D., & Xie, T. (2007). The Drosophila ovary: an active stem cell community. *Cell Research*, *17*(1), 15–25. https://doi.org/10.1038/sj.cr.7310123

Kisielnicka, E., Minasaki, R., & Eckmann, C. R. (2018). MAPK signaling couples SCF-mediated degradation of translational regulators to oocyte meiotic progression. *Proceedings of the National Academy of Sciences of the United States of America*, *115*(12), E2772–E2781. https://doi.org/10.1073/pnas.1715439115

Knaut, H., Pelegri, F., Bohmann, K., Schwarz, H., & Nüsslein-Volhard, C. (2000). Zebrafish vasa RNA but not its protein is a component of the germ plasm and segregates asymmetrically before germline specification. *The Journal of Cell Biology*, *149*(4), 875–888. https://doi.org/10.1083/jcb.149.4.875

Kocsisova, Z., Kornfeld, K., & Schedl, T. (2019). Rapid population-wide declines in stem cell number and activity during reproductive aging in C. elegans. *Development (Cambridge, England)*, *146*(8). https://doi.org/10.1242/dev.173195

Kodoyianni, V., Maine, E. M., & Kimble, J. (1992). Molecular basis of loss-of-function mutations in the glp-1 gene of Caenorhabditis elegans. *Molecular Biology of the Cell*, *3*(11), 1199–1213. https://doi.org/10.1091/mbc.3.11.1199

Komander, D. (2009). The emerging complexity of protein ubiquitination. *Biochemical Society Transactions*, *37*(Pt 5), 937–953. https://doi.org/10.1042/BST0370937

Kopan, R., Schroeter, E. H., Weintraub, H., & Nye, J. S. (1996). Signal transduction by activated mNotch: importance of proteolytic processing and its regulation by the extracellular domain. *Proceedings of the National Academy of Sciences of the United States of America*, *93*(4), 1683–1688.

https://doi.org/10.1073/pnas.93.4.1683

Kraemer, B., Crittenden, S., Gallegos, M., Moulder, G., Barstead, R., Kimble, J., & Wickens, M. (1999). NANOS-3 and FBF proteins physically interact to control the sperm-oocyte switch in Caenorhabditis elegans. *Current Biology : CB*, *9*(18), 1009–1018. https://doi.org/10.1016/s0960-9822(99)80449-7

Kubota, H., Avarbock, M. R., & Brinster, R. L. (2004). Growth factors essential for self-renewal and expansion of mouse spermatogonial stem cells. *Proceedings of the National Academy of Sciences of the United States of America*, *101*(47), 16489–16494. https://doi.org/10.1073/pnas.0407063101

Kuhn, L., Majzoub, K., Einhorn, E., Chicher, J., Pompon, J., Imler, J.-L., Hammann, P., & Meignin, C. (2017). Definition of a RACK1 Interaction Network in Drosophila melanogaster Using SWATH-MS. *G3 (Bethesda, Md.)*, *7*(7), 2249–2258. https://doi.org/10.1534/g3.117.042564

Lambie, E. J., Kimble, J., Lambie, E. J., Kimble, J., & Kimble, J. (1991). Two homologous regulatory genes, lin-12 and glp-1, have overlapping functions. *Development (Cambridge, England)*, *112*(1), 231–240.

Lamont, L. B., Crittenden, S. L., Bernstein, D., Wickens, M., & Kimble, J. (2004). FBF-1 and FBF-2 regulate the size of the mitotic region in the C. elegans germline. *Developmental Cell*, *7*(5), 697–707. https://doi.org/10.1016/j.devcel.2004.09.013

Lee, C., Sorensen, E. B., Lynch, T. R., & Kimble, J. (2016). C. elegans GLP-1/Notch activates transcription in a probability gradient across the germline stem cell pool. *ELife*, *5*. https://doi.org/10.7554/eLife.18370

Lee, M.-H., Ohmachi, M., Arur, S., Nayak, S., Francis, R., Church, D., Lambie, E., & Schedl, T. (2007). Multiple functions and dynamic activation of MPK-1 extracellular signal-regulated kinase signaling in Caenorhabditis elegans germline development. *Genetics*, *177*(4), 2039–2062. https://doi.org/10.1534/genetics.107.081356

Lee, M.-H., & Schedl, T. (2004). Translation repression by GLD-1 protects its mRNA targets from nonsense-mediated mRNA decay in C. elegans. *Genes & Development*, *18*(9), 1047–1059. https://doi.org/10.1101/gad.1188404

Lee, M.-H., & Schedl, T. (2010). *C. Elegans Star Proteins, Gld-1 And Asd-2, Regulate Specific RNA Targets to Control Development* (pp. 106–122). Springer, Boston, MA. https://doi.org/10.1007/978-1-4419-7005-3_8

Lee, M. H., & Schedl, T. (2001). Identification of in vivo mRNA targets of GLD-1, a maxi-KH motif containing protein required for C. elegans germ cell development. *Genes & Development*, *15*(18), 2408–2420. https://doi.org/10.1101/gad.915901

Lev, I., & Rechavi, O. (2020). Germ Granules Allow Transmission of Small RNA-Based Parental Responses in the "Germ Plasm". *IScience*, *23*(12), 101831.

https://doi.org/10.1016/j.isci.2020.101831

Lin, H. (2002). The stem-cell niche theory: lessons from flies. *Nature Reviews. Genetics*, *3*(12), 931–940. https://doi.org/10.1038/nrg952

Linden, L. M., Gordon, K. L., Pani, A. M., Payne, S. G., Garde, A., Burkholder, D., Chi, Q., Goldstein, B., & Sherwood, D. R. (2017). Identification of regulators of germ stem cell enwrapment by its niche in C. elegans. *Developmental Biology*, *429*(1), 271–284. https://doi.org/10.1016/j.ydbio.2017.06.019

Liu, M., Liu, P., Zhang, L., Cai, Q., Gao, G., Zhang, W., Zhu, Z., Liu, D., & Fan, Q. (2011). mir-35 is involved in intestine cell G1/S transition and germ cell proliferation in C. elegans. *Cell Research*, *21*(11), 1605–1618. https://doi.org/10.1038/cr.2011.102

Lock, P., Fumagalli, S., Polakis, P., McCormick, F., & Courtneidge, S. A. (1996). The human p62 cDNA encodes Sam68 and not the RasGAP-associated p62 protein. *Cell*, *84*(1), 23–24. https://doi.org/10.1016/s0092-8674(00)80989-7

Lublin, A. L., & Evans, T. C. (2007). The RNA-binding proteins PUF-5, PUF-6, and PUF-7 reveal multiple systems for maternal mRNA regulation during C. elegans oogenesis. *Developmental Biology*, *303*(2), 635–649. https://doi.org/10.1016/j.ydbio.2006.12.004

Macdonald, L. D., Knox, A., & Hansen, D. (2008). Proteasomal regulation of the proliferation vs. meiotic entry decision in the Caenorhabditis elegans germ line. *Genetics*, *180*(2), 905–920. https://doi.org/10.1534/genetics.108.091553

Maciejowski, J., Ugel, N., Mishra, B., Isopi, M., & Hubbard, E. J. A. (2006). Quantitative analysis of germline mitosis in adult C. elegans. *Developmental Biology*, *292*(1), 142–151. https://doi.org/10.1016/j.ydbio.2005.12.046

MacQueen, A. J., & Villeneuve, A. M. (2001). Nuclear reorganization and homologous chromosome pairing during meiotic prophase require C. elegans chk-2. *Genes & Development*, *15*(13), 1674–1687. https://doi.org/10.1101/gad.902601

Mahowald, A. P. (1968). Polar granules of Drosophila. II. Ultrastructural changes during early embryogenesis. *The Journal of Experimental Zoology*, *167*(2), 237–261. https://doi.org/10.1002/jez.1401670211

Mamidipudi, V, Dhillon, N. K., Parman, T., Miller, L. D., Lee, K. C., & Cartwright, C. A. (2007). RACK1 inhibits colonic cell growth by regulating Src activity at cell cycle checkpoints. *Oncogene*, *26*(20), 2914–2924. https://doi.org/10.1038/sj.onc.1210091

Mamidipudi, Vidya, Miller, L. D., Mochly-Rosen, D., & Cartwright, C. A. (2007). Peptide modulators of Src activity in G1 regulate entry into S phase and proliferation of NIH 3T3 cells. *Biochemical and Biophysical Research Communications*, *352*(2), 423–

430. https://doi.org/10.1016/j.bbrc.2006.11.034

Mamidipudi, Vidya, Zhang, J., Lee, K. C., & Cartwright, C. A. (2004). RACK1 regulates G1/S progression by suppressing Src kinase activity. *Molecular and Cellular Biology*, *24*(15), 6788–6798. https://doi.org/10.1128/MCB.24.15.6788-6798.2004

Manage, K. I., Rogers, A. K., Wallis, D. C., Uebel, C. J., Anderson, D. C., Nguyen, D. A. H., Arca, K., Brown, K. C., Cordeiro Rodrigues, R. J., de Albuquerque, B. F., Ketting, R. F., Montgomery, T. A., & Phillips, C. M. (2020). A tudor domain protein, SIMR-1, promotes siRNA production at piRNA-targeted mRNAs in C. elegans. *ELife*, *9*. https://doi.org/10.7554/eLife.56731

Maniates, K. A., Olson, B. S., & Abbott, A. L. (2021). Sperm fate is promoted by the *mir-44* microRNA family in the *Caenorhabditis elegans* hermaphrodite germline. *Genetics*, *217*(1), 1–14. https://doi.org/10.1093/genetics/iyaa006

Mantina, P., MacDonald, L., Kulaga, A., Zhao, L., & Hansen, D. (2009). A mutation in teg-4, which encodes a protein homologous to the SAP130 pre-mRNA splicing factor, disrupts the balance between proliferation and differentiation in the C. elegans germ line. *Mechanisms of Development*, *126*(5–6), 417–429. https://doi.org/10.1016/j.mod.2009.01.006

Marin, V. A., & Evans, T. C. (2003). Translational repression of a C. elegans Notch mRNA by the STAR/KH domain protein GLD-1. *Development (Cambridge, England)*, *130*(12), 2623–2632. https://doi.org/10.1242/dev.00486

Marnik, E. A., & Updike, D. L. (2019). Membraneless organelles: P granules in *Caenorhabditis elegans*. *Traffic*, *20*(6), 373–379. https://doi.org/10.1111/tra.12644

Martynovsky, M., Wong, M.-C., Byrd, D. T., Kimble, J., & Schwarzbauer, J. E. (2012). mig-38, a novel gene that regulates distal tip cell turning during gonadogenesis in C. elegans hermaphrodites. *Developmental Biology*, *368*(2), 404–414. https://doi.org/10.1016/j.ydbio.2012.06.011

McCulloch, E. A., & Till, J. E. (1960). The Radiation Sensitivity of Normal Mouse Bone Marrow Cells, Determined by Quantitative Marrow Transplantation into Irradiated Mice. *Radiation Research*, *13*(1), 115. https://doi.org/10.2307/3570877

McEwen, T. J., Yao, Q., Yun, S., Lee, C.-Y., & Bennett, K. L. (2016). Small RNA in situ hybridization in Caenorhabditis elegans, combined with RNA-seq, identifies germline-enriched microRNAs. *Developmental Biology*, *418*(2), 248–257. https://doi.org/10.1016/J.YDBIO.2016.08.003

McGovern, M., Voutev, R., Maciejowski, J., Corsi, A. K., & Hubbard, E. J. A. (2009). A "latent niche" mechanism for tumor initiation. *Proceedings of the National Academy of Sciences of the United States of America*, *106*(28), 11617–11622. https://doi.org/10.1073/pnas.0903768106

McLeod, M, Shor, B., Caporaso, A., Wang, W., Chen, H., & Hu, L. (2000). Cpc2, a fission yeast homologue of mammalian RACK1 protein, interacts with Ran1 (Pat1) kinase To regulate cell cycle progression and meiotic development. *Molecular and Cellular Biology*, *20*(11), 4016–4027. https://doi.org/10.1128/mcb.20.11.4016-4027.2000

McLeod, Maureen, & Beach, D. (1988). A specific inhibitor of the ran1+ protein kinase regulates entry into meiosis in Schizosaccharomyces pombe. *Nature*, *332*(6164), 509–514. https://doi.org/10.1038/332509a0

Meng, X., Lindahl, M., Hyvönen, M. E., Parvinen, M., de Rooij, D. G., Hess, M. W., Raatikainen-Ahokas, A., Sainio, K., Rauvala, H., Lakso, M., Pichel, J. G., Westphal, H., Saarma, M., & Sariola, H. (2000). Regulation of cell fate decision of undifferentiated spermatogonia by GDNF. *Science (New York, N.Y.)*, *287*(5457), 1489–1493. https://doi.org/10.1126/science.287.5457.1489

Merritt, C., Rasoloson, D., Ko, D., & Seydoux, G. (2008). 3' UTRs are the primary regulators of gene expression in the C. elegans germline. *Current Biology : CB*, *18*(19), 1476–1482. https://doi.org/10.1016/j.cub.2008.08.013

Minogue, A. L., Tackett, M. R., Atabakhsh, E., Tejada, G., & Arur, S. (2018). Functional genomic analysis identifies miRNA repertoire regulating C. elegans oocyte development. *Nature Communications*, *9*(1), 5318. https://doi.org/10.1038/s41467-018-07791-w

Mohammad, A., Vanden Broek, K., Wang, C., Daryabeigi, A., Jantsch, V., Hansen, D., & Schedl, T. (2018). Initiation of Meiotic Development Is Controlled by Three Post-transcriptional Pathways in Caenorhabditis elegans. *Genetics*, *209*(4), 1197–1224. https://doi.org/10.1534/genetics.118.300985

Mootz, D., Ho, D. M., & Hunter, C. P. (2004). The STAR/Maxi-KH domain protein GLD-1 mediates a developmental switch in the translational control of C. elegans PAL-1. *Development (Cambridge, England)*, *131*(14), 3263–3272. https://doi.org/10.1242/dev.01196

Morrison, S. J., & Spradling, A. C. (2008). Stem Cells and Niches: Mechanisms That Promote Stem Cell Maintenance throughout Life. *Cell*, *132*(4), 598–611. https://doi.org/10.1016/j.cell.2008.01.038

Nadarajan, S., Govindan, J. A., McGovern, M., Hubbard, E. J. A., & Greenstein, D. (2009). MSP and GLP-1/Notch signaling coordinately regulate actomyosin-dependent cytoplasmic streaming and oocyte growth in C. elegans. *Development (Cambridge, England)*, *136*(13), 2223–2234. https://doi.org/10.1242/dev.034603

Nayak, S., Santiago, F. E., Jin, H., Lin, D., Schedl, T., & Kipreos, E. T. (2002). The Caenorhabditis elegans Skp1-related gene family: diverse functions in cell proliferation, morphogenesis, and meiosis. *Current Biology : CB*, *12*(4), 277–287.

https://doi.org/10.1016/s0960-9822(02)00682-6

Nilsson, J., Sengupta, J., Frank, J., & Nissen, P. (2004). Regulation of eukaryotic translation by the RACK1 protein: a platform for signalling molecules on the ribosome. *EMBO Reports*, *5*(12), 1137–1141. https://doi.org/10.1038/sj.embor.7400291

Nousch, M., Minasaki, R., & Eckmann, C. R. (2017). Polyadenylation is the key aspect of GLD-2 function in C. elegans. *RNA (New York, N.Y.)*, *23*(8), 1180–1187. https://doi.org/10.1261/rna.061473.117

Núñez, A., Franco, A., Soto, T., Vicente, J., Gacto, M., & Cansado, J. (2010). Fission yeast receptor of activated C kinase (RACK1) ortholog Cpc2 regulates mitotic commitment through Wee1 kinase. *The Journal of Biological Chemistry*, *285*(53), 41366–41373. https://doi.org/10.1074/jbc.M110.173815

Otsuka, M., Takata, A., Yoshikawa, T., Kojima, K., Kishikawa, T., Shibata, C., Takekawa, M., Yoshida, H., Omata, M., & Koike, K. (2011). Receptor for Activated Protein Kinase C: Requirement for Efficient MicroRNA Function and Reduced Expression in Hepatocellular Carcinoma. *PLoS ONE*, *6*(9), e24359. https://doi.org/10.1371/journal.pone.0024359

Park, Y., O'Rourke, S., Taki, F. A., Alfhili, M. A., & Lee, M. H. (2020). Dose-Dependent Effects of GLD-2 and GLD-1 on Germline Differentiation and Dedifferentiation in the Absence of PUF-8. *Frontiers in Cell and Developmental Biology*, *8*, 5. https://doi.org/10.3389/fcell.2020.00005

Parker, W. N., Rönnfeldt, H., Weismann, A., & Rönnfeldt, H. (1893). *The germ-plasm; a theory of heredity, by August Weismann. Tr. by W. Newton Parker and Harriet Rönnfeldt.* Scribner's,. https://doi.org/10.5962/bhl.title.29345

Pepper, A. S.-R., Killian, D. J., & Hubbard, E. J. A. (2003). Genetic analysis of Caenorhabditis elegans glp-1 mutants suggests receptor interaction or competition. *Genetics*, *163*(1), 115–132.

Petcherski, A. G., & Kimble, J. (2000). LAG-3 is a putative transcriptional activator in the C. elegans Notch pathway. *Nature*, *405*(6784), 364–368. https://doi.org/10.1038/35012645

Phillips, C. M., Montgomery, T. A., Breen, P. C., & Ruvkun, G. (2012). MUT-16 promotes formation of perinuclear mutator foci required for RNA silencing in the C. elegans germline. *Genes & Development*, *26*(13), 1433–1444. https://doi.org/10.1101/gad.193904.112

Pickart, C. M. (2001). Mechanisms Underlying Ubiquitination. *Annual Review of Biochemistry*, *70*(1), 503–533. https://doi.org/10.1146/annurev.biochem.70.1.503

Pitt, J. N., Schisa, J. A., & Priess, J. R. (2000). P Granules in the Germ Cells of

Caenorhabditis elegans Adults Are Associated with Clusters of Nuclear Pores and Contain RNA. *Developmental Biology*, *219*(2), 315–333. https://doi.org/10.1006/dbio.2000.9607

Porta-de-la-Riva, M., Fontrodona, L., Villanueva, A., & Cerón, J. (2012). Basic Caenorhabditis elegans methods: synchronization and observation. *Journal of Visualized Experiments : JoVE*, *64*, e4019. https://doi.org/10.3791/4019

Praitis, V., Casey, E., Collar, D., & Austin, J. (2001). Creation of low-copy integrated transgenic lines in Caenorhabditis elegans. *Genetics*, *157*(3), 1217–1226.

Qiu, C., Bhat, V. D., Rajeev, S., Zhang, C., Lasley, A. E., Wine, R. N., Campbell, Z. T., & Hall, T. M. T. (2019). A crystal structure of a collaborative RNA regulatory complex reveals mechanisms to refine target specificity. *ELife*, *8*. https://doi.org/10.7554/eLife.48968

Qiu, S., Adema, C. M., & Lane, T. (2005). A computational study of off-target effects of RNA interference. *Nucleic Acids Research*, *33*(6), 1834–1847. https://doi.org/10.1093/nar/gki324

Ron, D., Chen, C. H., Caldwell, J., Jamieson, L., Orr, E., & Mochly-Rosen, D. (1994). Cloning of an intracellular receptor for protein kinase C: a homolog of the beta subunit of G proteins. *Proceedings of the National Academy of Sciences of the United States of America*, *91*(3), 839–843. https://doi.org/10.1073/pnas.91.3.839

Ron, D., Jiang, Z., Yao, L., Vagts, A., Diamond, I., & Gordon, A. (1999). Coordinated movement of RACK1 with activated betaIIPKC. *The Journal of Biological Chemistry*, *274*(38), 27039–27046. https://doi.org/10.1074/jbc.274.38.27039

Ron, D., Luo, J., & Mochly-Rosen, D. (1995). C2 region-derived peptides inhibit translocation and function of beta protein kinase C in vivo. *The Journal of Biological Chemistry*, *270*(41), 24180–24187. https://doi.org/10.1074/jbc.270.41.24180

Ron, D., & Mochly-Rosen, D. (1995). An autoregulatory region in protein kinase C: the pseudoanchoring site. *Proceedings of the National Academy of Sciences of the United States of America*, *92*(2), 492–496. https://doi.org/10.1073/pnas.92.2.492

Ruiz Carrillo, D., Chandrasekaran, R., Nilsson, M., Cornvik, T., Liew, C. W., Tan, S. M., & Lescar, J. (2012). Structure of human Rack1 protein at a resolution of 2.45 Å. *Acta Crystallographica. Section F, Structural Biology and Crystallization Communications*, *68*(Pt 8), 867–872. https://doi.org/10.1107/S1744309112027480

Scheckel, C., Gaidatzis, D., Wright, J. E., & Ciosk, R. (2012). Genome-Wide Analysis of GLD-1–Mediated mRNA Regulation Suggests a Role in mRNA Storage. *PLoS Genetics*, *8*(5), e1002742. https://doi.org/10.1371/journal.pgen.1002742

Schindelin, J., Arganda-Carreras, I., Frise, E., Kaynig, V., Longair, M., Pietzsch, T., Preibisch, S., Rueden, C., Saalfeld, S., Schmid, B., Tinevez, J.-Y., White, D. J.,

Hartenstein, V., Eliceiri, K., Tomancak, P., & Cardona, A. (2012). Fiji: an open-source platform for biological-image analysis. *Nature Methods*, *9*(7), 676–682. https://doi.org/10.1038/nmeth.2019

Schisa, J. A. (2012). New insights into the regulation of RNP granule assembly in oocytes. *International Review of Cell and Molecular Biology*, *295*, 233–289. https://doi.org/10.1016/B978-0-12-394306-4.00013-7

Schofield, R. (1978). The relationship between the spleen colony-forming cell and the haemopoietic stem cell. *Blood Cells*, *4*(1–2), 7–25.

Schumacher, B., Hanazawa, M., Lee, M.-H., Nayak, S., Volkmann, K., Hofmann, E. R., Hofmann, R., Hengartner, M., Schedl, T., & Gartner, A. (2005). Translational repression of C. elegans p53 by GLD-1 regulates DNA damage-induced apoptosis. *Cell*, *120*(3), 357–368. https://doi.org/10.1016/j.cell.2004.12.009

Schumacher, B., Hofmann, K., Boulton, S., & Gartner, A. (2001). The C. elegans homolog of the p53 tumor suppressor is required for DNA damage-induced apoptosis. *Current Biology*, *11*(21), 1722–1727. https://doi.org/10.1016/S0960-9822(01)00534-6

Seydoux, G., & Fire, A. (1994). Soma-germline asymmetry in the distributions of embryonic RNAs in Caenorhabditis elegans. *Development*, *120*(10), 2823–2834. https://doi.org/10.1242/dev.120.10.2823

Seydoux, Geraldine, & Schedl, T. (2001). The germline in C. elegans: Origins, proliferation, and silencing. In *International Review of Cytology* (pp. 139–185). https://doi.org/10.1016/S0074-7696(01)03006-6

Shin, H., Haupt, K. A., Kershner, A. M., Kroll-Conner, P., Wickens, M., & Kimble, J. (2017). SYGL-1 and LST-1 link niche signaling to PUF RNA repression for stem cell maintenance in Caenorhabditis elegans. *PLoS Genetics*, *13*(12), e1007121. https://doi.org/10.1371/journal.pgen.1007121

Song, X., Wong, M. D., Kawase, E., Xi, R., Ding, B. C., McCarthy, J. J., & Xie, T. (2004). Bmp signals from niche cells directly repress transcription of a differentiation-promoting gene, bag of marbles, in germline stem cells in the Drosophila ovary. *Development (Cambridge, England)*, *131*(6), 1353–1364. https://doi.org/10.1242/dev.01026

Sorensen, E. B., Seidel, H. S., Crittenden, S. L., Ballard, J. H., & Kimble, J. (2020). A toolkit of tagged glp-1 alleles reveals strong glp-1 expression in the germline, embryo, and spermatheca. *MicroPublication Biology*, *2020*. https://doi.org/10.17912/micropub.biology.000271

Speth, C., & Laubinger, S. (2014). RACK1 and the microRNA pathway: is it déjà-vu all over again? *Plant Signaling & Behavior*, *9*(2), e27909.

https://doi.org/10.4161/psb.27909

Speth, C., Willing, E.-M., Rausch, S., Schneeberger, K., & Laubinger, S. (2013). RACK1 scaffold proteins influence miRNA abundance in Arabidopsis. *The Plant Journal*, *76*(3), 433–445. https://doi.org/10.1111/tpj.12308

Spiegelman, M., & Bennett, D. (1973). A light- and electron-microscopic study of primordial germ cells in the early mouse embryo. *Journal of Embryology and Experimental Morphology*, *30*(1), 97–118. https://doi.org/10.1242/DEV.30.1.97

Spike, C. A., Bader, J., Reinke, V., Strome, S., Kohara, Y., Rhoads, R. E., & Strome, S. (2008). DEPS-1 promotes P-granule assembly and RNA interference in C. elegans germ cells. *Development (Cambridge, England)*, *135*(5), 983–993. https://doi.org/10.1242/dev.015552

Spradling, A., Fuller, M. T., Braun, R. E., & Yoshida, S. (2011). Germline stem cells. *Cold Spring Harbor Perspectives in Biology*, *3*(11), a002642. https://doi.org/10.1101/cshperspect.a002642

Stebbins, E. G., & Mochly-Rosen, D. (2001). Binding Specificity for RACK1 Resides in the V5 Region of βII Protein Kinase C. *Journal of Biological Chemistry*, *276*(32), 29644–29650. https://doi.org/10.1074/jbc.M101044200

Stirnimann, C. U., Petsalaki, E., Russell, R. B., & Müller, C. W. (2010). WD40 proteins propel cellular networks. *Trends in Biochemical Sciences*, *35*(10), 565–574. https://doi.org/10.1016/j.tibs.2010.04.003

Strome, S., & Wood, W. B. (1982). Immunofluorescence visualization of germ-line-specific cytoplasmic granules in embryos, larvae, and adults of Caenorhabditis elegans. *Proceedings of the National Academy of Sciences of the United States of America*, *79*(5), 1558–1562. https://doi.org/10.1073/pnas.79.5.1558

Suh, N., Crittenden, S. L., Goldstrohm, A., Hook, B., Thompson, B., Wickens, M., & Kimble, J. (2009). FBF and its dual control of gld-1 expression in the Caenorhabditis elegans germline. *Genetics*, *181*(4), 1249–1260. https://doi.org/10.1534/genetics.108.099440

Suh, N., Jedamzik, B., Eckmann, C. R., Wickens, M., & Kimble, J. (2006). The GLD-2 poly(A) polymerase activates gld-1 mRNA in the Caenorhabditis elegans germ line. *Proceedings of the National Academy of Sciences of the United States of America*, *103*(41), 15108–15112. https://doi.org/10.1073/pnas.0607050103

Sundby, A. E., Molnar, R. I., & Claycomb, J. M. (2021). Connecting the Dots: Linking Caenorhabditis elegans Small RNA Pathways and Germ Granules. *Trends in Cell Biology*, *31*(5), 387–401. https://doi.org/10.1016/j.tcb.2020.12.012

Tauber, D., Tauber, G., & Parker, R. (2020). Mechanisms and Regulation of RNA Condensation in RNP Granule Formation. *Trends in Biochemical Sciences*, *45*(9),

764–778. https://doi.org/10.1016/J.TIBS.2020.05.002

Theil, K., Imami, K., & Rajewsky, N. (2019). Identification of proteins and miRNAs that specifically bind an mRNA in vivo. *Nature Communications*, *10*(1), 4205. https://doi.org/10.1038/s41467-019-12050-7

Thompson, M. K., Rojas-Duran, M. F., Gangaramani, P., & Gilbert, W. V. (2016). The ribosomal protein Asc1/RACK1 is required for efficient translation of short mRNAs. *ELife*, *5*. https://doi.org/10.7554/eLife.11154

Thomson, J. A., Itskovitz-Eldor, J., Shapiro, S. S., Waknitz, M. A., Swiergiel, J. J., Marshall, V. S., & Jones, J. M. (1998). Embryonic stem cell lines derived from human blastocysts. *Science (New York, N.Y.)*, *282*(5391), 1145–1147. https://doi.org/10.1126/science.282.5391.1145

Trabucchi, M., Briata, P., Garcia-Mayoral, M., Haase, A. D., Filipowicz, W., Ramos, A., Gherzi, R., & Rosenfeld, M. G. (2009). The RNA-binding protein KSRP promotes the biogenesis of a subset of microRNAs. *Nature*, *459*(7249), 1010–1014. https://doi.org/10.1038/nature08025

Tran, A. T., Chapman, E. M., Flamand, M. N., Yu, B., Krempel, S. J., Duchaine, T. F., Eroglu, M., & Derry, W. B. (2019). MiR-35 buffers apoptosis thresholds in the C. elegans germline by antagonizing both MAPK and core apoptosis pathways. *Cell Death & Differentiation*, *26*(12), 2637–2651. https://doi.org/10.1038/s41418-019-0325-6

Tran, J., Brenner, T. J., & DiNardo, S. (2000). Somatic control over the germline stem cell lineage during Drosophila spermatogenesis. *Nature*, *407*(6805), 754–757. https://doi.org/10.1038/35037613

Tsukamoto, T., Gearhart, M. D., Spike, C. A., Huelgas-Morales, G., Mews, M., Boag, P. R., Beilharz, T. H., & Greenstein, D. (2017). LIN-41 and OMA Ribonucleoprotein Complexes Mediate a Translational Repression-to-Activation Switch Controlling Oocyte Meiotic Maturation and the Oocyte-to-Embryo Transition in Caenorhabditis elegans. *Genetics*, *206*(4), 2007–2039. https://doi.org/10.1534/genetics.117.203174

Ullah, H., Scappini, E. L., Moon, A. F., Williams, L. V., Armstrong, D. L., & Pedersen, L. C. (2008). Structure of a signal transduction regulator, RACK1, from Arabidopsis thaliana. *Protein Science : A Publication of the Protein Society*, *17*(10), 1771–1780. https://doi.org/10.1110/ps.035121.108

Updike, D. L., Knutson, A. K., Egelhofer, T. A., Campbell, A. C., & Strome, S. (2014). Germ-Granule Components Prevent Somatic Development in the C. elegans Germline. *Current Biology*, *24*(9), 970–975. https://doi.org/10.1016/J.CUB.2014.03.015

Updike, D., & Strome, S. (2010). P granule assembly and function in Caenorhabditis elegans germ cells. *Journal of Andrology*, *31*(1), 53–60. https://doi.org/10.2164/jandrol.109.008292

Villa, N., Do, A., Hershey, J. W. B., & Fraser, C. S. (2013). Human Eukaryotic Initiation Factor 4G (eIF4G) Protein Binds to eIF3c, -d, and -e to Promote mRNA Recruitment to the Ribosome. *Journal of Biological Chemistry*, *288*(46), 32932–32940. https://doi.org/10.1074/JBC.M113.517011

Volta, V., Beugnet, A., Gallo, S., Magri, L., Brina, D., Pesce, E., Calamita, P., Sanvito, F., & Biffo, S. (2013). RACK1 depletion in a mouse model causes lethality, pigmentation deficits and reduction in protein synthesis efficiency. *Cellular and Molecular Life Sciences : CMLS*, *70*(8), 1439–1450. https://doi.org/10.1007/s00018-012-1215-y

Voronina, E., Paix, A., & Seydoux, G. (2012). The P granule component PGL-1 promotes the localization and silencing activity of the PUF protein FBF-2 in germline stem cells. *Development*, *139*(20), 3732–3740. https://doi.org/10.1242/dev.083980

Voronina, E., Seydoux, G., Sassone-Corsi, P., & Nagamori, I. (2011). RNA granules in germ cells. *Cold Spring Harbor Perspectives in Biology*, *3*(12), a002774. https://doi.org/10.1101/cshperspect.a002774

Wall, M. A., Coleman, D. E., Lee, E., Iñiguez-Lluhi, J. A., Posner, B. A., Gilman, A. G., & Sprang, S. R. (1995). The structure of the G protein heterotrimer Gi alpha 1 beta 1 gamma 2. *Cell*, *83*(6), 1047–1058. https://doi.org/10.1016/0092-8674(95)90220-1

Wan, G., Fields, B. D., Spracklin, G., Shukla, A., Phillips, C. M., & Kennedy, S. (2018). Spatiotemporal regulation of liquid-like condensates in epigenetic inheritance. *Nature*, *557*(7707), 679–683. https://doi.org/10.1038/s41586-018-0132-0

Wang, C., Wilson-Berry, L., Schedl, T., & Hansen, D. (2012). TEG-1 CD2BP2 regulates stem cell proliferation and sex determination in the C. elegans germ line and physically interacts with the UAF-1 U2AF65 splicing factor. *Developmental Dynamics : An Official Publication of the American Association of Anatomists*, *241*(3), 505–521. https://doi.org/10.1002/dvdy.23735

Wang, L., Eckmann, C. R., Kadyk, L. C., Wickens, M., & Kimble, J. (2002). A regulatory cytoplasmic poly(A) polymerase in Caenorhabditis elegans. *Nature*, *419*(6904), 312–316. https://doi.org/10.1038/nature01039

Wang, Xiaobo, Ellenbecker, M., Hickey, B., Day, N. J., Osterli, E., Terzo, M., & Voronina, E. (2020). Antagonistic control of Caenorhabditis elegans germline stem cell proliferation and differentiation by PUF proteins FBF-1 and FBF-2. *ELife*, *9*. https://doi.org/10.7554/eLife.52788

Wang, Xiaobo, Olson, J. R., Rasoloson, D., Ellenbecker, M., Bailey, J., & Voronina, E. (2016). Dynein light chain DLC-1 promotes localization and function of the PUF protein FBF-2 in germline progenitor cells. *Development*, *143*(24), 4643–4653. https://doi.org/10.1242/dev.140921

Wang, Xin. (2013). *The Role of Protein Kinase CK2 in the Proliferative Fate vs. Differentiation Decision in the C. elegans Germ Line* [University of Calgary]. https://doi.org/http://dx.doi.org/10.11575/PRISM/28350

Wang, Xin, Gupta, P., Fairbanks, J., & Hansen, D. (2014). Protein kinase CK2 both promotes robust proliferation and inhibits the proliferative fate in the C. elegans germ line. *Developmental Biology*, *392*(1), 26–41. https://doi.org/10.1016/J.YDBIO.2014.05.002

Weismann, A. (1892). *Aufsätze über Vererbung und verwandte biologische Fragen*.

Wieschaus, E., & Szabad, J. (1979). The development and function of the female germ line in Drosophila melanogaster: a cell lineage study. *Developmental Biology*, *68*(1), 29–46. https://doi.org/10.1016/0012-1606(79)90241-0

Wu, S.-C., & Wong, S.-L. (2013). Structure-Guided Design of an Engineered Streptavidin with Reusability to Purify Streptavidin-Binding Peptide Tagged Proteins or Biotinylated Proteins. *PLoS ONE*, *8*(7), e69530. https://doi.org/10.1371/journal.pone.0069530

Xie, T., & Spradling, A. C. (2000). A Niche Maintaining Germ Line Stem Cells in the Drosophila Ovary. *Science*, *290*(5490), 328–330. https://doi.org/10.1126/science.290.5490.328

Xu, C., & Min, J. (2011). Structure and function of WD40 domain proteins. *Protein & Cell*, *2*(3), 202–214. https://doi.org/10.1007/s13238-011-1018-1

Xu, L., Paulsen, J., Yoo, Y., Goodwin, E. B., & Strome, S. (2001). Caenorhabditis elegans MES-3 is a target of GLD-1 and functions epigenetically in germline development. *Genetics*, *159*(3), 1007–1017.

Yamashita, Y. M., Jones, D. L., & Fuller, M. T. (2003). Orientation of asymmetric stem cell division by the APC tumor suppressor and centrosome. *Science (New York, N.Y.)*, *301*(5639), 1547–1550. https://doi.org/10.1126/science.1087795

Yomogida, K., Yagura, Y., Tadokoro, Y., & Nishimune, Y. (2003). Dramatic Expansion of Germinal Stem Cells by Ectopically Expressed Human Glial Cell Line-Derived Neurotrophic Factor in Mouse Sertoli Cells. *Biology of Reproduction*, *69*(4), 1303–1307. https://doi.org/10.1095/biolreprod.103.015958

Yu, X., Lu, N., & Zhou, Z. (2008). Phagocytic Receptor CED-1 Initiates a Signaling Pathway for Degrading Engulfed Apoptotic Cells. *PLoS Biology*, *6*(3), e61. https://doi.org/10.1371/journal.pbio.0060061

Zakrzewski, W., Dobrzyński, M., Szymonowicz, M., & Rybak, Z. (2019). Stem cells: Past, present, and future. In *Stem Cell Research and Therapy* (Vol. 10, Issue 1, p. 68). BioMed Central Ltd. https://doi.org/10.1186/s13287-019-1165-5

Zhang, B., Gallegos, M., Puoti, A., Durkin, E., Fields, S., Kimble, J., & Wickens, M. P. (1997). A conserved RNA-binding protein that regulates sexual fates in the C. elegans hermaphrodite germ line. *Nature*, *390*(6659), 477–484. https://doi.org/10.1038/37297

Zhang, L., Ding, L., Cheung, T. H., Dong, M.-Q., Chen, J., Sewell, A. K., Liu, X., Yates, J. R., Han, M., & Han, M. (2007). Systematic identification of C. elegans miRISC proteins, miRNAs, and mRNA targets by their interactions with GW182 proteins AIN-1 and AIN-2. *Molecular Cell*, *28*(4), 598–613. https://doi.org/10.1016/j.molcel.2007.09.014

Zhou, Z., Hartwieg, E., & Horvitz, H. R. (2001). CED-1 Is a Transmembrane Receptor that Mediates Cell Corpse Engulfment in C. elegans. *Cell*, *104*(1), 43–56. https://doi.org/10.1016/S0092-8674(01)00190-8